UNIVERSIDAD COMPLUTENSE DE MADRID

FACULTAD DE MEDICINA

TESIS DOCTORAL

Estrategias para la mejora de la persistencia y la eficacia de las células CAR NK para el tratamiento del mieloma múltiple refractario y en recaída

Strategies to improve persistence and efficacy of CAR NK cells for the treatment of relapsed and refractory multiple myeloma

MEMORIA PARA OPTAR AL GRADO DE DOCTOR

PRESENTADA POR

Jessica Encinas Mayoral

DIRECTORES

Antonio Valeri Lozano
Daniel Primo Ramos
Joaquín Martínez López

© Jessica Encinas Mayoral, 2024

UNIVERSIDAD COMPLUTENSE DE MADRID

FACULTAD DE MEDICINA

DOCTORADO EN INVESTIGACIÓN BIOMÉDICA

TESIS DOCTORAL

ESTRATEGIAS PARA LA MEJORA DE LA PERSISTENCIA Y LA EFICACIA DE LAS CÉLULAS CAR NK PARA EL TRATAMIENTO DEL MIELOMA MÚLTIPLE REFRACTARIO Y EN RECAÍDA

STRATEGIES TO IMPROVE PERSISTENCE AND EFFICACY OF CAR NK CELLS FOR THE TREATMENT OF RELAPSED AND REFRACTORY MULTIPLE MYELOMA

MEMORIA PARA OPTAR AL GRADO DE DOCTOR

PRESENTADA POR

Jessica Encinas Mayoral

DIRECTORES

Antonio Valeri Lozano

Daniel Primo Ramos

Joaquín Martínez López

Madrid, 2023

A mis padres, Asun y Jose,

A mi hermano Iván,

A mi familia,

AGRADECIMIENTOS / ACKNOWLEDGMENTS

Sin duda una tesis no es un trabajo que implique la dedicación de una sola persona y en ésta han participado muchísimas personas con las que he tenido la suerte de trabajar estos últimos años.

En primer lugar, quiero agradecer la cesión de muestras por parte de pacientes de mieloma múltiple y donantes sanos a este proyecto, porque sin su colaboración este trabajo no hubiera sido posible.

También quiero agradecer la dedicación de mis directores de tesis: Antonio, Joaquín y Dani. Muchas gracias, Joaquín, por darme la oportunidad de trabajar en el grupo de hematología y poder desarrollar esta tesis que, sin duda, tampoco habría sido posible sin la ayuda de Antonio y de Almu. Muchas gracias, Antonio, por guiarme, por enseñarme todo sobre las NKs, por corregirme los "le", que todavía sigo sin decir bien, y por tu apoyo estos años. Almu, que "como llegué tarde al reparto de postdocs, me tocó ella", y la verdad es que no podría haber tenido una mejor. Ha sido un pilar fundamental de esta tesis, de estos dos proyectos, y la que nos ha enseñado todo sobre citometría y cultivos. Muchísimas gracias por ayudarme y por cuidarme, y recuerda que vales mucho.

Muchas gracias también a Dani y a Joan por hacerme un hueco en Vivia, guiarme con los experimentos y apoyarme en esta tesis.

Elena y Eva, mis compañeras de tesis.

Elena, aquella muchacha a la que sentamos en una silla en mitad del despacho, porque no teníamos más sitio y que rápidamente se hizo hueco con sus "fantásticas" NK-92. Juntas aprendimos a hacer "calceínas", expandir NKs, pasar citometría y a infundir a los ratones por cola. Eso sí, si alguien necesita optimizar algún protocolo que no dude en hablar con ella. Mil gracias por tu ayuda durante toda la tesis, por tus consejos (sobre todo para pintarme las uñas permanentes, que obviamente no me quedan igual que a ti). Me hace muchísima ilusión volver a trabajar contigo.

Eva la pobre tampoco llegó en un buen día, por motivos que no voy a comentar aquí, pero ¿qué pensaría ese primer día como predoc? Menos mal que la cosa fue mejorando, o no. Muchas gracias mujer por tu apoyo durante estos años, por esas primeras producciones

de virus, por ayudarme con los experimentos cuando ya era tarde, por pesar a los ratones cuando me daba miedo y por enseñarme Villaviciosa junto a tu perrito, menos mal que le caí bien.

Raquel, sin duda mi mayor descubrimiento, y es que, aunque estudiamos juntas la carrera en Alcalá, creemos que no llegamos a hablar ni una sola vez. Yo no creo en el destino, si no en las casualidades, y me ha encantado que, "por casualidad", haya tenido la oportunidad de conocerte y compartir este último año y medio contigo. Gracias por ayudarme con las expansiones de las NKs, las producciones de virus, los *western* y por las recomendaciones de restaurantes, porque si hay alguien que más disfrute comiendo, es ella.

Elena y Marta, nuestras chicas de TFM y TFG. Mil gracias, chicas, por ayudarnos con nuestras tesis y espero que os hayamos enseñado alguna cosa útil. Yo creo que en el fondo echan de menos cultivos y el citómetro, podéis volver cuando queráis. Y, sobre todo, gracias, Marta, por amar mis audios (los que los sufren saben que mis audios, no son audios, si no *podcasts*).

Rebe, no te lo vas a creer, pero "la princesa de Asturias" va a defender por fin la tesis. Muchas gracias por cuidarme durante el TFM y ser uno de mis referentes durante mis primeros meses en el labo, te hemos echado mucho de menos.

Ana, muchas gracias por tu apoyo mientras escribía la tesis y por el tiempo que hemos compartido estos últimos meses.

Mis Lauris, Laura Córdoba y Laura Sánchez. No sé cuántas veces habremos reído/llorado en el despacho o en el comedor, y es que sois de lo mejor. Laura Córdoba sabe bien lo que cuesta expandir unas NKs, y ya si encima esa semana se transducen bien, todo un logro. Y es que ha sido una de mis compañeras de campana durante toda la tesis. ¡Qué maravilla eso de tener una campana de cultivos para dos! Y también de citómetro, sobre todo pasando Legendplex, una de nuestras actividades favoritas. Me ha encantado conocerte y compartir todos estos años contigo mujer. Laura Sánchez, no sabes lo que te hemos echado de menos estos meses, muchísimas gracias por tu apoyo y me alegro muchísimo de haber compartido este tiempo contigo.

La otra pecera, Roberto, Raquel, Irene, Ale Ortiz, Andrés, Alba, Richard y María. A María la conocí por primera vez cuando nos dio una clase en el máster y poco a poco fui

conociendo al resto del grupo, y la verdad es que sois todos estupendos. Muchas gracias, Richard, jefe del *Hemato Beer Team,* por ayudarnos con la secuenciación de ARN (y a Andrés por explicármela jaja). A Roberto, por ser como es, no se puede explicar, pero sin duda una de las personas a las que más le cunde el día, yo creo que el giratiempo de Hermione lo tiene él, porque si no, es imposible. Y por supuesto, para persona especial Raquel, reina de la fiesta, de los brindis y de los chupitos, que solo con encontrártela por el labo ya te alegra el día.

Natalia y Noe, desterradas en la tercera planta, pero parte esencial del grupo. Muchas gracias, chicas, por vuestro apoyo estos años, por las risas y por todos los momentos que hemos compartido. Sigue quedando pendiente una merienda en Alcorcón.

Isa, la primera persona que conocí del labo y que casualmente estaba estudiando la enfermedad de la que murió mi abuelo años antes, amiloidosis. Ojalá pronto se desarrollen también más terapias para las enfermedades raras. Ha sido un placer compartir estos años contigo.

Mariluz, de las veteranas del labo cuando aparecí por allí y a la que tenía frita preguntando donde estaba todo, pero bien que me dejó sola para que me entrevistaran los de Cris y les contara lo maravillosa que es la terapia CAR. Por cierto, no te preocupes que ya me voy del labo, dejo sitio en la campana para que puedan trabajar los demás y dejo de romper cámaras de Neubauer, aunque últimamente me están quitando el puesto.

Mis chicas de biobanco. Yo creo que a veces me temían cuando me veían aparecer, porque sabían que las iba a pedir algún favor y es que todas las muestras de pacientes que se han usado en esta tesis, y en otros tantos experimentos, han pasado por sus manos o me han ayudado a buscarlas en la Intranet, ya fueran de extracciones, de la HUNET o de Hospital de Día. Mil gracias, Vane, Ali, Laura Carneros (puberta y pepinera, a partes iguales), Laura Moreno, Lucía, María, Irene y Sandra, por ayudarme a conseguirlas prácticamente todas y por vuestras charlas y apoyo mientras marcaba citometría en la poyata a vuestro lado.

Paqui, el alma del labo y madre de todos. Mil gracias por cuidarme durante toda la tesis, por hacerme reír (sobre todo desde la mesa) y contarme anécdotas de Timoteo. Marijose, que escondía las puntas por todo el laboratorio y luego nos las iba repartiendo como si fuera contrabando. Paloma, Merche y Manu, los del turno de tarde, que menos mal que estaban por allí para amenizarnos esos ratos.

Citometría, Teresa Cedena, Fátima, Elvira, Lorena y Teresas (técnicos). Seguramente haya pasado la mitad de la tesis en su planta, pasando citometría. Muchas gracias a todas por enseñarme citometría, prestarme anticuerpos, hacerme "*spoiler*" del porcentaje de plasmáticas que tenían las muestras para poder poner los experimentos pronto, y por ayudarme a arreglar el citómetro cada vez que no funcionaba.

Hematólogos. Muchas gracias a todos por ayudarnos a conseguir muestras y en especial a Rafa, por ayudarnos siempre con los proyectos y los datos de los pacientes.

Sala blanca, Adri, Patri C, Patri del Moral, Ale Leivas y Fran. Ha sido un placer conoceros a todos y compartir estos años con vosotros, desde luego a vosotros tampoco os lo han puesto fácil. Muchas gracias, Ale, por tu ayuda desde que entré al labo, con la citometría, el sorter y el Legendplex.

Esther. Menuda guerra te hemos dado entre todos. Muchas gracias por los tantísimos pedidos que te hemos mandado tramitar y también por las charlas.

Mis chicos de Vivia, Miguel, Adri, Ana, Chechu, Vero y David. También se alegraban mucho de verme, sobre todo los días que tenían muchas muestras y yo me pasaba la mañana en el citómetro. Muchas gracias, chicos, por enseñarme a trabajar en vuestro labo, por las risas, los desayunos, la música de fondo (casi siempre canciones de verbena de pueblo), los puzles del Layton y sobre todo por vuestro apoyo, ya que la mayoría de las veces los experimentos no salían como esperaba, pero allí estabais vosotros para alegrarme el día.

CNIO, Pedro, Michel, Álvaro, Lara, Miguel y María Velasco. A pesar de que no he coincidido mucho con vosotros, los ratos que hemos pasado juntos han sido de los mejores, sois fantásticos. Muchísimas gracias por vuestro apoyo y por ayudarnos con las irradiaciones.

CIEMAT, Paula, Lauras, Irene, Marta y Bea. Muchísimas gracias, Paula, por ayudarnos con estos proyectos durante estos años y también a vosotras chicas, por tratarme tan bien y ayudarme cada vez que iba por el CIEMAT, sois estupendas.

Grupos UNICA y mitocondriales. Menos mal que no estábamos solos en la planta y hemos tenido la suerte de compartir cultivos con gente tan maravillosa y tan maja, para poder hacer intercambios de reactivos. Muchas gracias, chicos, por vuestro apoyo y ha

sido un placer conoceros y compartir tantas mañanas, y otras tantas tardes, con vosotros en cultivos. Y en especial, a Rocío y Pablo, por los experimentos de metabolismo.

Dana Farber team. First, I would like to thank Dr. Munshi and Mariateresa for taking me in and let me be part of their team during those months. It has been a great experience and I have enjoyed working with all of you. Thank you so much, Yao, for teaching me new techniques, helping me every time I needed it and taking care of me. Jessica, it has been a pleasure working with you, thank you for your help and your tips, above all related to good restaurants. The Italian team: Anna, Eugenio, Domenico and Marcello. Thank you so much for your help and the time we spent together. My dear Dori, thank you so much for taking care of me, for touring me around Boston and took me to incredible places, I have been very lucky to meet you.

Rocío y Ana. ¡Qué haría yo sin estas muchachas! Y es que valen para todo, da igual cual sea el problema que tenga, que me van a ayudar igual. Eso sí, primero se tienen que escuchar un audio de unos 10 minutos aproximadamente en el que yo, tranquilamente, explico los hechos acontecidos. Muchísimas gracias, chicas, por ser como sois, por vuestro apoyo incondicional y por vuestros consejos.

Mis biosanis, Marina, Elena, Rosa, Cris, Judith Abarca, Judith Ortega, Natalia, Luis y Javier. Ellos también saben lo que implica una tesis y lo difícil que es trabajar en ciencia. Muchas gracias, chicos, por apoyarme estos años y por todos los momentos que hemos compartido. Sobre todo, a Rosa, que menos mal que nos teníamos la una a la otra en el mismo huso horario cuando estuvimos de estancia para apoyarnos mutuamente.

Mis torrecillanos, María, Lidia, Andrea, Nuria, Raquel, Judith, Carlos, Víctor, Sergio y Miguel. Muchísimas gracias, a mi pequeña familia, por vuestro apoyo siempre, especialmente a Lidia, por esta maravillosa portada.

Mi familia. Muchísimas gracias a mis padres, Asun y Jose, a mi hermano Iván, a mis abuelos/as, tíos/as y primos/as, por su apoyo, no solo en estos años de tesis, si no siempre, porque a pesar de que no entendían muy bien que hacía tantas horas en el laboratorio o porque estaba tanto tiempo con el ordenador escribiendo la tesis, han hecho todo lo posible por ayudarme. Sobre todo, mi abuela Asu, que va a ser la que más se alegre de que, su nieta, la científica, haya terminado de escribir. Ahora cada vez que leen o ven por la tele algo sobre terapia CAR, se acuerdan de que está relacionado con mi trabajo y me mandan la noticia.

Y finalmente, muchas gracias a Perfecto, mi psicólogo y médico de mis abuelos desde que llegaron a Madrid. Gracias por ayudarme a entender lo que implica trabajar en ciencia y que, aunque es sacrificado, intentar desarrollar nuevas terapias para mejorar la vida de los pacientes merece la pena.

RESUMEN

Introducción

El mieloma múltiple (MM) es una neoplasia caracterizada por la proliferación clonal de células plasmáticas patológicas, principalmente en la médula ósea. Constituye el 10% de todos los tumores hematológicos y el 1,8% de todas las neoplasias. La sintomatología clásica se engloba en las siglas CRAB, hipercalcemia, fallo renal, anemia y enfermedad lítica ósea. Además, los pacientes con este tumor presentan una severa inmunosupresión, especialmente en las fases finales de la enfermedad. Aunque en los últimos años se han desarrollado una multitud de terapias para el tratamiento del MM, sigue siendo una enfermedad incurable. Este escenario justifica la necesidad de generar nuevos fármacos con distintos mecanismos de acción, especialmente en el contexto del MM refractario o en recaída.

La terapia con células CAR T autólogas ha revolucionado el tratamiento de tumores hematológicos y actualmente cuenta con 6 productos aprobados en el mercado, dos de ellos en MM. Sin embargo, su uso clínico conlleva toxicidades graves, dificultades de producción, un coste elevado y un control subóptimo de la enfermedad en una proporción destacable de pacientes. La generación de células CAR NK ha emergido como una estrategia más segura, con menores dificultades de producción y con un coste inferior. Además, la posibilidad de administración en contexto alogénico facilita la accesibilidad de los pacientes a este tratamiento. Sin embargo, estudios preclínicos y los primeros ensayos clínicos han mostrado que la inmunoterapia con células CAR NK también presenta una serie de impedimentos relacionados con una baja persistencia y eficacia limitada en el paciente, que pueden condicionar las respuestas clínicas.

Por un lado, una de las estrategias para aumentar la eficacia es la disrupción de puntos de control inmunológicos. Entre ellos, el eje HLA-E/NKG2A juega un papel importante en la inhibición de la célula NK. HLA-E, una molécula de histocompatibilidad de clase I no clásica, se encuentra sobre-expresada en una gran cantidad de tumores, en los que actúa como factor pronóstico. Estudios preclínicos han mostrado que el bloqueo de NKG2A con anticuerpos neutralizantes en combinación o la supresión del gen que codifica para este receptor inhibitorio aumentan la eficacia de las células NK en otros tipos de cáncer.

Por otro lado, a pesar de que las células NK pertenecen a la inmunidad innata, son capaces de adquirir propiedades de memoria en respuesta a virus, haptenos o citoquinas. En concreto, la breve exposición de células NK a IL-12, IL-15 e IL-18 induce cambios a

nivel transcripcional, epigenético, metabólico e inmunofenotípico, que incrementan la actividad antitumoral de las células NK, su capacidad proliferativa y su persistencia *in vivo*.

Estrategias en combinación para aumentar la eficacia mediante el bloqueo de puntos de control inmunes, así como para potenciar la capacidad citotóxica y la persistencia a través de la inducción de un fenotipo de memoria, podrían mejorar la actividad de las células CAR NK para el tratamiento del MM refractario o en recaída.

Objetivos

El objetivo principal de esta tesis es la generación de terapias CAR NK optimizadas en combinación para mejorar el tratamiento del MM refractario o en recaída: i) analizar la relevancia del eje HLA-E/NKG2A en MM; ii) potenciar la actividad anti-MM de las células NKG2D- y BCMA-CAR NK activadas y expandidas (NKAE) mediante la disrupción del eje HLA-E/NKG2A con un nuevo anticuerpo α-NKG2A; iii) incrementar la persistencia y eficacia de la inmunoterapia mediante la reprogramación de las células NKG2D-CAR NKAE hacia un fenotipo de memoria inducido por citoquinas.

Resultados

Nuestros resultados muestran que la expresión de HLA-E en células plasmáticas de pacientes de MM está incrementada con respecto a las de donantes sanos. Además, las células plasmáticas patológicas presentan una mayor expresión de HLA-E con respecto a células plasmáticas sanas y células $CD34^+$ del mismo paciente, especialmente en progresión. Aunque la supervivencia libre de progresión es menor en pacientes con un ratio alto de expresión de HLA-E en células plasmáticas patológicas con respecto a células $CD34^+$, no se observan diferencias significativas en este parámetro, ni en la supervivencia general, en nuestra cohorte de pacientes.

La concentración de IFN-γ en el plasma de médula ósea de pacientes de MM, sin signos analíticos ni clínicos de infección, es mayor que la de donantes sanos. El IFN-γ aumenta la expresión de HLA-E en células de líneas de MM y células primarias de pacientes al diagnóstico o en progresión. El bortezomib, inhibidor del proteasoma administrado como tratamiento de primera línea en pacientes de MM, disminuye la expresión de HLA-E incluso cuando es aumentada con IFN-γ, en células sensibles a este fármaco, pero no en las células resistentes.

Las células NK de los pacientes de MM presentan niveles incrementados del receptor inhibitorio de HLA-E, NKG2A, especialmente en pacientes en progresión. Sin embargo, el bloqueo de NKG2A con anticuerpos neutralizantes de ratón (Z199) o humano (BMS-936815) en muestras primarias de pacientes con MM, no impacta en la eliminación de células plasmáticas, lo que sugiere la falta de eficacia de estos tratamientos en monoterapia.

Durante la expansión y activación de las células NKG2D- o BCMA-CAR NKAE aumenta la expresión de NKG2A como respuesta compensatoria. Las células CAR NKAE producen altas concentraciones de IFN-γ en co-cultivo con líneas de MM, que a su vez aumenta la expresión de HLA-E como resultado de una retroalimentación positiva. La combinación de anticuerpos α-NKG2A con las terapias NKG2D- o BCMA-CAR NKAE aumenta significativamente la actividad antitumoral sobre líneas celulares de MM y células primarias, en cultivos en contexto nativo, sin toxicidad relevante sobre células $CD34^+$ del mismo paciente o PBMCs de donantes sanos. Asimismo, este aumento de función de las células CAR NKAE pretratadas con anticuerpos α-NKG2A está relacionado con mayores niveles de degranulación y producción de IFN-γ, y también se asocia a un balance positivo de la señal intracelular, que se refleja en una mayor fosforilación de ZAP70/Syk, con respecto a las células pretratadas con los isotipos correspondientes. No obstante, el bloqueo de NKG2A no altera significativamente la expresión fenotípica de receptores activadores e inhibidores en la membrana de la célula CAR NKAE. En los modelos de ratón de MM diseminado y ortotópico, la administración intraperitoneal del anticuerpo de bloqueo BMS-986315 en los animales reduce el porcentaje de células NKG2D- o BCMA-CAR NKAE, lo que elimina la eficacia de la combinación. Sin embargo, la infusión de células NKG2D-CAR NKAE pretratadas con el anticuerpo neutralizante no afecta a la proporción de células efectoras y disminuye significativamente la carga tumoral en los ratones.

Por otra parte, a partir de volúmenes reducidos de sangre periférica de donantes sanos se han podido generar células *cytokine-induced memory-like* (CIML)-NKAE con una expresión estable del CAR de NKG2D. La inducción de un fenotipo de memoria a través de la exposición breve de las células NKG2D-CAR NKAE a las citoquinas IL-12, IL-15 e IL-18 resulta en una mayor citotoxicidad, degranulación, producción de IFN-γ intracelular y un aumento en la liberación de IFN-γ, perforina y granzima A solubles, cuando las células de memoria se co-cultivan con líneas celulares de MM. Además, las

células NKG2D-CAR CIML-NKAE exhiben una mayor capacidad citotóxica sobre células primarias de pacientes de MM, sin afectar significativamente a la supervivencia de células $CD34^+$ del mismo paciente o procedentes de cordón umbilical. Asimismo, esta población de memoria tiene una mayor capacidad proliferativa y presenta cambios a nivel epigenético, transcriptómico, metabólico y fenotípico, comparado con las células NKG2D-CAR NKAE. En el modelo de ratón de MM U-266 ffLucGFP, las células NKG2D-CAR CIML-NKAE han demostrado un mayor control del tumor *in vivo,* que se asocia a un aumento en la proporción de las células NKG2D-CAR CIML-NKAE en los ratones y no a una persistencia superior de esta población, porque no se observa un mayor sostenimiento de esta terapia frente a las células NKG2D-CAR NKAE.

Finalmente, hemos demostrado *in vitro* que el pretratamiento de las células NKG2D-CAR CIML-NKAE con el anticuerpo de bloqueo de NKG2A supera la eficacia anti-MM de las células NKG2D-CAR NKAE neutralizadas con este anticuerpo.

Conclusiones

La sobreexpresión de HLA-E en células plasmáticas patológicas y de NKG2A en células NK de pacientes de MM en progresión sugiere un papel relevante del eje HLA-E/NKG2A en el desarrollo del tumor, aunque el tratamiento con el anticuerpo α-NKG2A, BMS-986315, en monoterapia no restaura la actividad de la célula NK.

Las células CAR NKAE destinadas a inmunoterapia sobre-expresan NKG2A, que aumenta la susceptibilidad a la inhibición por la célula plasmática de MM, por lo que la combinación de terapias CAR NKAE con anticuerpos α-NKG2A es capaz de superar la resistencia a MM mediada por HLA-E *in vitro* e *in vivo*.

La reprogramación de memoria inducida por citoquinas en combinación con la terapia NKG2D-CAR NKAE supone la generación de un nuevo efector con mayor eficacia anti-MM *in vitro* e *in vivo* comparado con las células NKG2D-CAR NKAE.

Tomadas en conjunto, ambas estrategias de tratamiento pueden ser potencialmente utilizadas no solo para aumentar la vulnerabilidad de las células de MM refractario o en recaída, si no administradas en el contexto de otro tipo de tumores, fundamentalmente HLA-E positivos.

ABSTRACT

Introduction

Multiple myeloma (MM) is a neoplasm characterized by the clonal proliferation of pathologic plasma cells (PC), mainly in the bone marrow (BM). It constitutes 10% of hematologic tumors and 1.8% of all neoplasms. Classic symptomatology is included in CRAB acronym, hypercalcemia, renal failure, anemia, and bone lytic lesions. Moreover, MM patients have severe immunosuppression, especially at the late stages of the illness. Although in the last decades, a plethora of therapies for MM treatment have been developed, it is still an incurable disease. This scenario justifies the unmet need to generate new drugs with different mechanisms of action, especially in the relapsed/refractory MM (RRMM) context.

Autologous CAR T therapy has revolutionized the treatment of hematologic tumors and currently, there are 6 market-approved treatments, two of them in MM. However, CAR T cell clinical use implies severe toxicities, manufacturing challenges, a high cost and suboptimal control of the disease in a remarkable proportion of patients. CAR NK cell generation has emerged as a safer, less cumbersome production and cost-effective strategy. Furthermore, the possibility of administering CAR NK cells in allogeneic context facilitates the accessibility of every patient to this treatment. However, preclinical studies and first clinical trials have shown that CAR NK immunotherapy also has certain shortcomings, regarding the low persistence and limited efficacy in patients, which may affect clinical responses.

On the one hand, one of the strategies to enhance efficacy is the disruption of immune checkpoints. In concrete, the HLA-E/NKG2A axis plays a key role in NK cell inhibition. HLA-E, a non-classical class I histocompatibility molecule, is overexpressed in a high number of tumors, acting as a prognostic factor. Preclinical studies have shown that NKG2A blockade with neutralizing Abs in combination or the deletion of the gene that encodes NKG2A increases the efficacy of NK cells in other types of cancer.

On the other hand, although NK cells belong to the innate immunity, they are able to acquire memory properties in response to viruses, haptens or cytokines. In concrete, a brief exposure of NK cells to IL-12, IL-15, and IL-18 induces transcriptional, epigenetic, metabolic, and immunophenotypic changes, which increase the NK cell antitumor activity, proliferative capacity, and persistence *in vivo*.

Strategies in combination to augment the efficacy through immune checkpoint blockade, as well as to potentiate the cytotoxic capacity and persistence through memory-phenotype induction, could enhance CAR NK cell activity for RRMM.

Objectives

The main objective of this thesis is the generation of optimized therapeutic combinations for CAR NK cells to enhance RRMM treatment: i) to analyze the relevance of the HLA-E/NKG2A axis in MM; ii) to potentiate the anti-MM activity of NKG2D- and BCMA-CAR activated and expanded NK (NKAE) cells by disrupting the HLA-E/NKG2A axis with a novel α-NKG2A antibody; iii) to increase the immunotherapy persistence and efficacy by reprogramming NKG2D-CAR NKAE cells towards a cytokine-induced memory-like phenotype.

Results

Our results show that HLA-E expression on MM patient PC is increased with respect to healthy donor (HD) PC. Moreover, pathologic PC have higher HLA-E expression compared to normal PC and $CD34^+$ cells from the same patient, especially at progression. Although PFS is lower in patients with a high HLA-E expression ratio with respect to $CD34^+$ cells, no significant differences are observed regarding this parameter or OS in our patient cohort.

BM plasma IFN-γ concentration from MM patients, without analytic or clinical signs of infection, is higher than HD'. IFN-γ increases HLA-E expression on MM cell lines and primary PC from patients at diagnosis or progression. Bortezomib (BTZ), a proteasome inhibitor administered in first-line for MM treatment, reduced HLA-E expression even if it is increased with IFN-γ in BTZ sensitive cells, but not in resistant cells.

NK cells from MM patients have augmented levels of the HLA-E inhibitory receptor, NKG2A, especially in patients at progression. However, NKG2A blockade with neutralizing mouse (Z199) or human (BMS-986315) Abs over MM primary samples does not impact on PC elimination, suggesting the lack of efficacy of these treatments in monotherapy.

Along NKG2D- or BCMA-CAR NKAE cell expansion and activation, the expression of NKG2A augments as a compensatory response. CAR NKAE cells produce high concentration of IFN-γ in co-culture with MM cells, which at the same time increases

HLA-E expression as positive feedback. Combination of α-NKG2A Abs with NKG2D- or BCMA-CAR NKAE cells significantly increases antitumor activity against MM cells and primary cells, in native context cultures, without producing relevant toxicity against $CD34^+$ cells from the same patient or HD PBMCs. Furthermore, this enhanced function of CAR NKAE cells pretreated with α-NKG2A Abs is related to superior degranulation and IFN-γ levels, and it is also associated with a positive balance of the intracellular signaling, reflected by a higher ZAP70/Syk phosphorylation, compared to CAR NKAE cells pretreated with the corresponding isotypes. Nevertheless, NKG2A blockade does not alter activating or inhibiting receptor phenotypic expression on CAR NKAE cell surface. In disseminated and orthotopic MM-bearing mice, the intraperitoneal administration of BMS-986315 blocking Ab reduce NKG2D- or BCMA-CAR NKAE cell percentage, which eliminates the combination efficacy. However, pretreated NKG2D-CAR NKAE cell with the neutralizing Ab infusion does not affect effector cell proportion and significantly reduce tumor burden in mice.

Additionally, generation of cytokine-induced memory-like (CIML)-NKAE cells with a NKG2D-CAR stable expression is feasible starting from low volumes of HD PB. The cytokine-induced memory phenotype through a brief IL-12, IL-15, and IL-18 exposure on NKG2D-CAR NKAE cells provokes higher cytotoxicity, degranulation, intracellular IFN-γ production and augments IFN-γ, perforin and granzyme A release, when memory cells are co-cultured with MM cell lines. Moreover, NKG2D-CAR CIML-NKAE cells exhibit an increased cytotoxic capacity over primary MM cells, without significantly affecting $CD34^+$ cell survival from the same patients or cord blood samples. Furthermore, this memory population has a higher proliferative capacity and experiment epigenetic, transcriptomic, metabolic and phenotypic changes, compared to NKG2D-CAR NKAE cells. In a U-266 ffLucGFP-bearing mouse model, NKG2D-CAR CIML-NKAE cells have demonstrated an increased tumor control *in vivo*, associated with a higher NKG2D-CAR CIML-NKAE proportion and not with a superior persistence, as there is not a higher sustenance of this therapy compared to NKG2D-CAR NKAE cells.

Finally, we have demonstrated that NKG2D-CAR CIML-NKAE cell pretreatment with a NKG2A blocking Ab improves α-NKG2A blocked NKG2D-CAR NKAE cell anti-MM efficacy.

Conclusions

Overexpression of HLA-E on pathologic PC and NKG2A on NK cells from RRMM patients suggest a relevant role of HLA-E/NKG2A in tumor progression, although BMS-986315 α-NKG2A Ab monotherapy treatment does not restore NK cell activity.

CAR NKAE cells intended for immunotherapy overexpress NKG2A, augmenting their susceptibility to MM PC inhibition, thus CAR NKAE therapy combination with α-NKG2A Abs is able to overcome HLA-E mediated MM resistance *in vitro* and *in vivo*.

Cytokine-induced memory reprogramming in combination with the NKG2D-CAR NKAE therapy implies the generation of a new effector with higher anti-MM efficacy *in vitro* and *in vivo,* compared to NKG2D-CAR NKAE cells.

Taken together, both treatment strategies can be potentially used not only to increase RRMM cells vulnerability, but also to be administered in other tumors, principally the HLA-E positive ones.

INDEX

LIST OF FIGURES

LIST OF TABLES

1. INTRODUCTION

1.1. Multiple myeloma

1.1.1. Definition and general features

Multiple myeloma (MM) is a clonal B cell malignancy, characterized by the accumulation of tumor plasma cells (PC), mainly in the bone marrow (BM) [1]. This tumor is called "myeloma" because it is generated in the BM, and "multiple" because it affects different parts of the axial skeleton, especially the vertebral column, ribs, pelvis and skull [2].

Malignant PC produce monoclonal immunoglobulins (Igs), also called M proteins. Monoclonal proteins can be a complete Ig or its κ or λ chains. The presence of these free light chains in urine is called Bence-Jones proteinuria. Around 15-20% of patients have light-chain MM, characterized by the secretion of κ or λ chains instead of a complete Ig in urine and/or blood [3].

MM can be developed from premalignant status, called monoclonal gammopathy of undetermined significance (MGUS), or asymptomatic MM, known as smoldering multiple myeloma (SMM). In late stages, MM can become independent from BM signals and exert to the bloodstream, although extramedullary disease can also appear at diagnosis. When 5% of PC are found in blood, it is called PC leukemia (PCL) [1, 4].

Clinical manifestations of this tumor are hypercalcemia, renal failure, bone lesions, anemia as well as recurrent infections, caused by the severe immunosuppression in the BM [1, 5].

1.1.2 Epidemiology

MM accounts for 10% of all hematologic tumors and it is the 2nd most common hematologic cancer, after non-Hodgkin lymphoma [1, 6].

According to the American Cancer Society, during 2023, there is an estimation of 35,730 new cases of MM (1.8% of all new cancer cases) and 12,590 deaths associated with this tumor (2.1% of all cancer deaths) in the United States. The 5-year relative survival of MM calculated between 2013-2019 is 59.8%, the median age at diagnosis is 69 years (31.9% of MM patients are diagnosed at 65-74 years) and the median age of death is 75 [6, 7].

In Spain, the *Asociación Española Contra el Cáncer* estimated 3,251 MM cases in 2021 [8].

Generally, MM is slightly more common in men than women [9] and more than 64% of patients are diagnosed over the age of 65 (less than 4% of MM patients are below 44) [7]. In addition, African-American people have a 2-fold MM incidence and a 2- to 3-fold MGUS prevalence compared to Caucasians [10, 11].

1.1.3. Etiology

MM etiology is still unknown. However, environmental and hereditary factors have been described to influence MM development.

Environmental factors such as radiation [12-14], products used in farming (herbicides, pesticides and organic solvents, like benzene) [15, 16] and hair dyes [17] have been described to promote MGUS or MM development, although some studies reported these data are not conclusive [18].

Obesity has also been associated with increased MM incidence (1.11-fold) and mortality. However, other studies have suggested that obesity can prevent cancer patient risk of death due to cachexia [19].

Recently, our group has identified 4 MM responder patients to HCV antiviral treatment, suggesting that those MM which are developed by chronic antigen-stimulation can be controlled, or even cured, by eradicating the initiating viral infection [20]. In line with this, Igs from MGUS and MM patients have been found to specifically bind lysolipids from Gaucher's disease, implying another antigenic stimulation role in MM [21, 22].

Hereditary genetic factors can also influence MM appearance [23] and a compilation of studies has determined a 2- to 4-fold familial risk for MM in an autosomal dominant pattern [24, 25].

1.1.4. Physiopathogenesis

B cells are generated in the BM and migrate to germinal centers due to antigen recognition. Through somatic hypermutation and antigen selection, B cells undergo

affinity maturation to secrete antibodies (Abs). After class switch recombination, these post-germinal B cells, called plasmablasts, egress to the bloodstream. Mutations or failures during these processes result in an accumulation of malignant clonal PC in the BM, which originate MM [26].

MM can be developed from a premalignant status, called MGUS, or an asymptomatic neoplastic stage, commonly known as SMM, with an average risk of progression to MM of 1% and 10% by year, respectively, [11]. Moreover, between 1-2% of patients have extramedullary disease since the first examination and around 8% of MM patients may progress to PCL [1].

Primary genetic events normally occur in these previous MM stages (MGUS and SMM) and are related to hyperdiploidy and translocations (Fig. 1) [27].

MM can be classified in hyperdiploid (h-MM) or non-hyperdiploid MM (nh-MM). In h-MM (approximately 55-60% of patients), there are trisomies in the odd chromosomes (3, 5, 7, 9, 11, 15, 19 and/or 21) and in nh-MM, 70% of cases have mutations in the Ig heavy chain locus [28, 29]. Most common IgH translocations involves cyclin D, followed by WHSC1 and FGFR3 dysregulation [30].

Along MM progression, second hits, including monosomies (chromosomes 13, 14 and 17), deletions, duplications (chromosome 1q), secondary translocations, recurrent point mutations or epigenetic alterations, appear. Deletions in several chromosomes affect tumor suppressor genes, among others: 17p (TP53), 1p (FAM46C/CDKN2C), 13q (BRCA2/RB1), 12p (CDKN1B), 16q (WWOX) and 11q (BIRC2/3/MMP) [27]. Moreover, oncogenes (MYC and RAS), cell cycle regulators (eg. CDKN2A and CDKN2C) and transcription factors genes involved in the NF-κB pathway, emerge as second anomalies [28]. Other recurrent point mutations are DIS3, BRAF, TRAF and RB1 [27]. In the last MM stage, PCL, there is an accumulation of abnormalities that correlates with a lower overall survival (OS) [31]. In addition, epigenetics alterations are involved in MM progression, such as DNA methylation changes on cyclin-dependent kinase inhibitors, WNT and JAK/STAT signaling pathway and tumor suppressor genes; alterations in histone methylation (upregulation of MMSET domain gene) and tumor suppressor miRNAs inactivation [28, 32].

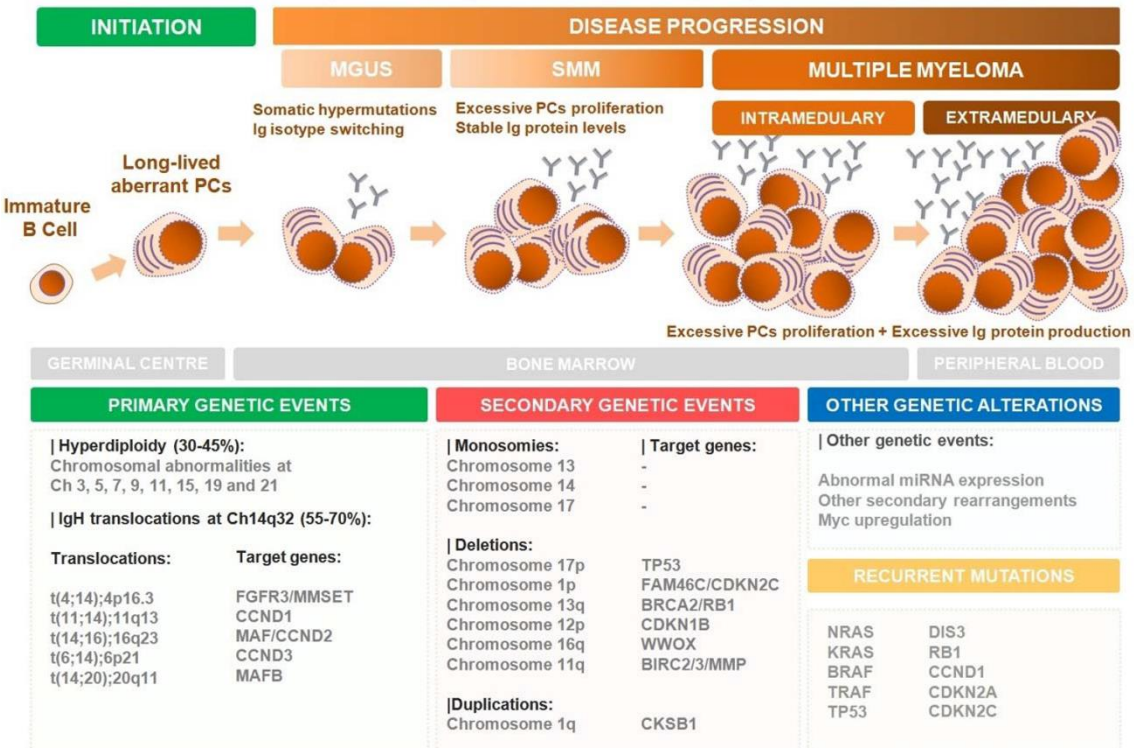

Figure 1. Development of MM and genetic alteration events. MGUS: Monoclonal gammopathy of uncertain significance; SMM: smoldering multiple myeloma. Extracted from Pinto et al. 2020 [27].

Not only do genetic abnormalities trigger MM proliferation, but also BM microenvironment (soluble factors and accessory cells) participate in the proliferation, sustenance, and drug resistances of this tumor (Fig. 2).

Initially, the interaction of CXCR4 and α4β1, present in malignant PC, with the soluble factor CXCL12 and VCAM-1, respectively, expressed by BM stromal cells (BMSCs), favors tumor cell homing and adhesion to the BM. [33]. Apart from these relations, BMSCs express proangiogenic molecules (eg. vascular endothelial growth factor (VEGF)) and unleash IL-6 production, through NF-κB signaling pathway activation, which enhances MM development [34, 35].

Moreover, MM cells promote a dysregulation between bone formation, generated by osteoblasts, and bone destruction, characteristic of this tumor and performed by osteoclasts. Principally, both BMSC and PC produce high levels of the receptor activator of NF-κB ligand (RANKL) that binds RANK on the surface of osteoclasts, enhancing their activity. Under normal conditions, osteoblasts and BMSC produce osteoprotegerin (OPG) to compete with RANKL, impeding its interaction with RANK in the osteoclast surface and regulating bone destruction. In MM, tumor cell interactions with BMSCs

reduce OPG secretion, favoring RANKL-RANK binding. In addition, MM cells release Dickkopf 1 (DKK1), which inhibits osteoblast function and therefore, impairs OPG production, fostering osteoclast activity. Other factors as macrophage inflammatory protein-1α (MIP-1α), IL-3 and IL-6, mostly secreted by MM cells, favor this disbalance between osteoblasts and osteoclasts, enhancing tumor growth and bone loss [34, 36, 37]. All these interactions produce bone resorption, hypercalcemia, and pathological fractures. Thus, these patients can be treated with an antibody (Ab) against RANKL (denosumab) or bisphosphonates (pamidronate and zoledronic acid) to decrease bone destruction [38].

In late stages, tumor microenvironment (TME) becomes hypoxic. In this context, there is a downregulation of CXCL12 levels [36] and MM cells reduce the expression of the CXCL12 receptor, CXCR4, losing tumor cell interactions with stromal cells and favoring their egression to the bloodstream [33].

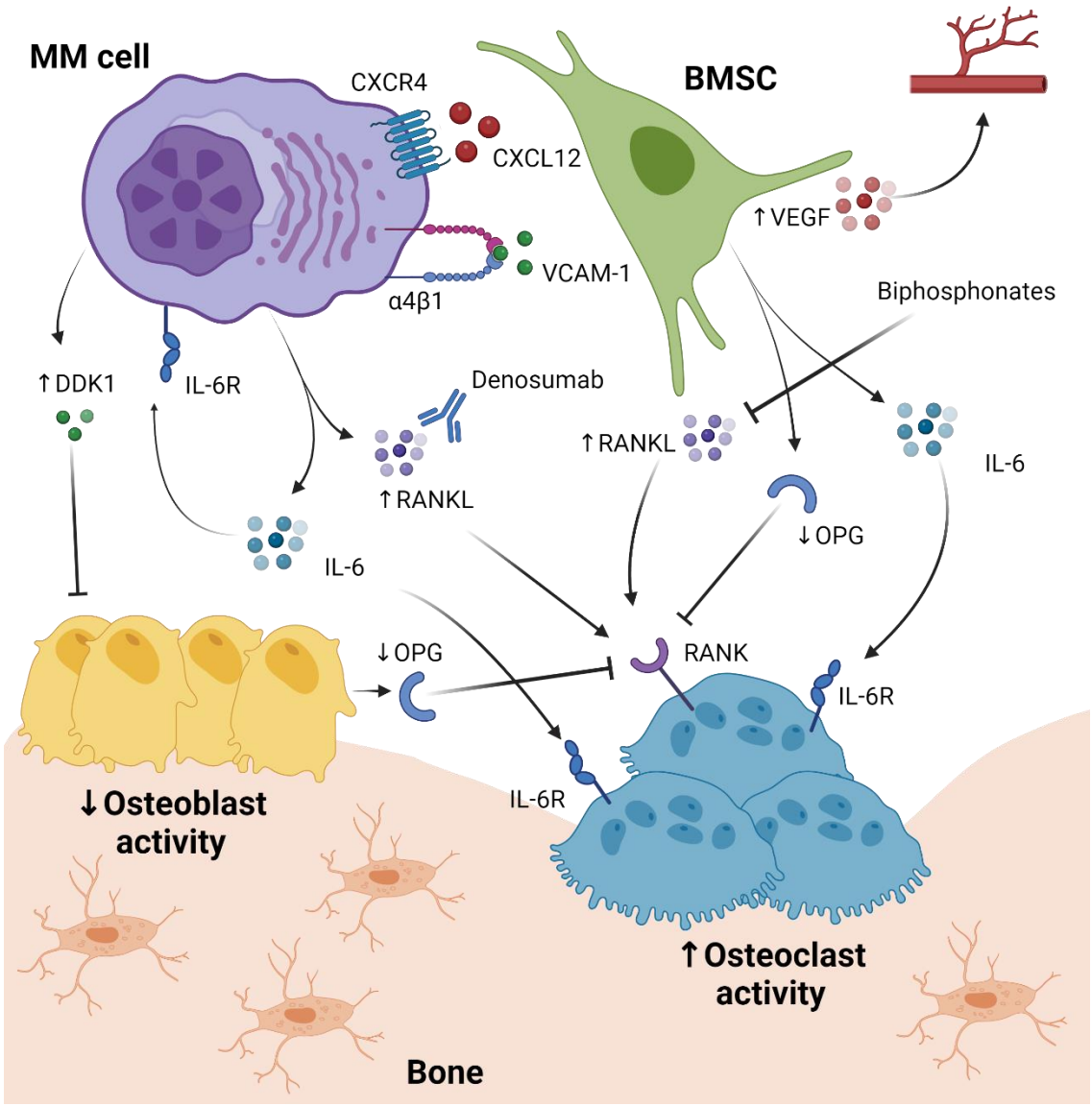

Figure 2. MM physiopathogenesis. MM: multiple myeloma; BMSC: bone marrow stromal cell; VEGF: vascular endothelial growth factor; CXCR4: CXC chemokine receptor 4; CXCL12: CXC chemokine ligand 12; VCAM-1: vascular cell adhesion protein 1; DKK1: Dickkopf 1; RANK: receptor activator for nuclear factor κ B. RANKL: RANK ligand; OPG: osteoprotegerin; IL: interleukin; IL-6R: IL-6 receptor. Adapted from Palumbo and Anderson, 2011 [35]. Created with BioRender.com.

1.1.5. Clinical development

The typical course of MM is characterized by periods of remission and relapse with increasingly shorter response periods and an increasing number of rescue treatments [39]. Most clinical manifestations are due to the accumulation of PC in BM and other tissues and the high release of monoclonal proteins. The emergence of the well-known CRAB symptoms confirms MM diagnosis. CRAB stands for hypercalcemia, renal failure, anemia and bone lesions [1].

Bone lytic lesions, which can be detected by imaging, generate fractures, vertebral collapse, spinal cord compression and hypercalcemia. Osteoclast activity produces bone destruction, being the main cause of morbidity. This activity correlates with tumor burden and MM prognosis [1, 40].

Due to this high osteoclastic activity and bone resorption, enhanced by MM cells, there is an increase in the levels of calcium in the bloodstream. In addition, there is an association between hypercalcemia and altered renal function, detected by a decreased glomerular filtration rate (GFR) [37, 41].

In 19-30% of the MM patients, renal failure is resulting from the precipitation and accumulation of light chains from the monoclonal Igs secreted by MM cells. This accumulation induces the formation of urinary casts in the kidney tubules, causing cast nephropathy. Normally, renal impairment can be detected by high levels of serum creatinine or a low GFR, and high light chains serum levels can be a prognostic factor of this damage [41-43].

Normocytic and normochromic anemia is also a common symptom in MM patients (70-85% of cases), characterized by low levels of hemoglobin in the blood, which correlates with tumor burden and a worse prognosis [43, 44]. Lately, it has been discovered that MM BM microenvironment inhibits hematopoietic stem cell proliferation, affecting their differentiation to erythrocytes and diminishing the levels of hemoglobin [44]. Moreover, this anemia can be produced by a relative erythropoietin (EPO) deficiency, caused by renal impairment [45].

Infections are the main cause of death related to MM [42]. Seventy-five percent of patients at diagnosis have immunoparesis, caused by the lack of one or more Igs [46], and a reduction of immune cells, which lack of function originate a severe immunosuppression in MM patients, increasing the risk of infections. In addition, typical MM treatments such as bortezomib (BTZ), melphalan and stem cell transplant induce neutropenia, which increases the risk of viral infections [47, 48].

1.1.6. Diagnosis

Since 2014, MM has been diagnosed if the BM contains more than 10% of malignant PC and one CRAB symptom or myeloma-defining biomarker (SLiM criteria) or

plasmacytoma. SLiM criteria can be ≥ 60% malignant PC in the BM, ≥ 100 serum free light chain ratio, and more than one focal lesion (≥ 5mm) detected by magnetic resonance imaging (MRI) [43].

MM clinical symptoms are similar to other illnesses; therefore it is normally discovered by chance in a routine blood test. First diagnostic testing usually comprises blood and urine analysis, including hemogram, biochemistry, and protein studies [43]. High calcium levels (>11 mg/dL or >1 mg/dL above normal limit), detection of monoclonal Igs in blood and urine by electrophoresis with immunofixation, increased serum β2-microglobulin, high creatinine (>2 mg/dL) and serum free light chain ratio (≥ 100) may indicate MM. In addition, an imaging study is normally performed, comprising a low-dose whole-body computed tomography (CT), MRI, or PET-CT to identify bone lesions [1, 43, 49-51].

If the results of these determinations suggest MM disease, a BM aspirate with cytogenetic analysis is carried out to assure the MM diagnosis [43].

BM analysis includes cytogenetics, the detection of translocations, trisomies, and deletions through fluorescent in situ hybridization (FISH), as well as flow cytometry determination of malignant PC. Common immunophenotype of MM cells is defined by $CD138^{+}$ $CD38^{+}$ $CD56^{+}$ $CD45^{+}$ $CD117^{+}$ $CD19^{-}$ [1, 52-54]. Moreover, CD81 has been described as a new prognostic factor that correlates with MM development [55] and other authors have suggested that MM clonogenic cells are $CD138^{-}$ [27]. However, these discoveries should be confirmed in further studies.

1.1.7. Staging and prognosis

In 2005, the International Staging System (ISS) was proposed to stratify MM patients at diagnosis based on serum β2-microglobulin and albumin levels. ISS-I was determined by < 3.5 mg/L of serum β2-microglobulin and ≥ 3.5 g/dL of albumin; ISS-III when the serum β2-microglobulin was higher than 5.5 mg/L and ISS-II, not ISS stage I or III. In 2015, a revision of the ISS (R-ISS) was proposed including LDH values and high-risk cytogenetics, del(17p) and translocations t(4;14) and t(14;16), to the prior classification. Patients were then stratified as R-ISS-I when serum albumin > 3.5 g/dL, serum β2-microglobulin < 3.5 mg/dL and no high-risk cytogenetics or LDH abnormal values were detected. R-ISS-3 comprised serum β2-microglobulin > 5.5 mg/L and high cytogenetics

risk or high LDH levels. Neither R-ISS-I nor R-ISS-III patients were stratified as R-ISS-II [56]. However, a new revision of this R-ISS staging, the R2-ISS, was done in 2022 to stratify better these intermediate-risk patients, including the risk feature 1q+ and deleting t(14;16) as a staging factor [57, 58].

Currently, depending on the following features (ISS-III 1.5 points, ISS-II 1 point, del(17p) 1 point, high lactate dehydrogenase 1 point, t(4;14) 1 point, and 1q+ 0.5 points), values are summed to calculate a new score. Then, patients are stratified in these new R2-ISS risk groups: low, low-intermediate, intermediate-high, and high. Thus, median OS and progression-free survival (PFS) values from these new groups define better the prognosis and outcome of MM patients (Table 1) [57].

Risk factor	Score
ISS-III	1.5
ISS-II	1
Del(17p)	1
High LDH	1
t(4;14)	1
1q+	0.5

R2-ISS (risk)	Score	OS (months)	PFS (months)
I (low)	0	Not reached	68
II (intermediate-low)	0.5-1	109.2	45.5
III intermediate-high)	1.5-2.5	68.5	30.2
IV (high)	3-5	37.9	19.9

Table 1. R2-ISS characteristics. ISS: international staging system; OS: overall survival; PFS: progression-free survival; LDH: lactate dehydrogenase. Data extracted from D'Agostino et al. 2022 [57]

1.1.8. Treatment for newly diagnosed MM (NDMM) patients

From mid-50s, the combination of alkylating agents with corticosteroids achieved a median OS of 7.5 months [59]. Nowadays, without taking into account the outcomes with adoptive therapies, the 5-year survival of MM patients has increased up to 59.8% [7] and the median OS is 6 years [60].

Currently, treatments for NDMM patients are based on autologous stem cell transplant (ASCT) eligibility and risk-stratification (Fig. 3). Fit for transplant patients are chosen based on their adequate physical conditions and lack of comorbidities [1].

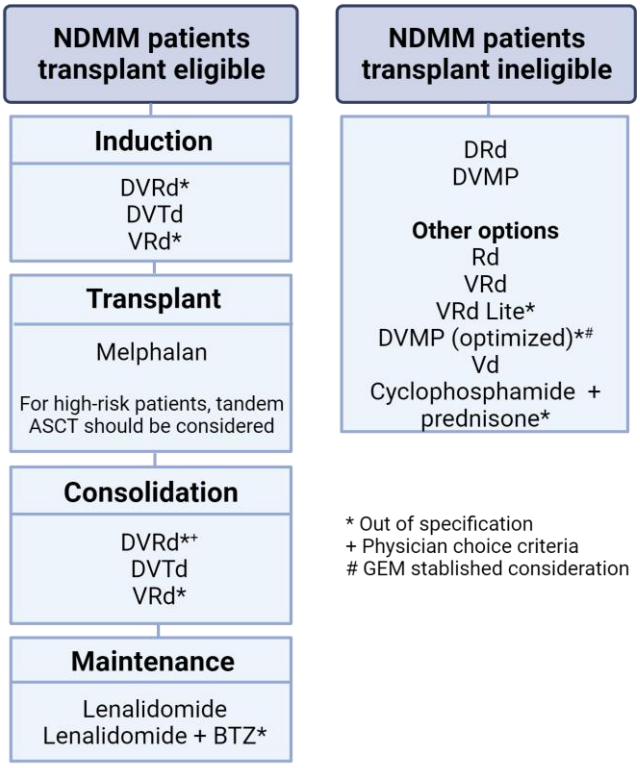

Figure 3. Schematic description of NDMM treatments. D: Daratumumab; V or BTZ: Bortezomib; R: lenalidomide; d: dexamethasone; T: thalidomide; M: melphalan; P: prednisone. GEM: *Grupo Español de Mieloma*. Data extracted from *Grupo de Estudio de Gammapatías Monoclonales de Castilla y León* clinical practice guideline 2023 [61]. Created with BioRender.com.

Patients eligible for ASCT receive 3-4 cycles of induction therapy (DVTd, DVRd, or VRd) prior to stem cell collection and after ASCT, lenalidomide, or BTZ plus lenalidomide for high-risk cytogenetic patients, maintenance. If patients are not fit for transplant, a combination of 3 or 4 drugs containing immunomodulatory drugs (IMIDs), proteasome inhibitors (PIs), daratumumab, alkylating agents, and/or corticoids are indefinitely administered [1, 5]. At a median follow-up of 35.4 months, DVTd plus ASCT median PFS was not reached and 73% of complete responses (CR) were achieved in the CASSIOPEIA study [62]. Patients ineligible for transplant and treated with DVMP in the ALCYONE study obtained a median PFS of 32.9 months, after 40.1-month median follow-up [63].

Autologous stem cell transplant (ASCT)

Within this first scenario, some reports have suggested that, despite new agents being available for MM, the ASCT role in the first-line remains indispensable for achieving deep responses in NDMM patients [64-66]. Furthermore, the treatment with triplet or quadruplet regimens before ASCT, as induction therapies, is key for the impressive results obtained after this regimen [67, 68]. In addition, tandem ASCT, a second ASCT in less than 6 months, benefits the PFS and OS of high-risk NDMM, although this strategy is not routinely recommended outside clinical trials [69].

ASCT also impacts on immune cell recovery. In particular, $CD56^{bright}$ $NKG2A^{+}$ NK cells are first reconstituted after 13 days from ASCT, while T cell recovery may take up to one year. At that moment, cytotoxic $CD8^{+}$ T cells outnumber the inhibitory Tregs, although their PD-1 expression is high [70, 71]

Immunomodulatory drugs (IMiDs)

The first-line drugs that most affect immune effectors are IMiDs. Thalidomide, a synthetic derivative of glutamic acid, was the first IMiD used for MM treatment [72]. However, its neurological toxicities have arisen the discovery of new generation analogues with less adverse events, such as lenalidomide and pomalidomide, and recently avadomide, iberdomide and mezigdomide. IMiDs main target is cereblon, a member of the E3 ubiquitin ligase complex. Activation of this complex causes the polyubiquitination of the transcription factors IKZF1 (Ikaros) and IKZF3 (Aiolos) and their degradation via proteasome. The lack of these factors, highly involved in PC development and differentiation, triggers MM cell death. Furthermore, IMiDs possess anti-inflammatory and anti-angiogenic effects in the TME together with immunomodulation properties [73-76]. In particular, lenalidomide increases NK cell function via antibody-dependent cellular cytotoxicity (ADCC) [77] and upregulates TRAIL expression on NK cells [78] and the NK cell receptor ligand expression, PVR and MICA, on MM cells [75]. Remarkably, this drug is able to lower NK cell activation threshold, which means that the recognition of low levels of NK cell ligands on MM cells is able to trigger NK cell antitumor activity [79]. Moreover, lenalidomide inhibits TNF-α, IL-1β, and IL-6 production and boosts clonal T cell proliferation [80, 81]. Nevertheless, toxicities as

thromboembolic events, teratogenicity, neutropenia, and infections have been described after IMiD treatment [82].

Proteasome inhibitors (PIs)

Proteasome degrades cell polyubiquitin proteins to recover amino acids that can be reused for protein generation [83]. MM cells produce high levels of Igs and therefore the correct functioning of the proteasome is critical for maintaining the homeostasis of these cells. Proteasome inhibitors, which target the β5 subunit of the proteasome, produce an accumulation of ubiquitinated or misfolded proteins, leading to ER stress and apoptosis, preferentially on MM cells [84]. BTZ, a dipeptide derived from boronic acid, belongs to first class PI, followed by carfilzomib and ixazomib (second generation), and new PI (oprozomib, delanzomib and marizomib) are under research. BTZ, ixazomib and delanzomib are reversible PI, while carfilzomib, marizomib and oprozomib irreversibly bind the β5 subunit of the proteasome. [83, 85]. As well as IMiDs, BTZ also possess immunomodulation features. Not only BTZ inhibits the NF-κB canonical signaling pathway and decreases the expression of anti-apoptotic proteins, promoting DC and T cell apoptosis, but also diminishes proinflammatory cytokine secretion and costimulatory molecule expression on T cells [86, 87]. In addition, proteasome can also degrade signal peptides derived from HLA class I molecules, which are loaded on HLA-I and HLA-E molecules and expressed on the cell surface [88]. Therefore, the inhibition of proteasome caused by BTZ downregulates the expression of HLA-I and HLA-E, sensitizing MM cells to NK cell-mediated recognition and killing (Fig. 4) [85, 89]. Of note, BTZ also increases NKG2D ligands (NKG2D-L), DR5, and PVR expression on the MM cell membrane, enhancing NK cell cytotoxicity through NKG2D, TRAIL, and DNAM-1 receptors, respectively [85, 90]. Moreover, this inhibitor enhances FasL-dependent NK cell cytotoxicity against tumor cells [91]. Toxicities as neuropathy, Herpes virus reactivation, thrombocytopenia, neutropenia, cardiovascular events, especially after carfilzomib treatment, and risk of infections have been described after PI administration [47, 83, 92].

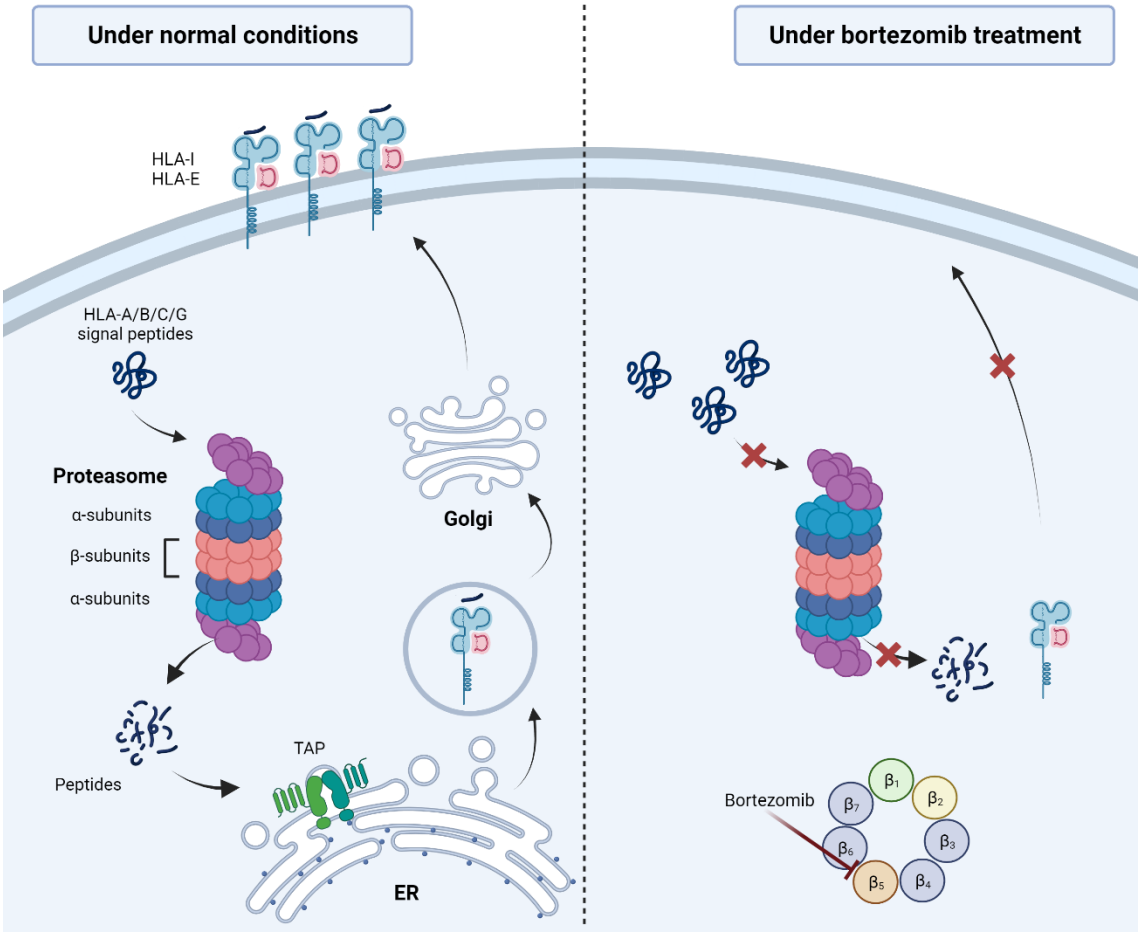

Figure 4. Bortezomib modulates HLA-E expression. ER: endoplasmic reticulum. HLA: human leukocyte antigen

Alkylating agents

Melphalan, a DNA alkylating agent, has been used for MM treatment since 1960s [9], although high doses of this drug have many side effects, such as prolonged BM suppression, cardiotoxicity [93] and increased mutational burden on surviving MM cells [94]. Currently, the ALCYONE phase III study results have considered the use of oral melphalan at low doses in combination with Daratumumab, BTZ, and prednisone for NDMM transplant ineligible patients, as this combination achieved 45.7 months of PFS and 83.6% OS at 3 years [63].

Daratumumab

Recently, daratumumab, an α-CD38 Ab, has been established as a first-line treatment due to the longer PFS obtained in combination with VTd [62] or VMP [63] with weak adverse

events (higher risk of infection and hematological toxicities) [95, 96]. Daratumumab characteristics and mechanisms of action will be explained below.

1.1.9. Relapsed/refractory treatments in MM (RRMM)

RRMM comprises patients who have not achieved at least minimal response to prior line treatments (primary refractory myeloma), have reached minimal response at some point but have not responded to salvage therapy, within 60 days of the last treatment (relapsed or refractory), or after 60 days from last treatment (relapsed) [97].

Lenalidomide-resistant patients are normally treated with second-generation IMiDs, as pomalidomide, in combination with other drugs as daratumumab, PIs, cyclophosphamide, or dexamethasone. If they are not refractory to lenalidomide, but they have been treated with BTZ, other combinations with second-generation PI, as KRd, or DRd, are considered. However, the OS in triple- or quad-refractory patients is 9.2 months and in penta-refractory (refractory to anti-CD38 Abs, 2 PIs and 2 IMiDs) is 5.6 months [98]. Thus, there is an unmet medical need to find new strategies to target MM (Fig. 5). Of note, these measurements do not include last updates from chimeric antigen receptor (CAR) T cells and bispecific antibody (BiAB) responses.

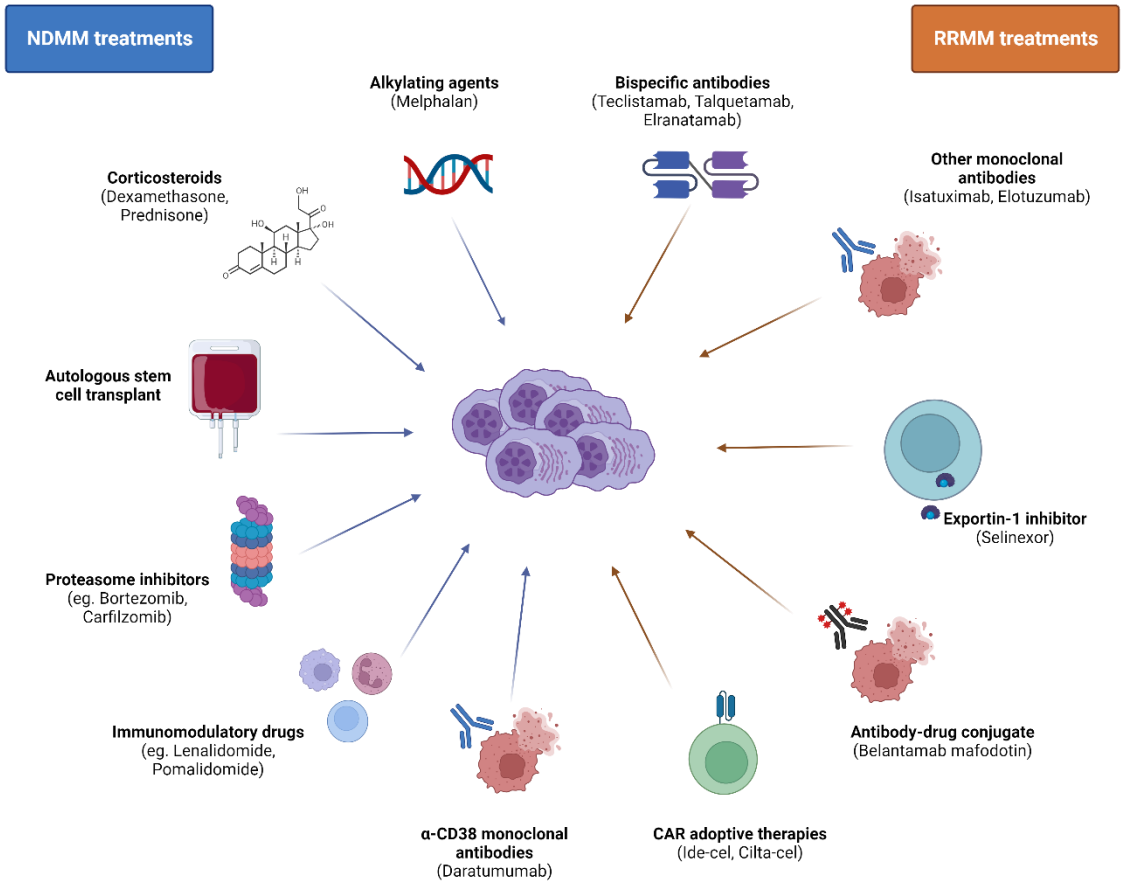

Figure 5. Current FDA-approved treatments for NDMM and RRMM patients. NDMM: newly diagnosed multiple myeloma; RRMM: relapsed or refractory multiple myeloma; CAR: chimeric antigen receptor. Created with BioRender.com.

Selinexor is a nuclear export inhibitor that blocks exportin 1 (XPO1), whose expression has been correlated with a shorter PFS and OS in MM patients. This inhibitor blocks XPO1-mediated transport through the nuclear membrane, retaining tumor suppressor proteins, as p53, RB, IκB or BRCA1/2, which maintain the cell cycle arrest, and oncogenes mRNA (eg. c-Myc, D1 cyclin and BCL-2), impeding their translation [99]. Selinexor activity has been tested in combination with the abovementioned conventional drugs for MM, showing promise and synergistic results. Nevertheless, its toxicities, gastrointestinal and side effects, asthenia, diarrhea, nauseas, hyporexia, weight loss, hyponatremia, neurological effects, neutropenia, and infections, are the main drawbacks [99, 100]. Furthermore, Selinexor also displays immunomodulatory effects on NK cells. This drug downregulates the expression of HLA-E [101], which preferentially binds the NKG2A inhibitory receptor, and upregulates the expression of the activating receptor NK

cell ligands PVR, ULBP-1, -2 and -3 on MM cells. This way, Selinexor favors MM susceptibility to NK cell lysis [102, 103].

Melphalan flufenamide (Melflufen) is another alkylating peptide. When it enters in the MM cells, it takes advantage of the high concentration of peptidases and esterases to quickly release the melphalan and trigger PC apoptosis. Compared to melphalan, Melflufen enhances melphalan intracellular concentration, being a more effective anti-MM treatment [104]. This drug is approved for RRMM patients in combination with dexamethasone. A recent phase III, the LIGHTHOUSE study, has tested the efficacy of melflufen in combination with daratumumab and dexamethasone. Median PFS of this group has not been reached yet and overall response rate (ORR) was superior to the control group (59% melflufen-daratumumab-dexamethasone vs 30% daratumumab). Hematological toxicities, including neutropenia, thrombocytopenia and anemia, were described [105].

Remarkably, B-cell maturation antigen (BCMA) and G protein-coupled receptor class C group 5 member D (GPRC5D)-targeted immune therapies have been recently authorized for RRMM patients with ≥4 prior lines of therapy by the FDA and EMA [106, 107]. Two BCMA-CAR T therapies (ide-cel and cilta-cel) [108, 109], two BCMA-bispecific T cell engager (BiTE) (teclistamab and elranatamab) [110, 111], as well as a GPRC5D BiAb (talquetamab) [112] have been approved for patients with a poor prognosis, achieving impressive outcomes that will be reported below.

Another salvage therapy for RRMM patients is a second autologous transplant. Stem cells, previously collected from NDMM transplant eligible patients or collected after relapse, can be administered after 24 months from the first ASCT [113], although patients who relapsed after 36 months achieved better results (94% OS) [114].

Other drugs used for RRMM patients, but not approved by the FDA, are BCL-2 inhibitors (venetoclax), histone deacetylase (HDAC) inhibitors (panobinostat, vorinostat) and DNA hypomethylating drugs (5-azacitidine and decitabine) [28].

Venetoclax is used for patients harboring t(11;14) or high BCL-2 expression levels [115, 116], and it can be administered in combination with dexamethasone (CANOVA trial NCT03539744) or BTZ and dexamethasone (BELLINI trial) [117] in clinical trials. Although these treatments enhance PFS in RRMM patients, diverse cytopenias and gastrointestinal side effects have been reported.

Although Panobinostat was withdrawn in 2022 by the FDA, it has been used in clinical trials in combination with PIs, IMiDs and steroids, obtaining an OS ranging from 10-19 months and most common adverse effects are hematological and gastrointestinal [118, 119].

Despite all this therapeutic armamentarium, MM remains an incurable disease and patients relapse with increasingly shorter response periods. In this regard, there is an urgent need to find new treatments with novel mechanisms of action to surmount this refractory setting.

1.1.10. RRMM immunosuppression

During previous MM stages, MGUS and SMM, there is an immune equilibrium that is completely impaired along progression to active MM, especially in the RRMM context. Due to the predominance of M protein in the BM, polyclonal Ig production and other Ig isotypes are reduced, causing immunoparesis. Simultaneously, pathologic PC evade from immunosurveillance due to the rise of immunosuppressor cells and the enhanced levels of soluble factors. Both foster MM cell proliferation, while diminishing NK and T cell function [46, 120]. Moreover, PC clones from triple-refractory MM patients become more proliferative, being less dependent on inflammation factors as IL-6 and TGF-β and, at the same time, downregulate critical pathways, IFN and TNF signaling, to avoid immunosurveillance [121].

Despite the percentage of NK and cytotoxic T cells in the BM from MM patients is superior compared to HD, there is a dysfunction in these immune effector cells that hampers MM proliferation control (Fig. 6) [122]. On the one hand, the efficacy of activating receptors (DNAM-1, NKG2D, NKp30) is downregulated on MM patient immune effectors. DNAM-1 expression has been found reduced on NK cells from active MM patients compared to patients in remission, diminishing NK cell DNAM-1-mediated cytotoxicity [123]. In addition, NKG2D activating receptor activity is impaired in NK and $CD8^+$ T cells due to the decrease of its ligand expression, MICA, along MM progression to late extramedullary stages [124]. Contrary to most tumors, MM cells augment their HLA class I, classical and non-classical molecules, HLA-E. However, defects in the antigen processing-presenting machinery disrupt MM cell TCR-mediated recognition by T cells. In line with this, NK cells are also inhibited via KIR-HLA-I and

NKG2A-HLA-E interactions [125, 126]. Remarkably, KIR expression is upregulated on NK cells from MM patients [127]. Furthermore, immune effector efficacy is reduced via immune checkpoints. PD-1 and CTLA-4 expression is augmented on T cells from MM patients [128] and their binding to their corresponding ligands, PD-L1, highly expressed on MM cells, and CD80/86, respectively, impair their antitumor efficacy [129]. Additionally, BM T cells have an increased CD4/CD8 ratio, which may justify their lower degranulation and decreased TNF-α and IFN-γ signaling [121].

Moreover, different interleukins, IL-6 and IL-10, cytokines, TGF-β and IFN-γ, together with other inhibitory soluble factors, soluble MICA, IDO, and adenosine (ADO), are highly expressed in the BM of MM patients, impairing immune effector function [33, 130, 131]. MM cell as well as myeloid-derived suppressor cell (MDSC) and BMSC production of IL-6 not only enhances tumor proliferation, but also diminishes NK cell function [33, 132] and inhibits dendritic cell (DC) generation from $CD34^+$ progenitors and therefore, T cell stimulation [133]. Similarly, IL-10 hampers effector T cell proliferation [33] and blocks the production of a potent IFN-γ inducer on NK cells, reducing one of the major mechanisms of these cells to exert their antitumor activity [134]. TGF-β strongly suppresses NK cell activity, as it diminishes IFN-γ production as well as NKG2D and NKp30 activating receptor and T-bet transcription factor expression [135]. Moreover, this cytokine is able to decrease T cell activation and proliferation, since it inhibits the presence of T cell costimulatory molecules on DCs, which allow antigen presentation [136]. IFN-γ is able to increase PD-L1 expression on tumor cells through JAK/STAT signaling, inducing T and NK cell exhaustion via PD-1/PD-L1 interaction [137]. In addition, an enhanced concentration of IDO generates a lower availability of tryptophan in the TME, as it is converted to kynurenine. The lack of tryptophan, an indispensable amino acid for T cell survival, causes the cell cycle arrest and apoptosis of these immune cells. At the same time, the obtained metabolite, kynurenine, impairs interactions among DCs, T, and NK cells [138, 139]. Furthermore, ADO release by MM cells, mediated by CD38, inhibits T and NK cell cytotoxicity [140]. Apart from these molecules, shedding of the NKG2D-L, MICA, from the surface of MM cells acts as decoy, neutralizing NKG2D function, and also fosters its internalization, impairing both NK and cytotoxic T cell function [131]. Of note, high soluble MICA levels correlate with a poor OS and PFS in MM patients [141].

Additionally, there is a recruitment of immunosuppressive cells in the BM from MM patients that fosters tumor cell proliferation, while hampers T and NK cell function. M2 macrophages produce VEGF, which enhances tumor angiogenesis and other suppressor cytokines, such as IL-10 and ADO. Moreover, high infiltration of these type of macrophages has been correlated with a lower prognosis as well as with an augmented MDSCs proportion [33, 142]. MDSCs diminish T cell proliferation, together with DCs, and release different soluble factors that induce Tregs differentiation. Tregs are highly activated in this tumor due to the soluble factors released to the TME by MM cells. Moreover, cytokines produced by Tregs, such as IL-10 and TGF-β, attenuate effector T and NK cell function [33, 143]. Altogether, direct interaction with immune suppressive cells or the release of soluble factors by the latter or MM cells, enhances tumor proliferation and reduces endogenous T and NK cell function. This persistent immunosuppressive status suggests the need of new adoptive treatments with ex vivo stimulated immune effectors for MM patients.

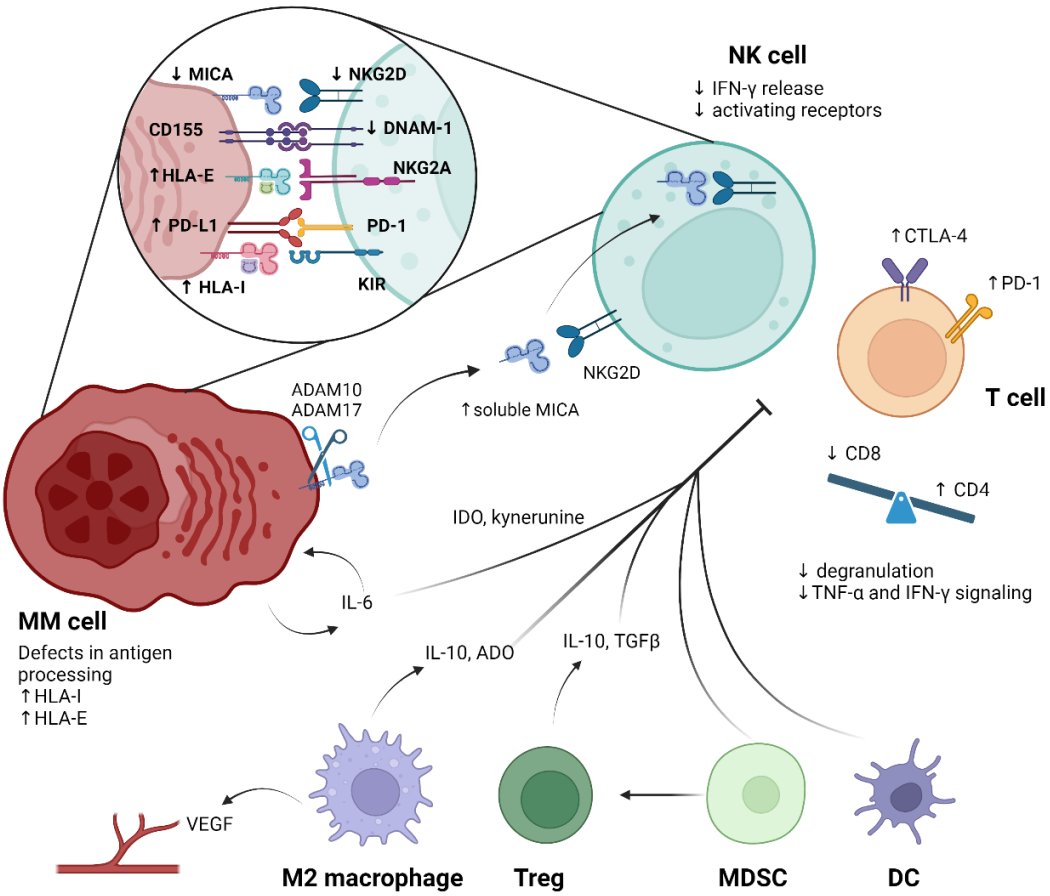

Figure 6. Immunosupression in MM. MICA: major histocompatibility complex class I chain-related protein A; HLA: human leukocyte antigen; KIR: killer-cell immunoglobulin-like receptors; MM: multiple myeloma; ADAM10/17: a disintegrin and metallopeptidase 10/17; VEGF: vascular endothelial growth factor; IDO: indoleamine-pyrrole 2,3-dioxygenase; ADO: adenosine; TGF-β: transforming growth factor-β; CTLA-4: cytotoxic T-lymphocyte antigen 4; PD-1: programmed cell death 1; TNF-α: tumor necrosis factor α; IFN-γ: interferon-γ; Treg: regulatory T cells; MDSC: myeloid-derived suppressor cells; DC: dendritic cells. Created with BioRender.com.

1.2. Immunotherapy in MM

Over the last decades, several approaches to enhance immune effector cell activity against tumors have been developed. In MM, monoclonal Abs (mAbs) targeting CD38 [96, 144] as well as BiAbs [110, 112] and BCMA-CAR T therapies [108, 109], have been already approved by the FDA, as it has been previously described. The most relevant feature of these therapies is choosing an appropriate target antigen, with high expression on malignant cells and low expression or absence on healthy tissues, to increase antitumor responses, avoiding on-target off-tumor toxicities (Fig. 7).

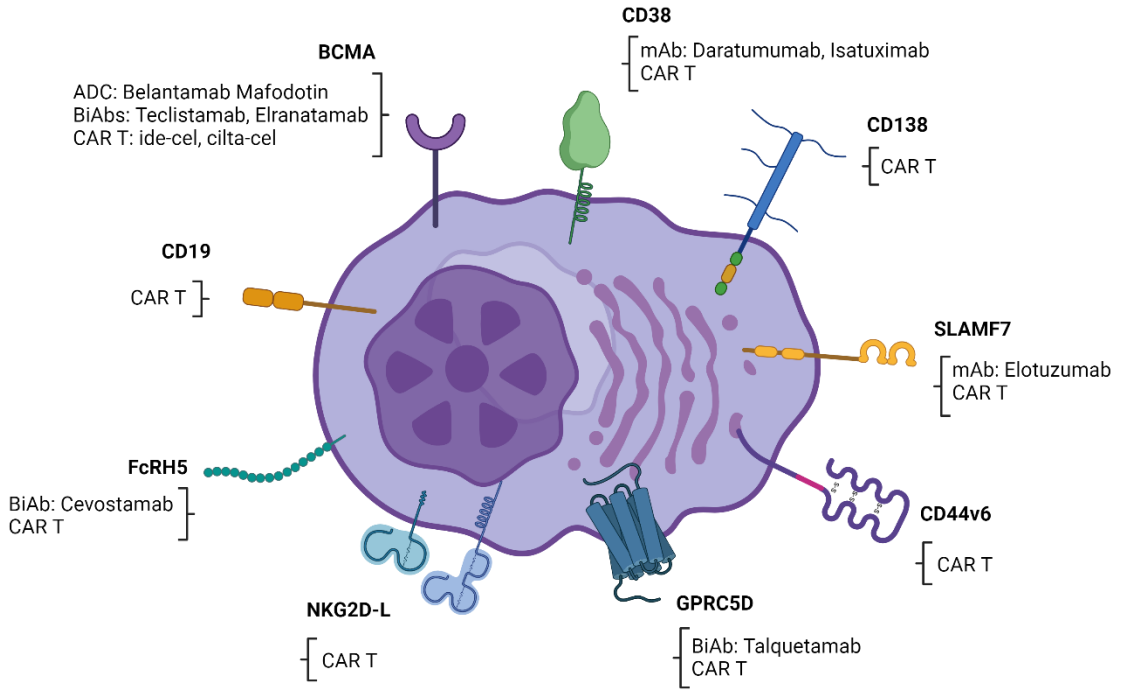

Figure 7. MM targets and associated immunotherapies. ADC: antibody-drug conjugate; BiAbs: bispecific antibodies; CAR: chimeric antigen receptor; mAb: monoclonal antibody. BCMA: B-cell maturation antigen; SLAM: signaling lymphocyte activation molecule family member 7; CD44v6: CD44 variant domain 6; GPRC5D: G protein-coupled receptor class C group 5 member D; NKG2D-L: natural killer group 2 member D ligands; FcRH5: Fc receptor-homolog 5; ide-cel: idecabtagene vicleucel; cilta-cel: ciltacabtagene autoleucel. Created with BioRender.com.

1.2.1. MM immunotherapeutic targets

- B-cell maturation antigen (BCMA; TNFRSF17; CD269)

BCMA, also called CD269 or TNFRSF17, is a type III transmembrane glycoprotein and a member of the TNF-receptor superfamily. The expression profile of this protein is very limited. BCMA is present in mature B cells, plasmablasts and PC, and its expression is augmented on malignant PC along MM progression [145]. However, neurons and astrocytes placed in basal ganglia also have BCMA expression and few Parkinsonism cases have been reported after BCMA-CAR T therapies [146]. BCMA recognizes two ligands: B-cell activation factor (BAFF), which enhances MM cell adhesion to stromal cells, and, with higher affinity, a proliferation-inducing ligand (APRIL), which promotes MM cells survival and proliferation (Fig. 8). In addition, BAFF, normally expressed on monocytes, neutrophils and DCs, can bind BCMA, BAFF-R and the transmembrane activator and calcium modulator and cyclophilin ligand interactor (TACI) [147, 148]. However, APRIL, found on monocytes and tumors cells, only recognize TACI and, with

higher affinity, BCMA [147, 149]. Of note, APRIL and BAFF serum levels have been found increased on MM patients compared to HD [150].

BCMA binding to its ligands triggers pathways (PI3K/AKT and MAPK/ERK) involved in the proliferation and survival of malignant PC and the sustenance of the immunosuppressive TME, through the induction of anti-apoptotic and immunosuppressive proteins in PC (PD-L1 and TGF-β) [147, 151, 152].

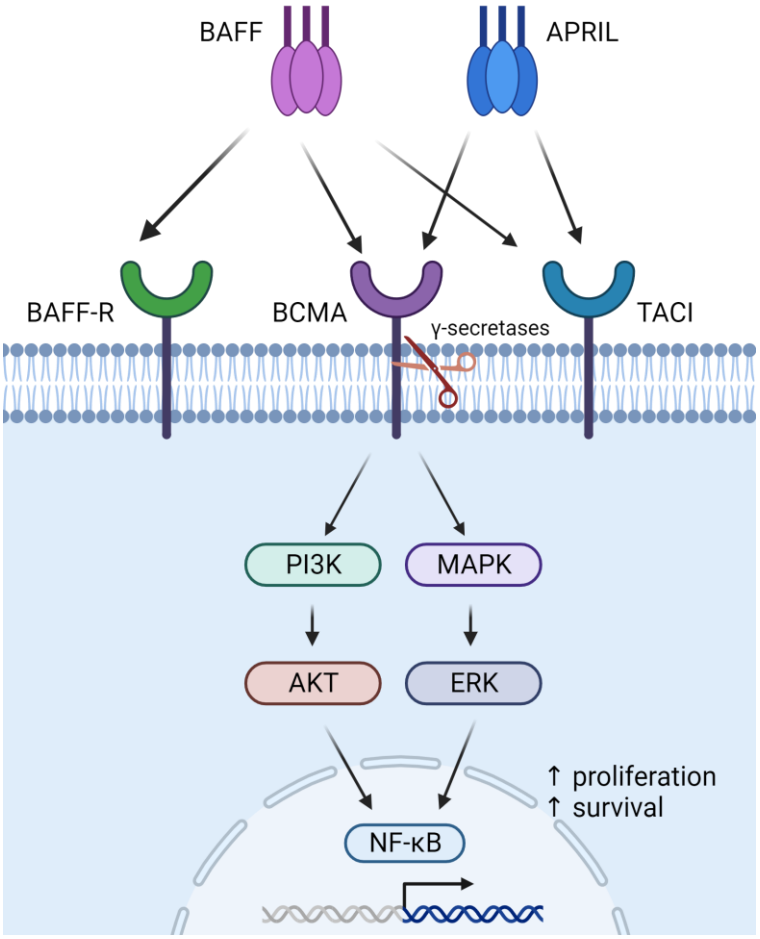

Figure 8. BCMA signaling. BAFF: B-cell activating factor; APRIL: a proliferation-inducing ligand; TACI: transmembrane activator and calcium modulator and cyclophilin ligand interactor; BCMA: B-cell maturation antigen; BAFF-R: BAFF receptor; PI3K: phosphoinositide 3-kinase; MAPK: mitogen-activated protein kinase; AKT: Ak strain transforming; ERK: extracellular signal-regulated kinase; NF-κB: nuclear factor κ B. Created with BioRender.com.

Nevertheless, BCMA-targeted therapy efficacy can be reduced by the excessive levels of the soluble form of BCMA, found in the BM from MM patients, blocking their interaction with malignant PC [153]. In line with this, an augmented shedding of BCMA diminishes

the presence of this glycoprotein on the surface of MM cells, and the soluble BCMA acts as a decoy, avoiding tumor cell recognition by BCMA-targeted treatments. BCMA shedding is caused by γ-secretases, a multisubunit protease complex that mediates protein cleavage. Inhibition of these proteases recovers α-BCMA therapy activity [154].

- NKG2D-L

NKG2D, a type II homodimer, belongs to the C-type lectin superfamily. NKG2D is a potent activating receptor of NK cells, but it is also expressed on the surface of $CD8^+$ T cells, γδ T cells and NKT cells [155]. Under pathological conditions, as Crohn's disease [156] or cytomegalovirus infection [157], this receptor can be found on $CD4^+$ T cells. NKG2D does not contain ITAM motifs to promote activating signals, but it forms a hexamer complex with DAP10, which contains the sequence YINM. This complex recruits PI3K/AKT and Grb2/Vav1 to trigger cytotoxicity when binding to NKG2D-L (Fig. 9) [158, 159].

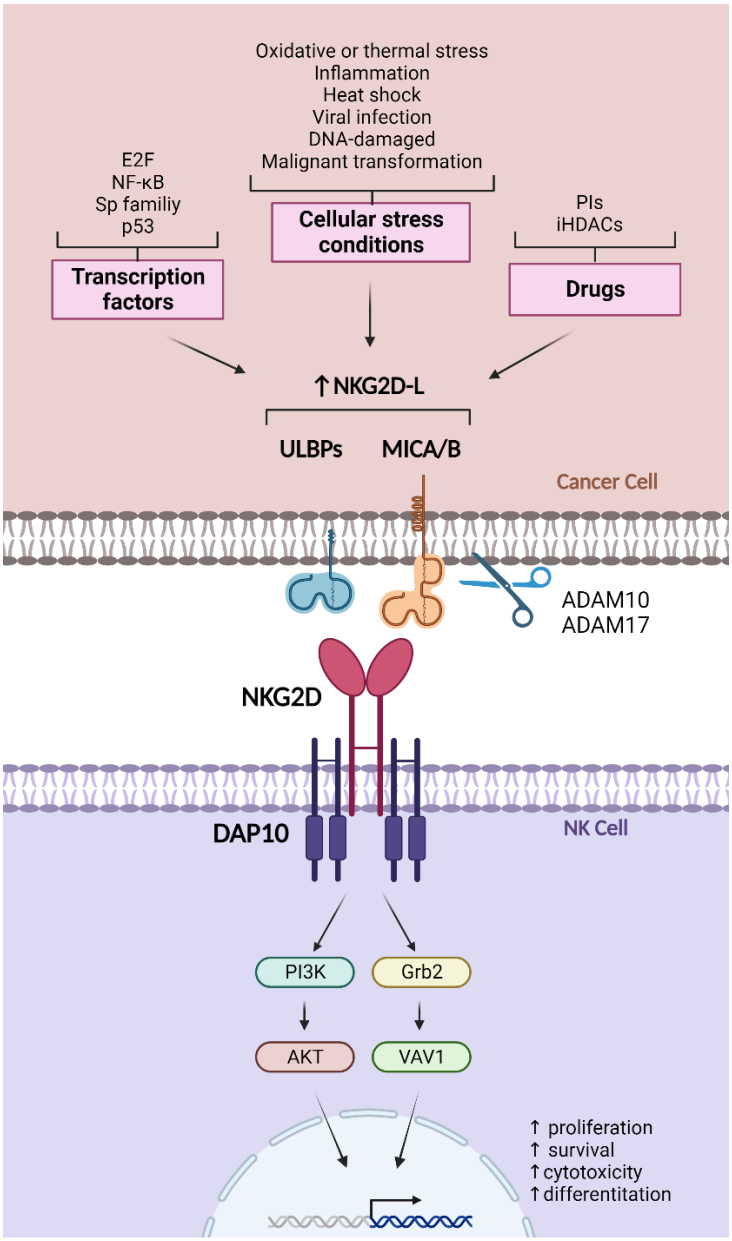

Figure 9. NKG2D-L/NKG2D axis. NF-κB: nuclear factor κ B; PIs: proteasome inhibitors; iHDACs: histone deacetylase inhibitors; NKG2D-L: NKG2D ligands; ULBPs: unique long 16 binding proteins; MICA/B: major histocompatibility complex class I chain-related protein A/B; ADAM10/17: a disintegrin and metallopeptidase 10/17; DAP10: DNAX-activating protein 10; PI3K: phosphoinositide 3-kinase; Grb2: growth factor receptor-bound protein 2; AKT: Ak strain transforming. Created with BioRender.com.

NKG2D-L comprise 8 molecules: the MHC class I chain-related (MIC) proteins A and B, and the unique long 16 binding proteins (ULBP) 1 to 6. These ligands are normally induced by stress, including oxidative or thermal stress, heat shock or inflammation [160], DNA-damage [161], viral infection [162] or malignant transformation. Remarkably, at least one of these ligands is expressed on more than 85% of tumor cells, including stem-like MM cells [124, 155, 163]. However, NKG2D-L expression has been also detected in

healthy tissues as gastrointestinal epithelium [164]. NKG2D-L expression is transcriptionally and post-transcriptionally regulated. The transcription factors E2F, NK-κB, Sp family and p53 are involved in NKG2D-L expression. For example, p53 is able to amplify some NKG2D-L transcription and the drug-mediated induction of p53 has been associated with a higher expression of ULBP1 and 2. In addition, NF-κB induction enhances MICA expression [165]. At a protein level, some genotoxic drugs and chemotherapeutic agents, as PI and HDAC inhibitors, can increase NKG2D-L presence on the cell membrane [166]. However, the matrix metalloproteases (MMPs) ADAM10 and ADAM17 participate in MICA, MICB, and ULBP2 shedding, augmenting the levels of these soluble forms in the TME, as we have described previously in RRMM immunosuppression, and impairing NKG2D-mediated cytotoxicity of NK and cytotoxic T cells [165]. Of note, supraphysiological levels of sMICA do not hamper NKG2D-CAR T cell efficacy [167].

- GPR5CD

GPRC5D is an orphan receptor, which still does not have a recognized ligand, with seven transmembrane segments that belongs to the G protein-coupled receptor family. GPRC5D is highly expressed on MM cells and it is unlikely to be shed, being a suitable target for targeted therapies, although GPRC5D expression has been also detected in hard keratinized tissues and hair follicles [168, 169]. In addition, on-target off-tumor toxicities as mucosal toxicity [170] and nail- and skin-related events have been reported in more than 60% of MM patients, after treatment with GPRC5D BiAbs [112]. However, GPRC5D-CAR T cells have not induced alopecia in mice and cynomolgus monkeys [171]. Although in MM GPRC5D expression correlates with high-risk myeloma markers and could be related to tumor PC proliferation, its function is still unknown [168].

- Fc receptor-homolog 5 (FcRH5)

FcRH5, another orphan receptor, also called FcRL5, IRTA2 or CD307, is encoded by one of the last 6 new genes that have been discovered from the Ig superfamily. FcRH5 is a differentiation antigen expressed on B cells, from pre-B cells and especially on their late stages, memory B cells and PC, after the development of antigen-primed B cells [172].

Considering MM, this receptor is highly found in malignant PC, especially in patients with the gain 1q21, being associated to high-risk MM [173]. Although its ligands are still unknown, FcRH5 has been found to increase proliferation and possible toxicities are suggested to affect skin, eyes, and gastrointestinal tract [172, 174].

- CD38

The ectoenzyme CD38 is a type II transmembrane protein that belongs to the ADP-ribosyl cyclase family. It is expressed on almost all hematopoietic cells: B, NK, and T cells and myeloid cells [175]. CD38 is high and uniformly expressed on MM cells compared to healthy tissues. However, this expression, positively controlled by STAT1 and negatively controlled by STAT3, can be downregulated due to selective pressure after CD38-targeted treatments [176, 177]. CD38 catalyzes two reactions: the cleavage of NAD^+ into ADP-ribose and the transglycosylation of NADP and nicotinic acid to obtain NAADP. Substrates from these reactions are involved in calcium release and ADO secretion, which participates in MM immunosuppression [177]. Moreover, CD38 has been described to also mediate cell migration and adhesion when binding CD31 or hyaluronic acid [178]. On-target off-tumor toxicities involve the reduction of B and T cell number [179] but remarkably, NK cell fratricide after α-CD38 Ab therapies [180].

- CD138

CD138, also known as syndecan-1, as it belongs to the syndecan family, is a heparan sulfate proteoglycan. Although it can be found on squamous epithelial cells from liver, bladder, and gastrointestinal tract [181], this molecule is a lineage marker of PC and it is highly expressed on MM cells [182]. Of note, it is used to identify tumor PC by flow cytometry. However, in late stages, CD138 can be shed from MM cells. Both a high number of $CD138^{low}$ cells and high levels of soluble CD138 correlate with a worse prognosis [183-185]. CD138 can bind a multitude of proteins as integrins and extracellular matrix molecules, playing a key role in adhesion. Moreover, this proteoglycan binds growth factors [186], cytokines [187], and chemokines [188], and mediates wound healing, endocytosis and micropinocytosis [182]. In addition, it can bind

APRIL and TACI, promoting tumor growth and survival [189]. Possible on-target off-tumor may affect the bladder, liver, or gastrointestinal tract tissues [181].

- CD44 variant domain 6 (CD44v6)

CD44v6 is a spliced isoform of the CD44 protein, a group of type I transmembrane proteins. CD44 gene alternative splicing can generate different variants with different extracellular domains [190]. Ten different proteins can be generated between exon 5 and 16 from CD44, and CD44v6 corresponds to alternative splicing in exon 11. This aberrant protein is commonly found in tumor cells, including MM, acute myeloid leukemia (AML) and pancreatic, colon, breast, and head/neck cancers, with low expression on activated T cells, monocytes, and keratinocytes and no expression on hematopoietic stem cells. Remarkably, it has been associated with a poor prognosis and metastasis [191], probably due to its expression on tumor stem cells [192]. Standard CD44 binds hyaluronic acid [193], collagen, matrix metalloproteinases [194] and E-selectin [195] to promote cell migration and tumor cell survival. Moreover, the addition of the exon 11-codified peptide to CD44 protein allows CD44v6 binding to osteopontin [196], hepatocyte growth factor (HGF) [197] and VEGF [198]. Due to its expression on keratinocytes, skin toxicities have been reported after CD44v6-targeted therapies [199], but not with CD44v6-CAR T cells [200]. Moreover, these treatments might reduce the number of $CD44v6^{+}$ monocytes and macrophages [201], cells involved in cytokine release syndrome (CRS), diminishing the grade of this side effect [202].

- SLAMF7

SLAMF7, CD319, CRACC or CS1 is a glycoprotein receptor, member of the signaling lymphocytic activation molecule and of the CD2 subset of the immunoglobulin superfamily [203]. SLAMF7 can be found in lymphocytes and mature DCs and it is expressed on healthy and pathologic PC [204]. SLAMF7 is a homophilic receptor, it interacts with itself when it is expressed on the cell membrane of other cells or with its soluble form, promoting PC proliferation [205]. Moreover, IMiD downregulation of Ikaros reduces both SLAMF7 forms, soluble and on the membrane, diminishing MM

progression [147]. As it has been described for CD38, SLAMF7 expression in NK and T cells promotes fratricide after SLAMF7-targeted immunotherapies [206, 207].

- CD19

CD19 is a type I glycoprotein transmembrane protein, a member of the Ig superfamily, and a BCR co-receptor molecule. Similarly to FcRH5, it is expressed on all the B cell lineage, but it has a low expression in late stages, as PC. CD19 is involved in B cell maturation, differentiation and activation [208]. Although CD19-targeted therapies have shown great results against acute lymphocytic leukemia (ALL) [209] and B-cell lymphomas [210], CD19 expression on tumor PC is restricted to MM stem-like cells [208, 211], characterized by a higher proliferation and drug resistance [212]. CD19-CAR T cell combinations with other BCMA therapies [213, 214] and ASCT, together with melphalan, have shown synergistic effects [212].

Other promising targets for MM treatment are CD229 [215], integrin β7 [216], TACI [217], and SEMA4a [218].

1.2.2. Monoclonal antibodies (mAbs)

mAbs are an alternative approach for cancer patients, engineered to specifically target antigens that are overexpressed on tumor cells. Most mAbs can exert their antitumor activity through four mechanisms of action: ADCC, antibody-dependent cellular phagocytosis (ADCP), complement-dependent cytotoxicity (CDC), and direct tumor killing (Fig. 10) [219].

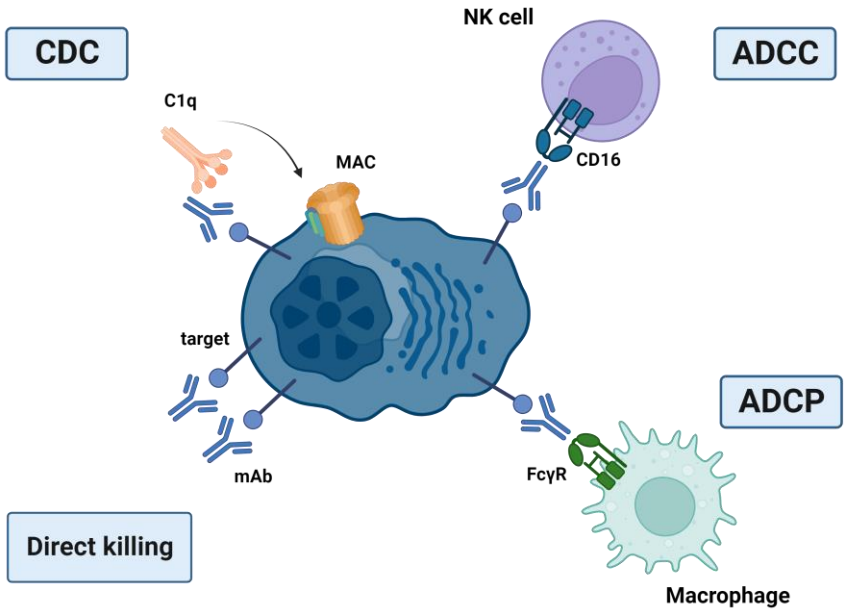

Figure 10. Mechanisms of action of mAbs. CDC: complement-dependent cytotoxicity; ADCC: antibody-dependent cellular cytotoxicity; ADCP: antibody-dependent cellular phagocytosis; mAb: monoclonal antibody; MAC: membrane attack complex. Created with BioRender.com.

Daratumumab

Daratumumab is a first-in-class α-CD38 human naked IgG1κ mAb [177]. This Ab was approved by the FDA in 2015 and is currently used as a first-line treatment in NDMM patients together with PI, IMiDs, and corticosteroids [1]. Apart from the mAb properties described above, Daratumumab also modulates the TME through the decrease of ADO production and the reduction of $CD38^{+}$ Tregs, Bregs and MDSCs, while augmenting T cell proliferation [177, 220].

In RRMM patients, the last results of phase III trial POLLUX reported a higher OS of Daratumumab in combination with lenalidomide and dexamethasone, 67.6 months, compared to 51.8 months obtained after lenalidomide and dexamethasone, and PFS, 45 vs 17.5 months, respectively [221]. Another phase III (CASTOR) has compared Daratumumab together with BTZ and dexamethasone versus BTZ and dexamethasone. Last update has described an enhanced OS (49.6 vs 38.5 months, respectively) and PFS (16.7 vs 7.1 months, respectively) [222].

However, acquired resistance to this treatment has been described. Firstly, one of the events that leads MM progression after Daratumumab is the loss of CD38 in MM cells. It has been described that $CD38^{-}$ clones persist after treatment or that there is a

downregulation within the first weeks and CD38 expression is recovered after 3-6 months [223]. Another challenge is that NK cells also express CD38 on their surface, being a Daratumumab target. Thus, NK cell number is significantly decreased, affecting ADCC function, and NK cells that remain are exhausted and lack CD16 and granzyme B production. Some groups have reported the use of CD38 KO exogenous NK cells in combination with Daratumumab to recover NK cell-mediated tumor killing [224, 225]

Toxicities associated with these treatments are infusion reactions, neutropenia, anemia, lymphopenia, pneumonia, thrombocytopenia, and diarrhea [221, 222].

Isatuximab

Another α-CD38 Ab commonly used in RRMM treatment is isatuximab. It is a naked chimeric IgG1 mAb approved by the FDA and EMA in 2020 [226, 227]. IKEMA phase III trial has reported a PFS of 35.7 months in the isatuximab, carfilzomib, and dexamethasone group, compared to the 19.2 months from the carfilzomib and dexamethasone arm [228]. Moreover, in the ICARIA study, the PFS of the isatuximab, pomalidomide and dexamethasone group was 17.5 months versus 12.9 months in the control group (pomalidomide and dexamethasone) [144].

Most common adverse effects are related to infusion reactions along with respiratory infections [144, 229]. Moreover, reactivation of hepatitis B has been described in patients after daratumumab or isatuximab treatments [230].

New mAbs targeting CD38, as MOR202 and TAK-079, are still under research [231]. In addition, new approaches include the HexaBody-CD38 described by Hiemstra et al, which highly fosters CDC compared to Daratumumab [232] and its efficacy is being studied in a clinical trial (NCT04824794).

Elotuzumab

The α-SLAMF7 humanized naked IgG1κ mAb elotuzumab, was the first-in-class mAb approved for MM treatment in 2015 by the FDA and in 2016 by the EMA [226, 233]. Mechanisms of action of elotuzumab are principally ADCC and NK cell-mediated activation, but it is also capable of inhibiting MM cell adhesion to BMSCs [234, 235].

However, as it has been described for other mAbs, elotuzumab treatment also reduced NK cell count due to the expression of CS1 in this immune subset [236].

ELOQUENT-3 phase II trial in RRMM patients demonstrated a significantly higher OS (29.8 months) in the elotuzumab plus pomalidomide and dexamethasone arm compared to the 13.8 months obtained by the pomalidomide and dexamethasone group [237].

Few adverse events have been reported after elotuzumab treatment: anemia, neutropenia, and respiratory infections [237].

Anti-MM efficacy of other mAbs, as siltuximab (α-IL-6) and SEA-BCMA (α-BCMA), is being studied in clinical trials [219].

1.2.3. Antibody-drug conjugate (ADC)

ADCs are recombinant mAbs frequently conjugated to small cytotoxic molecules, as a payload. When ADCs specifically target the antigens expressed on the cell surface, they are endocytosed and release the toxin after lysosomal cleavage, eliminating the tumor cells [219]. The payload can be tubulin inhibitors, DNA damaging agents, topoisomerase I inhibitors or RNA polymerase II inhibitors [238].

Belantamab mafodotin

Belantamab Mafodotin is an afucosylated humanized α-BCMA Ab conjugated to monomethyl auristatin F (mafodotin), a microtubule polymerization blocker. It was the first-in-class ADC approved by the FDA in 2020 for RRMM treatment [239], after DREAMM-2 results. In this phase II study including 97 patients in the 2.5 mg/kg cohort, 31% of them achieved OR and 2.9 months of PFS. Most common grade 3-4 toxicities were keratopathies, including reduced visual acuity, blurred vision, dry eye, photophobia, thrombocytopenia, and anemia [240]. However, the subsequent phase III trial (DREAMM-3) showed no improvement in PFS, when patients were treated with this ADC, compared to the pomalidomide and dexamethasone arm. For this reason, the FDA provisionally halted its approval in 2022 [241, 242]. In Spain this drug remains approved and there are still clinical trials with this ADC. In 2023, a national compilation of results

of its compassionate use has revealed a median OS rate of 41.8% and a median PFS of 3.61 months [243].

Other promising BCMA ADCs as AMG 224 (NCT02561962) and CC-99712 (NCT04036461) as well as α-CD138 (indatuximab) and an α-CD38 conjugated to IFN-α2 (TAK-573) are being studied in clinical trials. However, ADCs targeting BCMA and other specificities are being discarded due to their low efficacy and severe adverse events, like lorvotuzumab mertansine (α-CD56), MEDI2228 (α-BCMA), DFRF4539A (α-FcRH5), and azintuxizumab vedotin (α-SLAMF7) [244].

1.2.4. Bispecific T-cell engagers (BiTEs) and bispecific antibodies (BiAbs)

BiTEs and BiAbs are designed to concomitantly bind immune cells and tumor cells. BiTEs are made by linking two scFv and BiAbs are recombinant Abs with a Fc region and two epitope-binding sites. One specific domain normally binds CD3 in T cells and the other, a tumor antigen on the surface of the malignant cells. In this way, these molecules redirect T cells to tumor cells and enhance the formation of immune synapses, favoring cancer cell elimination and T cell activation and expansion, independently of TCR-MHC recognition, antigen-presenting cells and costimulation [245]. Thus, these molecules represent an off-the-self therapy.

Teclistamab

Teclistamab (JNJ-64007957) is a humanized IgG4 BiAb, recently approved for RRMM patients. This BCMAxCD3 BiAb fosters T cell activation after tumor cell killing, exhibiting incredible efficacy against MM cells *in vitro*, even in whole blood cultures, and *in vivo*. Of note, soluble BCMA does not impair Teclistamab-mediated T cell cytotoxicity [246]. In the first clinical trial evaluating this molecule, MajesTEC-1, RRMM patients achieved an ORR of 63%, 39.4% of these responses were CR, and median PFS was 11.3 months. Most common toxicities were CRS, neutropenia, thrombocytopenia, neurotoxicity, and infections, in the 76% of patients [110]. In addition, new phase Ib and III clinical trials, MajesTEC-2 (NCT04722146) and MajesTEC-7 (NCT05552222), respectively, are testing teclistamab efficacy compared to current triplets in RRMM patients.

Elranatamab

Elranatamab (PF-06863135) is a humanized IgG2a BCMAxCD3 BiAb [245]. Last update of the phase II MagnetisMM-3 (NCT04649359) clinical trial shown 61% of ORR and 35% CR. PFS has still not been reached. Neutropenia, anemia, CRS and infections were the most common adverse events described, slightly reduced in the biweekly dosing arm [111]. These outcomes gave the green light for its approval in 2023.

The activity of other BCMAxCD3 BiAbs is being currently tested in clinical trials:

- Linvoseltamab (REGN5458): an IgG4κ-based CD3xBCMA bispecific (NCT03761108).
- Alnuctamab (CC-93269; EM901): a BiAb that recognizes two different epitopes of BCMA (NCT03486067).
- TNB-383B (ABBV-383): a BiAb with 2 BCMA binding domains and low affinity for CD3 (NCT03933735).
- Pacanalotamab (AMG 420, Bi 836909; NCT02514239) and Pavurutamab (AMG 701; NCT03287908): BCMAxCD3 BiTEs.

Talquetamab

Talquetamab (JNJ-64407564) is a humanized BiAb that targets GPRC5D on PC and CD3 on T cells. Preclinical studies highlighted the increased talquetamab efficacy over MM cells *in vitro* and *in vivo,* along with T cell proliferation [169], although BMSCs and Tregs impaired talquetamab-mediated T cell killing [247]. Clinical experience with talquetamab within MonumenTAL-1 study resulted in 73% ORR and 11.9 months of PFS with the higher dose. Although 79% of patients experienced CRS and 75% developed neutropenia, together with dysgeusia and skin-related adverse events, great efficacy outcomes promoted its approval in 2023 by the FDA and EMA. Moreover, a phase Ib/II clinical trial (RedirecTT-1) is studying the antitumor activity of talquetamab in combination with teclistamab (NCT04586426) and a phase Ib (TRIMM-2), its efficacy combined with daratumumab. First results demonstrated 84% of ORR (34% CR) and 78% of ORR (45% CR), respectively [112, 248].

Another relevant GPRC5DxCD3 BiAb is Fortintamig (RG6234; NCT04557150).

Cevostamab

Cevostamab (BFCR4350A) is an IgG FcRH5xCD3 BiAb [245]. Li et al. have demonstrated specific and effective killing of Cevostamab against primary MM cells as well as against MM cell lines, showing no toxicity against FcRH5 negative cells. In addition, they showed that the BiAb specifically binds the membrane-proximal epitope (gD) of the FcRH5 protein [249]. Currently, there are 6 clinical trials ongoing. The phase I clinical trial (NCT03275103) reported a 54.5% ORR at the higher dose, although CRS within the first 24 hours occurred in more than 80% of the patients. Due to this quick and common CRS in almost all patients, tocilizumab, an α-IL-6R Ab, is administered prior to the BiAb infusion [250].

Another promising BiAb is ISB 1342 (GBR 1342), the first CD38xCD3 BiAb engineered (NCT03309111).

1.2.5. Oncolytic viruses, vaccine peptides and marrow-infiltrating lymphocytes

Other immunotherapeutic strategies designed to target MM are oncolytic viruses, vaccines peptides and marrow-infiltrating lymphocytes (MILs).

Oncolytic virotherapy consists of engineered self-replicating viruses that selectively infect tumor cells, causing cancer cell killing and antigen spreading, which favors the patient immune system reaction to the tumor. Oncolytic virus can recognize adhesion antigens or receptors, overexpressed on tumor cells, and, alterations in intracellular signaling pathways and metabolism favor their infection on malignant cells [251]. Moreover, the viral genome can be modified to increase tumor cell recognition (eg. adenovirus targeting E2F/Rb pathway), while decreasing pathogenicity, and to express anti-oncogenic or suicide genes. Different types of oncolytic viruses with distinct surface attachment receptors have been edited for this purpose for MM treatment. These oncolytic viruses can be intratumorally or systemically administered. Of note, the efficacy of reovirus, measles virus and VSV is currently being tested in clinical trials and first results have been modest [252, 253].

Peptide-based vaccines are used to enhance antigen recognition by the immune system. In MM, due to the immune cell exhaustion generated by the TME, most approaches have combined immunogenic peptides with DCs to potentiate antitumor responses. Some of

the current clinical trial target selected for this cancer are MUC1, RHAMM-R3, Bcl-2 family, XBP1, CD138 and CS1, as well as idiotype Igs, suggesting promising results [219, 254].

In addition, adoptive immunotherapy is being studied, including MILs. These are tumor-specific T cells that reside in the BM [254]. Due to the high proportion of T cells that selectively target cancer cells, a clinical trial combining ex vivo activated autologous MILs with ASCT, and an allogenic myeloma vaccine has been carried out. This triplet combination achieved a median of 81.3% ORR, 18.6 months PFS and 31.3% CR (NCT01045460).

Moreover, other adoptive approaches are activated and expanded NK cells [255], DCs [256], and engineered T and NK cells to express a CAR against tumor antigens, as it is described below.

1.2.6. CAR adoptive immunotherapy

Although the abovementioned treatments have obtained substantial results in clinical trials, CAR adoptive therapy has revolutionized the treatment of cancer patients, especially with hematologic tumors. Effector cells are frequently extracted through apheresis, activated, and transduced with CAR molecules. Then, these CAR cells are expanded and infused into the patient, to specifically kill target-positive cells, after lymphodepletion to avoid patient immune system rejection [254]. First studies were developed using T cells as CAR hosts, but there are other immune cells, as NK, iNKT, γδ T cells, macrophages and DCs that have been efficiently modified to express CAR sequences (Fig. 11) [257].

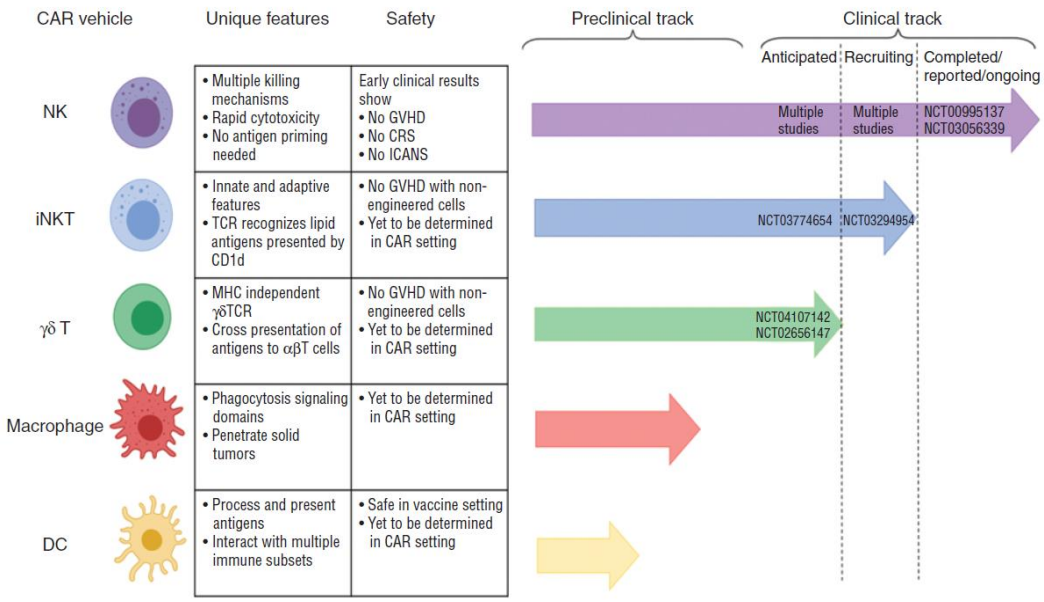

Figure 11. Track record of CAR immune effectors in preclinical and clinical studies. GVHD: graft versus host disease; CRS: cytokine release syndrome; ICANS: immune effector cell-associated neurotoxicity syndrome; DC: dendritic cell; CAR: chimeric antigen receptor; MHC: major histocompatibility complex; TCR: T cell receptor. Extracted from Daher and Rezvani, 2021 [257]

CAR molecules contain an extracellular domain that recognizes an antigen on the surface of the tumor cells. This domain can be a fragment of a natural receptor, whose ligands are overexpressed on malignant cells, or the single chain variable fragment (scFv) from a mAb that specifically binds a tumor antigen. Then, it contains a hinge region, a transmembrane domain, and a signaling endodomain. Depending on the latter, CAR structures can be classified into 5 groups. First generation CAR molecules only contain the CD3ζ chain from the TCR, second generation also have a costimulatory domain, and third generation include two costimulatory domains and the CD3ζ. In addition, fourth generation CARs, also known as armored CARs, have been developed to incorporate a cytokine expression inductor into second generation structures or to express interleukins from a bicistronic transgene. Recently, next or fifth generation CARs have been designed. These molecules incorporate a signaling domain of an interleukin receptor (normally IL-2) to foster JAK/STAT activation pathway. Most common costimulatory domains used are 4-1BB, CD28, OX40, CD27, CD40, and ICOS, among others [258].

1.2.7. CAR T immunotherapy in MM

CAR T cells are an innovative therapy that has reported impressive results against hematological malignancies as $CD19^+$ lymphomas and B-cell lymphoblastic leukemias. CAR T cell therapy first approval by the FDA, Tisagenlecleucel, was in 2017 against CD19 for children and young adults with relapse or refractory B-ALL, obtaining 76% OS and 50% PFS at 12 months [259, 260] and to date, a total of 6 CAR T products have been globally approved for BCMA or CD19 positive tumors [261]. In addition, other two therapies have been approved by the Chinese National Medical Products Administration (NMPA), Relmacabtagene autoleucel, an α-CD19 CAR T, and Equecabtagene Autoleucel, an α-BCMA CAR T. Recently, the EMA has granted the α-CD19 varnimcabtagene autoleucel the PRIME designation. In Spain, this CD19-CAR T therapy, also called ARI-0001, is administered under hospital exemption. These groundbreaking achievements have paved the way for the development of new CAR T treatments, not only for hematological malignancies, but also for solid tumors. The two CAR T therapies that have been recently authorized for clinical use in MM against BCMA are idecabtagene vicleucel (ide-cel) and ciltacabtagene autoleucel (cilta-cel). Ide-cel was approved in early 2021 by the FDA and later by the EMA, due to KarMMa1 trial outcomes. Recently, the KarMMA-3 phase III clinical trial reported 71% of responses and a median PFS of 13.3 months in the ide-cel arm compared to the 4.4 obtained by the control group, which included 5 different standard regimens combining Daratumumab, PI, IMiDs and corticosteroids for the treatment of RRMM patients. Toxicities grade 3 or 4 were observed in 93% of the patients, above all CRS and immune effector cell-associated neurotoxicity syndrome (ICANS) [108]. A year later, the FDA and EMA gave the green light for cilta-cel, based on 89% OS and 77% 12-month progression free rate outcomes obtained in the CARTITUDE-1 clinical trial [262]. Lately, a total of 208 patients were enrolled in the CAR T therapy arm within the phase III CARTITUDE-4 clinical trial. OS was 84.6% in this group with 73.1% of CR and 60.6% MRD^-. Nevertheless, 76.1% of patients suffered CRS, but only a small percentage developed neurotoxic adverse events (4.5% of patients) or severe CRS (1.1% of patients) [109]. Results from FDA-approved immunotherapies are summarized in Table 2.

Treatment	Trial phase	No. of patients	ORR	Median duration of response	Median PFS	Median OS	CRS	Neurotoxicity	Nonrelapse death
		nº	nº (%)	months	months	months	% of any grade (≥grade 3)		nº (%)
FDA-approved therapies									
Selinexor	2	122	32 (26)	4,4	3,7	8,6	NA	NA	12 (10)
Belantamab mafodotin	2	97	31 (32)	11	2,8	13,7	NA	NA	7 (7)
Idecabtagene vicleucel	2	128	94 (73)	10,7	8,8	24,8	84 (5)	18 (3)	17 (14)
Ciltacabtagene autoleucel	1B-2	97	95 (98)	NR	NR	NR	95 (5)	22 (12)	16 (17)
Teclistamab	1-2	165	104 (63)	18,4	11,3	18,3	72 (1)	14 (1)	19 (12)
Talquetamab (GPRC5D-CD3)	1-2	74	49 (66)	10.2-13 at two doses	NA	NA	78 (1)	NA	NA
Elranatamab	2	94	57 (61)	NA	NA	NA	61 (0)	2 (0)	1 (1)
BCMA-CD3 bispecific antibody in clinical development									
ABBV-383	2	94	57 (61)	NA	NA	NA	61 (0)	2 (0)	1 (1)
Linvoseltamab (REGN5458)	1	118	NA	NA	NA	NA	54 (3)	5 (NA)	6 (5)
Pavurutamab (AMG701)	1	73	37 (51)	NA	NA	NA	38 (0)	4 (0)	5 (7)
Alnuctamab (CC-93269)	1	30	13 (43)	NA	NA	NA	77 (3)	NA	3 (10)
Non-BCMA-CD3 bispecific antibody in clinical development									
Cevostamab (FCRH5-CD3)	1-2	161	64 (45)	11,5	NA	NA	81 (1)	14 (1)	6 (4)

Table 2. FDA-approved immunotherapies in clinical development for patients with RRMM. ORR: overall response rate; PFS: progression-free survival; OS: overall survival; CRS: cytokine release syndrome; FDA: Food and Drug Administration; GPRC5D: G protein-coupled receptor class C group 5 member D; FCRH5: Fc receptor-homolog 5; BCMA: B-cell maturation antigen; NR: not reached. NA: not available. Adapted from Mailankody et al. 2022 [263]. Point-of-care these outcomes have to be carefully compared due to the differences in basal populations.

Currently, there are a total of 195 clinical trials testing CAR T therapies in MM patients, most of them targeting BCMA. Moreover, GPRC5D, SLAMF7, CD38, FcRH5, NKG2D-L, and CD138 specificities are also being studied, among others. In particular, two clinical trials (NCT03018405 and NCT02203825) have examined NKG2D-CAR T cell efficacy

against MM. THINK phase I study tested the activity of NKR-2, also known as CYAD-01, which demonstrated great cytotoxicity and cytokine production against MM cell lines *in vitro*. Apart from tumor cells, these NKG2D-CAR T cells have unique properties, as they also target the tumor neovasculature, MDSCs, and Tregs present in the TME [264, 265]. However, only 3 MM patients were enrolled in the THINK study and just one could be evaluated, who did not respond to the treatment, but treatment-related toxicities were low-grade, including CRS in 71% of patients [160]. The second study (NCT02203825) enrolled 5 MM patients and NKG2D-CAR T cells could be detected in 2 of them within the first two weeks. Nevertheless, efficacy was limited, no severe adverse events were reported, and all patients had to be treated with other therapies after relapse [266]. Of note, both treatments were first generation CAR (NKG2D ectodomain and CD3ζ signaling), no lymphodepletion was realized prior to NKG2D-CAR T therapy infusions and these MM patients expressed low levels of NKG2D-L. All these characteristics may have impacted on the poor NKG2D-CAR T cell efficacy reported.

Contrary to CD19-CAR T therapy, BCMA-CAR T cell responses did not achieve *plateaus* [267]. This lack of stability in the responses might be caused by the following limitations.

On the one hand, effector cell-dependent resistances, referring to T cells, include scFv immunogenicity and CAR T cell exhaustion. Most CAR scFv are derived from mice or are not completely human and the immune system can secrete human anti-mouse Abs (HAMAs). This fact limits CAR T cell expansion and persistence, and also annuls the effect of following doses. Some strategies such as changing scFv origin for fully-human sequences, applying a conditioning regimen before CAR T therapy to deplete endogenous lymphocytes, or using natural receptor- or ligand-based CARs instead of scFv, have been proposed [268].

Exhaustion is a reversible state that can be defined as lack of function, high expression of inhibitory receptors (PD-1, TIM-3, LAG-3, TIGIT, and CTLA-4), and T cell differentiation. This phenotype has been reported in most non-responders CAR T cell patients. CAR T cell exhaustion can be caused by the CAR structure. CD28 costimulatory domain within CAR molecule has been reported to enhance exhaustion compared to other signaling domains, such as 4-1BB or ICOS. In addition, accumulation of scFv on the cell membrane can result in tonic signaling and persistence antigen exposure also causes T cell exhaustion [269, 270].

Both immunogenicity and exhaustion directly impact on CAR T cell persistence, being partially responsible for low stability in the responses. Moreover, TME, as it has been described previously, not only affects patients NK and T cells, but also CAR T cells, through the expression of inhibitory ligands, the release of cytokines (TGF-β, IL-10), or the interaction with immunosuppressive cells [269-271]. These factors inhibit CAR T cell activity and persistence, diminishing therapy efficacy.

On the other hand, there are also target cell-dependent resistances that impair CAR T cell cytotoxicity. Principally, antigen loss or negative clone appearance are the main obstacles. Many tumors downregulate the CAR-target antigen, therefore they cannot be killed by the infused therapy. One solution is the use of Dual-CARs, carrying two different CARs in the same cell [272], or changing the specificity of the CAR T cell depending on the antigens expressed on the tumor cell, as Ruffo et al. have proposed [273]. This self-labeling protein tag (SNAP)-synthetic Notch (synNotch) technology allows the binding of different Abs with diverse specificities to the CAR T cell, avoiding tumor cell escape. Moreover, target antigens such as BCMA or FcRH5 can be cleaved from the cell membrane and bind CAR T cells, impairing their cytotoxicity [154, 173]. The combination of γ-secretase inhibitors and BCMA-CAR T cells has been studied to avoid BCMA shedding and to augment this therapy efficacy [154]. Of note, NKG2D-CAR T therapy has been demonstrated in several reports to overcome this resistance, as soluble NKG2D ligands do not affect NKG2D-CAR T cell antitumor activity [167]. Furthermore, extramedullary disease and high-risk cytogenetics have been reported as risk factors for CAR T therapy failure [274].

In addition, new strategies are being developed to enhance CAR T cell trafficking to the tumor (especially in solid tumors), increase expansion and survival *in vivo*, augment cancer recognition (dual targeting, switch CAR specificity), control therapy growth (suicide genes) or target the immunosuppressive microenvironment [258]. Moreover, different studies have suggested the efficacy of a second CAR T treatment or BiAbs after BCMA-CAR T relapses, even with the same target-specificity, therefore sequential administration of immunotherapies enhances patient outcomes [275, 276].

One of the major limitations of CAR T therapies is treatment-related toxicity. Main adverse events are CRS, ICANS and on-target off-tumor toxicities. CRS, developed in almost all patients, cause fever and, in severe cases, hypotension, hypoxia and/or organ dysfunction, although these symptoms are normally controlled by α-IL-6R Ab infusions.

In most cases, ICANS is developed in patients who have already experienced CRS. This neurotoxicity mainly causes confusion, impaired motor skills, apraxia, dysphasia, aphasia, and, in severe cases, seizures, cerebral oedema, motor weakness or coma [277]. Other relevant toxicities are hemophagocytic lymphohistiocytosis, a second inflammatory state after CRS [278] and prolonged cytopenias that can persist for more than 90 days [279].

Related to manufacturing, autologous individualized CAR T therapies have a high cost, vein-to-vein time is quite long and there is a high rate of production failure, due to tumor contaminations or lack of expansion, as most patients have a high tumor burden or have been treated with multiple lines of treatment, respectively [280].

This scenario highlights the need to find alternative immune effectors to enhance CAR therapy persistence and efficacy, avoiding toxicities (CRS and ICANS), TME immunosuppression or antigen loss consequences, as the use of NK cells.

1.3. CAR NK immunotherapy in MM

NK cells have emerged as safer and universal effectors for CAR treatment. Most relevant advantage regarding NK cells as CAR effectors is the low probability of graft versus host disease (GvHD). Contrary to T cells [281], NK cells lack TCR, which means that its function is not restricted to HLA recognition, facilitating its use in an allogeneic context without engineering. This fact guarantees the accessibility of every patient to this therapy, as CAR-NK cells can be already prepared from different sources (eg. peripheral blood (PB), cord blood (CB)) and rapidly infused into the patient, reducing costs, time, and manufacturing failures [282, 283]. In addition, multiple infusions of CAR NK cells can be safely administered, as NK cells release a different cytokine profile (IFN-γ, TNF-α, and GM-CSF) and have a limited expansion capacity, diminishing CRS probability. Moreover, neurotoxicity has not been described in CAR NK therapies [284, 285]. Additionally, on-target off-tumor toxicities disappear when using CAR NK cells instead of CAR T cells, redirected to the same target [286]. This effect could be attributed to KIR restriction or the short half-life of mature NK cells in circulation (around 2 weeks). For this reason, suicide switch is not needed to control this therapy proliferation [287-289] but the addition of cytokines as IL-2 and IL-15 can improve CAR NK cell lifespan [290].

NK cells as CAR effectors can overcome some CAR-T cell resistances, regarding CAR target antigen loss. Not only CAR NK cells can exert their antitumor activity through CAR signaling, but also through their native activating receptors, such as natural cytotoxicity receptors (NCRs), DNAM-1, and NKG2D, guaranteeing NK cell efficacy, even if the CAR target is downregulated [282].

1.3.1. Unique biological properties of NK cells over T cells for CAR engineering

NK cells are innate cytotoxic lymphocytes that represent 5-15% of lymphocytes in PB. Their main function, as the first line of defense, is to identify and quickly eliminate abnormal, stressed, virally infected, senescent, and tumor cells, including metastatic cells [291-294]. NK cells are differentiated along 6 stages from lymphoid progenitor cells in the BM. After maturation in primary lymphoid organs, NK cells recirculate in the PB and tissues. Along differentiation, NK cells acquire activating receptor expression, as CD16 and NKG2D, as well as perforin and granzymes to foster their cytolytic functions. Furthermore, NK cells increase KIR expression while downregulating CD62L, NKG2A, CCR7 and CXCR3 expression (Fig. 12) [295]

Although the NK population is highly heterogeneous, it has been traditionally classified into two main groups based on their CD56 expression. Cytotoxic $CD56^{dim}$ NK cells, comprising 90-95% in PB, represent a more mature subset and express CD16, while regulatory $CD56^{bright}$ NK cells, around 5% in PB, are more immature and normally $CD16^{-}$. When NK cells are activated, CD56 expression increases, but this $CD56^{bright}$ population does not resemble the regulatory characteristics of this traditional subset [296]. Remarkably, NK cells lack CD3 and TCR expression, not being restricted to antigen presentation, as T cells [284, 285].

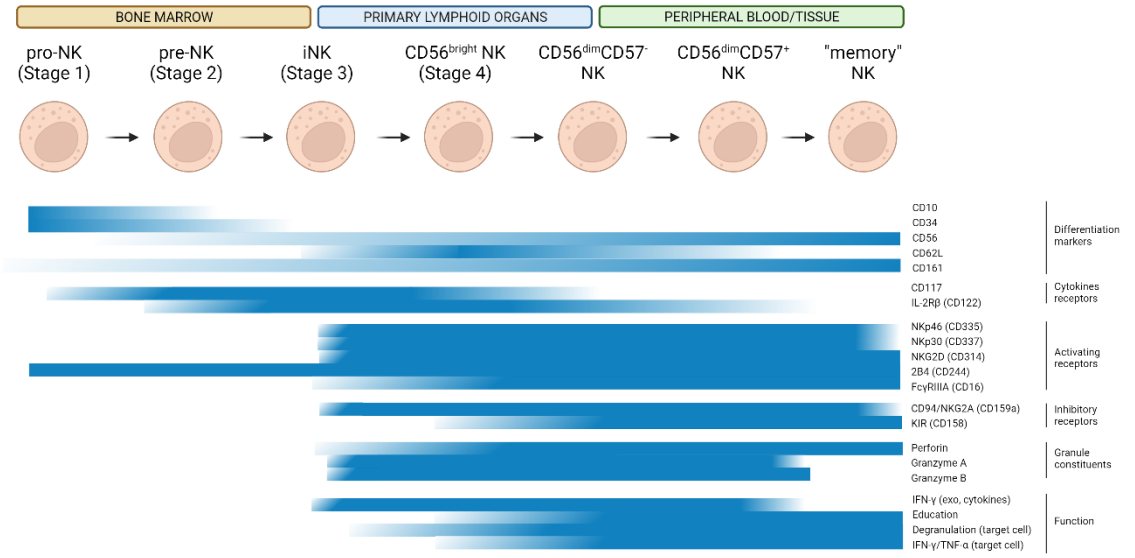

Figure 12. NK cell differentiation and maturation. Adapted from Cichocki et al. 2013 [295]. Created with BioRender.com.

The action of these effector cells depends on a balance between germline-encoded activating and inhibiting receptors (Fig. 13). NK cells are educated to identify and tolerate the own cells due to the recognition of HLA class I molecules, through a process called licensing. NK cells are able to eliminate tumor cells that do not express HLA-I molecules ("non-self") or have downregulated HLA-I expression ("missing-self"), as well as damaged or stressed cells through the recognition of activating-receptor ligands, overcoming the KIR-HLA inhibitory signal ("induced self") [284, 292]. This NK cell tolerance is regulated by HLA receptors, KIRs, expressed on the NK cell surface. NK cells need the recognition of at least one self-inhibitory KIR binding HLA-I molecules to acquire functional education or licensing. When these effector cells lose KIR expression, also known as unlicensed NK cells, they become hyporesponsive [297].

KIRs are high polymorphic receptors, expressed on NK, NKT, and $CD8^+$ T cells, which comprise 15 gene loci, located on chromosome 19, and their allelic variants [298, 299]. Their nomenclature depends on their structure and function. KIRs can possess a long cytoplasmic tail, normally containing ITIM motifs, which display an inhibiting response and a few KIRs have a short cytoplasmic tail, which normally includes ITAM motifs (activating responses). Of note, KIR2DL4 can conduct both responses, although it has ITIM motifs. To increase even more KIR complexity, KIRs can contain 2 or 3 Ig-like

domains, called KIR2D or KIR3D, respectively [285, 298]. Apart from KIRs, other inhibitory receptors have been identified on NK cells, including TIGIT, PD-1, CD96, KLRG1, and TIM-3.

PD-1 is an inhibitory receptor with an extracellular IgV domain, expressed on T, B and NK cells, as well as on DCs under inflammatory conditions [282]. PD-1 binds to their ligands PD-L1, highly expressed on tumor cells, including MM [129], and PD-L2, also expressed on malignant cells and DCs, macrophages, and B cells [300, 301]. Both PD-L1 and PD-L2 are transmembrane glycoproteins which contain IgC and IgV domains [282]. When binding to its ligands, PD-1 recruits SHP2 and SHP3 to exert their inhibitory activity, inducing effector cell exhaustion. However, although PD-1 is one of the main inhibitory signals in T cells, its role in NK cells has not been dilucidated yet [302].

TIGIT belongs to the PVR-like proteins family and contains an extracellular Ig variable domain and an intracellular ITIM and Ig tyrosine tail (ITT)-like motif. It shares homology with another inhibitory receptor, CD96 (TACTILE), both expressed on T and NK cells. These receptors recognize their ligands, PVR and Nectin-2, expressed on tumor cells and involved in cell adhesion and polarization, although TIGIT has more affinity for PVR than CD96 [303, 304]. Remarkably, TIGIT expression on NK cells that infiltrate the tumor has been found higher compared to those outside the tumor [285].

TIM-3, located in chromosome 5, belongs to the TIM family of immunoregulatory proteins, encoded by three genes, HAVCR1, HAVCR2 and TIMD4. When binding to galectin 9, it interacts with BAT3 through its cytoplasmic tail containing five tyrosines. TIM-3 can be found on T, NK, myeloid and mast cells and it is involved in the regulation of immune responses in cancer and autoimmunity [305]. Of note, its expression on NK cells is a prognostic factor in solid tumors [306] and it has been reported that PD-1^{+} and TIM-3^{+} NK cells have impaired IFN-γ and granzyme B production [285].

KLRG1 is a transmembrane glycoprotein containing an ITIM domain. It is expressed on NK and T cells and their ligands, E-, N and R-cadherin, are involved in cell adhesion. This receptor inhibits AKT phosphorylation, impairing NK and T cell proliferation [307] and it has been associated with effector cell senescence [308].

NKG2 family members play a key role in the NK cell function balance. These receptors are members of the C-type lectin-like receptor superfamily and are expressed on NK cells and cytotoxic T cells [309]. Depending on the ITIM or ITAM motifs of each member,

they can be classified into activating (NKG2C, NKG2D, and NKG2E) or inhibiting (NKG2A and NKG2B) receptors. Moreover, NKG2A, NKG2C, and NKG2E form disulfide-linked heterodimers with the unfunctional CD94 protein, while NKG2D is a homodimer. NKG2A, NKG2C and NKG2E bind the HLA class-I non-classical molecule, HLA-E, although NKG2A has 6 times more affinity for this molecule than NKG2C [310]. The relevance of this inhibitory interaction will be later described. The activating NKG2D receptor specifically binds their ligands (MICA/B and ULBP1-6), as previously mentioned.

NCRs comprise the activating receptors NKp30, NKp44, and NKp46, type I transmembrane proteins that belong to the Ig superfamily and are expressed on NK cells. They bind several ligands, such as BAG6, B7-H6, PCNA, and 21spe-MLL5, among others, as the complete panel of ligands has not been discovered yet. NKp30, NKp44 and NKp46 contain ITAM domains and besides, NKp30 and NKp46 are associated with FcεRIγ and/or CD3ζ intracellular domains, while NKp44 is associated with DAP12 to trigger NK cell killing function through Syk and ZAP70 phosphorylation [311]. Soluble NCR ligands, as well as the soluble factors IDO, TGF-β, and PGE2 can downregulate these receptors surface expression, diminishing NK cell activity [282].

The well-known CD16 receptor (FcγRIII), encoded by the *FCGR3A* gene, is associated with CD3ζ and FcRγ, forming homodimers or heterodimers. It has two isoforms, CD16A, highly expressed on NK cells, which is a transmembrane glycoprotein that recognizes Fc domains of IgG1 and IgG3, and CD16B mainly found on neutrophils. Binding of CD16A to Ab-coated cells principally fosters ADCC, although it is also involved in NK cell proliferation. However, this receptor can be cleaved and shed, or downregulated by ADAM17 metalloproteases or soluble factors, respectively, within TME, impairing NK cell ADCC function [291, 311].

Another activating and adhesion receptor is DNAM-1. It is a transmembrane glycoprotein that contains two Ig-like extracellular domains and three tyrosine residues in the cytoplasmic tail. DNAM-1, normally expressed on NK, T cells and other immune subsets such as monocytes, competes with TIGIT and CD96 for binding PVR and Nectin-2, although the TIGIT receptor has more affinity for these ligands. DNAM-1 binding to their ligands triggers Fyn phosphorylation and participates in IFN-γ secretion and NK antitumor activity [282, 312, 313].

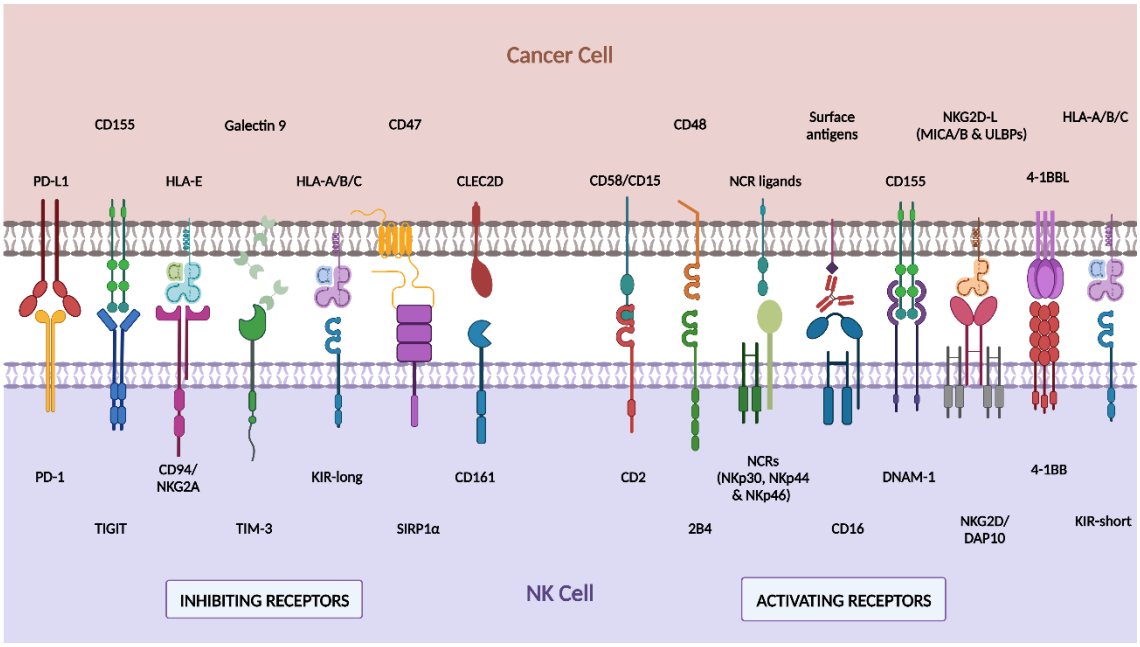

Figure 13. Main NK cell activating and inhibiting receptors. PD-L1: programmed cell death ligand 1; HLA: human leukocyte antigen; CLEC2D: C-type lectin domain family 2 member D; NCR: natural cytotoxicity receptors; NKG2D-L: NKG2D ligands; MICA/B: major histocompatibility complex class I chain-related protein A/B; ULBP: unique long 16 binding protein; 4-1BBL: 4-1BB ligand; KIR: killer-cell immunoglobulin-like receptor; DAP10: DNAX-activating protein 10; DNAM-1: DNAX accessory molecule-1; SIRPα: signal regulatory protein α; TIM-3: T cell immunoglobulin domain and mucin domain-3; TIGIT: T cell immunoreceptor with Ig and ITIM domain; PD-1: programmed cell death 1. Adapted from Valeri et al. 2022 [280]. Created with BioRender.com.

Based on this activating/inhibiting balance, NK cells exert their cytotoxicity through 4 mechanisms: direct killing, mediated by perforin and granzyme release, cytokine production, which also implies an immunomodulatory function (eg. IFN-γ and TNF-α), ADCC, through CD16, and death-receptor pathways, mediated by TRAIL and FasL apoptosis induction [314, 315]. Therefore, compared to CAR T cells, which can only display their antitumor efficacy through CAR signaling and mainly release IL-6, IL-8 and IL-1β causing CRS, NK cells possess a variety of mechanisms and activating receptors to target tumor cells and secrete a different cytokine profile including IFN-γ, GM-CSF, TNF-α, and IL-3, which produces a low CRS probability. Therefore, the high expression of chemokine receptors and chemokine release, as CCL2, CCL3, CCL4, CCL5 and XCL1 favor their trafficking to tumor niches. All these advantages enhance NK cell suitability as a CAR effector [287, 316, 317].

1.3.2. NK cell sources for CAR NK therapy

Adoptive therapy using CAR NK cells can be generated from multiple sources: PB NK cells, CB NK cells, NK cell lines (as NK-92), decidual NK cells extracted from placenta [318] and NK cells derived from undifferentiated progenitors as hematopoietic stem/progenitor cells (HSPCs) from CB [319] or placenta [320], human embryonic stem cells (hESC), or induced pluripotent stem cells (iPSC) (Fig. 14).

Peripheral blood (PB) NK cells

Most CAR NK cell preclinical and clinical studies have been developed using NK cells derived from PB in an allogeneic context [321], where they represent 5-15% of all lymphocytes [294]. Although it is a low percentage, large volumes of PB samples can be obtained from apheresis and buffy coat samples and the same donor can be used for further product generations [296]. Then, PB mononuclear cells (PBMCs) are expanded with feeder cells along with cytokines (eg. IL-2 and IL-15) to promote NK cell activation and expansion, reaching 90% of NK cells in around 7 days [306, 322]. Of note, PB NK cells are very heterogeneous and display a more mature profile. These cells display a higher expression of activating receptors, as DNAM-1, NKG2D, and NCRs as well as CD16. In addition, PB NK cells highly express KIRs, adhesion molecules, as CD2 and CD62L, and the maturation antigen CD57 [293, 323]. Final balance results in an increased direct killing, ADCC and apoptosis-induction, through TRAIL [322]. However, NK cells from PB are refractory to engineering with lentivectors, due to several intrinsic antiviral mechanisms that hamper DNA insertion [293, 324]. In addition, it has been also reported that long NK cell cultures drive telomerase shortening, meaning that CAR NK therapy persistence could be decreased [293].

Umbilical CB NK cells

NK cells derived from umbilical CB have been also used as CAR effectors in preclinical and clinical studies. Although the percentage of these heterogeneous NK cells is superior (around 20-30%) compared to PB NK cells, the total volume is limited to one unit of CB, much lower than apheresis, and it is not possible to obtain repeated samples for the same donor [296]. However, these cells have several advantages, as the immediate availability

of CB samples, better transduction efficiency with viral vectors, lower risk of GvHD, due to the reduced percentage of T cells in these samples, less KIR and NKG2A expression and a higher expression of CXCR4 and expansion capacity with feeder cells and cytokines. Moreover, CB NK cells can be cryopreserved, facilitating the infusion of multiple doses from the same donor. Contrary to PB NK cells, CB NK cells display a more immature phenotype and express less natural activating receptors as DNAM-1, NKG2C, and CD16, therefore they display a lower ADCC capacity [282, 293, 306, 321]. Nevertheless, when CB CAR NK cells are activated and expanded, they acquire a more mature phenotype and demonstrate similar antitumor activity, compared to PB CAR NK cells [325]. Of note, CB CAR NK cells engineered to express IL-15 have been detected in patients after 12 months from infusion [326].

NK cell lines

Described NK cell lines are NK-92, NKT, HANK-1, YT, KHYG-1, SNK-6, NK-YS and NK3.3. Except from NK3.3, which has been established from healthy donor (HD) blood, these cell lines have been generated from NK cell lymphomas and leukemias. To date, the only NK cell line approved by the FDA for clinical use is the NK-92 [321, 327]. The use of NK cell lines represents a universal and unlimited source of NK cells. Advantages of using NK-92 cells as CAR effector are their rapid expansion, easy genetic modifications, and homogeneity, although they do not express CD16, being incapable of exerting ADCC. On the contrary, NK-92 cell line main disadvantage is the necessity of irradiation prior to infusion, which reduces its cytotoxicity and persistence *in vivo*. Thus, the efficacy of these NK cell effectors in clinical studies is limited [293].

Stem cell-derived NK cells

Other sources are NK cells derived from $CD34^+$ hematopoietic stem/progenitor cells (HSPCs), human embryonic stem cells (hESC), or induced pluripotent stem cells (iPSC). These stem cell-derived cells are homogenous, unlimited, due to the possibility of differentiating NK cells from the same donor multiple times, and have a low expression of KIRs and CD16. Since these cells display a more immature profile and require multiple differentiation steps, their manufacturing is longer than NK cells from PB or CB (around

3-5 weeks) and they do not recapitulate all the NK cell receptor repertoire [293, 296, 328, 329]

Preclinical and clinical studies developed with iPSC-derived NK cells have obtained clinical infusion numbers and have been easily genetically engineered [327].

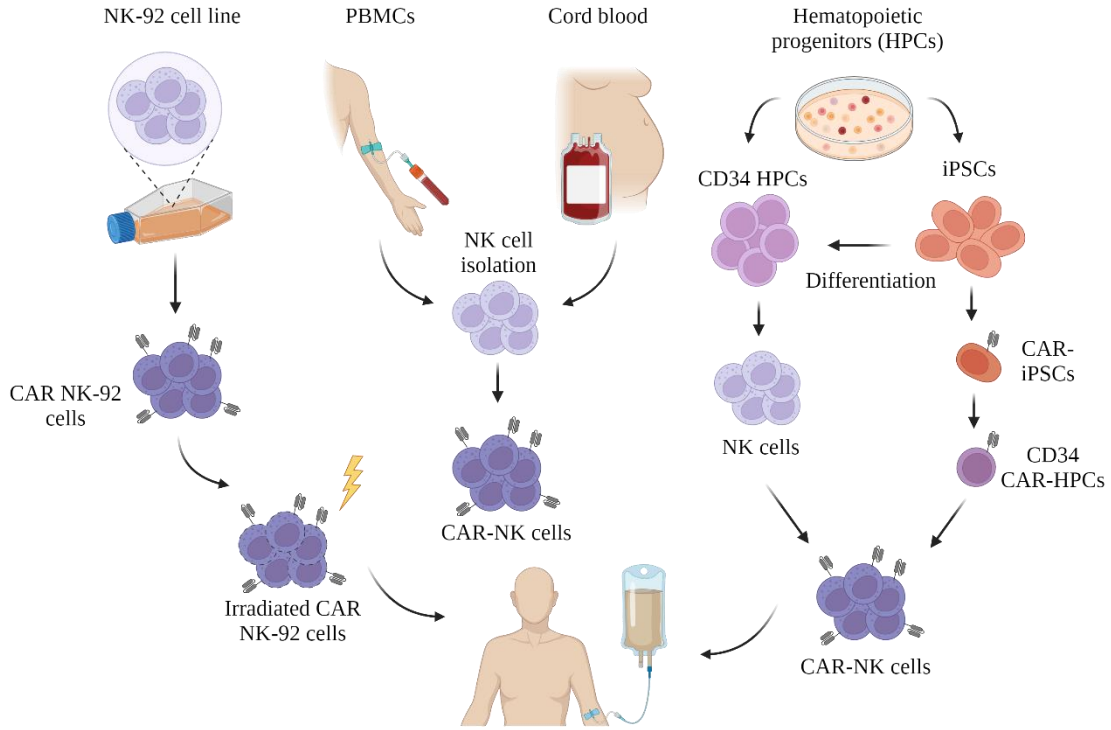

Figure 14. NK cell sources for immunotherapy. CAR: chimeric antigen receptor; HPCs: hematopoietic progenitors; PBMCs: peripheral blood mononuclear cells; iPSCs: induced pluripotent stem cells. Created with BioRender.com.

1.3.3. CAR NK preclinical and clinical studies in MM

During the last decade, several groups have been studying CAR NK cell efficacy against hematological tumors, demonstrating the feasibility of this therapy as a new cancer treatment. This fact has fostered their use in clinical trials, where preliminary data have shown a higher safety and similar responses, compared to CAR T cells.

Regarding MM, different CAR specificities, as well as NK cell sources, have been tested in preclinical studies. First strategies were conducted using the NK-92 cell line targeting CS1 [206] and CD138 [330]. Both groups demonstrated high efficacy *in vitro* and *in vivo*, paving the way for further studies using CAR NK cells in MM. Recently, NK-92 cells have been also engineered to express two specificities within the same cell, dual-CAR

NK cells: BCMA and CD19 [331], CD138 and CD19 [332] as well as BCMA and NKG2D, using different CAR costimulatory domains (unpublished results from our group). This strategy assures CAR NK cell efficacy even if one CAR-target antigen is downregulated. Moreover, Motais et al. have modified BCMA-CAR NK-92 cells to express soluble TRAIL, enhancing TRAIL-R expressing tumor cells apoptosis [333].

N°	Status	Study start	Treatment	CAR construction	NK cell source	Phase	Pat	Location	NCT
1	Recruiting	2021	RRMM	BCMA CAR	CB	I	27	China	NCT05008536
2	Unknown	2019	MM	BCMA CAR	NK-92	I/II	20	China	NCT03940833
3	Recruiting	2022	MM	BCMA CAR	Allogeneic	I	19	China	NCT05652530
4	Recruiting	2023	RRMM and PCL	BCMA CAR	Allogeneic	I	18	China	NCT06045091
5	Not yet recruiting	2022	MM	LUCAR-B68 (BCMA CAR)	Allogeneic	I	34	China	NCT05498545
6	Recruiting	2021	MM	FT576 (BCMA CAR) + Daratumumab	iPSCs	I	168	USA	NCT05182073
7	Terminated	2022	AML	NKG2D CAR	CB	I	9	China	NCT05247957
8	Recruiting	2023	AML	NKG2D CAR	Unknown	Unknown	30	China	NCT05734898
9	Recruiting	2020	RR MDS, RR AML	NKX101 (NKG2D CAR/mbIL-15)	PB	I	90	USA	NCT04623944
10	Recruiting	2021	NHL	CAR-NK019 (CD19 CAR)	PB	I	25	China	NCT04887012
11	Not yet recruiting	2020	NHL	CD19 CAR	Unknown	I	9	China	NCT04639739
12	Unknown	2019	Refractory B-cell lymphoma	CD19 CAR	Unknown	I	9	Unknown	NCT03690310
13	Recruiting	2021	ALL, CLL, NHL	CD19 CAR	CB	I	27	China	NCT04796675
14	Unknown	2016	B-cell leukemia and lymphoma	CD19 CAR	NK-92	I/II	10	China	NCT02892695
15	Completed	2009	AML	CD19 CAR	PB	I	14	USA	NCT00995137
16	Withdrawn	2019	DLBCL	CD19 CAR	Modified NK-92 (haNK)	I	0	USA	NCT04052061
17	Recruiting	2022	ALL, CLL, NHL	CD19 CAR	PB	I	15	China	NCT05410041
18	Completed	2022	ALL	CD19 CAR	Unknown	I	2	China	NCT05563545
19	Withdrawn	2022	B-cell leukemia and lymphoma	CD19 CAR	Allogeneic	I/II	0	China	NCT05570188
20	Recruiting	2023	DLBCL	CD19 CAR	Unknown	I	12	China	NCT05673447
21	Recruiting	2022	B-cell lymphoblastic leukemia/ lymphoma	CD19 CAR	Allogeneic	I	30	China	NCT05654038
22	Active, not recruiting	2020	B-cell lymphoma	FT596 (CD19 CAR)	iPSCs	I	3	USA	NCT04555811
23	Recruiting	2022	Relapsed or Refractory B-cell malignancies	JD010 (CD19 CAR)	Allogeneic	I	12	China	NCT05645601
24	Recruiting	2022	RR B-cell NHL	CAR-NK019 (CD19 CAR)	CB	I	48	China	NCT05472558
25	Recruiting	2023	ALL, CLL, B-cell lymphoma	JD001 (CD19 CAR)	Allogeneic	I	12	China	NCT05739227
26	Recruiting	2021	B-cell malignancies	NKX019 (CD19 CAR/mbIL-15)	PB	I	150	USA and Australia	NCT05020678
27	Suspended	2013	ALL	CD19 CAR + IL-2	PB	I	20	Singapore	NCT01974479

28	Completed	2017	B-cell leukemia and lymphoma	iCasp9/CAR CD19/IL-15 + AP1903	CB	I/II	44	USA	NCT03056339
29	Withdrawn	2019	B-cell lymphoma	CAR CD19/iCasp9/IL-15 + Rituximab	CB	I/II	0	USA	NCT03579927
30	Active, not recruiting	2020	CLL, B-cell lymphoma	FT596 (CD19 CAR) + Rituximab	iPSCs	I	98	USA	NCT04245722
31	Recruiting	2021	B-ALL, B-cell lymphoma	QN-019a (CD19 CAR) +/- Rituximab	Allogeneic	I	24	USA	NCT05379647
32	Not yet recruiting	2023	RR NHL	CD19 t-haNK ± N-803 and rituximab	NK-92	I	20	USA	NCT05618925
33	Recruiting	2021	B-cell NHL	CD19/IL-15 CAR	CB	II	242	USA	NCT05020015
34	Recruiting	2023	$CD19^+$ tumors	CNTY-101 (CD19/EGFR/ IL-15 CAR) + IL-2	iPSCs	I	75	Unknown	NCT05336409
35	Unknown	2019	Refractory B-cell lymphoma	CD19/CD22 CAR	Unknown	I	10	Unknown	NCT03824964
36	Recruiting	2023	RR B-cell NHL	CD19/CD70 CAR	CB	I/II	48	China	NCT05842707
37	Recruiting	2022	B-cell NHL	CD19/CD70 CAR	CB	I	48	China	NCT05667155
38	Unknown	2016	Lymphomas or $CD7^+$ leukemias	CD7 CAR	NK-92	I/II	10	China	NCT02742727
39	Unknown	2019	Refractory B-cell lymphoma	CD22 CAR	Unknown	I	9	Unknown	NCT03692767
40	Recruiting	2021	AML	CD33 CAR	Unknown	I	27	China	NCT05008575
41	Unknown	2016	AML, ANLL	CD33 CAR	NK-92	I/II	10	China	NCT02944162
42	Recruiting	2022	AML	QN-023a (CD33 CAR)	iPSC	I	18	China	NCT05601466
43	Recruiting	2022	AML	QN-023a (CD33 CAR)	iPSC	I	19	China	NCT05665075
44	Recruiting	2020	AML	CD33/CLL1 CAR	Unknown	I	18	China	NCT05215015
45	Not yet recruiting	2023	AML	CD33/CLL1 CAR	iPSC	I	102	China	NCT05987696
46	Recruiting	2023	AML	CLL1 CAR	iPSC	I	24	China	NCT06027853
47	Not yet recruiting	2023	Hematological malignancies	CD5/IL-15 CAR	CB	I/II	48	USA	NCT05110742
48	Recruiting	2022	B-cell lymphoma, MDS, AML	CD70/IL-15 CAR	CB	I/II	94	USA	NCT05092451
49	Recruiting	2023	RR leukemia, AML BPDCN	CD123 CAR	Unknown	I/II	36	China	NCT06006403
50	Recruiting	2022	RR AML	JD023 (CD123 CAR)	Allogeneic	I	12	China	NCT05574608

Table 3. Current clinical trials with CAR NK cells against hematologic tumors. NCT: national clinical trial; RRMM: relapsed or refractory multiple myeloma; PCL: plasma cell leukemia; AML: acute myeloid leukemia; MDS: myelodysplastic syndrome; NHL: non-Hodgkin lymphoma; CLL: chronic lymphocytic leukemia; DLBCL: diffuse large B cell lymphoma; ALL: acute lymphocytic leukemia; ANLL: acute

nonlymphocytic leukemia; BPDCN: blastic plasmacytoid dendritic cell neoplasm; BCMA: B-cell maturation antigen; CB: cord blood; iPSC: induced pluripotent stem cell; PB: peripheral blood; CAR: chimeric antigen receptor; Modified from Valeri et al. 2022 [280].

CAR NK cells have been also generated from primary cells obtained from PB, CB, and iPSCs for MM treatment. Our laboratory has engineered PB NKG2D-CAR NK cells that efficiently target MM cells *in vitro* and *in vivo* [155] and Golubovskaya et al. have developed PB BCMA-CAR NK cells, which have shown enhanced cytotoxicity and cytolytic cytokine production against MM cell lines [334]. Moreover, different approaches have been conducted to enhance PB CAR NK cell efficacy. Ng et al. have modified BCMA-CAR NK cells including CXCR4 to increase their migration to the BM [335]. Moreover, Wang et al. have incorporated the inducible MyD88/CD40 protein switch coupled with ectopic IL-15 to foster BCMA-CAR NK cell proliferation and anti-MM killing [336]. Karvouni et al., in order to avoid CD38-CAR NK cells fratricide, as NK cells also express CD38, have carried out the knock out of CD38 in these cells using CRISPR-Cas9 technology [337]. The same strategy was conducted by Brophy et al. using CD38-CAR NK cells from CB [338]. In addition, our group has expertise in CB CAR NK cells, generating NKG2D- or BCMA-CAR NK cells that have shown efficacy in killing MM cells (unpublished results). Regarding NK cells derived from iPSC, FT555 therapy, which co-targets GPRC5D and CD38, has been used against MM cells in combination with daratumumab [339] and Cichocki et al. have introduced 4 modifications into iNK cells to augment their efficacy and proliferation, avoiding fratricide: a BCMA-CAR, a non-cleavable version of CD16, a membrane-bound IL-15/IL-15R fusion knock-in, and a CD38 knock out. These CAR NK cells have been called FT576 [340].

Nowadays, there a total of 69 clinical trials testing CAR NK cell efficacy and safety against cancer cells, 50 in hematologic tumors (Table 3) and 6 of them in MM: BCMA-CAR NK-92 cells (NCT03940833), CB BCMA-CAR NK cells (NCT05008536), iPSC-derived FT576 therapy (described by Cichocki et al; NCT05182073) [340], and BCMA-CAR NK cells (unknown NK cell origin; NCT05652530, NCT06045091 and NCT05498545). However, only the multiengineered FT576 product has reported its preclinical activity [340]. Thus, there is a lack of preclinical studies supporting the use of CAR NK cells in MM treatment.

Regarding hematological malignancies, most of these studies are phase I clinical trials and only 6 have updated their preliminary results (Table 4), one of them including MM patients.

First-in-human CB CAR NK cells were reported by Rezvani's group for the treatment of $CD19^+$ non-Hodking's lymphomas or CLL. CB NK cells were expanded ex vivo using K562-mb21-41BBL and engineered to express a CD19 CAR, IL-15 and an iCas9 safety switch. The phase I trial reported objective responses in 8 out of 11 patients (73%), 7 of them achieved CR. Of note, CAR NK cells persist at low levels for 12 months. CD19-CAR NK cells did not produce severe adverse events as CRS, neurotoxicity, hemophagocytic lympho-histiocytosis, or GvHD, despite the HLA mismatch. Moreover, the use of rimiducid, to activate the suicide switch, was not needed [326].

Regarding MM, preliminary results of FT576 reported a 22% ORR in combination with daratumumab. Notably, this combination did not produce CRS, ICANs or GvHD. Due to the low efficacy, dose escalation is ongoing in both monotherapy and in combination with daratumumab [341].

Product	NCT	Source	Type of tumor	Results	Toxicities
CD19 -CAR NK	NCT03056339	CB	NHL or CLL	72.7% ORR (8/11) 63,6% CR (7/11)	Post-remission therapy was administered to five of the responding patients. No patients experienced CRS or neurotoxicity.
CD33-CAR NK	NCT05008575	CB	AML	60% CR (6/10)	No ICANS, 1 patients CRS grade 2
BCMA-CAR NK (FT576) ± daratumumab	NCT05182073	iPSCs	MM	1 VGPR in monotherapy 1 PR and 1 MR in combination 22% ORR	There were no events of any grade of CRS, ICANS, or GvHD
CD19-CAR NK (NKX019)	NCT05020678	PB	B-cell malignancies	70% CR (7/10)	Early safety profile supports outpatient administration and shows no neurotoxicity / ICANS, GvHD, or >Gr3 CRS
NKG2D-CAR NK (NKX101)	NCT04623944	PB	AML and MDS	67% CR (4/6; 2 of them CRs are MRD^-)	No CRS, no ICANs or GvHD. 50% hematologic events (anemia and neutropenia)
CD19-CAR NK (FT596) ± rituximab: Discontinued Jan 2023 after promising initial data Aug 2021	NCT04555811	iPSCs	B-cell lymphoma	71.4% OR (10/14; 7 of them CR)	No Dose-limiting Toxicities, and No Adverse Events of Any Grade of ICANS or GVHD, were Observed; Two Low-grade Adverse Events of CRS were Reported

Table 4. Published results from oncohematologic CAR NK cell clinical trials. BCMA: B-cell maturation antigen; NCT: national clinical trial; CB: cord blood; iPSCs: induced pluripotent stem cells; PB: peripheral blood; NHL: non-Hodgkin lymphoma; CLL: chronic lymphocytic leukemia; AML: acute myeloid

leukemia; MM: multiple myeloma: MDS: myelodysplastic syndrome; ORR: overall response rate; CR: complete response; VGPR: very good partial response; PR: partial response; MR: minimal response; MRD: minimal residual disease; CRS: cytokine release syndrome; ICANS: immune effector cell-associated neurotoxicity syndrome; GvHD: graft versus host disease.

These data suggest that CAR NK cells are highly safe, they do not exert CAR T-related toxicities as CRS and ICANs, but their efficacy outcomes can be improved overcoming some of the following limitations. First, although there are multiple sources of NK cells available for CAR engineering, expansion protocols and viral transduction are challenging. Cell-cytokine priming using soluble cytokines or feeder cells engineered to express membrane-bound cytokines and/or T cell costimulators, generates a great amount of NK cells but its GMP-implementation for clinical use is still being developed. In addition, NK cells are refractory to viral transduction and low percentages of CAR^+ NK cells may be also limiting their efficacy. Related to this low efficacy, NK cells can be killed through fratricide via Fas/FasL or due to self-recognition CAR target-ligand, when CAR NK cells are engineered to express a CAR, whose ligands are also expressed on CAR NK cells (eg. CD38 and SLAMF7). Similarly, CAR NK cells can acquire the expression of the CAR-target ligand from the target cell through trogocytosis, being susceptible to CAR NK cell killing [342].

Loss of efficacy can also occur when homing into the tumor bed is reduced due to the downregulation of chemokine receptors. In addition, once CAR NK cells reach the tumor, their function can be impaired via cell-cell contact with immunosuppressive cells or the interaction with soluble factors released by both, tumor cells and immunosuppressive cells in the TME. Furthermore, CAR NK cells can become senescent or even exhausted, by the inhibitory interaction with tumor cells via immune checkpoints. In terms of persistence, CAR NK cells can be rejected by the host T cells when they recognize non-self HLA molecules on CAR NK cell surface, diminishing CAR NK cell number or affected by the TME, limiting their *in vivo* sustenance [280]. However, some studies have been focused on overcoming these limitations with different approaches.

1.4. Combination of CAR NK cells with other strategies in MM

1.4.1. Strategies to enhance CAR NK cell efficacy

As it has been mentioned above, most CAR NK cell limitations affect CAR NK cell efficacy. Small inhibitory molecules (eg. GSK3) [343] and activating receptor Ab agonists (eg. 2B4, 4-1BB, and SLAMF7) [296] can enhance their cytolytic function as well as IMiDs and HDAC inhibitors have been described to modulate their activity, increasing activating receptor expression on CAR NK cells and target ligands on the surface of tumor cells [344]. Another strategy is the combination of CAR NK cells with mAbs to enhance ADCC function (eg. Daratumumab: NCT05182073), oncolytic viruses, as oHSV-1, which enhances EGFR-CAR NK cell efficacy against breast cancer brain metastases [345], or with bispecific killer cell engagers (BiKEs), facilitating CAR NK cell redirecting to the tumor. In this regard, NKG2DxBCMA and CD16xBCMA BiKEs have been designed to simultaneously bind NK cells and MM cells, which has demonstrated efficacy both *in vitro* and in *vivo* [213, 346]. In addition, taking advantage of the CAR specificity, NKG2D-CAR NK cell activity has been tested in combination with a NKG2DxErbB2 BiAb against solid tumors [347]. Furthermore, difficulties in trafficking to tumor sites or inhibition caused by the TME can be overcome by engineering CAR NK cells to express chemokines receptors (CXCR4) [335] to redirect them to the tumor or knocking out the expression of inhibitory soluble factors receptors, as A2AR and TGFβR, as well as by designing CAR molecules, to directly target immunosuppressive cells, respectively (eg. CD73-CAR NK cells) [296]. Additionally, CAR NK cell exhaustion can be overcome by using blocking Abs [348] or deleting inhibitory receptors [349] to avoid immune checkpoint inhibition. Moreover, knocking out negative NK cell regulators as CIS, which impairs IL-15 signaling, also improves CAR NK cell function [350] (Fig. 15).

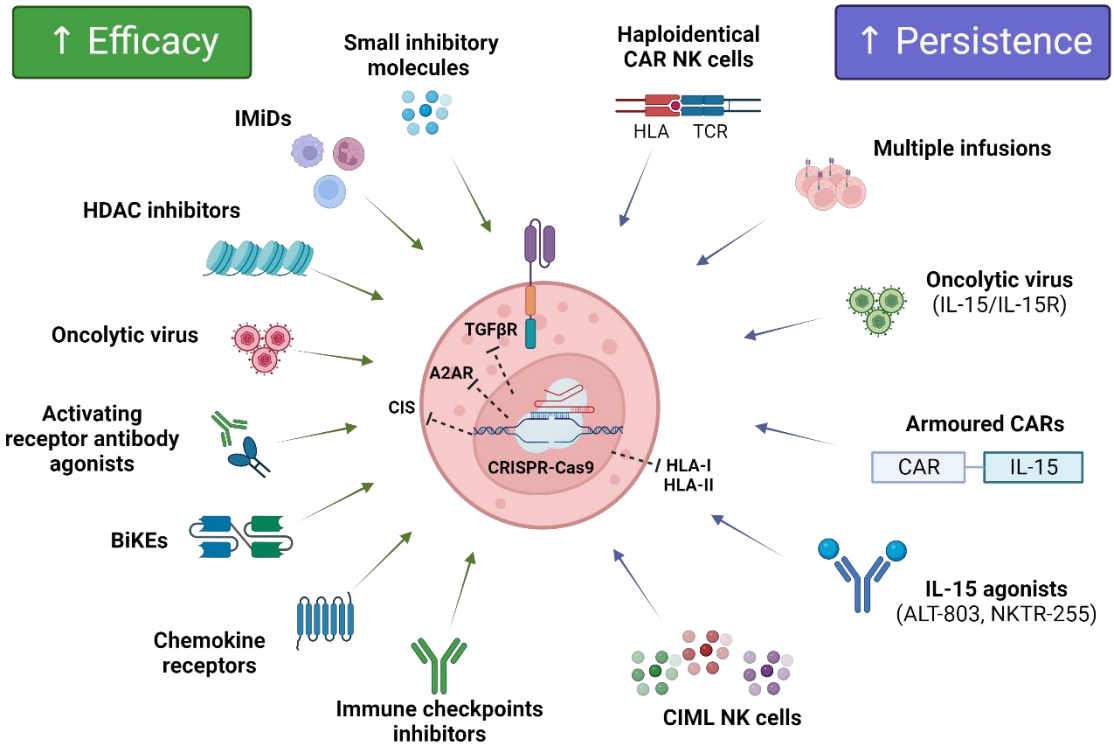

Figure 15. Main strategies to enhance CAR NK cells efficacy and persistence. HLA: human leukocyte antigen; TCR: T cell receptor; IL-15R: IL-15 receptor; CAR: chimeric antigen receptor; CIML: cytokine-induced memory-like; BiKE: bispecific killer cell engager; HDAC: histone deacetylase; IMiDs: immunomodulatory agents. TGFβR: transforming growth factor-β receptor; A2AR: adenosine A2a receptor. Created with BioRender.com.

1.4.1.1. Immune checkpoint inhibitors

NK cells display inhibitory receptors on the cell surface to avoid toxicity against healthy cells. However, the high expression of these molecules on CAR NK cells also decreases their antitumor efficacy. In this way, several groups are studying the combination of these modified effector cells with blocking Abs or the deletion of the genes encoding inhibitory receptors to disrupt immune checkpoint suppression.

The inhibition of KIRs, one of the main brakes of the NK cell, has been recently object of study. The mAb IPH2101 (1-7F9), also called lirilumab, which targets KIR2D, has exhibited enhanced preclinical NK cell activity against MM cells, without affecting healthy tissues, as well as in combination with lenalidomide [351] and daratumumab [352]. Clinical trials did not observe objective responses as a single agent in MM [353]. NK cells isolated from these patients had less degranulation and cytokine production, probably due to the removal of KIR2D surface molecules through target cell trogocytosis

[354] or lack of NK cell licensing, as maintained KIR blockade may impair NK cell activity [355]. However, a phase I trial administering IPH2101 in combination with lenalidomide (NCT01217203) described 5 objective responses and no autoimmunity effects [356].

Although PD-1 expression is low on NK cells [357], some groups have studied the disruption of the PD-1/PD-L1 axis in the cancer field. Yang et al. reported very preliminary data about an increased tumor control of BCMA/GPRC5D-CAR NK cells against MM cells when they are combined with an α-PD-L1 mAb [358]. Another preclinical analysis studying pidilizumab (CT-011), an α-PD-1 mAb, enhanced NK cell killing, in an autologous context, against MM cells [359]. However, clinical trial results using pembrolizumab, another α-PD-1 Ab, were controversial. Some studies showed activity as monotherapy or in combination with lenalidomide, but lack of long-term responses and a low benefit:risk ratio, due to the high immune-mediated adverse events, dismissed the use of this Ab for MM patients [360-362].

In MM, TIGIT ligands (PVR and Nectin-2) have been found overexpressed after BTZ treatment [90], inhibiting NK and T cell efficacy. A preclinical study has exhibited enhanced anti-MM killing after blocking TIGIT on NK cells [363]. The same strategy has been carried out in other tumors, deleting TIGIT expression on CAR NK cells [364] or blocking TIGIT through mAbs on NK cells [365-367]. Both approaches have shown increased NK cell activity against tumors and could be implemented for MM treatment with CAR NK cells.

Another inhibitory receptor that could hamper CAR NK cell efficacy is TIM-3. Its blockade has been described to increase cytokine production and enhance NK cell anti-MM activity [368]. However, in AML setting, TIM-3^{+} NK cells have been defined to be more mature and TIM-3 blockade diminished IFN-γ secretion [369, 370]. More studies are needed to fully understand TIM-3 role in NK cell inhibition.

Apart from these inhibitory receptors, a main inhibitory immune checkpoint in cancer is the HLA-E/NKG2A axis.

1.4.1.1.1. Description and modulation of the HLA-E/NKG2A axis

HLA class I can be classified into classical (Ia) including HLA-A, -B, and -C, and nonclassical (Ib), comprising HLA-E, -G, and -F, CD1 antigens and MICA and MICB [88, 371]. HLA-E, Qa-1b in mice, is located in the MHC complex on chromosome 6, between *HLA-A* and *HLA-C* genes, and contains 8 exons. Although HLA-E is known for displaying a low polymorphism, with two dominant protein variants expressed in 99% of cases (HLA-E*01:01 and HLA-E*01:03), a recent study has updated HLA-E number of proteins to 110, from 256 different alleles [372]. HLA-E is composed of three extracellular α domains (α1-3), encoded by exons 2-4, and it is displayed on the cell surface together with β2-microglobulin. Moreover, it has a leader peptide (exon 1) before the extracellular domains and, after them, a transmembrane region (exon 5) and the intracellular domains (exons 6-7) [372]. In order to stabilize its expression, HLA-E needs to bind peptides. Most common peptides are derived from intracellular proteins or pathogens, amino acid residues 3-11 of signal peptides of HLA-A, -B, -C, and -G molecules, and Hsp60 [88, 373]. These peptides, containing 8 to 10 amino acids, are normally generated in the cytosol, after protein degradation by the proteasome, and transported into the ER by a transporter associated with antigen processing (TAP) [374]. Therefore, a functional TAP, the availability of these peptides and their binding affinity to HLA-E, determine HLA-E expression on the cell surface (Fig. 4) [373, 375]. This nonclassical molecule is expressed in all nucleated healthy cells, at low levels [88], except from trophoblasts cells in the placenta and ductal epithelial cells in the testis and epididymis [376], which indicates a key role in immune tolerance [375]. Moreover, HLA-E can be overexpressed in neoplastic cells.

HLA-E expression is elevated in several tumors as Ewing sarcoma [377], MM [378], cervical cancer [379], AML [380, 381], melanoma [382], and pancreatic ductal adenocarcinoma (PDAC) metastatic cells [383], correlating with a poor prognosis in non-small cell lung carcinoma [384], breast [385], ovarian [379, 386], MM [125, 387], glioblastoma [388], and colon cancer [389]. Regarding MM studies, Lagana et al. inferred HLA-E expression on MM patients from HLA-A data included in the CoMMpass study [387] and Yang et al. demonstrated that high expression of HLA-E correlates with an advances ISS stage and high-risk cytogenetics, proposing HLA-E as biomarker for high-risk MM [125]. Thus, an appropriate correlation between HLA-E expression and worse prognosis in MM patients has not been analyzed yet.

Furthermore, HLA-E expression can be modulated by different cytokines or drugs. BTZ treatment reduces HLA-E surface expression on MM cells, due to the ER stress generated by this drug and the reduction of signal peptides from HLA molecules degradation, caused by the proteasome impaired function [85]. At the same time, BTZ increases NKG2D-L expression, being more susceptible to NK cell killing [390]. Another MM drug, Selinexor, also downregulates HLA-E expression on lymphoma cells [101], as well as dinaciclib, a CDK inhibitor, on AML cells [391]. In addition, selenite, an inorganic selenium compound, has been found to abrogate HLA-E protein expression due to oxidative stress induction [392].

On the contrary, many studies have reported that IFN-γ upregulates HLA-E expression on MM cells [349, 393], AML cells [394], chronic lymphocytic leukemia (CLL) B-cells [348], and even on solid tumor cells [395]. However, it has been also reported that this cytokine can also induce HLA-E shedding by MMP [382]. Regarding MM, Pérez-Andrés et al. discovered that this cytokine, mainly produced by NK cells and T cells, is expressed at high levels in patients with MM [130].

As it has been previously described, NKG2A is a type II transmembrane glycoprotein that belongs to the C-type lectin-like receptor superfamily, which includes the NKG2 family. NKG2C and NKG2E (activating receptors) and NKG2A (inhibiting receptor) bind HLA-E, although HLA-E affinity binding to NKG2A is 6 times higher. Therefore, NK cell common response to HLA-E-bearing cells is inhibitory [375, 396].

NKG2A protein is encoded by the *KLRC1* gene, consists of 7 exons, and it is located in chromosome 12, as well as the gene that encodes CD94, another C-lectin type II receptor. NKG2A is displayed in the cell membrane forming a heterodimer with CD94, a receptor that lacks intracellular signaling [397]. NKG2A possesses a cytoplasmic tail containing ITIM domains, which recruits SHP-1/2 and triggers VAV1, ZAP70 and src-family kinases, as Fyn and Lck, dephosphorylation, reducing NK cell activity. This inhibitory complex, NKG2A/CD94, is expressed on NK cells, invariant NKT cells, activated $CD8^+$ T cells and γδ T cells [103].

NKG2A, as well as KIRs, is indispensable for NK cell education and autoimmune control [396]. However, under certain circumstances, as the cytokine-mediated activation of NK cells, typical education rules are not needed, thus unlicensed NK cells can acquire complete functions and mediate NK cell response [398].

Fifty percent of unstimulated PB circulating NK cells and around 60% of tumor-infiltrating NK cells express NKG2A [399]. Of note, NKG2A expression correlates with a poor prognosis in AML, liver, and head and neck cancer patients [103].

NKG2A expression can be also modulated by cytokines and drugs. Remarkably, dasatinib, a tyrosine kinase inhibitor, used for chronic myeloid leukemia (CML) treatment, reduces NKG2A expression, while augmenting NK cell antitumor efficacy. However, other tyrosine kinase inhibitors as imatinib and nilotinib do not downregulate NKG2A expression. Cytokines IL-21, IL-15, IL-12, IL-10, and TGF-β are known to overexpress NKG2A presence on the immune effectors cell membrane [396].

The interaction of HLA-E and NKG2A disrupts the actin network, impairing effector-target immune synapse [400]. NKG2A binding to HLA-E is tuned depending on the peptides that HLA-E is presenting and therefore NKG2A inhibitory signaling can be modulated or attenuated. For example, HLA-G peptides presenting on HLA-E molecules induce the strongest inhibition reaction [401], while Hsp60 loading of HLA-E molecules impairs NKG2A binding to HLA-E [402].

Due to the high expression of HLA-E in diverse tumors and the increased expression of NKG2A, above all on NK cells, as well as in activated or CAR-modified NK cells, diverse alternatives have been proposed to impair this immune checkpoint inhibitory response (Fig. 16).

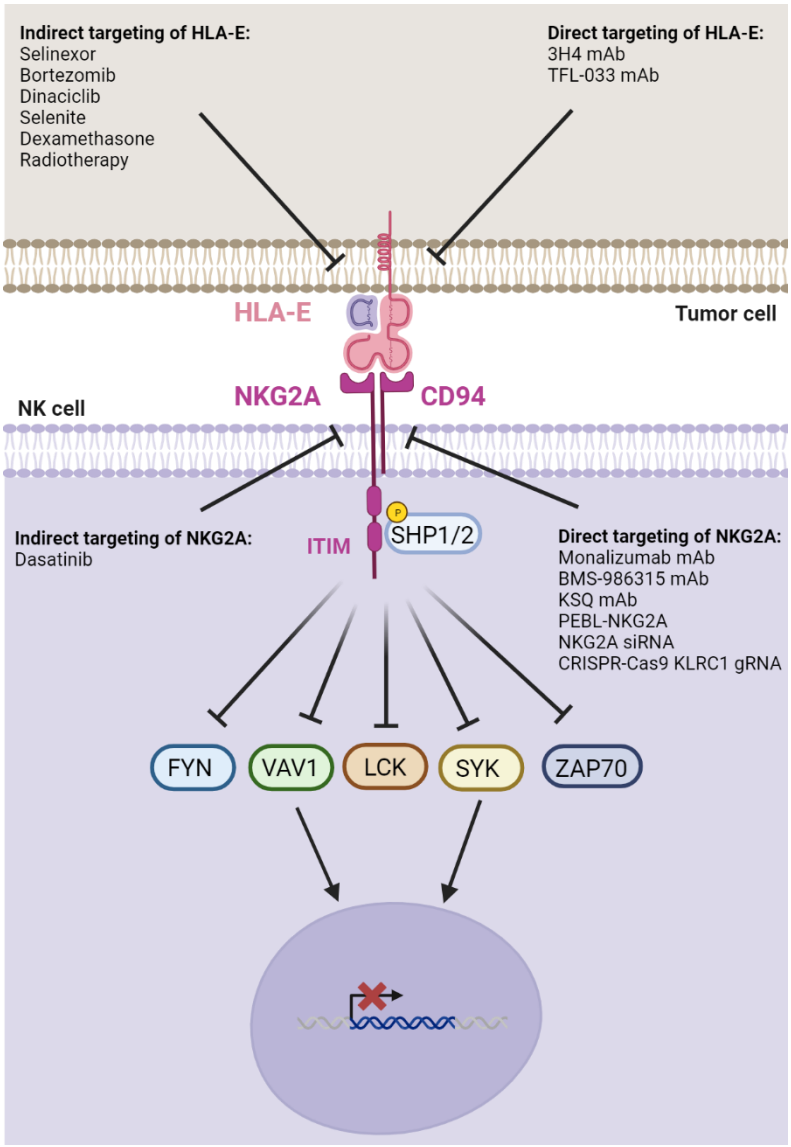

Figure 16. Modulation and signaling of HLA-E/NKG2A axis. HLA: human leukocyte antigen; mAb: monoclonal antibody; PEBL: protein expression blocker; ITIM: immunoreceptor tyrosine-based inhibitory motif; SHP-1: Src homology region 2 domain-containing phosphatase-1; LCK: lymphocyte-specific protein tyrosine kinase; SYK: spleen tyrosine kinase; ZAP-70: Zeta-chain-associated protein kinase 70. Adapted from Fisher et al. 2022 [103]. Created with BioRender.com.

Direct targeting of HLA-E has been proposed, using the 3H4 and TFL-033 mAbs. Despite these Abs have demonstrated efficacy *in vitro* [103], most studies have been focused on targeting the NKG2A receptor instead.

1.4.1.1.2. Preclinical studies targeting NKG2A

The elimination of NKG2A to improve NK cell responses has been also carried out against different types of cancers. A siRNA has been used to permanently reduce NKG2A

mRNA levels in NK cells, which has enhanced NK cell efficacy against B lymphoblastoid cells [403]. A new strategy to retain NKG2A receptor by the ER was developed by Kamiya et al. Fragments from the mouse anti-human NKG2A blocking Ab (Z199) were linked to ER-retention domains to generate NKG2A protein expression blockers (PEBLs). These proteins hampered NKG2A expression on NK cell surface, enhancing their cytotoxic activity against different HLA-E^+ tumors, even more than blocking NK cells with the mouse α-NKG2A Ab Z199 [394]. Moreover, Ruggeri et al. demonstrated the efficacy of monalizumab, a humanized α-NKG2A IgG4 blocking Ab, on NK cells against engrafted leukemia mice and proposed the use of this Ab in combination with adoptive NK cell therapy or after stem cell transplant recovery, to foster tumor reduction [404]. In CLL and EBV^+ lymphomas, the improvement of NK cell cytotoxicity due to NKG2A blockade with monalizumab, has been demonstrated, suggesting its use in clinical trials [348]. In solid tumors, monalizumab treatment significantly enhances antitumor NK cell killing against HLA-E^+ tumor cells [383, 395], although its combination with an α-PDL1 Ab (durvalumab) was needed to reduce tumor burden *in vivo* [399]. In addition, intratumoral co-injection of human PB NK cells with monalizumab was able to reduce tumor growth in immunodeficient mice bearing head and neck squamous cell carcinoma (HNSCC) [405]. Remarkably, Battin et al. have discovered that monalizumab blocking efficacy on NK cells depends on the peptides presented by HLA-E, as monalizumab was more effective when HLA-E loaded HLA-A, -B, and -C peptides, instead of HLA-G peptide [402].

Regarding MM and out of the CAR setting, first approaches isolating $NKG2A^+$ and $NKG2A^-$ NK cells reported that $NKG2A^-$ degranulation was not impaired by HLA-E^+ MM cells, while $NKG2A^+$ NK cells degranulation was affected [378]. Although Mahaweni et al. reported that NKG2A blockade with the Z199 Ab did not enhance $NKG2A^+$ NK cells degranulation against primary MM cells, other studies have demonstrated the relevance of targeting this inhibitory receptor in this tumor [406]. Tognarelli et al. shown that the blockade of NKG2A with the same Ab, the Z199, consistently increases the killing activity of activated NK cells, expanded from diagnosed MM patients or HD PB [393]. In 2022, during the development of this thesis, Bexte et al. deleted the NKG2A-encoding *KLRC1* locus in NK cells by CRISPR-Cas9, demonstrating their enhanced efficacy against MM primary cells [349].

Concerning CAR NK cells, combination of this adoptive therapy with complete or partial NKG2A elimination or with NKG2A neutralization has not been reported yet.

1.4.1.1.3. Clinical trials with α-NKG2A neutralizing antibodies

Despite these impressive preclinical results interfering the HLA-E/NKG2A axis, clinical study results are controversial. Most trials are currently testing monalizumab, in monotherapy or in combination with other blocking Abs or chemotherapy (Table 5).

However, monalizumab efficacy as a single agent against solid tumors did not meet the expected results, only achieving stable disease responses against gynecologic malignancies [407]. In addition, first HNSCC patients from the phase II UPSTREAM trial were treated only with monalizumab, obtaining an OS of 6.7 months and 1.7 months of median PFS. Due to these poor results, they decided to combine this α-NKG2A Ab with durvalumab, an α-PD-L1 Ab, in the following cohort of patients [408]. Similar and other combinatorial strategies were carried out by other groups. Regarding HNSCC patients (NCT02643550), Cohen et al. tested the efficacy and safety of the combination of monalizumab and cetuximab, an α-EGFR Ab. In a cohort that included patients who had relapsed after platinum-based therapies, an 8.5-month median OS, a 27.5% ORR and a 4.5-month median PFS were reported. Moreover, a second cohort including patients, who not only had relapsed to platinum therapies, but also to PD-L1 inhibitors, an ORR of 20% and a median duration of response of 5.2 months were obtained. More than 10% of patients suffered from dermatitis acneiform, dry skin, pruritus, fatigue, hypomagnesemia, skin fissures, infusion-related reaction, mucosal inflammation, nausea, paronychia, rash, asthenia and diarrhea after treatment [409]. Additionally, a new triplet regimen including monalizumab, cetuximab, and durvalumab has been proposed for HNSCC patients within the same clinical trial (NCT02643550). Last results reported an ORR of 32.5% (3 patients achieved CR) and the median PFS was 6.9 months. Most common adverse events were increased lipase or amylase and dermatitis acneiform [410]. The phase II study COAST for non-small cell lung cancer (NSCLC) patients has combined monalizumab and durvalumab, obtaining a 72.7% 12-month PFS and 35.5% ORR, better results than its control (only durvalumab). Median PFS was 15.1 months. Most frequent adverse events found after durvalumab plus monalizumab were also described for durvalumab monotherapy (cough, dyspnea, pneumonitis, asthenia, and pruritus) [411]. Moreover,

MIMOSA phase II trial was designed for $HER2^+$ breast cancer patients, combining trastuzumab and monalizumab. Unfortunately, recently published results reported that, although both treatments were well tolerated, they did not achieve objective responses [412].

Regarding hematologic tumors, a phase I trial with a short follow-up has shown promising results. Monalizumab efficacy and safety has been determined after allogeneic stem cell transplant in patients with AML, myelodysplastic syndrome (MDS), lymphoma, CLL, and myelofibrosis. This drug was highly tolerated, with no side effects, and the short-term efficacy analysis revealed that 13 out of 15 patients had CR. Of note, the blockade of NKG2A on circulating NK cells after 14 weeks from infusion was detected [413].

These results indicate that monalizumab monotherapy is not able to restore NK and T cell cytotoxicity against tumor cells within the patient, especially in solid tumors, probably due to their exhausted phenotype induced by tumor cells and the TME. However, fostering these immune cells efficacy with other blocking Abs or new approaches, such as CAR NK cell adoptive therapy, may result in better clinical outcomes.

Another human α-NKG2A Ab that is being clinically studied is BMS-986315. This α-NKG2A is an inert IgG1.3, which contains 3 mutations in the heavy chain, L234A, L235E and G237A, to prevent Fc-mediated activity, through CD16 recognition, and C1q binding. Estimated half-life of this Ab in circulation is approximately 16.5 days [414]. Remarkably, the efficacy and toxicity of this Ab has been never compared to other α-NKG2A Abs as monalizumab or KSQ. Although preclinical data with BMS-986315 Ab has not been found, its efficacy is being tested against solid tumors, in combination with nivolumab or cetuximab (NCT04349267), and NSCLC, together with nivolumab and chemotherapy (NCT06094296). Of note, neither this Ab has been used against hematologic tumors, including MM, nor in combination with CAR NK cells.

Nº	Status	Study start	Treatment	Condition	Phase	Pat	Location	NCT
1	Recruiting	2022	Monalizumab plus Durvalumab	NSCLC	III	999	Global	NCT05221840
2	Recruiting	2022	Monalizumab plus durvalumab plus platinum doublet chemotherapy	NSCLC	II	350	Global	NCT05061550
3	Active, not recruiting	2020	Monalizumab plus Cetuximab	HNSCC	III	370	Global	NCT04590963
4	Active, not recruiting	2021	Monalizumab plus Trastuzumab	Breast cancer	II	38	Netherlands	NCT04307329
5	Recruiting	2019	Monalizumab plus Durvalumab	NSCLC	II	120	France	NCT03833440
6	Active, not recruiting	2019	Monalizumab plus Durvalumab	NSCLC	II	188	Global	NCT03822351
7	Recruiting	2017	Monalizumab	HNSCC	II	340	Europe	NCT03088059
8	Unknown	2016	Monalizumab	Hematologic malignancies	I	18	France	NCT02921685
9	Completed	2015	Monalizumab plus Cetuximab ± anti-PD-L1	HNSCC	I/II	143	Global	NCT02643550
10	Terminated	2015	Monalizumab plus Ibrutinib	CLL	I/II	22	USA	NCT02557516
11	Active, not recruiting	2016	Monalizumab plus Durvalumab	Solid tumors	I/II	383	Global	NCT02671435
12	Recruiting	2023	Monalizumab plus Durvalumab plus Chemotherapy	SCLC	II	38	USA	NCT05903092
13	Withdrawn	2017	Monalizumab plus Chemotherapy plus radiotherapy	Esophagus and gastroesophageal junction carcinomas	I/II	0	Belgium	NCT03307941
14	Completed	2019	Monalizumab plus Durvalumab	NSCLC	II	84	Global	NCT03794544
15	Completed	2020	Monalizumab	Hematological and solid tumors	I	19	France	NCT04333914
16	Withdrawn	2020	Monalizumab plus Durvalumab	Colorectal cancer	II	0	Unknown	NCT04145193
17	Recruiting	2020	BMS-986315 ± nivolumab or cetuximab	Solid tumors	I/II	308	America	NCT04349267
18	Not yet recruiting	2023	BMS-986315 plus nivolumab and chemotherapy	NSCLC	II	196	Global	NCT06094296

Table 5. Current clinical trials using α-NKG2A antibodies for cancer treatment. NCT: national clinical trial; NSCLC: non-small cell lung cancer; HNSCC: head and neck squamous cell carcinoma; PD-L1: programmed cell death ligand 1; CLL: chronic lymphocytic leukemia; SCLC: small-cell lung cancer; NSCLC: non-small cell lung cancer.

1.4.2. Strategies to enhance CAR NK cell persistence

Within efficacy challenges, one of the relevant limitations of CAR NK cells is their low lifespan. *In vivo* persistence after adoptive transfer has been previously reported to correlate with clinical responses [415]. Mature NK cell persistence in circulation is around 1-2 weeks and activated and expanded human NK cells can survive from 4 to 5 weeks without cytokine stimulation and up to 68 days when they are engineered to express IL-15, in xenografted immunodeficient mice [280]. First approaches tested multiple CAR NK cell infusions to enhance their sustenance in circulation, but the

persistence of CAR NK cells after subsequent infusion doses was even shorter [416]. After lymphodepletion recovery, T cells from the host generate allorejection of CAR NK cells via HLA-TCR mismatch, reducing their number in the bloodstream. For this reason, administration of haploidentical CAR NK cells has been carried out by many groups [417, 418]. In line with this, multiengineered CAR NK cells can avoid recognition through knocking out HLA-I molecules or expressing the HLA-E ones, reducing T and NK cell allorejection, respectively, by the host [296]. Alternatively, CAR sequences can be modified to induce interleukin secretion (armoured CAR) [419], enhancing NK cell cytotoxicity and persistence *in vivo*. This time, second infusions of CD19-CAR/IL-15 NK cells achieved a longer CAR NK cell persistence [420]. Other strategies are the administration of exogenous IL-15, using IL-15 superagonists as NKTR-255 [421] or ALT-803 [422]. In line with this, oncolytic virus carrying IL-15/IL-15R complexes have enhanced EGFR-CAR NK cell proliferation (Fig. 14) [296].

It has been reported that, although NK cells belong to the innate immunity, they can acquire memory properties after their interaction with haptens, viruses or tumor cells as well as after an activation with a combination of cytokines (cytokine-induced memory-like; CIML). One of the main properties of these cells is their improved persistence compared to conventional NK cells [423, 424].

1.4.2.1 Cytokine-induced memory-like NK cells

First studies reported memory-like properties in mouse NK cells after their exposure to haptens or viruses (MCMV, Zika) [423, 425]. Mouse Ly49H^{+} NK cells were found to proliferate after MCMV interaction and remain for months at low frequency, as happens with T cells. The same reaction was found in human NK cells regarding CMV, hantavirus, and chikunguya virus [423]. In the case of CMV, NKG2C^{+} NK cells proliferated and then contracted, persisting for up to a year. These cells displayed a mature phenotype (CD56^{dim} CD57^{+}), reduced NKG2A expression and produced high amounts of IFN-γ [426]. A gene expression array comparing these memory-like NK cells (NKG2C^{+}) with NKG2C^{-} revealed 89 upregulated and 102 downregulated genes, suggesting that the response to virus exposure triggers several gene expression modifications that lead to memory properties in NK cells [427]. However, chronic CMV stimulation fostered PD-1 and LAG-3 expression and consequently, NK cell exhaustion [428].

Alternatively, tumor-priming is also able to induce a memory-like phenotype in NK cells (TIML-NK cells). These cells have been described to be tumor-specific, show a higher cytotoxicity and perforin release and display maturity markers ($CD57^+$ $KLRG1^+$ KIR^+). Remarkably, exposure to tumor cells rapidly induces S-phase entry [424]. TIML-NK cells, primed with the tumor product INKmune™, have been tested in AML and MDS patients, proving safety and quick peripheral NK cell activation [429].

In 1999, Fehniger et al. tested the effect of IL-18, IL-15, or IL-12 on human NK cells, where IL-18 and IL-12 induced more IFN-γ, the combination of IL-15 and IL-12 significantly increased IL-10, TNF-α, and MIP-1β, while IL-15 and IL-18 augmented GM-CSF production [430]. In 2009, Cooper et al. cultured mouse NK cells overnight with the combination of the three cytokines, IL-18, IL-15, and IL-12. These preactivated NK cells had enhanced IFN-γ secretion and persisted over 3 weeks in the mice. Moreover, these cells strongly responded upon stimulation compared to conventional NK cells, suggesting that the combination of these three cytokines induces a memory-like phenotype, calling them CIML-NK cells (Fig. 17). Notably, all these properties passed on to their daughter cells, therefore this preactivation promotes DNA changes that can be inherited [431]. In 2012, Romee et al. corroborated these memory properties in human NK cells. These CIML-NK cells had improved IFN-γ production, enhanced response after stimulation, higher proliferation, and their daughter cells also inherited all these characteristics [432].

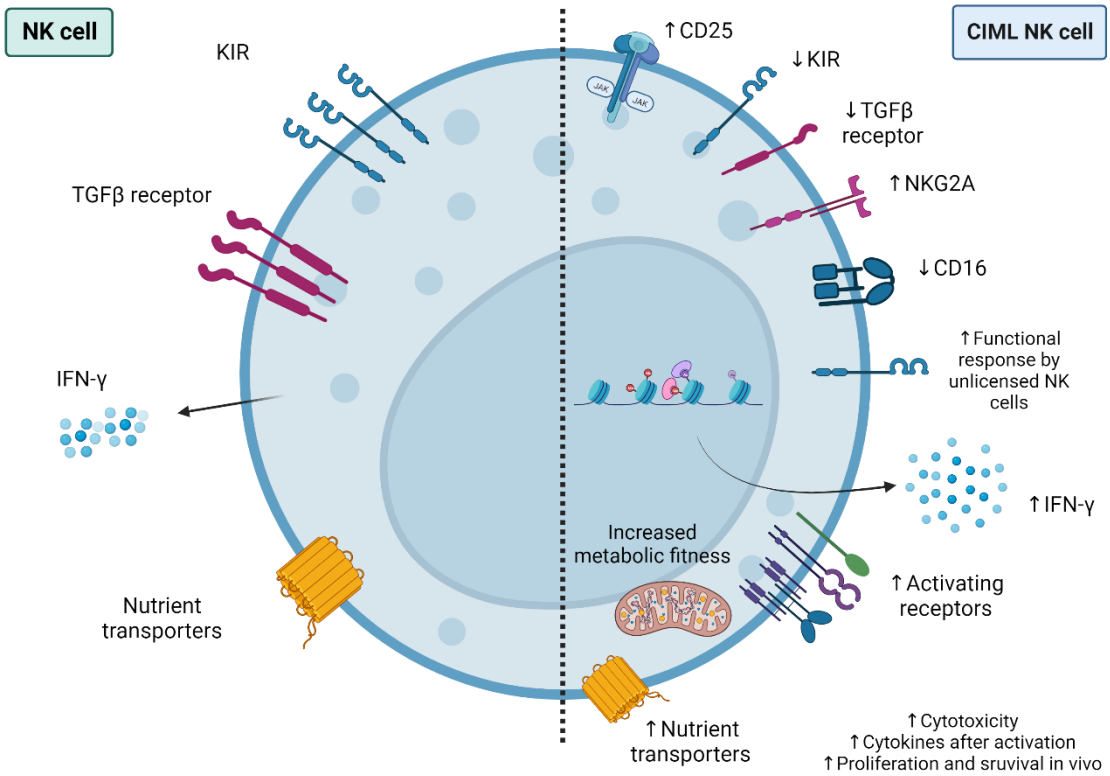

Figure 17. CIML-NK cells display a different phenotype compared to conventional NK cells. KIR: killer-cell immunoglobulin-like receptor; TGFβ: transforming growth factor-β; CIML: cytokine-induced memory-like. Adapted from Tarannum et al., 2021 and Berrien-Elliott et al. 2023 [296, 433]. Created with BioRender.com.

Since then, several studies have been focused on this new population, mainly in describing its phenotype. CIML-NK cells have been described to overexpress activation receptors such as CD25 [434-436] and CD69, NKG2A, CD56 [437], and Sca-1 while decreasing CD62L, CD16 [435, 438], and CXCR4 expression [439]. Moreover, they had enhanced SEMA7A (a potent cytokine stimulator) [440], TNF-α [441], IFN-γ [398, 435, 442], FasL, and perforin production, and the transcription factors T-bet and Blimp-1 were upregulated [438]. In contrast, CIML-NK cells possess a lower expression of TGFβR, being less inhibited by the presence of TGFβ in the TME, and KIRs [443]. Of note, the exposure of NK cells to IL-12, IL-15, and IL-18 has been reported to restore the functional activity of unlicensed NK cells [444].

Recently, mass cytometry analysis revealed that CIML-NK cells have high CD56, Ki-67, NKG2A, NKG2D, NKp30, and NKp44 expression and low CD16 and CD11b expression *in vitro,* as well as an increased frequency of TRAIL, CD69, NKG2A, NKp30, and CD62L positive NK cells and a reduced CD27 and CD127 NK cell percentage *in vivo*,

compared to baseline NK cells [445]. Another CyTOF report described that CIML-NK cells exhibit reduced CD16, CD57, CD8, NKp30, NKp46, and NKG2D expression and increased CD56 and CD69 expression [446]. Additionally, a transcriptomic study shown an enrichment in KLRC1 mRNA and GATA3 target genes compared to conventional NK cells [445].

CIML-NK cells have shown *in vitro* efficacy against hematological malignancies as ALL [437, 447], AML [437, 442, 445], as well as against solid tumors such as ovarian [441], hepatocellular carcinoma [448], melanoma [449, 450], sarcoma, and renal cell carcinoma [437].

Additionally, CIML-NK cells proliferated more compared to conventional NK cells *in vitro* and *in vivo* [436, 439], although a higher apoptosis rate has been also associated [441].

Furthermore, some groups have focused their studies on unveiling CIML-NK cell metabolism. These cells have an increased metabolic activity, demonstrated by an enhanced glycolytic capacity and oxidative phosphorylation (OXPHOS), above all during the initial days after preactivation with IL-12, IL-15, and IL-18, compared to IL-15 control NK cells [451, 452]. Of note, limiting OXPHOS flux during preactivation, strongly impaired CIML-NK cell IFN-γ production and cytotoxicity, suggesting the importance of nutrients for CIML-NK correct differentiation [452]. Furthermore, CIML-NK cells overexpress nutrient transporter expression, including the glucose transporters GLUT1 and GLUT3, the amino acid transporter CD98, and the transferrin receptor CD71 [453].

Although CIML-NK cells have shown efficacy in preclinical studies, there are several modifications or combinations that can be carried out to optimize these effector cells responses. Since CIML-NK cells overexpress NKG2A, and based on previously described results blocking or knocking out NKG2A expression on conventional NK cells, Berrien-Elliot et al. impaired NKG2A inhibitory signaling in CIML-NK cells with an α-NKG2A Ab, enhancing transfectant HLA-E^{+} leukemia cell killing [445]. Moreover, this group has also combined CIML-NK cells with cetuximab, resulting in increased NK cell activity against HNSCC [454]. In addition, Kerbauy et al. have combined CIML-NK cells with a bispecific CD30xCD16 Ab (AFM13), enhancing CD30^{+} lymphoma tumor killing [455].

Recently, CIML-NK cells have been modified to enhance their efficacy through CAR redirection. First study engineered CIML-NK cells to express a CD19-CAR, achieving improved *in vivo* responses against NK-resistant lymphomas, [456]. In line with this, He et al. also modified CIML-NK cells to express a CD19-CAR and demonstrated enhanced antitumor efficacy against B cell malignancies [457]. Dong et al. incorporated a TCR-like CAR structure that recognizes the intracellular neoepitope NPM1 presented by HLA-A2 on the cell membrane, targeting AML cells with NPM1c mutations [458]. CIML-NK cells have been also redirected to solid tumors through CAR expression. Jacobs et al. incorporated an α-EphA2 CAR in CIML-NK cells, resulting in a higher IFN-γ production and cytotoxicity against HNSCC [454].

Due to the impressive preclinical results, CIML-NK cell safety and antitumor efficacy are being tested in several clinical trials, most of them in AML patients (Table 6). First-in-human treatment with CIML-NK cells (NCT01898793) started in 2014. First results considering 9 AML patients described 55% of ORR and 45% CR [442]. Moreover, the NCT02782546 study revealed that 87% of the AML patients had achieved CRs after one month from CIML-NK cells infusion. Of note, these cells persisted for over 2 months in AML patients [417]. Another AML trial in pediatric and young adult patients, achieved CRs in 4 out of 8 evaluable patients, with no significant toxicities. NK cells were the dominant lymphocyte subset in BM of these patients until day 100 after CIML-NK cells infusion and ex vivo analysis demonstrated that these NK cells retained their increased function for at least 4 weeks after administration [418]. Additionally, the NCT04024761 study described the rapid expansion of CIML-NK cells after infusion, although 4 out of 6 myeloid malignancies patients developed pancytopenia and all of them had fever, due to IL-2 administration during the first 12 days. Remarkably, 66.67% of patients achieved CR [459].

Recently, a CIML-NK cell product, WU-NK-101, has been generated by the company Wugen. These allogeneic PB CIML-NK cells have shown the same phenotypic characteristics, as previously described by other groups. They have improved glycolytic and OXPHOS capacity and exhibited an enhanced cytotoxic capacity that is not impaired by cytokines or inhibitory cells present in the TME [460]. Nowadays, this product is being tested as monotherapy (NCT05470140) and in combination with cetuximab (NCT05674526).

Of note, a clinical trial is testing autologous CIML-NK cell efficacy in NDMM patients who are MRD^+ and eligible for ASCT, in combination with low dose IL-2, intravenous Igs (IVIGs) and the molecule BHV-1100 (also known as KP1237). It is a CD38 Ab recruiting molecule (ARM) that binds CD38 on the target cell and also the exogenous IVIGs [461]. However, preliminary results have not been published yet and no preclinical data from these trials is available, indicating the lack of knowledge of CIML-NK cell efficacy against MM. Moreover, to date, no clinical data showing CAR CIML-NK cells against hematologic tumors have been published.

N°	Status	Study start	Treatment	Condition	Phase	Pat	Location	NCT
1	Recruiting	2023	CIML NK	AML	I/II	20	USA	NCT05580601
2	Not yet recruiting	2023	Autologous or allogeneic ML NK cells plus nivolumab and relatlimab	Melanoma	I	33	USA	NCT05629546
3	Withdrawn	2022	CIML NK plus IL-2	AML and MDS	II	0	USA	NCT04893915
4	Recruiting	2020	CIML NK plus N-803 ± ipilimumab or cetuximab	HNSCC	I	25	USA	NCT04290546
5	Withdrawn	2023	CIML NK	AML	II	0	USA	NCT04354025
6	Recruiting	2017	CIML NK	AML	I/II	110	USA	NCT03068819
7	Terminated	2014	CIML NK plus IL-2	AML and MDS	I/II	89	USA	NCT01898793
8	Recruiting	2017	CIML NK plus ALT-803	AML	II	60	USA	NCT02782546
9	Active, not recruiting	2019	CIML-NK	AML, MDS, myeloproliferative neoplasm and juvenile myelomonocytic leukemia	I	50	USA	NCT04024761
10	Recruiting	2021	Autologous ML NK plus BHV-1100	MM	I	25	USA	NCT04634435
11	Recruiting	2023	WU-NK-101	AML	I	24	USA and Australia	NCT05470140
12	Not yet recruiting	2023	WU-NK-101 plus Cetuximab	Colorectal and HNSCC	I	30	-	NCT05674526
13	Terminated	2021	CT101a (CIML-NK)	AML	I	3	China	NCT05256277

Table 6. Current clinical trials using CIML-NK cells against tumor malignancies. NCT: national clinical trial; CIML: cytokine-induced memory-like; AML: acute myeloid leukemia; MDS: myelodysplastic syndrome; HNSCC: head and neck squamous cell carcinoma; MM: multiple myeloma.

2. HYPOTHESIS AND OBJECTIVES

Despite all the therapeutic strategies approved for the treatment of MM, most patients progress, with increasingly shorter response periods, and MM is still an incurable disease. MM microenvironment is characterized by a high immunosuppression, mainly in late stages of the disease. The discovery of new targeted therapies, as CAR T cells, has revolutionized the treatment of hematologic malignancies, although severe toxicities, such as CRS, neurotoxicity and prolonged cytopenias, together with CAR T cell exhaustion, responsible for suboptimal responses, have arisen the need to find new CAR effectors. Allogeneic CAR NK cells have emerged as a safer, off-the-self, cost-effective approach, compared to CAR T. However, CAR NK cell reduced activity via inhibitory immune checkpoints and low persistence *in vivo*, mainly caused by the immunosuppressive TME, are limiting CAR NK antitumor responses in preclinical studies and clinical trials. Published studies have described the HLA-E/NKG2A axis as a main inhibitory signal in other tumors, correlating with a poor overall survival, and combinatorial strategies to disrupt this interaction have reported promising results in cancer patients. In addition, cytokine-induction of a memory-like phenotype on NK cells is able to enhance NK cell lifespan and proliferative capacity, which have an impact on NK cell efficacy.

2.1. Hypothesis

Combined strategies of CAR activated and expanded NK (NKAE) cells with α-NKG2A Abs or the induction of a memory phenotype can enhance CAR NK immunotherapy anti-MM efficacy and persistence.

2.2. Objectives

Considering the current limitations of CAR NK cells in the treatment of hematologic tumors, the main objective of this thesis is the generation of optimized therapeutic combinations for CAR NK cells to enhance RRMM treatment. Specific objectives of this thesis are:

1. To analyze the relevance of the HLA-E/NKG2A axis in MM.
2. To potentiate the anti-MM activity of NKG2D- and BCMA-CAR NKAE cells by disrupting the HLA-E/NKG2A axis with a novel α-NKG2A antibody.
3. To increase the immunotherapy persistence and efficacy by reprogramming NKG2D-CAR NKAE cells towards a cytokine-induced memory-like phenotype

3. MATERIALS AND METHODS

3.1. Cell lines and primary samples

3.1.1. Cell lines

MM cell lines NCI-H929 (ACC 163), L-363 (ACC 49) and RPMI-8226 (ACC 402) were purchased from DSMZ (Leibniz Institute, Germany) and U-266B1 (TIB-196) from ATCC, XG-1 cell line was provided by Dr. Shelly Lawson (Sheffield University, UK), ARP-1 cell line (CVCL_D523) was provided by Dr. Joshua Epstein (Arkansas Cancer Research Center, Arkansas, USA) and BTZ-resistant cell lines NCI-H929 R20 and RPMI-8226 R7 were kindly provided by Dr. Joaquín Teixidó (*Centro de Investigaciones Biológicas Margarita Salas*, Madrid) [462].

K562-mb21-41BBL cell line (Clone 9.mbIL21 or CSTX002), provided by Dr. Dean A. Lee (Nation Wide Children, Ohio, USA), has been used to promote NK cell *in vitro* activation and expansion. For this purpose, K562, an erythroleukemic cell line with positive Philadelphia chromosome, was modified to constitutively express membrane-bound IL-21 (mb21), 4-1BB ligand (4-1BBL or CD137-L), CD64, CD86 and truncated CD19. Both IL-21 and 4-1BBL promote NK cell activation and proliferation [463].

HEK293T, an embryonic cell line modified to express SV40 T antigen, was required for lentiviral packaging. This cell line was obtained from DSMZ.

All cell lines, except HEK293T, were cultured in Roswell Park Memorial Institute (RPMI)-1640 medium (Biowest) supplemented with 10% fetal bovine serum (FBS; Hyclone), 2 mM L-glutamine and 100 IU/mL penicillin/streptomycin (P/S; Lonza) at 37ºC in a humidified atmosphere with 5% CO_2. Additionally, XG-1 cell line were cultured with 1 ng/ml recombinant human IL-6 (Miltenyi). HEK293T cell line was cultured in Iscove´s Modified Dulbecco´s Medium (IMDM; Lonza) supplemented with 10% FBS and 100 IU/ml P/S. The medium was changed every 2-3 day and cell count was assessed in a Neubauer chamber (VWR) using 0.4% Trypan Blue (Gibco) exclusion method. The absence of mycoplasma was regularly tested by Polymerase Chain Reaction (PCR) and cell line integrity was tested through short tandem repeat (STR) analysis in the Genomic Unit from *Centro Nacional de Investigaciones Oncológicas* (CNIO), Madrid.

3.1.1.1. Cell lines modified in the laboratory

Additionally, some cell lines were modified due to experiment requirements.

For BTZ-resistant RPMI-8226 R20 cell line generation, RPMI-8226 R7 cells were gradually cultured with 2 nM BTZ (MedChemExpress) up to 20 nM BTZ, until culture viability was up to 80%.

For mouse models, U-266 and RPMI-8226 cell lines were lentivirally transduced with ffLucGFP vector to constitutively express luciferase and GFP for tumor burden detection.

All these cells were cultured as indicated in 3.1.1.

3.1.2. Primary samples

HD PB samples (n=52), as well as MGUS and MM patients BM aspirates (n=76), were obtained from *Hospital 12 de Octubre* (H12O). Healthy BM samples from orthopedic patients (n=20) were obtained from *Hospital de parapléjicos de Toledo*, hereinafter referred to as HD BM samples, and CB samples (n=4) from *Centro de Transfusiones de la Comunidad de Madrid*. Both HD and MM patients gave their written informed consent to collaborate in the study (nº20/326), previously approved by the H12O ethics committee, in accordance with the Declaration of Helsinki protocol. All primary samples were analyzed, according to the arrival order of patients at hospital.

3.2. Expansion, culture and CAR transduction of activated and expanded NK cells (NKAE)

3.2.1. Generation of CAR NKAE and CAR CIML-NKAE cells from PB samples

NKAE and CIML-NKAE cells were generated from PB mononuclear cells (PBMCs). Two 9ml-EDTA PB tubes, collected from HDs, were diluted 1:4 with Phosphate-Buffered Saline (PBS; Gibco) and added 3:1 over Ficoll-Paque (Sigma-Aldrich). Samples were centrifuged at 1,800 rpm for 20 minutes (acceleration 6; deceleration 3). PBMCs layer was collected, washed with PBS, and centrifuged at 1,600 rpm for 10 minutes. PBMCs were then co-cultured at a ratio of 1:1.5 with K562-mb21-41BBL cells, previously irradiated under 100 Gy, at 1.2 x 10^6 cells/ml in RPMI-1640 medium

supplemented with 10% human AB serum (Sigma-Aldrich), 2 mM L-glutamine, 100 IU/mL P/S and 50 IU/ml IL-2 (Miltenyi). After 3 days, the medium was changed, maintaining the culture at 1.2 x 10^6 cells/ml. On day 6 of culture, NKAE cells were isolated by immunomagnetic negative selection following the manufacturer´s instructions (NK cell Isolation Kit, Human, Miltenyi). NKAE cell purification was analyzed using flow cytometry. On day 8, purified NKAE cells were lentivirally transduced with NKG2D- or BCMA-CAR vectors (as described in 3.2.5) for 16 hours. After washing with PBS, NKG2D- and BCMA-CAR NKAE cells were preferentially used between days 14-18 of culture and maintained until a maximum time of 23 days, changing the medium every 3 days (Fig. 18A).

To obtain CAR CIML-NKAE cells, after removing lentivector-containing medium, CAR NKAE cells were exposed to 100 ng/ml IL-18 (MBL), 20 ng/ml IL-15 (Miltenyi), 10 ng/ml IL-12 (Miltenyi) and 50 IU/ml IL-2 and cultured at 3.7 x 10^6 cells/ml using the medium described above. Control NKG2D-CAR NKAE cells were also incubated at 3.7 x 10^6 cells/ml with 50 IU/ml IL-2. After 16h, cells were washed three times with PBS, to remove residual cytokines, and resuspended in the culture medium with a maintenance dose of 50 IU/ml of IL-2 at 1.5 x 10^6 cells/ml until day 23 of culture, changing the medium every 3 days, but experiments were mainly performed from day 14 to 18 of culture (Fig. 18B).

Considering that transgene stable expression using lentivectors is achieved between 5-7 days [464], at day 6 after transduction, CAR expression was confirmed.

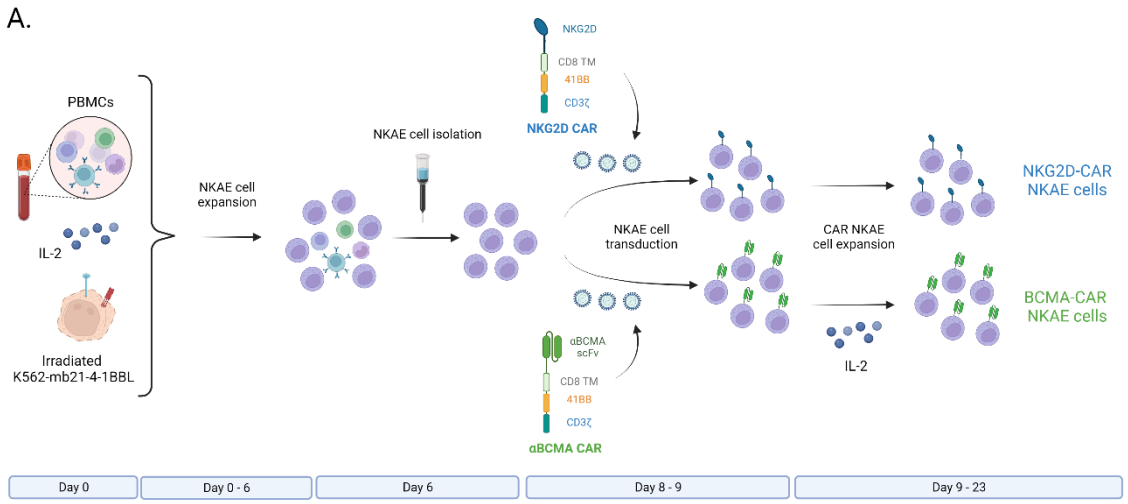

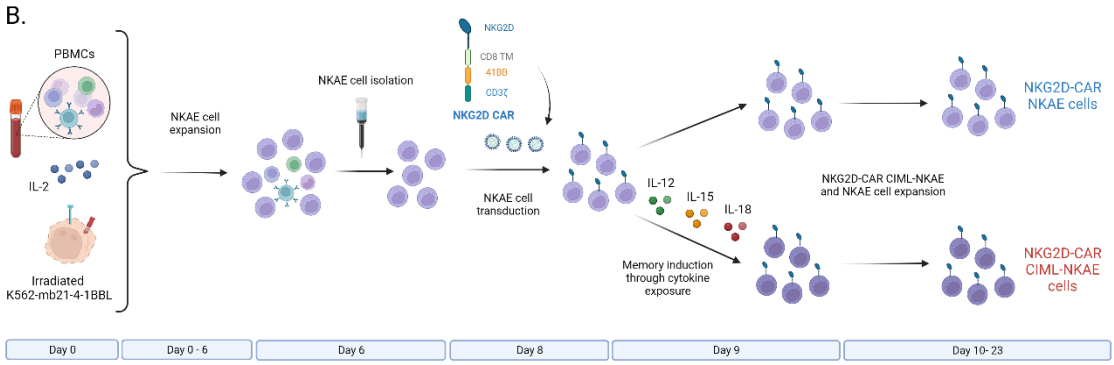

Figure 18. CAR NKAE cell generation protocol. Schematic representation of A) NKG2D- and BCMA-CAR NKAE cell and B) NKG2D-CAR CIML-NKAE and NKAE cell generation and expansion from HD PB samples. PBMCs: peripheral blood mononuclear cells; IL: interleukin; mb21: membrane-bound IL-21; NKAE cells: activated and expanded NK cells; CIML: cytokine-induced memory-like. Created with BioRender.com.

3.2.2. CAR molecule design and transfer plasmid amplification

Second generation NKG2D- and BCMA-CAR molecules as well as ffLucGFP reporter gene were needed for the development of this thesis. CAR molecule design and lentivector production were performed in collaboration with the Division of Hematopoietic Innovative Therapies from CIEMAT, Madrid.

NKG2D-CAR transfer plasmid (pTRPE_NKG2D-ECD_4-1BBz) was kindly provided by Daniel J. Powell Jr. (Perelman School of Medicine, Pennsylvania, USA). The extracellular domain contains the 82-216 amino acid sequence from the human NKG2D receptor ectodomain [465], and the intracellular region contains 4-1BB costimulatory domain, bound to the CD3ζ chain.

For the BCMA-CAR transfer plasmid (pTRPE_BCMA_4-1BBz) design, the NKG2D-CAR lentiviral backbone was used. This sequence was designed using SnapGene™ software and synthesized at GeneArt (Thermofisher). NKG2D ectodomain sequence was replaced by the kappa light chain signal peptide (κLC) followed by clone 4ZFO α-BCMA single-chain variable fragment (scFv) (mouse/human chimera J22.9-xi mAb) and the hinge and transmembrane domain of the CD8a receptor. The sequence was flanked by the restriction sites of the Nhe I and Nde I enzymes (New England Biolabs) and inserted in NKG2D-CAR backbone using a one-step cloning with T4 DNA ligase (Biolabs). The product was transformed into One Shot Stbl3 chemically competent *E.coli* by heat shock (Thermofisher).

PRRL_Luc_EGFP transfer plasmid was used for the luciferase and GFP expression in U-266 and RPMI-8226.

For transfer plasmid DNA amplification, transformed bacteria were cultured over ampicillin selective plates containing 2% (p/v) Luria Bertani (LB) agar (Condalab) and 50 ug/ml ampicillin and then, plates were incubated overnight at 37ºC. The following day, bacteria colonies were picked and cultured in ampicillin LB liquid medium (Condalab) overnight at 37ºC in an orbital shaker. Plasmid DNA was then extracted using QIAprep Spin Miniprep Kit (Qiagen) and evaluated by restriction digestion pattern using gel electrophoresis. After this step, 4-5 confirmed bacteria clones were selected and cultured in antibiotic-treated LB liquid medium overnight at 37ºC with constant shaking. Plasmid DNA was then extracted with QIAGEN Plasmid Maxi Kit (Qiagen) and restriction digestion pattern was corroborated. Plasmid DNA quantity and quality were measured using a Nanodrop ND-1000 Spectrophotometer (Thermo Fisher Scientific) and Sanger sequencing was carried out by the company Stab Vida to confirm the transfer plasmid sequence.

3.2.3. Production of 3rd generation lentivector supernatants

Once DNA transfer plasmids are amplified, HEK293T cells were used to produce 3rd generation self-inactivating lentivector supernatants containing NKG2D-CAR, BCMA-CAR or ffLucGFP vectors. Nine million HEK293T cells were cultured in a treated-P150 plate (ThermoFisher Scientific) and the following reagents were added to carry out the transfection: 4 plasmids, including pMD2.VSV.G (viral envelope; PlasmidFactory), pMDLg/pRRE (VIH-1 Gag/Pol plasmid; PlasmidFactory), pRSV-Rev 10 (transactivator; PlasmidFactory), pAdvantage™ (to enhance translation initiation, Promega Biotech) and the corresponding transfer plasmid; and 2.5M $CaCl_2$ (Sigma), 2X HBS (containing 281 mM NaCl, 100 mM HEPES, 1.5 mM Na_2HPO_4, at pH 7.12 and 0.22µm-filtered) and 0.1X buffer TE (10 mM Tris (pH 8), 1 mM EDTA (pH 8); diluted 1:10 in sterile distilled H_2O (dH_2O) and 0.22 µm filtered). After 2 days, supernatants were collected and 0.45 µm filtered (Fig. 19). Ultracentrifugation at 20,000 rpm during 2 hours at 4ºC was done to concentrate and purify the lentiviral particles. Later, the supernatant was removed, and lentiviral particles were resuspended in RPMI-1640 medium. After 30 minutes of shaking, lentivector supernatants were aliquoted and stored at -80ºC.

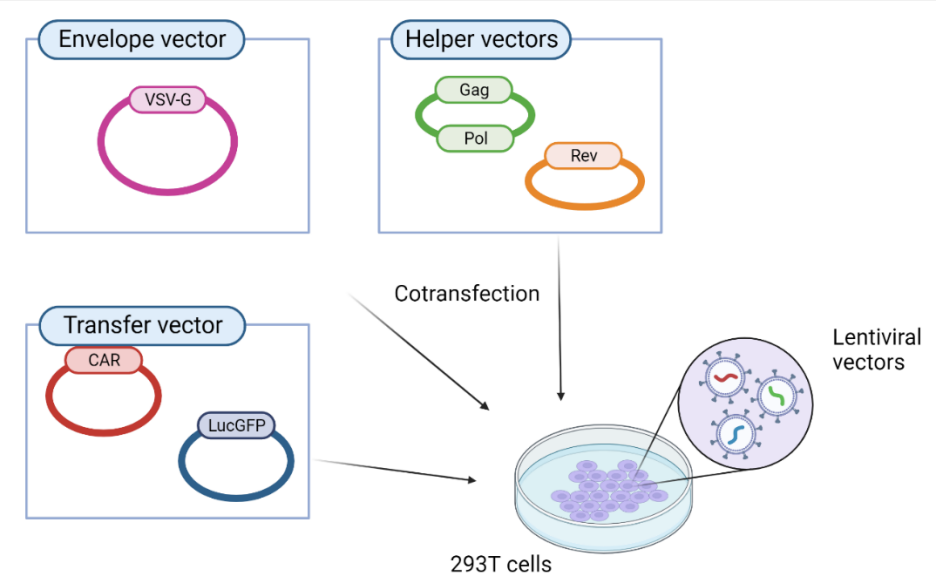

Figure 19. Schematic representation of lentivector production. Created with BioRender.com.

3.2.4. Titration of lentivector supernatants

To calculate the lentivector particles contained in the supernatants, 1 x 10^5 HEK293T/well were cultured in 24-well treated-plates (Thermo Fisher Scientific) using serial dilutions of the lentiviral particles. After 7 days, cells were collected and the transduction percentage in each dilution was tested by flow cytometry using recombinant human BCMA protein (rhBCMA), α-NKG2D Ab or GFP fluorescence (see 3.3.1.1 and table 9). Lentivector titer was determined, taking into account the number of cells initially cultured, and assuming one copy of vector per cell, by the following formula:

Titer (viral particles/ml) = number of cells x % CAR^+/GFP^+ cells x Dilution/100.

3.2.5. Lentiviral transduction

Non-treated plates were coated with retronectin at 2 µg/cm^2 24 hours before their use and stored at 4ºC or 3-4 hours before and stored at RT. Due to cell size variability, cells were plated differently: 1 x 10^6 NKAE cells were cultured at 1.33 x 10^6 cells/ml per well in non-treated 12-well plates and 5 x 10^5 MM cells were cultured at 1 x 10^6 cells/ml per well in non-treated 24-well plates. Moreover, a distinct multiplicity of infection (MOI) was also used for each lentivector: MOI 5 for all NKG2D-CAR NKAE cell transductions, MOI 8 BCMA-CAR and MOI 10 ffLucGFP.

Cells were then spinoculated at 2,000 rpm for 20 minutes at 24ºC and incubated at 37ºC. After 16 hours, cells were washed with PBS and resuspended in their corresponding medium (see 3.2.1 and 3.1.1). Only in the case of BCMA-CAR transduction, a second round of transduction was performed at MOI 8, following the conditions described above, thus, total MOI for this CAR is 16.

After 6 days from transduction, stable CAR or ffLucGFP expression was determined by flow cytometry.

3.2.6. Study of vector copy number (VCN) per cell in transduced NK cells

In addition to flow cytometry transduction determination, VCN per cell was carried out. One week after transduction, DNA and RNA from CAR effector cells were first extracted using AllPrep DNA/RNA/Protein Mini Kit (Qiagen) following the manufacturer´s instructions. DNA and RNA quantity and quality were measured using the Nanodrop ND-1000 (Thermo Fisher Scientific). RNA was stored at -80ºC for RNA-seq (described in 3.11) and DNA at -20ºC for VCN.

To determine VCN, the viral packaging signal sequence, Psi, was amplified by quantitative-PCR (q-PCR) using the Applied 7500 Fast Real-Time PCR system (Thermo Fisher Scientific) and the copy number was normalized to albumin. The primers used are included in Table 8. Albumin amplification was detected by a VIC fluorescent probe, and Psi sequence by a FAM probe. Duplicates were carried out per sample and VCN was calculated by interpolating the cycle threshold values (Ct) from the DNA sample to the Ct of a standard curve of a known concentration of dsDNA that contains albumin and Psi sequences.

Psi forward (Psi.F)	5’ CAGGACTCGGCTTGCTGAAG 3’
Psi reverse (Psi.R)	5’ TCCCCCGCTTAATACTGACG 3’
Albumin forward (Alb.F)	5’ GCTGTCATCTCTTGTGGGCTG 3’
Albumin reverse (Alb.R)	5’ ACTCATGGGAGCTGCTGGTTC 3’

Table 8. Primers used to amplify Psi and albumin sequences.

3.3. Multiparametric flow cytometry and cell sorting

3.3.1. Multiparametric flow cytometry

Cells were collected (~1-2 x 10^5), washed with PBS, centrifuged at 1,400 rpm for 5 minutes and resuspended in 100 µl of the Ab cocktail, prepared in PBS, in a 5 ml round bottom test tube (Falcon). Abs used are compiled in table 9. Cells were stained during 30 minutes at 4ºC in darkness, then washed with PBS and resuspended in 100 µl of PBS with 0.2 µg/ml 4',6-diamidino-2-phenylindole (DAPI).

The flow cytometer FACSCanto™ II (BD Biosciences) contains 3 laser lines: 405 nm (violet), 488 nm (blue) and 633 nm (red), and detects 8 different fluorescence channels.

Antigen	Dilution	Clone	Fluorochrome	Source	Catalog number
CD2	1:100	RPA-2.10	PE	Biolegend	300208
CD3	1:100	UCHT1	PE/Cy7	Biolegend	300420
CD3	1:100	UCHT1	APC/Cy7	Biolegend	300426
CD8	1:100	HIT8a	PerCP/Cy5.5	Biolegend	300924
CD16	1:100	3G8	APC/Cy7	Biolegend	302018
CD19	1:100	SJ25C1	APC/Cy7	Biolegend	363010
CD25	1:100	BC96	APC	Biolegend	302610
CD34	1:100	4H11	PE/Cy7	Life Technologies	25-0349-42
CD34	1:100	4H11	APC	Life Technologies	17-0349-42
CD38	1:100	LD38	FITC	Cytognos	CYT-38F
CD45	1:100	2D1	PerCP/Cy5.5	Biolegend	368504
CD56 (NCAM)	1:100	HCD56	APC	Biolegend	318310
CD56 (NCAM)	1:100	HCD56	PerCP/Cy5.5	Biolegend	318322
CD56 (NCAM)	1:200	HCD56	PE	Biolegend	318306
CD57	1:100	HNK-1	PE	Biolegend	359612
CD69	1:100	FN50	PE	Biolegend	310906
CD62L	1:100	DREG-56	APC	Biolegend	304810
CD71	1:100	M-A712	APC-H7	BD Biosciences	655408
Fas (CD95)	1:100	DX2	Alexa Fluor 488	Biolegend	305616
CD107a	1:100	H4A3	PE	BD Biosciences	555801
CD138	1:100	MI15	PE/Cy7	Biolegend	356514
CD138	1:100	MI15	BV 421	Biolegend	356516
NKG2A (CD159a)	1:100	Z199	PE	Beckman Coulter	IM3291U
NKG2C (CD159c)	1:100	134591	Alexa Fluor 488	R&D Systems	FAB138G
KIR2DL2/L3 (CD158b)	1:100	DX27	PerCP/Cy5.5	Biolegend	312614

KIR3DL1 (CD158e1)	1:100	DX9	PE/Cy7	Biolegend	312720
KIR3DL2/CD158k	1:100	539304	PE	R&D Systems	FAB-2878P
KIR2DL1/KIR2DS5	1:100	143211	Alexa Fluor 488	R&D Systems	FAB1844G
FasL (CD178)	1:100	NOK-1	APC	Life Technologies	17-9919-42
CCR7 (CD197)	1:100	G043H7	PE	Biolegend	353204
IL-15Rα (CD215)	1:100	JM7A4	PE	Biolegend	330208
DNAM-1 (CD226)	1:100	TX25	FITC	Biolegend	337104
TRAIL (CD253)	1:100	RIK-2	PE	Biolegend	308206
PD-1 (CD279)	1:100	EH12.2H7	PE	Biolegend	329906
NKG2D (CD314)	1:100	149810	PE	R&D Systems	FAB139P
NKp46 (CD335)	1:100	29A1.4	PE	Biolegend	137604
NKp44 (CD336)	1:100	P44-8	PE	Biolegend	325108
NKp30 (CD337)	1:100	P30-15	PE	Biolegend	325208
KLRG1	1:100	14C2A07	PE	Biolegend	368610
TIGIT	1:100	A15153G	PE	Biolegend	372704
GLUT1	1:100	202915	Alexa Fluor 488	R&D Systems	FAB1418G
Ki67	1:100	Ki-67	Brilliant Violet 421™	Biolegend	350506
BCMA (CD269)	1:100	19F2	PE	Biolegend	357504
HLA-E	1:100	3D12HLA-E	APC	ThermoFisher	17-9953-42
ULBP2/5/6	1:100	165903	PE	R&D Systems	FAB1298P
ULBP1	1:100	170818	PE	R&D Systems	FAB1380P
ULBP3	1:100	166510	PE	R&D Systems	FAB1517P
MICA/B	1:100	6D4	PE	Biolegend	320906
IFN-γ	1:100	45-15	PE	Miltenyi Biotec	130-113-493

Other reagents	Dilution	Clone	Fluorochrome	Source	Catalog number
Biotinylated rhBCMA (CD269)	1:200	-	-	Adipogen	ANC-519-030
IgG1, κ	1:100	MOPC-21	PE	BD Biosciences	555749
IgG1, κ	1:100	P3.6.2.8.1	APC	Life Technologies	17-4714-42
IgG2a, κ	1:100	MOPC-173	PE	Biolegend	400211
IgG2b, κ	1:100	MPC-11	PE	Biolegend	400314
Streptavidin	1:300	-	PE	BD Biosciences	554061
Propidium Iodide	-	-	-	Sigma Aldrich	P4864
DAPI	-	-	-	Sigma Aldrich	D9542

Table 9. Reagents and primary Abs used for flow cytometry. FITC: Fluorescein isothiocyanate; PE: Phycoerythrin; PerCP/Cy5.5: Peridinin chlorophyll protein-Cyanine5.5; PE/Cy7: PE-Cyanine7; APC: Allophycocyanin; APC/Cy7: APC-Cyanine7; DAPI: 4',6-diamidino-2-phenylindole.

Using FACSDiva v.8.0.1 software, debris was first excluded by Forward Side Channel-Area (FSC-A) vs Side Scatter Channel-Area (SSC-A). Once cells are gated, single cells were selected by FSC-A and FSC-Height (FSC-H), avoiding aggregates, which show a deviation from the linearity. To analyze live cells, $DAPI^-$ cells were selected, determining the population of interest. A range of 10,000-20,000 live cells per tube were acquired in most experiments. Data analysis was later performed using FlowJo Vx 10.0.7 software (BD Biosciences).

Unstained controls were needed to set the laser voltages and single-stained controls were used to compensate the spectral overlap among fluorochromes. Fluorescence minus one (FMO) controls were needed to identify the additive effect of spreading from multiple fluorochromes into the detector of interest. Relative fluorescence intensity (RFI) was then calculated as the mean fluorescence intensity of Ab staining divided by the FMO, isotype or unstained.

3.3.1.1. Immunophenotype

Characterization of CAR effector cell and MM cell line phenotype was mainly performed by flow cytometry. CAR-target ligands (NKG2D-L and BCMA) on MM cells as well as CAR expression on NKAE cells (NKG2D-CAR and BCMA-CAR) were evaluated by this technique. NKG2D-CAR expression on NKAE cells was detected with a human α-NKG2D Ab, while BCMA-CAR expression was analyzed on NKAE cells by the incubation with a rhBCMA protein conjugated to biotin and detected by streptavidin-PE. Quantibrite™ beads (Biolegend) were used to calculate the number of NKG2D molecules in NKG2D-CAR populations.

In addition, the following expression markers were studied on the cell surface of CAR NKAE cells.

- Activating or activation receptors: CD69, NKp30, NKp44, NKp46 and NKG2C
- Inhibitory or exhaustion receptors: KIR2DL1/2DS5, KIR2L2/L3, KIR3DL1, KIR3DL2, NKG2A, PD-1, TIGIT and KLRG1
- Adhesion receptors: DNAM-1 and CD62L
- Costimulatory receptors: CD2
- Maturation: CD57

- Cytokine receptors: CD25 (IL-2Rα), IL-15Rα and TGFBR-II
- Apoptosis induction: TRAIL and FasL
- Metabolic receptors: GLUT1 and CD71
- ADCC and degranulation: CD16 and CD107a
- Other receptors: Fas (FasL receptor) and CCR7

HLA-E expression on primary MM cells as well as NKG2C, NKG2A and PD-1 expression on cytotoxic T and NK cells from BM samples were analyzed using the panels below (table 10). We differentiated PC population into pathologic PC (pPC; $CD138^+$ $CD38^+$ $CD19^-$ $CD56^+$) and normal PC (nPC; $CD138^+$ $CD38^+$ $CD19^-$ $CD56^+$), following flow cytometry phenotype described for each patient by the Hematology Service from H12O. Then, RFI was calculated for each population. In order to obtain HLA-E expression ratio between pPC and healthy populations, pPC RFI was divided by nPC or $CD34^+$ RFI.

HLA-E expression on PC							
	450	**FITC**	**PE**	**PerCP/Cy5.5**	**PE/Cy7**	**APC**	**APC/Cy7**
HLA-E	CD138	CD38	CD56	CD45	CD34	HLA-E	CD19
IgG1κ	CD138	CD38	CD56	CD45	CD34	IgG1κ	CD19

NKG2C, NKG2A and PD-1 expression on cytotoxic T and NK cells							
	450	**FITC**	**PE**	**PerCP/Cy5.5**	**PE/Cy7**	**APC**	**APC/Cy7**
T/NK cells 1	DAPI	NKG2C	NKG2A	CD8	CD3	CD56	CD16
T/NK cells 2	DAPI	-	PD-1	CD8	CD3	CD56	CD16
FMO	DAPI	-	-	CD8	CD3	CD56	CD16

Table 10. Description of Abs used for HLA-E expression on PC and NKG2C, NKG2A and PD-1 expression on $CD8^+$ T cells and $CD56^+CD16^+$ NK cells.

3.3.2. U-266 and RPMI-8226 ffLucGFP cell line sorting

U-266 and RPMI-8226 cells were transduced with the ffLucGFP vector, as described in 3.2.5. After one week, GFP signal was detected by flow cytometry to confirm transduction and GFP^+ cells were sorted using BD FACSAria™ Fusion Cell Sorter (BD Biosciences), which contains 3 laser lines: 405 nm (violet), 488 nm (blue) and 640 nm (red).

3.4. Cytotoxicity assays

3.4.1. Calcein release cytotoxicity assay against MM cell lines

CAR CIML-NKAE and NKAE cell cytotoxicity against MM cell lines was evaluated *in vitro* through calcein release assay. Calcein-acetoxymethylester (calcein-AM) is a lipophilic ester that penetrates the plasma membrane. It is hydrolyzed in the cytosol by esterase enzymes to a polar green-fluorescent product (calcein) that is retained into the cells with intact membrane. When a cell is destroyed, calcein is released to the supernatant and the cytotoxicity can be evaluated due to the fluorescence detected in the supernatants of co-cultures.

Target MM cells (50,000 per well) were stained with 3 µM Calcein-AM during 30 min at 37ºC in RPMI-1640 medium with 100 IU/ml P/S. Target cells were then washed with PBS and co-cultured with CAR NK cells at different target:effector (T:E) ratios. Moreover, spontaneous lysis (calcein-stained target cells alone, in the absence of effector cells) and maximum lysis (calcein-stained target cells with 1% Triton X 100; Sigma Aldrich) controls were included. Every condition was carried out per triplicate in a non-treated U-bottom 96-well plate (Corning) using NK cell corresponding medium without IL-2. Plates were centrifuged for 5 minutes at 1,200 rpm and incubated for 3 hours at 37ºC. After the incubation, plates were again centrifuged, and supernatant was transferred into a 96-well black microplate (Corning). Fluorescence (excitation 488 nm; emission 520 nm) was detected by the spectrophotometer VICTOR Nivo™ (PerkinElmer) (Fig. 20) and specific lysis was calculated using the following formula:

$$\text{Specific lysis (\%)} = \frac{\text{Co-culture lysis fluorescence} - \text{Spontaneous lysis fluorescence}}{\text{Maximun lysis fluorescence} - \text{Spontaneous lysis fluorescence}} \text{ x } 100$$

In NKG2A blocking assays, CAR NKAE cells were pre-treated with 10 µg/ml mouse α-NKG2A clone Z199 (Beckman Coulter) or its corresponding isotype IgG2b (R&D systems) or human α-NKG2A BMS-986315 (Bristol-Myers-Squibb) or its corresponding isotype IgG1κ (Bristol-Myers-Squibb) Abs for 30 minutes at 37ºC. Later, blocked CAR NKAE cells were incubated with target calcein-stained cells, as described above.

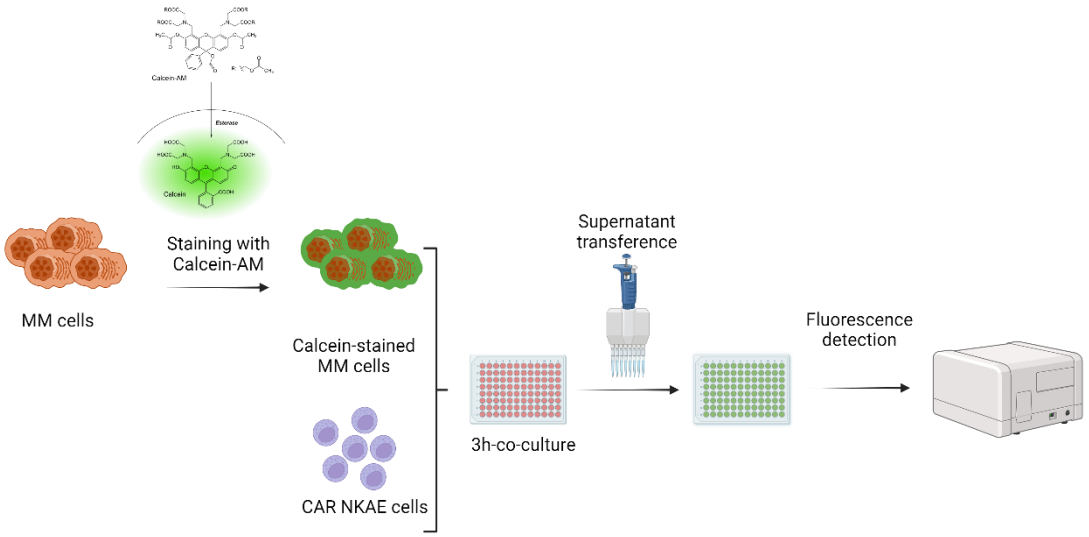

Figure 20. Schematic representation of calcein release cytotoxicity assay. Created with BioRender.com.

3.4.2. Clonogenic cytotoxicity assay against MM cell lines

Cytotoxicity of CAR CIML-NKAE and NKAE cells was also performed against the MM cell line L-363. Around 40-50% of these tumor cells are clonogenic, which can grow forming colonies in semi-solid culture medium [466].

CAR CIML-NKAE or NKAE cells were co-cultured at different T:E ratios with L-363 cells, in non-treated U-bottom 96-well plates, in NK cell medium without IL-2. To establish the maximum number of colonies, L-363 cells were cultured in the absence of CAR NKAE cells and a control with NK cells alone was also included. Plates were centrifuged and incubated at 37ºC for 3 hours. Then, each co-coculture was seeded over methylcellulose-based medium without cytokines (MethoCult™ H4230; Stem cell) per triplicate in p35mm plates (Corning). Each plate contained 250 L-363 cells. After 14 days of incubation at 37ºC, colonies were counted using an inverted bright-field microscope (Nikon Diaphot, objective 4X).

3.4.3. Cytotoxicity assay against primary MM cells through flow cytometry

CAR NKAE cell cytotoxicity over primary MM cells and toxicity over $CD34^+$ cells were performed by flow cytometry at 24 hours in a native context.

BM samples from MM patients at diagnosis or progression were centrifuged at 350 g for 10 minutes and plasma was collected and stored at 4 ºC. Then, BM samples were diluted

1:10 with PBS and added over 2:1 Ficoll-Paque. BM mononuclear cells (BMMCs) layer was collected, washed with PBS, and centrifuged at 1,600 rpm for 10 minutes. 1-2 x 10^5 BMMCs were stained to analyze the percentage of PC in each sample ($CD138^+CD38^+$) by flow cytometry. 30,000 PC were plated per well within BMMCs and co-cultured with NKG2D-CAR NKAE cells at 1:10 T:E ratio or BCMA-CAR NKAE cells at 1:5 T:E ratio (pretreated with the α-NKG2A Ab or the corresponding isotype, as described in 3.4.1). A control with BMMCs alone was also used to determine the maximum PC survival within the experiment. Each condition was plated per triplicate in a non-treated U-bottom 96-well plate using the NK cell medium, without IL-2, supplemented with 6% of the BM plasma. Plasma is added to maintain the TME present in the MM BM, which sustain PC survival, and could negatively impact in the adoptive cell therapy efficacy. Plates were centrifuged for 5 minutes at 1,200 rpm and incubated for 24 hours at 37ºC. After this time, plates were centrifuged again, supernatants were removed, and cells were washed with PBS. Then, cells were stained with CD38 FITC, CD138 PE/Cy7, CD45 PerCP/Cy5.5, CD34 APC and CD56 PE, as described in 3.3.1. After washing the staining, cells were resuspended in 150 µl of PBS-DAPI and 120 µl from each well were acquired by the cytometer at 500 µl/min. This experiment was performed using the Attune CytPix Flow Cytometer (Thermofisher), located in Vivia Biotech company. This cytometer allows the analysis of a concrete volume of sample, assuring more accurate results. The number of $CD38^+$ $CD138^+$ cells as well as $CD34^+$ cells that remained in each condition was then analyzed. PC cytotoxicity and $CD34^+$ toxicity were calculated using the following formula:

$$\text{Survival (\%)} = \frac{\text{Number of PC or CD34+ cells per condition}}{\text{Number of PC or CD34+ in the absence of effector cells}} \text{ x } 100$$

$$\text{Cytotoxicity or toxicity (\%)} = 100 - \text{survival (\%)}$$

3.4.4. Degranulation assay

CAR CIML-NKAE and NKAE cell antitumor activity was also studied by measuring their degranulation levels. U-266, XG-1, ARP-1, RPMI-8226 and K562-mb21-41BBL target cells, 1 x 10^5 cells, were co-cultured with effector cells at 1:1 ratio per duplicate in NK cell medium without IL-2. CAR NK cells without target cells were also seeded as basal degranulation control. In α-NKG2A blocking assays, CAR NK cells were pre-

treated as described in 3.4.1. CD107a PE or its isotype, IgG1κ PE, were added to each condition and incubated for 1 hour at 37ºC. Then, GolgiStop (BD) was added to all wells, following the manufacturer's indications, and plates were centrifuged and incubated for 3 more hours. Later, cells were centrifuged, washed with PBS and stained with CD56 PerCP/Cy5.5 (XG-1 and K562-mb21-41BBL co-cultures and CAR NK cell controls), CD138 PE/Cy7 (U-266 and ARP-1 co-cultures) or CD45 PerCP/Cy5.5 (RPMI-8226 co-cultures) Abs, as described in 3.3.1, to discriminate NK cells from MM cell lines in each case. Cells were resuspended in PBS-DAPI solution and acquired by the cytometer. $CD107a^+$ cell percentage within live NK cells was analyzed.

3.5. Cytokine detection assays

3.5.1. Intracellular IFN-γ detection assay

To detect intracellular IFN-γ production in CAR CIML-NKAE and NKAE cells, 1 x 10^5 target cells (U-266, XG-1, ARP-1, RPMI-8226 and K562-mb21-41BBL) were co-cultured with effector cells at 1:1 ratio per duplicate using NK cell medium without IL-2 in non-treated U-bottom 96-well plates. GolgiStop was added and plates were centrifuged and incubated at 37ºC for 4 hours. Later, cells were centrifuged again, washed with PBS and stained with CD56 PerCP/Cy5.5 (XG-1 and K562-mb21-41BBL co-cultures and CAR NK cell controls), CD138 PE/Cy7 (U-266 and ARP-1 co-cultures) or CD45 PerCP/Cy5.5 (RPMI-8226 co-cultures) Abs, to discriminate CAR NKAE cells from MM cell lines. After 30 minutes, cells were centrifuged, washed with PBS with 0.5% Bovine Serum Albumin (BSA) and 2 mM Ethylenediaminetetraacetic acid (EDTA) (PBE), centrifuged at 1,400 rpm for 5 minutes and resuspended in fix Solution A (Fix&Perm, Cytognos). After 10 minutes at RT, cells were washed with PBE buffer and resuspended in permeabilization Solution B (Fix&Perm, Cytognos) with the IFN-γ PE Ab or its isotype IgG1κ PE for 30 minutes at RT. Cells were washed again with PBE and resuspended in PBS to be acquired by the cytometer. IFN-γ^+ cell percentage within live NK cells was analyzed.

3.5.2. Soluble cytokines quantification assay

CAR NKAE effectors, 50,000 cells, were cultured with target cells (U-266, XG-1, RPMI-8226 and K562-mb21-41BBL) at 1:2 T:E ratio in NK cell medium, without IL-2, in non-treated U-bottom 96-well plates. For α-NKG2A studies, CAR NKAE cells were blocked with α-NKG2A Ab or its corresponding isotype for 30 minutes before the co-culture, as described in 3.4.1. After 24 hours, supernatants were collected and stored at -80ºC.

Quantification of soluble cytokines from NK and target cell co-culture supernatants was performed by flow cytometry using LEGENDplex™ Human CD8/NK Panel (13-plex) (Biolegend), following the manufacturer´s instructions (Fig. 21). This panel allows simultaneous quantification of 13 human proteins, including IL-2, IL-4, IL-10, IL-6, IL-17A, TNF-α, sFas, sFasL, IFN-γ, granzyme A, granzyme B, perforin, and granulysin.

Besides, a customized LEGENDplex™ panel (IL-1β, IFN-α2, IFN-γ, TNF-α, MCP-1, IL-6, IL-8, IL-10, IL-18, IL-15, IL-2, IL-3, TGF-β1) was designed for cytokines detection in MM patients and HD BM plasmas.

LEGENDplex™ Data Analysis Software Suite was then used to analyze the flow cytometry data files.

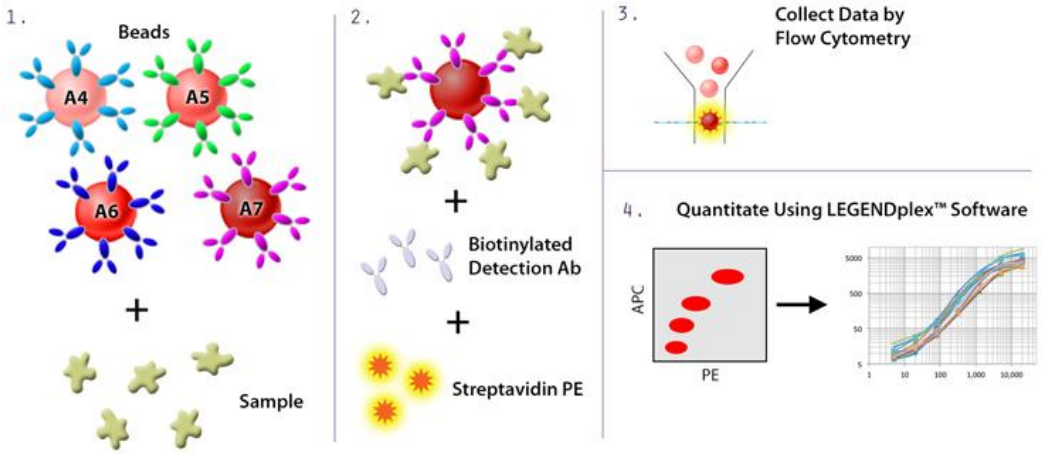

Figure 21. Schematic representation of LEGENDplex™ assay. Obtained from LEGENDplex™ protocol guide (Biolegend).

3.6. Toxicity assays

3.6.1. Toxicity against PBMCs

Evaluation of NKG2D- and BCMA-CAR NKAE cell toxicity was carried out against PBMCs from HD. PBMCs were isolated by density gradient centrifugation, as described in 3.2.1. Then, PBMCs were stained with calcein-AM and co-culture with the NKAE populations in NK cell medium without IL-2, as described in 3.3.1.

3.6.2. Toxicity against $CD34^+$ hematopoietic cells from CB

The hematotoxicity of CAR CIML-NKAE and NKAE cells was evaluated over $CD34^+$ cells isolated from CB samples. First, mononuclear cells were obtained by Ficoll density gradient centrifugation. Cells were then lysed with ACK lysis buffer (Gibco) and $CD34^+$ cells were purified by immunomagnetic positive selection using CD34 MicroBead Kit (Miltenyi), following the manufacturer´s instructions. Purification of $CD34^+$ cells was confirmed by flow cytometry (see 3.3.1) and these cells were frozen in 80% FBS with 20% dimethyl sulfoxide (DMSO).

On the day of the experiment, $CD34^+$ cells were thawed in NK cell medium without cytokines. Thereafter, CAR CIML-NKAE or NKAE cells were co-cultured with $CD34^+$ cells at different T:E ratios, using NK cell medium without IL-2, in non-treated U-bottom 96-well plates. To establish the maximum number of colonies, $CD34^+$ cells were cultured in the absence of effector cells and a negative control with NK cells alone was included. Plates were centrifuged and incubated at 37ºC, in normoxic conditions, for 4 hours. Then, each condition was seeded over a methylcellulose-based medium containing recombinant human stem cell factor (SCF), IL-3, EPO and granulocyte-macrophage colony-stimulating factor (GM-CSF) (MethoCult™ H4434; Stem cell), per triplicate in p35mm plates. After 14 days incubation at 37ºC, Colony Forming Units-Granulocyte-Macrophage (CFU-GM) and Burst Forming Units-Erythroid (BFU-E) were counted using an inverted bright-field microscope (Nikon Diaphot, objective 4X).

3.7. Proliferation assays

3.7.1. Cell cycle analysis

NKG2D-CAR CIML-NKAE or NKAE cells, 5 x 10^5 cells, were collected and washed with PBS in 5 ml round bottom test tubes. Cells were fixed by adding 70% cold ethanol drop by drop while vortexing for 1 minute. Samples were stored at -20ºC for at least 12 hours.

Before cell cycle analysis by flow cytometry, samples were washed twice with PBS and cell pellets were resuspended in PBS and incubated with 0.2 mg/ml RNAse A for 30 minutes in darkness at RT. Propidium iodide (PI) at 0.04%, was added to each tube and PI staining was then analyzed by flow cytometry in linear scale (see 3.3.1).

3.7.2. Ki67 cell proliferation analysis

Ki67 protein expression indicates cell proliferation because this marker can be detected when cells are in G_1, S, G_2 and mitosis phases, but not in G_0 [467].

As described for cell cycle assay, 5 x 10^5 NKG2D-CAR CIML-NKAE cells or NKAE cells were collected, washed, fixed with ethanol and stored at -20ºC for further analysis.

Cells were then washed three times with Cell Staining Buffer (Biolegend) and stained with the Ki67 BV421 Ab. After 30 minutes in darkness at RT, cells were washed twice with this buffer and resuspended in 0.5ml of buffer for flow cytometry analysis (see 3.3.1).

3.8. Metabolism assays

3.8.1. MitoTracker staining

NKG2D-CAR CIML-NKAE or NKAE effectors, 1 x 10^5 cells, were collected, washed with PBS in 5 ml round bottom test tubes, and incubated for 10 min at 37ºC with 100 nM Mitotracker Green (Life Technologies). After incubation, cells were rinsed with PBS, centrifuged, and resuspended with PBS-DAPI solution prior to flow cytometry acquisition (see 3.3.1).

3.8.2. Mitochondrial Oxidative Phosphorylation (OXPHOS) system function

Mitochondrial and glycolysis stress experiments with NKG2D-CAR CIML-NKAE or NKAE cell populations were performed by the Rare, Mitochondrial and Neuromuscular Diseases group from H12O, Madrid.

To assess the OXPHOS system function, Oxygen Consumption Rate (OCR) was determined through high-resolution respirometry in a Seahorse XFp Extracellular Flux Analyzer (Agilent, Santa Clara, California; Fig. 22A). Mitochondrial stress test was performed through sequential injections of 2.5 µM oligomycin, 2 injections of fluoro-carbonyl cyanide phenylhydrazone (FCCP), first one of 1.1 µM and the second one of 2.5 µM, and then a mix of 1.3 µM rotenone and 1.3 µM antimycin A, prepared from XFp Cell Mito Stress Test (Agilent) reagents. Oligomycin, a complex V inhibitor, inhibits the ATP synthase and diminishes OCR; the mitochondrial uncoupler FCCP disrupts ATP synthesis, obtaining the maximal OCR; and rotenone and antimycin A inhibit the electron transport chain and decrease the OCR to a minimal value (Fig. 22B).

NKG2D-CAR CIML-NKAE or NKAE cells, 30,000 per well, were resuspended in XF Seahorse Base pH 7.4 medium supplemented with 4.44 mM glucose, 0.08 mM sodium pyruvate and 0.66 mM glutamine and seeded on a XFp Cell Culture Miniplate. This plate was incubated at 37ºC without CO_2 for 20 minutes. Then, the plate was introduced into the analyzer and sequential injections of the indicated compounds were carried out. The test determines the following parameters:

- Basal OCR: OCR obtained before any compounds were added minus non-mitochondrial OCR (nmOCR).
- Oligomycin-sensitive OCR or ATP-linked respiration: it calculates the amount of OCR needed to pump protons that complex V would use to produce ATP. It is the basal OCR minus OCR after oligomycin injection.
- Proton leak: it determines the proton flux that is not directed to ATP production. It is calculated as the oligomycin-sensitive OCR minus nmOCR.
- Maximal OCR (maxOCR): FCCP forces a high energy demand to calculate the highest OCR the cell can achieve. It is the OCR value obtained after FCCP injection minus nmOCR.
- Spare capacity: it is the reaction capacity of a cell to an energy demand. It is the difference between the maxOCR and the basal OCR.

- NmOCR: it is measured after rotenone and antimycin A injection, when all the electron transport chain is inhibited.

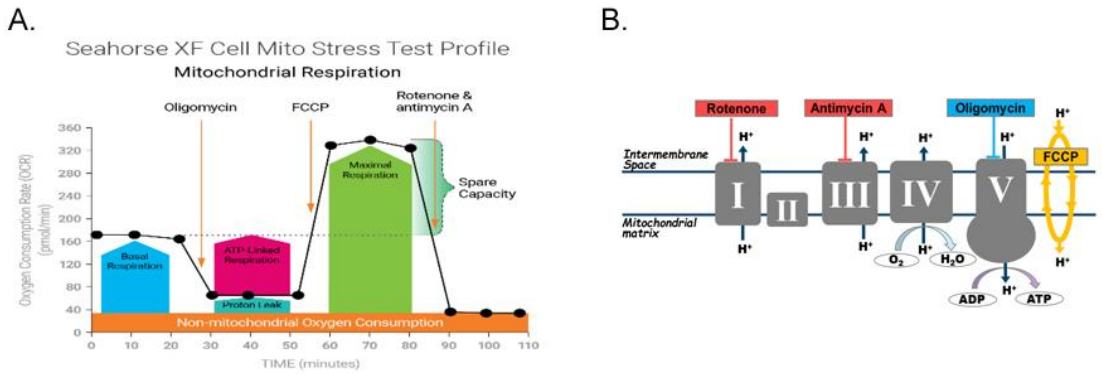

Figure 22. Schematic representation of Seahorse OCR test. A) Seahorse XF Cell Mito Stress test profile. B) Target of action of Mito Stress test modulators on the electron transport chain. Obtained from Agilent.

Moreover, the extracellular acidification rate (ECAR), which measures the concentration of free protons, was determined using the XFp Glycolysis Stress Test in the Seahorse XFp Extracellular Flux analyzer. For this assay, cells were resuspended in the same XF Seahorse Base medium without glucose and supplemented with 100 mM sodium pyruvate and 200 mM glutamine. Three sequential injections of 25 mM glucose, 2.6 µM oligomycin and 100 mM 2-desoxy-D-glucose (2-DG) were carried out to determine the following parameters (Fig. 23):

- Non-glycolytic acidification: acidification that is not attributed to glycolysis. It is obtained after 2-DG injection.
- Basal glycolysis: basal glycolytic activity of the cell, obtained from ECAR value after glucose injection minus non-glycolytic acidification or initial ECAR.
- Maximal glycolytic capacity: obtained after mitochondrial ATP production disruption, due to oligomycin injection. It is determined by ECAR value after oligomycin injection minus initial ECAR.
- Glycolytic reserve: capacity to increase glycolytic activity in response to an increase in energy demand. It is determined as ECAR after oligomycin addition minus basal glycolysis.

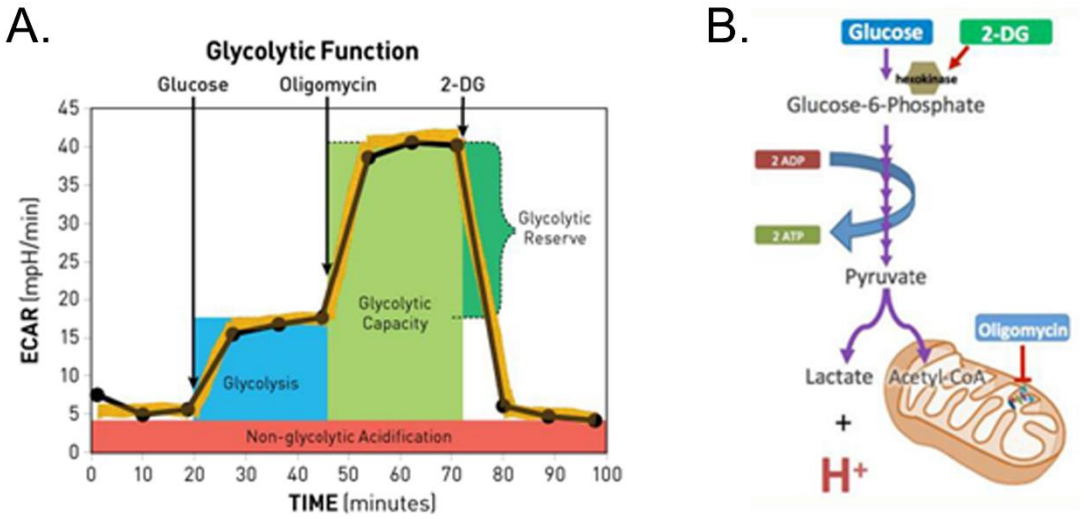

Figure 23. Schematic representation of Seahorse ECAR test. A) Seahorse XF Glycolysis Stress test profile. B) Target of action of Glycolysis Stress test modulators. Obtained from Agilent

All measurements were normalized to the amount of protein in each well. Cells seeded in the microplates were lysed and proteins were quantified by Bradford assay (Bio-Rad).

3.9. Western Blot (WB)

To extract proteins from CAR NK cells, cell pellets were lysed in RIPA lysis buffer with protease (Roche) and phosphatase inhibitors (Merck). Samples were incubated for 1 hour on ice, vortexing occasionally. Then, they were centrifuged at 15,000 rpm for 30 minutes at 4ºC and supernatants, containing the extracted proteins, were collected. Protein samples were diluted in Laemmli loading buffer (Bio-Rad) containing sodium dodecyl sulfate (SDS) and 5% β-mercaptoethanol and incubated at 99ºC for 10 minutes in a block heater. These proteins were separated following a SDS-polyacrylamide gel electrophoresis (SDS-PAGE) under denaturing conditions. Electrophoresis was performed at constant voltage (120V) in electrophoresis buffer (25 mM Tris-HCl, 200 mM glycine, 0.1% SDS, pH 8.3).

After electrophoresis, proteins were transferred from the gels to nitrocellulose membranes (Amersham) at a constant current (350 mA) for 90 minutes using wet transfer. Then membranes were blocked with PBS containing 3% of BSA for 30 minutes at RT in

agitation. After this step, membranes were washed with TBS with 0.1% Tween20 (TBS-T) and incubated with primary Abs overnight. The following day, membranes were washed three times with TBS-T and incubated with the secondary anti-mouse or anti-rabbit Abs conjugated to Horseradish Peroxidase (HRP; Cell Signaling) for 30 minutes. Then, membranes were again washed three times with TBS-T and Abs bound to the target proteins were detected using commercial enhanced chemiluminescence (ECL) kits (Amersham) in the Gel Doc^{TM} EZ Documentation System (Bio-Rad).

3.9.1. Detection of CAR expression on CAR NKAE cells

Five million CAR NKAE cells were pelleted and processed, as previously described, to analyze the presence of CAR molecules in transduced NKAE cells. The CD3ζ signaling domain is present in the NKG2D- and BCMA-CAR sequences. Therefore, an α-CD3ζ primary Ab (#551033, BD Pharmigen) was used to identify the expression of CAR molecules within NKAE cell populations. P150 (#610473, BD Biosciences) detection was utilized as loading control.

3.9.2. NKG2A signaling pathway

To evaluate the phosphorylation state of ZAP-70/Syk, involved in NKG2A signaling pathway (Fig. 16), 5 x 10^6 isotype- or NKG2A-pretreated CAR NKAE cells were stimulated with 5 x 10^5 RPMI-8226 cells for 1h in NK medium with 2% AB serum and then pelleted. CAR NKAE cells as well as RPMI-8226 cells alone were also collected. Pellet samples were processed, as previously described, and a specific Ab against phospho-Zap-70 (Tyr^{319})/Syk (Tyr^{352}) (#2701S; Cell Signaling) was used. ZAP-70 (#2705S, Cell Signaling) detection was utilized as loading control.

3.10. Mass cytometry

Surface and intracellular protein expression was studied by mass cytometry. For this purpose, 5 x 10^6 NKG2D-CAR NKAE cells were pretreated with either the human α-NKG2A or its corresponding isotype IgG1κ, co-cultured at 1:10 T:E ratio with the MM cell line RPMI-8226 for 24 hours and frozen in 90% FBS + 10% DMSO. This experiment

was carried out and analyzed by the Department of Medical Oncology from Dana Farber Cancer Institute, Boston, USA.

On the day of the experiment, cells were quickly thawed in a water bath, resuspended in PBS and pelleted. Cells were then stained with a viability stain. After washing with Maxpar cell staining buffer (Fluidigm), samples were stained with a cocktail of surface Abs (Table 11) (Standard Bio) for 15 minutes at RT. Next, cells were washed and fixed. After washing, cells were stained with Cell ID Intercalator Ir to label nucleated cells. Then, cells were rinsed with PBS and stored until acquisition on the same day. Samples were acquired on the Fluidigm XT (Standard Bio) mass cytometer. Data were analyzed with FlowJo and R programming.

Antigen	Metal
CD16	145Nd
CD27	167Er
CD56	176Yb
CD94	170Er
CD117 (c-kit)	143Nd
CD122 (IL-2/15Rβ)	156Gd
CD127 (IL-7Rα)	165Ho
CD158b (KIR2DL2/DL3)	173Yb
CD159a (NKG2A)	169Tm
CD161	164Dy
CD294 (CRTH2)	163Dy
CD314 (NKG2D)	166Er
CD328 (SIGLEC7)	152Sm
CD335 (NKp46)	162Dy
CD336 (NKp44)	155Gd
CD337 (NKp30)	159Tb
KIR3DL3	147Sm

Table 11. Abs used for CyTOF experiment.

3.11. Transcriptomic analysis by RNA sequencing (RNA-seq)

NKG2D-CAR CIML-NKAE and NKAE cells RNA expression differences from 4 experiments were studied by RNA-seq. This technique was performed by the Department

of Hematology from H12O, Madrid, and analyzed by the Department of Biochemistry and Molecular Biology from *Universidad Complutense de Madrid*.

RNA from these populations was extracted, as described in 3.2.6, and total RNA quality was determined in Bioanalyzer 2100 (Agilent Technologies). For this purpose, Agilent RNA 6000 Pico kit (Agilent Technologies) was used following the manufacturer's instructions.

RNA library generation was performed from 10 ng to 1 µg of total RNA following the KAPA RNA HyperPrep Kit with RiboErase (HMR) (KR1351 – v1.16) protocol for Illumina (San Diego, USA). KAPA RNA HyperPrep Kit and KAPA HyperPlus Kit (Roche) were utilized.

First, oligonucleotides hybridization to rRNA was performed, rRNA was depleted through RNAse H and RNA was purified using 2.2X KAPA Pure Beads (Roche). Subsequently, hybridized oligonucleotides were digested by DNAse and RNA was again purified with 2.2X KAPA Pure Beads. rRNA-free RNA was then eluted, heat-fragmented and the first cDNA chain was generated. Afterwards, a second cDNA was synthesized and SeqCap Adapter Kit B (Roche) was used for adapter ligation.

Later, samples were again purified using 0.63X and 0.7X KAPA Pure Beads and libraries were amplified utilizing HiFi polymerase. Libraries were 1X KAPA Pure Beads purified and quantified using KAPA Library Quant Kit (Illumina) ROX Low qPCR Mix (Roche), according to Ct comparison regarding 6 standards of Ct known concentrations (20 pM, 2 pM, 0.2 pM, 0.02 pM, 0.002 pM and 0.0002 pM).

Then, libraries were diluted until 4 nM, denaturalized, and again diluted following the NextSeq System: Denature and Dilute Libraries Guide (15048776 v09), until 1.8 pM. The 8 samples from 4 paired experiments were loaded in a chip and sequenced in NextSeq 500/550 System (Illumina) (Fig. 24).

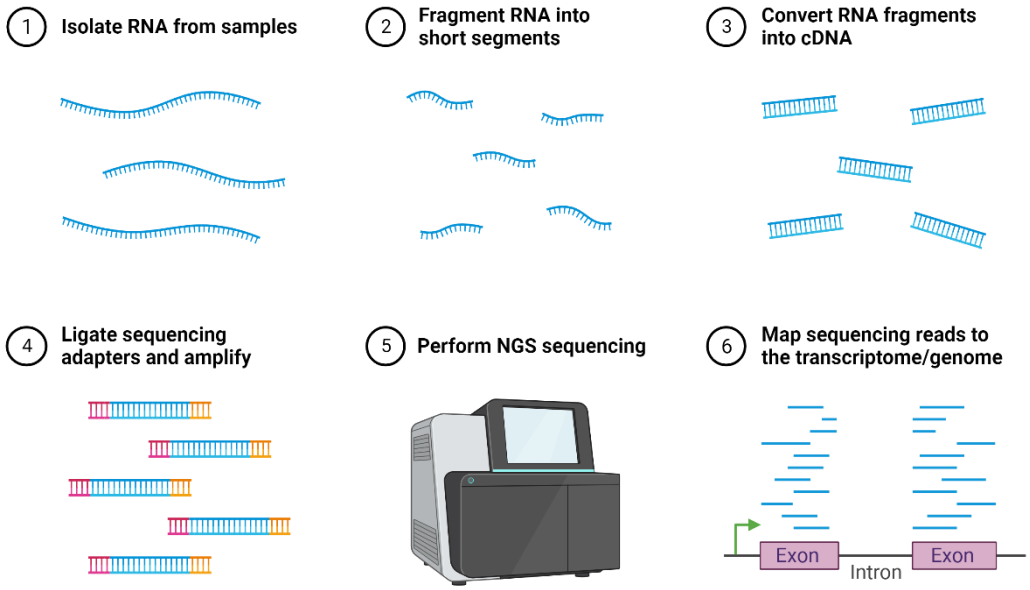

Figure 24. Schematic representation of RNA-seq protocol. Obtained from BioRender gallery.

Time and temperature specifications of each process developed in ProFlexTM Base (Applied Biosystems) or QuantStudioTM 5 Real-Time PCR Instrument (96-Well 0.1 ml Block; Applied Biosystems) are detailed in table 12.

Procedure	Cycles	Conditions
Oligonucleotides hybridization and rRNA depletion	1	95ºC / 2’
	1	45ºC: - 0.1ºC / second
	1	45ºC / ∞
	1	45ºC / 30’
	1	4ºC / ∞
DNA digestion	1	37ºC / 30’
	1	4ºC / ∞
Fragmentation	1	85ºC / 6’
First cDNA chain synthesis	1	25ºC / 10’
	1	42ºC / 15’
	1	70ºC / 15’
	1	4ºC / ∞
Second cDNA chain synthesis	1	16ºC / 30’
	1	62ºC / 10’
	1	4ºC / ∞
Libraries amplification	1	98ºC / 45’’
	11-15	98ºC / 15’’
		60ºC / 30’’
		72ºC / 30’’
	1	72ºC / 1’
	1	4ºC / ∞
Quantitative PCR	1	95ºC / 5’
	35	95ºC / 30’’
		60ºC / 45’’
	1	95ºC – 65ºC – 95ºC

Table 12. Detailed description of all procedures carried out along RNA sequencing.

RNA-seq data processing and analysis workflow were performed following these steps. First of all, RNA-seq data quality control was carried out using FastQC, to test sequencing quality and adapter presence. Then, reads were mapped to the homo sapiens GRCh38 genome version (available in GENCODE v29), not only to align the reads to the reference genome but also for gene annotation. Fastq RNA-seq data were mapped using STAR-2.7.0e and gene abundances were internally estimated using the HT-seq algorithm. Before the differential expression analysis, expression genes were filtered, keeping the genes whose read counts are above 1, and normalized, considering the estimates of the library size. Differential expression analysis was then performed using DESeq2 [468]. In order to detect differentially expressed genes between NKG2D-CAR NKAE and NKG2D-CAR CIML-NKAE cells, analysis was performed comparing differences between these populations, taking into account HD variability. Finally, principal components (PC) analysis was carried out, selecting the 3,000 genes with the higher variability among NK cell populations. PC1 reveals the most variation and PC2, the second most variation.

3.12. Bulk DNA methylation analysis

Epigenomic analysis of NKG2D-CAR CIML-NKAE and NKAE cells was performed by Cancer epigenetic group, at Josep Carreras Leukaemia Research Institute, Barcelona.

Following manufacturer recommendations, NK cells Genomic DNA was bisulfite-converted using an EZ DNA Methylation Gold kit (Zymo Research, Orange, CA, USA). DNA methylation was then interrogated using the Infinium MethylationEPIC Kit (Illumina). Raw signal intensity data were initially preprocessed from resulting idat files using minfi Bioconductor package (v1.36.0). Several quality control steps were applied to minimize errors and remove erratic probe signals, such as failed probes (probes with detection P value > 0.01 in at least 10% of samples were removed), cross-reacting probes and probes that overlapped SNPs within ±1 bp of CpG sites, followed by background correction and dye-based normalization using ssNoob algorithm (single-sample normal-exponential out-of-band). Normalized intensities were used to calculate DNA methylation levels (Beta values) for each CpG evaluated. All analyses were performed under R statistical environment (v4.0.3).

3.13. Mouse models

Non-obese diabetic (NOD) Cg-Prkdcscid Il2rgtm1Wjl Tg(IL15)1Sz/SzJ (NSG-Tg(Hu-IL15)) mice were procured from Jackson Laboratory (#030890) and used to study CAR effector *in vivo* efficacy. NSG-Tg(Hu-IL15) strain has been modified with a rhIL-15 knock-in to constitutively express physiological concentrations of human IL-15 (7.1 ± 0.3 pg/ml) [469]. All the procedures were approved by the *Comunidad de Madrid* (under the PROEX 191.2/20) and according to the European Union Directive 2010/63/EU and the Spanish Royal Decree-Law RD53/2013. Mice were maintained in pathogen-free conditions and housed in ventilated cages at 20-25ºC, 55 ± 10% relative humidity, *ad libitum* fed and exposed to 12 hours light:dark (LD) cycles. At the time of experiments, 6-8 week-old female mice were randomly assigned to the different experiment groups (n=4 mice per group).

NSG-Tg(Hu-IL15) mice were sublethally irradiated with a whole-body 1.5 Gy gamma ray dose, 24 hours before tumor infusion. At day 0, 5 x 10^5 U-266 or RPMI-8226

ffLucGFP cells were intravenously administered via tail vein. After 72 hours, CAR NK effectors were intravenously injected.

Mice body weight was measured weekly and end point criteria (20% weight loss, asthenia or paraplegia) were evaluated daily. At this point, mice were sacrificed by anaesthesia (75 µg/gr ketamine and 500 µg/gr dexmedetomidine intraperitoneal (i.p)) and tissues were collected for further analysis.

3.13.1. *In vivo* tumor biodistribution analysis by bioluminescence imaging (BLI)

Tumor burden monitoring was weekly or fortnightly performed by BLI using In-Vivo Xtreme Preclinical Optical/X-ray Imaging System (Bruker Sciences) or IVIS Lumina XRMS Series III (Perkin Elmer) until the end of the experiment. Mice were anaesthetized with 2% isoflurane and 200 mg/kg of an aqueous solution of D-luciferin potassium salt (Thermosfisher) were intraperitoneally administered 10 minutes prior to image acquisition. Binning, f-stop and time exposure were automatically set for each picture and luminescence was expressed in photons per second per mm^2 and overlaid on the white light image.

3.13.2. CAR NK cell infiltration analysis in PB samples

CAR effector *in vivo* follow-up was carried out at 7-, 14- and 29-days post-administration. PB from tail vein was extracted in EDTA tubes and CAR NK cells were detected by flow cytometry. CD45 PerCP/Cy5.5 and CD56 APC Abs were used for NK cell gating and rhBCMA/Streptavidin PE or NKG2D PE for CAR^+ cells detection, as described in 3.3.1.

3.13.3. Human population engraftment analysis in PB and BM at necropsy

At end point, mouse necropsy was conducted and PB, femurs and tibias were extracted for further analysis. BM was flushed out into PBE with a syringe. Samples were filtered (0.3 µm) and erythrocytes were lysed with the ACK lysis buffer. MM cells were detected by GFP expression and CD138 PE/Cy7 staining, while CAR NK cells were analyzed by CD45 PerCP/Cy5.5, CD56 APC and rhBCMA/Streptavidin PE or NKG2D PE staining, after flow cytometer acquisition.

3.14. Statistical analysis

GraphPad Prism 8 was used for all statistical analysis (GraphPad Software, CA, USA). Data are shown as mean ± Standard Error of Mean (SEM). First, Shapiro-Wilk and Levene tests were conducted to evaluate normality and homoscedasticity, respectively in the studied variables.

Paired or unpaired two-tailed Student t-tests were applied between two parametric groups, one-way analysis of variance (ANOVA) following Tukey's post-hoc test was carried out for two groups with only one variable and two-way ANOVA analysis was performed following Tukey´s multiple comparison post-hoc test for two groups that had two different variables. Mann-Whitney-Wilcoxon U test was used to compare two independent non-parametric variables, while Kruskal-Wallis test was performed for three or more groups comparison. *In vivo* mouse model survival curves were analyzed by applying the Kaplan-Meier method and Mantel-Cox test. Additionally, Kaplan-Meier analysis of PFS and OS between MM patients at diagnosis was carried out. Hazard ratio (HR) and corresponding 95% CIs are from a Cox proportional hazard model. One-sided p value was derived from a log-rank test. Statistical significance was shown as follows: $p < 0.05$ (*), $p < 0.01$ (**), $p < 0.001$ (***), $p < 0.0001$ (****).

4. RESULTS

4.1. HLA-E/NKG2A immune checkpoint is upregulated in MM patients but α-NKG2A blocking antibodies are not efficient as monotherapy treatment

4.1.1. HLA-E is overexpressed across the progression of MM

To evaluate whether HLA-E is overexpressed in MM cells, we first studied HLA-E expression on malignant PC from MM patients in comparison to PC from HD. A compilation of 20 HD BM samples as well as 54 MM patient samples showed that HLA-E is overexpressed on PC from MM patients (17.31 ± 1.99 RFI) with respect to PC from HD (10.31 ± 1.29 RFI) (Fig. 25A).

We further assessed HLA-E expression on pPCs compared to healthy populations, such as nPCs and $CD34^+$ progenitor cells, from those MM patients at different disease stages. We stratified MM patient samples into diagnosis (n=31) and progressions (n=25), and incorporated MGUS patients (n=12) into the study. The analysis of HLA-E expression levels revealed that this biomarker is overexpressed in pPC with respect to nPC in 59% of MM symptomatic patients and 78% of patients at progression. The expression ratio achieves significantly higher values in patients at progression (1.72 ± 0.2-fold), compared to patients at diagnosis (1.08 ± 0.12-fold) or MGUS (0.96 ± 0.19-fold) (Fig. 25B). By the same token, we also detected superior levels of HLA-E in pPC over $CD34^+$ cells in 70% of MM symptomatic patients and 84% of patients at progression, with the highest overexpression values in progression cases (2.2 ± 0.24-fold) (Fig. 25B).

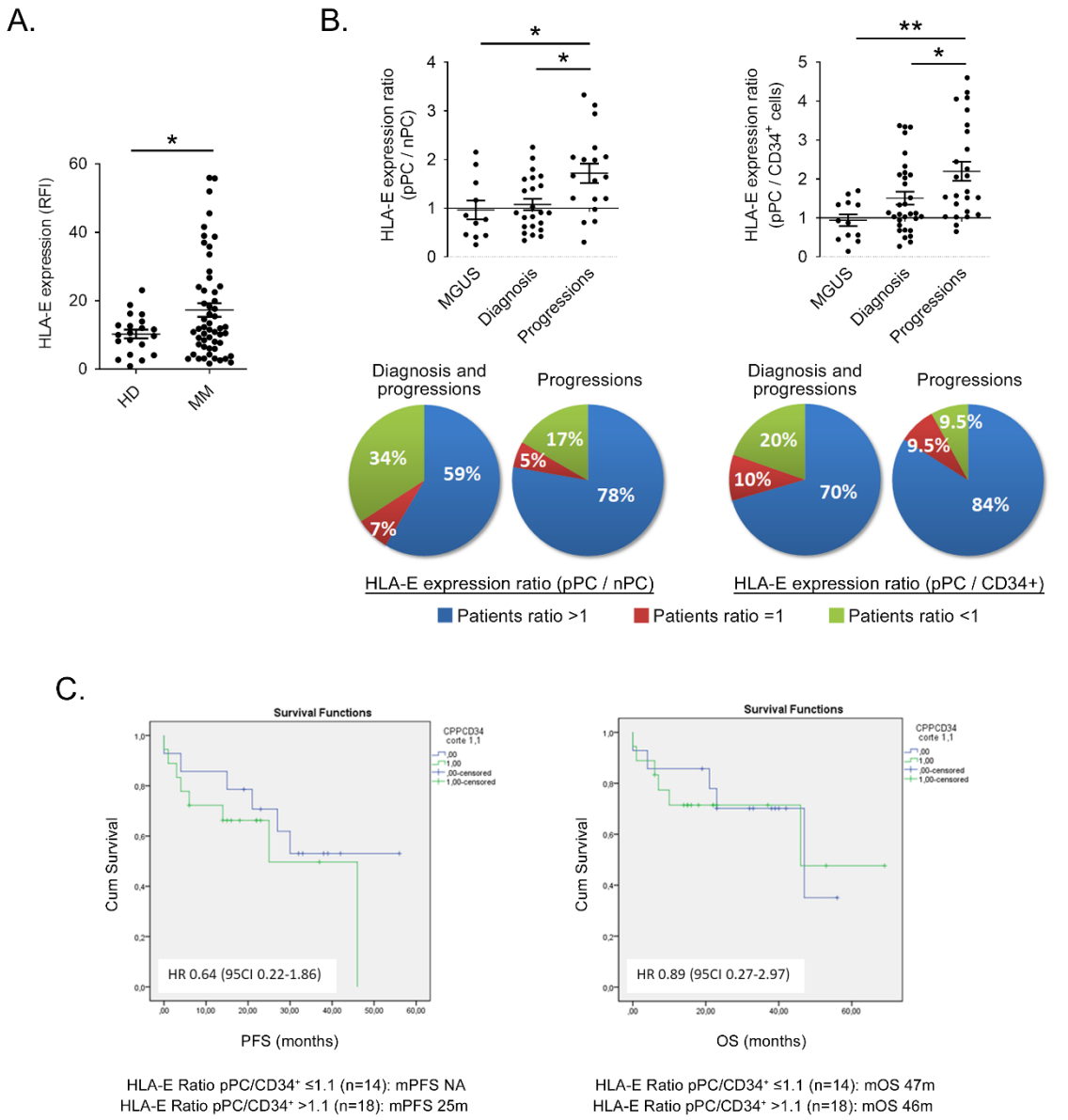

Figure 25. HLA-E is overexpressed on PC from MM patients, especially at progression, but it does not significantly correlate with a higher OS or PFS. A) Flow cytometry analysis of HLA-E expression on PC from HD (n=20) or symptomatic MM patient BM samples (n=54). The mean ± SEM is shown. B) At the left, flow cytometry analysis of HLA-E expression ratio between pPC and nPC from MGUS (n=11) or symptomatic MM patient samples at diagnosis (n=23) or progression (n=18). At the right, HLA-E expression ratios between pPC and $CD34^+$ cells from MGUS (n=12) or symptomatic MM patient samples at diagnosis (n=31) or progression (n=25). The mean ± SEM is shown. Below, percentages of patients with pPC/nPC or pPC/CD34+ HLA-E expression ratios >, < or equal to 1 are represented as circle chart. C) Kaplan-Meier analysis of progression-free survival (PFS) and overall survival (OS) between MM patients at diagnosis (n=32). Hazard ratio (HR) and corresponding 95% CIs are from a Cox proportional hazard model stratified by HLA-E ratio pPC/$CD34^+$ ≤ 1.1 or > 1.1. *p<0.05; **p<0.01.

High HLA-E expression has been associated with poor patient survival in solid tumors [379, 384-386, 388, 389], but its relevance as biomarker in MM progression has not been

properly studied. Our latter analysis, which shows HLA-E overexpression on MM cells with regard to healthy populations across MM progression, raised the evaluation of HLA-E as a prognostic factor in MM. For this purpose, we stratified MM patients at diagnosis in two groups: high HLA-E expression (patients with a pPC/CD34$^+$ HLA-E expression ratio >1.1; n=14) and low HLA-E expression (patients with a pPC/CD34$^+$ HLA-E expression ratio ≤1.1; n=18). No significant differences were found neither in OS nor in PFS. However, high HLA-E expression patients had a median PFS of 25 months, while the median PFS within the low HLA-E expression group was not reached (HR 0.64; 95CI 0.22-1.86) (Fig. 25C).

Altogether, these results suggest that HLA-E expression increases with the progression of MM but a further study, in a larger number of patients, would be required to better evaluate the use of this biomarker to predict MM patient prognosis.

4.1.2. IFN-γ is highly expressed in BM MM patients and increases HLA-E levels, while BTZ decreases its expression on MM cells

To understand the possible effect of TME on HLA-E expression on MM cells, we studied the presence of different immunosuppressive or inflammatory cytokines (TGF-β1, IL-1β, IL-6, IL-3, TNF-α, MCP-1, IL-2, IL-8, IFN-α, IL-15, IL-18, IL-10 and IFN-γ) in MM patient BM plasmas, including patients at diagnosis and progression, compared to HD. Of note, neither HD nor patients had any sign of infection at the time BM samples were extracted. Results show that the concentration of TGF-β1 (66.76 ± 13.81 pg/ml vs 16.97 ± 2.95 pg/ml), MCP-1 (2,807 ± 398.6 pg/ml vs 1,316 ± 120.9 pg/ml), IL-6 (23.78 ± 3.49 pg/ml vs 6.91 ± 1.69 pg/ml) and IFN-γ (14.35 ± 2.9 pg/ml vs 6.85 ± 0.27 pg/ml) were significantly higher in the plasma of BM from MM patient compared to HD (Fig. 26A).

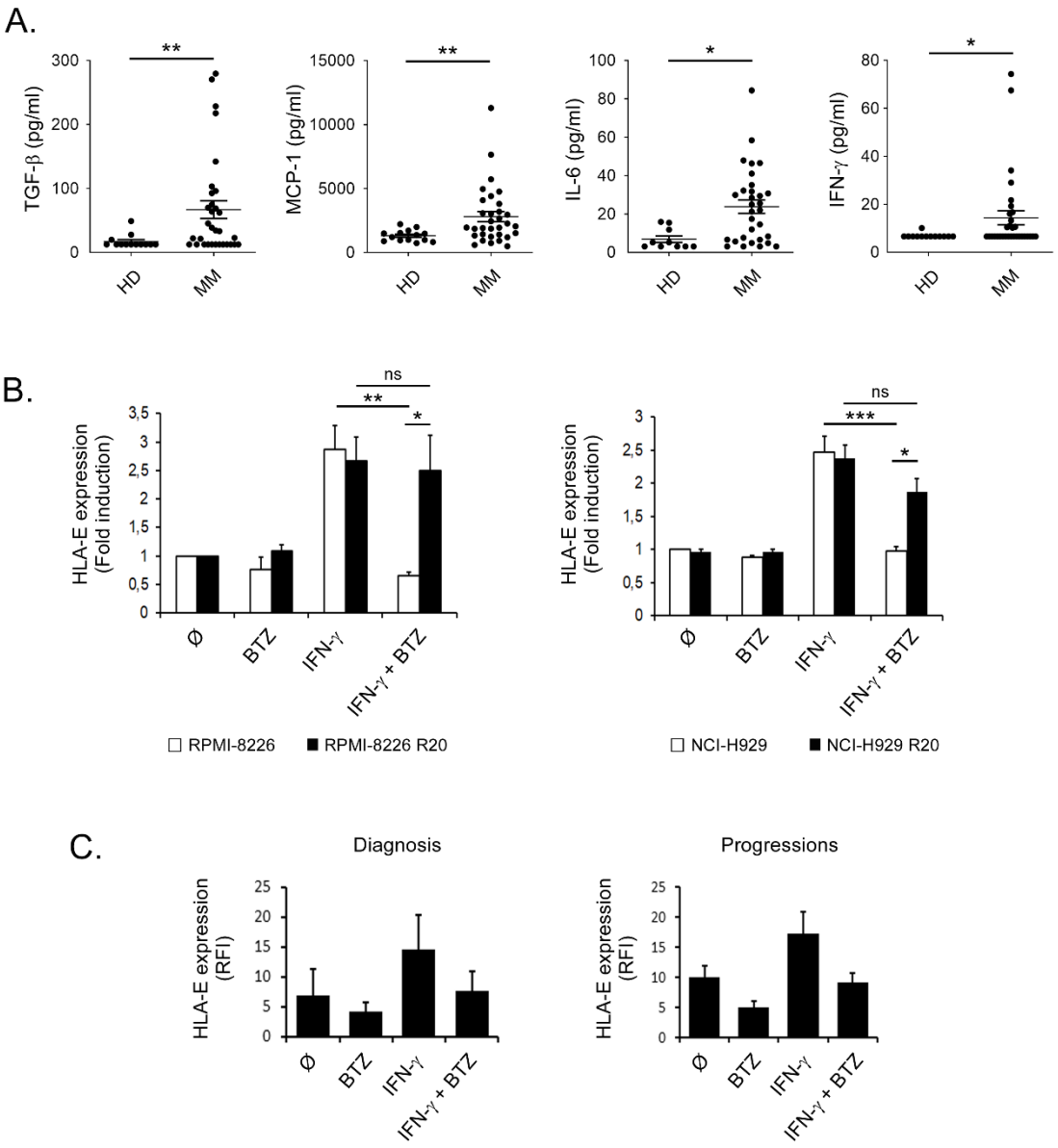

Figure 26. BM plasma of MM patients has an increased concentration of IFN-γ, cytokine that, along with BTZ, modulates HLA-E expression. A) Cytokine quantification in BM plasma from HD (n=14) and MM patients (n=32) by LEGENDplex bead-based immunoassay. The mean ± SEM is shown. B) Flow cytometry analysis of HLA-E expression modulation on MM cell lines RPMI-8226 and NCI-H929 and the 20 nM BTZ-resistant RPMI-8226 R20 and NCI-H929 R20 cells (n=3) or C) on MM patient PC at diagnosis (n=3) or progression (n=2), without treatment or after 24-hour treatment with 20 nM BTZ, 500 ng/ml IFN-γ or both. The mean ± SEM is shown. ns: not significant; *p<0.05; **p<0.01; ***p<0.001.

Given that IFN-γ has been described to increase HLA-E expression on MM cells [393], we studied this association in depth.

With this aim, NCI-H929 and RPMI-8226 MM cells were treated with IFN-γ for 24 hours. Flow cytometry analysis demonstrated that IFN-γ is able to significantly increase HLA-

E expression, 2.87 ± 0.42-fold on RPMI-8226 and 2.48 ± 0.24-fold NCI-H929 MM cells, over untreated MM cells (Fig. 26B). In addition, we tested the induction of HLA-E in MM primary cells after 24-hour IFN-γ exposure over BMMC cultures. Similarly, IFN-γ treatment is capable of enhancing HLA-E expression on PC of MM patients at diagnosis (from 6.89 ± 4.39 RFI without treatment to 14.59 ± 5.76 RFI) and progression (from 10.13 ± 1.84 RFI without treatment to 17.28 ± 3.6 RFI) (Fig. 26C).

Since previous studies demonstrated that BTZ treatment reduces HLA-E expression on MM cells [85], we asked whether the activity of this proteasome inhibitor might be compromised in the presence of IFN-γ. BTZ treatment slightly decreases HLA-E expression on the studied MM cell lines, but it is able to significantly counteract the induction of HLA-E expression caused by IFN-γ on RPMI-8226 cells (2.87 ± 0.42-fold after IFN-γ vs 0.66 ± 0.07-fold after IFN-γ and BTZ) and NCI-H929 cells (2.48 ± 0.24-fold after IFN-γ vs 0.98 ± 0.07-fold after IFN-γ and BTZ) (Fig. 26B). HLA-E reduction due to BTZ treatment is also observed in PC, even after IFN-γ exposure from patients at diagnosis (14.59 ± 5.76 RFI vs 7.77 ± 3.22 RFI) and progressions (17.28 ± 3.6 RFI vs 9.18 ± 1.54 RFI) (Fig. 26C).

MM patients can acquire BTZ resistance after first-line standard treatments [98]. Therefore, we studied the combination effect of IFN-γ and BTZ over MM cells resistant to 20 nM of BTZ: RPMI-8226 R20 and NCI-H929 R20. HLA-E expression induction on RPMI-8226 R20 treated with IFN-γ is 2.67 ± 0.42-fold, but BTZ treatment cannot significantly decrease this value (2.49 ± 0.62-fold). Similarly, the increment of HLA-E expression caused by IFN-γ on NCI-H929 R20 (2.38 ± 0.2-fold), is maintained after BTZ exposure (1.87 ± 0.2-fold) (Fig. 26B).

These results indicate that IFN-γ treatment augments HLA-E presence on the surface of both cell lines and primary MM cells, while BTZ decreases HLA-E expression, even the higher levels achieved after IFN-γ exposure. However, BTZ treatment cannot reduce IFN-γ-induced HLA-E expression on BTZ-resistant MM cell lines, which could mimic the BTZ-resistant MM patient scenario.

4.1.3. NKG2A is overexpressed on MM cytotoxic NK cells at progression but α-NKG2A treatment does not reactivate their cytotoxicity against tumor cells in native cultures

In addition to the HLA-E study on PC from MM patients, we analyzed the expression of their activating and inhibiting receptors, NKG2C and NKG2A, respectively, on cytotoxic NK ($CD56^{dim}CD16^{+}$) and T ($CD3^{+}CD8^{+}$) cells from these patients.

Flow cytometry results revealed that there is a higher percentage of cytotoxic NK cells expressing NKG2A than NKG2C in all stages (Fig. 27A). No differences were found regarding NKG2C expression on NK cells (17.17 ± 4.1% on MGUS, 12.2 ± 2.52% on MM at diagnosis and 28.71 ± 6.11% at progression). Remarkably, the percentage of $NKG2A^{+}$ cells is significantly higher in patients at progression (49.24 ± 7.61%), compared to patients at diagnosis (29.56 ± 4.82%), which suggests that the NK population from these patients may be inhibited by the HLA-E/NKG2A immune checkpoint. Regarding T cells, NKG2C and NKG2A expression is minimal in all the studied patients, less than 20% of positive cells.

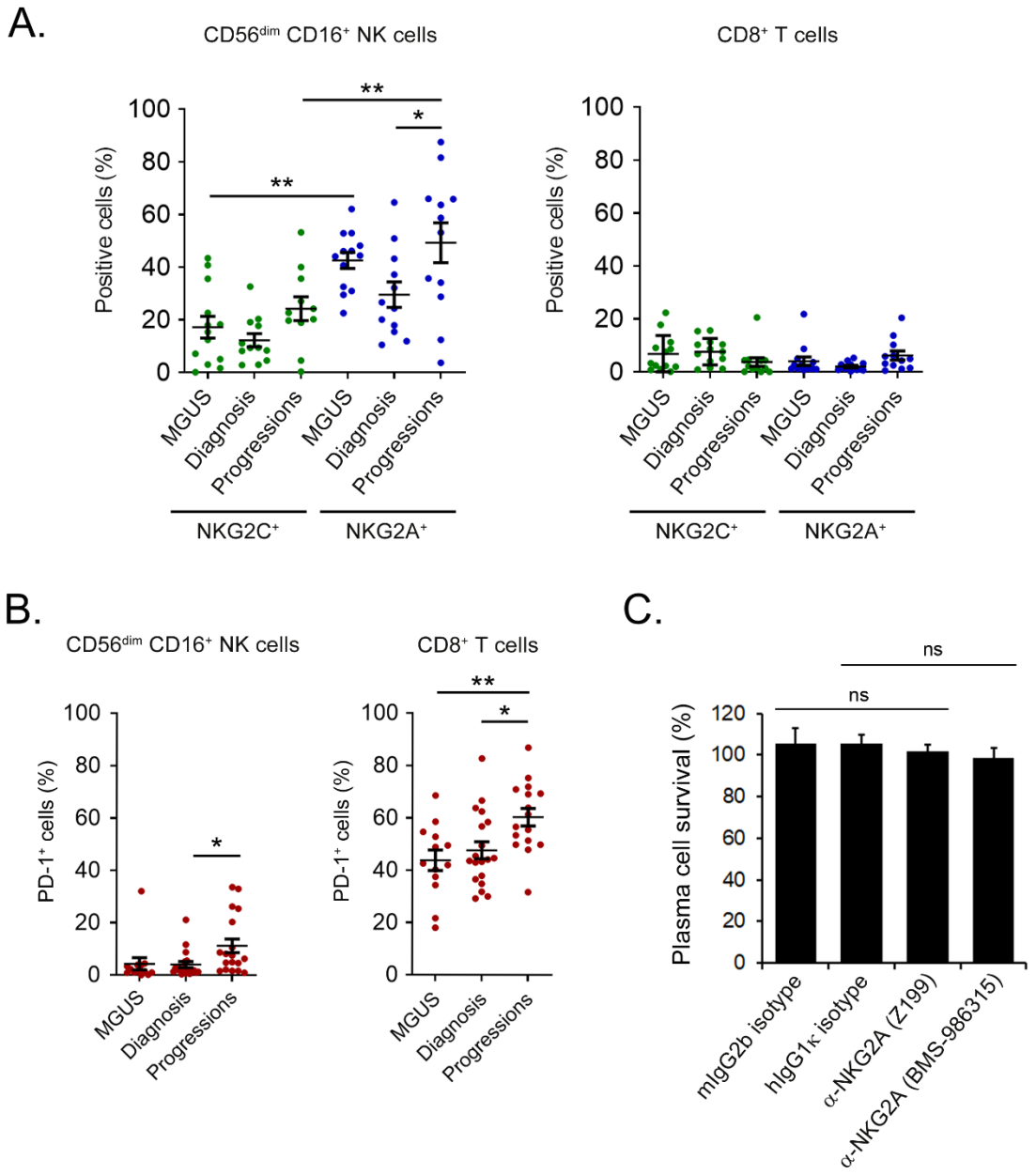

Figure 27. Cytotoxic NK cells from MM patients at progression have increased NKG2A expression, but α-NKG2A Abs in monotherapy cannot restore NK cell activity against primary PC. Flow cytometry analysis A-B) of NKG2C, NKG2A (A) and PD-1 (B) expression on $CD8^+$ T and $CD56^{dim}$ $CD16^+$ NK cells from BM MGUS (n=13) and MM patient samples at diagnosis (n=19) or at progression (n=16). C) Flow cytometry analysis of PC survival in cultures of BMMCs from MM patients after treatment with the mouse (Z199) or human (BMS-986315) α-NKG2A Abs or their corresponding isotypes (mouse IgG2b and human IgG1κ, respectively) (n=5). Means ± SEM are shown. ns: not significant; *p<0.05; **p<0.01.

In addition, we have studied the expression of another relevant immune checkpoint in MM, PD-1. The percentage of $PD\text{-}1^+$ T cells is 43.78 ± 3.91% at MGUS, 47.61 ± 3.26% at diagnosis, increasing significantly in patients at progression 60.3 ± 3.36% (Fig. 27B). By contrast, low percentages of MM cytotoxic NK cells express this inhibitory receptor

(4.29 ± 2.35% on MGUS, 4.06 ± 1.17% on MM at diagnosis and 11.26 ± 2.64% at progression). Altogether, these results suggest that NKG2A is not the predominantly inhibitory receptor expressed in MM $CD8^+$ T cells, where PD-1 might be a relevant inhibitory signal.

Since both HLA-E on pPC and NKG2A on cytotoxic NK cells are highly expressed on MM patients at progression, we assessed the disruption of the inhibitory signal in order to reactivate NK cell cytotoxicity against the tumor cells. BMMCs from MM patients were cultured for 24 hours with a mouse (Z199) or human (BMS-986315) α-human NKG2A Ab or their corresponding isotypes, mouse IgG2b (mIgG2b) or human IgG1κ (hIgG1κ), respectively. Neither the Z199 nor the BMS-986315 Abs are able to restore patient NK cell activity against primary MM cells, not exceeding 8% of lysis reduction (Fig. 27C).

Taken together, these results demonstrate that, despite the HLA-E/NKG2A immune checkpoint axis is upregulated in MM patients at progression, the treatment with α-NKG2A Abs, as single agents, is not effective reducing pPC number *in vitro*.

4.2. NKG2A blockade improves NKG2D-CAR and BCMA-CAR NKAE cell anti-MM cytotoxic activity

4.2.1 NKG2D- and BCMA-CAR NKAE cells are efficiently generated

Based on HLA-E overexpression on MM cells and considering that α-NKG2A monotherapy has not restored NK cell activity, correlating with clinical trial results in solid malignancies [407, 408], we studied the combination of α-NKG2A Abs with a novel immunotherapy approach. Regarding that clinical responses obtained with CAR NK cells might be improved, we determined to evaluate the combination of α-NKG2A blocking Abs with two CAR NK cell therapies for MM treatment.

To generate CAR NKAE cells from HD, PBMCs were obtained from 18 ml of PB and co-cultured with the irradiated feeder cell line, K562-mb21-41BBL. Once NKAE cells were purified at day 6 of culture, these cells were transduced with NKG2D- or BCMA-CAR lentivectors at MOI 5 and 16, respectively.

Phenotype analysis of these populations, NKG2D-CAR NKAE and BCMA-CAR NKAE cells, was performed by flow cytometry (Fig. 28A). Although NK cell percentage is lower than 10% in PBMCs at day 0 of culture (7.98 ± 2.96% among cultures for NKG2D-CAR NKAE cells and 9.91 ± 2.4% for BCMA-CAR NKAE cells), after activation, expansion, purification, and transduction, an average purity of 91.96 ± 2.05% $CD56^{+}CD3^{-}$ cells in NKG2D-CAR and 94.1 ± 3.11% $CD56^{+}CD3^{-}$ cells in BCMA-CAR NKAE cell cultures was obtained at day 14. Of note, NK cells at both time points are mainly cytotoxic (around 70-90% $CD56^{+}CD16^{+}$). Moreover, despite T cells are a predominant subset at the beginning of NKAE cell expansion, with a mean percentage above 40% (38.64 ± 10.22% among cultures for NKG2D-CAR NKAE cells and 50.14 ± 9.14% for BCMA-CAR NKAE cells), NK cell expansion and subsequent purification reduce $CD3^{+}$ cells in both cultures to values lower than 0.5% (0.19 ± 0.1% in NKG2D-CAR NKAE cell cultures and 0.43 ± 0.38 in BCMA-CAR NKAE cell cultures at day 14) (Fig. 28B).

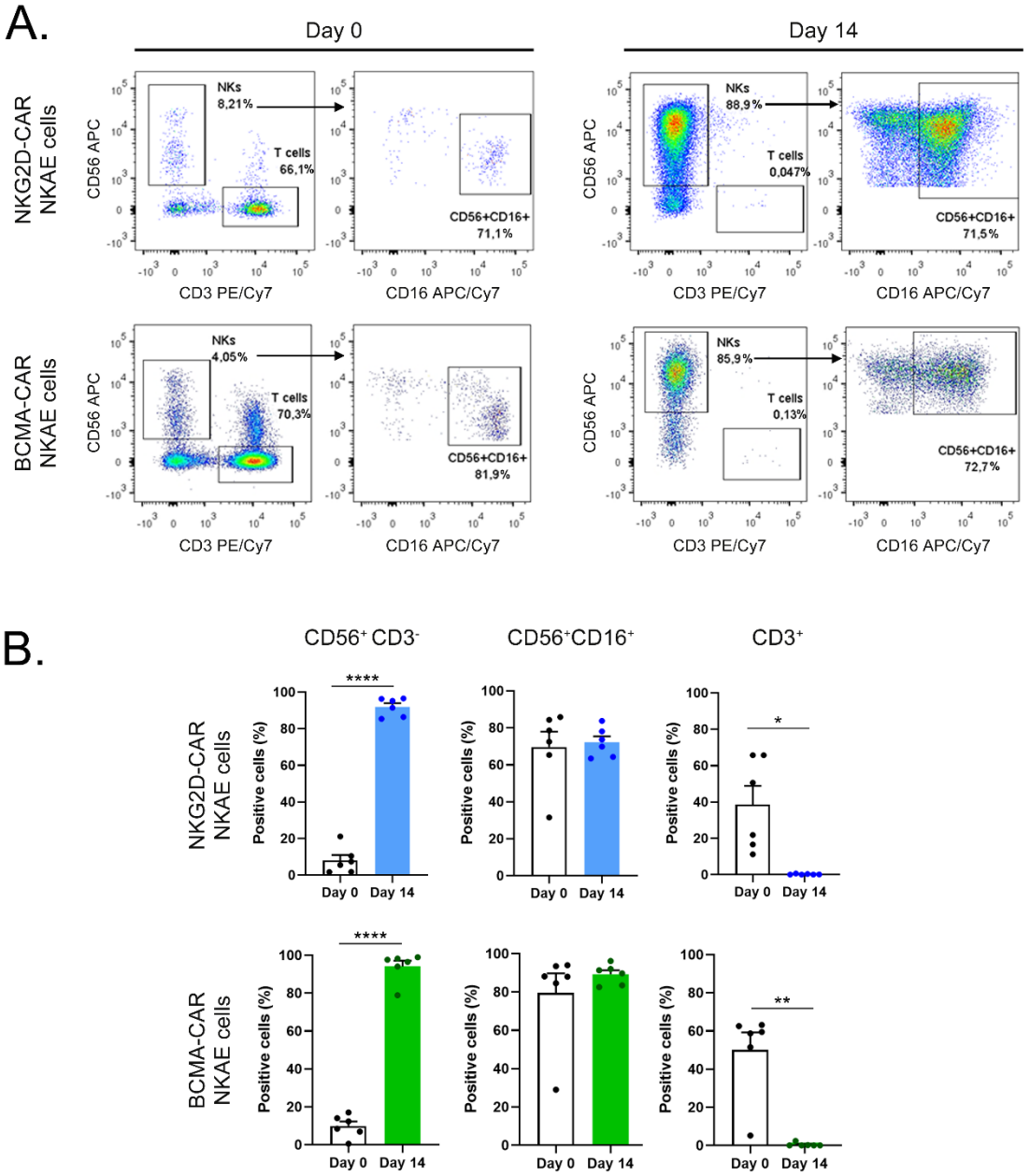

Figure 28. High-purity and cytotoxic NKG2D- and BCMA-CAR NKAE cell generation from HD PB. A) Representative flow cytometry dot plot of NK cells ($CD56^+CD3^-$), cytotoxic NK cells ($CD56^+CD3^-CD16^+$), and T cells ($CD3^+$) from NKG2D- and BCMA-CAR NKAE cell cultures at day 0 and day 14. B) Flow cytometry analysis of the percentage of NK cells ($CD56^+CD3^-$), cytotoxic NK cells ($CD56^+CD3^-CD16^+$), and T cells ($CD3^+$) cells in NKG2D- or BCMA-CAR NKAE cell cultures at day 0 and day 14 (n=6). Means ± SEM are shown. *p<0.05; **p<0.01; ****p<0.0001.

At day 6 after transduction, flow cytometry and q-PCR analysis were performed to evaluate CAR transduction efficiency in NKAE cells. The percentage of transduction, analyzed by flow cytometry, is 34.05 ± 6.32% for NKG2D-CAR and 22.21 ± 4.83% for BCMA-CAR (Fig. 29A, B). q-PCR data show there to be 0.82 ± 0.22 and 0.55 ± 0.17 vector copies per cell on average of NKG2D- and BCMA-CAR, respectively (Fig. 29B).

The protein expression of both CAR in NKAE cells was also corroborated by western blotting using an α-CD3ζ Ab. To obtain the theoretical molecular weight of CAR molecules, nucleotide sequences were translated to protein sequence with ExPASy translate tool and these amino acid sequences were applied to calculate the protein molecular weight with ExPASy compute pI/Mw. Western blot analysis shows proteins at the expected molecular mass of NKG2D-CAR (43.5 kDa) and BCMA-CAR (53.9 kDa) (Fig. 29C).

These results demonstrate the feasibility of generating NKG2D- and BCMA-CAR NKAE cells, achieving a high percentage of pure and cytotoxic NK cells, with a low percentage of T cell contamination, and being potently transduced with CAR molecules.

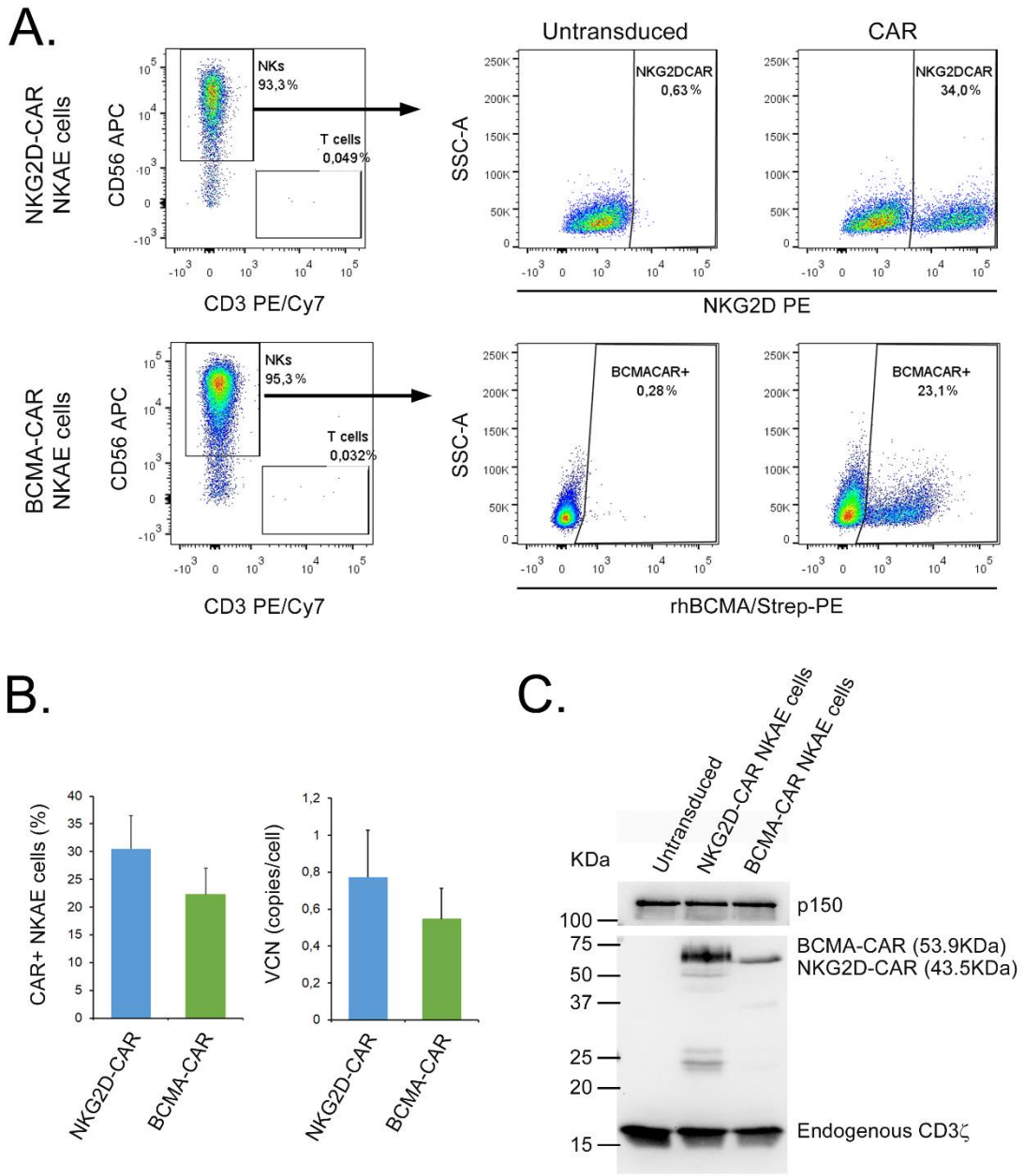

Figure 29. NKAE cells are stable and efficiently transduced with lentivectors containing NKG2D- or BCMA-CAR. A-B) Representative flow cytometry dot plot (A) and analysis (B, left) of NKG2D- and BCMA-CAR expression on the surface of NKAE cells at 6 days post-transduction (n=7). Vector copy number (VCN) quantification (B, right) of NKG2D- and BCMA-CAR in NKAE cells by q-PCR (n=7). The mean ± SEM is shown. C) Western blot analysis of NKG2D- and BCMA-CAR expression in NKAE cells after 6 days post-transduction. Lysates of untransduced, NKG2D-CAR and BCMA-CAR NKAE cells were separated by SDS-PAGE. A mouse anti-human CD3ζ Ab was used to detect the expression of endogenous and chimeric CD3ζ proteins. p150 was used as loading control.

4.2.2. NKG2A is highly expressed on CAR NKAE cells

To study the modulation of NKG2 family receptors along NK cell expansion, we analyzed NKG2C and NKG2A expression on NKG2D- and BCMA-CAR NKAE cells. Regarding

NKG2D, we only studied the differential expression of this receptor between day 0 and day 14 on BCMA-CAR NKAE cells, to avoid NKG2D-CAR expression bias.

Flow cytometry results show that 12.91 ± 5.2% of NKG2D-CAR NKAE cells were NKG2C^{+} at day 0 vs 17.11 ± 4.23% at day 14, whereas 31.3 ± 13.37% of BCMA-CAR NKAE cells were NKG2C^{+} at day 0 vs 13.35 ± 3.69% at day 14 (Fig. 30A). While NKG2C levels remained stable after NK cell expansion, NKG2A expression significantly enhanced on NKG2D-CAR NKAE cells (59.27 ± 4.24% at day 0 vs 90.49 ± 2.76% at day 14) and BCMA-CAR NKAE cells (48.46 ± 6.05% at day 0 vs 85.23 ± 3.66% at day 14). The expression of NKG2D also increased from 11.1 ± 1.74% at day 0 to 64.79 ± 11.52% at day 14 in BCMA-CAR NKAE cells (Fig. 30A).

Since the majority of CAR NKAE cells were NKG2A^{+}, we studied the effect of several cytokines, present in MM TME (IL-6, IL-10, TGF-β, and IFN-γ) or normally used to stimulate NK cells (IL-2, IL-15, IL-21, and 4-1BBL), to determine which of them can induce NKG2A expression on NK cells. NKG2A expression on regulatory (CD56^{bright}CD16^{-}) and cytotoxic (CD56^{dim}CD16^{+}) NK cells, purified from HD PBMCs, was measured by flow cytometry. IL-15 significantly increases NKG2A expression on both regulatory (162.21 ± 25.37 RFI with IL-15 vs 102.56 ± 7.14 RFI without stimulation) and cytotoxic (101.7 ± 11.05 RFI with IL-15 vs 54.94 ± 4.59 RFI without stimulation) NK cell subpopulations (Fig. 30B), as well as its combination with cytokines utilized in ex vivo culture and expansion of NK cells. Moreover, IL-2 in combination with IL-21, with or without 4-1BBL, also augments NKG2A expression. Notably, this last combination, IL-2, IL-21, and 4-1BBL, the one employed by our group to generate NKAE cells (IL-21 and 4-1BBL are expressed on the membrane of the feeder cell), significantly increases NKG2A expression on regulatory (149.55 ± 10.75 RFI with IL-2, IL-21, and 4-1BBL vs 102.56 ± 7.14 RFI without stimulation) and cytotoxic (101.9 ± 12 RFI with IL-2, IL-21, and 4-1BBL vs 54.94 ± 4.59 RFI without stimulation) NK cells.

These results suggest that all the cytokines commonly used in NK cell ex vivo expansion protocols increase the expression of the inhibitory receptor NKG2A, probably to counteract the high activation and expansion of these cells, defined by the increase of NKG2D expression.

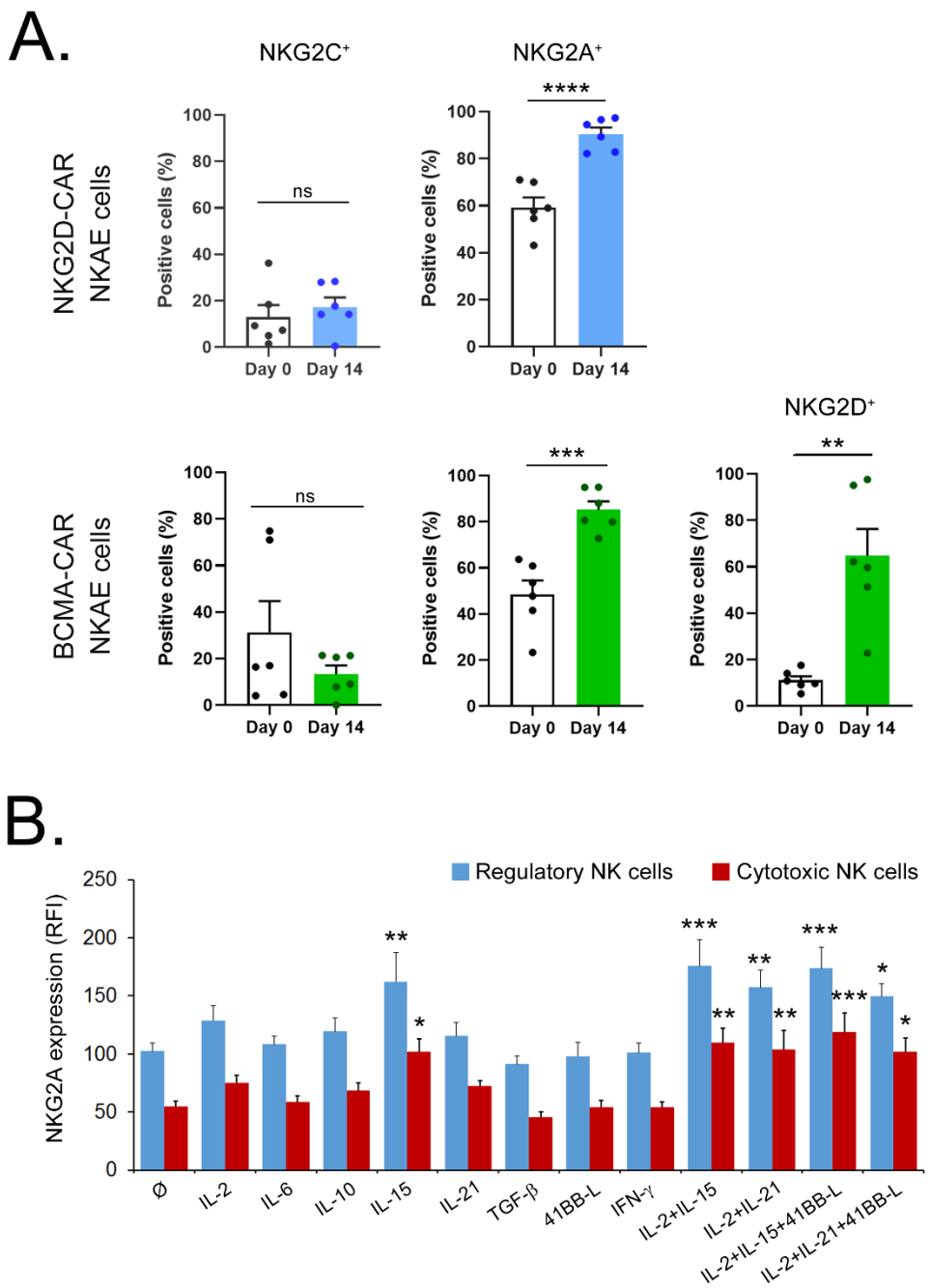

Figure 30. Cytokines used to expand NK or CAR NK cells ex vivo promote NKG2A expression. A) Flow cytometry analysis of the percentage of NKG2C^{+}, NKG2A^{+}, and NKG2D^{+} cells within CD56^{+}CD3^{-} populations on NKG2D- or BCMA-CAR NKAE cell cultures at day 0 and day 14 (n=6). Means ± SEM are shown. B) Flow cytometry analysis of NKG2A expression on regulatory (CD56^{bright}CD16^{-}) and cytotoxic (CD56^{dim}CD16^{+}) NK cells after 48-hour NK cell culture with different cytokines: IL-2 (50 IU/ml), IL-6 (20 ng/ml), IL-10 (50 ng/ml), IL-15 (50 ng/ml), IL-21 (50 ng/ml), TGF-β (10 ng/ml), 4-1BBL (200 ng/ml), and IFN-γ (500 ng/ml) or combinations of these cytokines (n=9). Means ± SEM are shown. ns: not significant; *p<0.05; **p<0.01; ***p<0.001; ****p<0.0001

4.2.3. CAR NKAE cells produce a high concentration of IFN-γ and increase HLA-E tumor expression after co-culture with MM cells

Once we have studied the NKG2A modulation on NK cells by cytokines present in the TME or used in NK cell activation protocols, we investigated whether CAR NKAE cells can modulate HLA-E expression on MM cell lines.

We first studied HLA-E expression on the MM cell lines used in the subsequent experiments: 2.64 ± 0.23 RFI on U-266, 3.64 ± 0.54 RFI on RPMI-8226, 4.48 ± 0.28 RFI on ARP-1 and 4.48 ± 0.18 RFI on XG-1. Moreover, we included the feeder cell line, K562-mb21-41BBL, as a HLA-E$^-$ cell line (RFI of 0.23 ± 0.09) (Fig. 31A).

To study the impact of CAR NKAE treatments on HLA-E expression on MM cell lines, we co-cultured both CAR therapies with the XG-1 MM cell line and analyzed HLA-E presence on its surface at 0, 3, and 24 hours. At 3 hours, HLA-E expression is similar to basal levels but, at 24 hours, HLA-E RFI significantly increases up to 10.17 ± 2.44 on XG-1 cells after NKG2D-CAR NKAE cell co-culture (vs 2.33 ± 0.1 RFI on XG-1 without NK treatment) and 11.61 ± 5.81 after BCMA-CAR NKAE cell co-culture (vs 2.29 ± 0.25 RFI on XG-1 without NK treatment) (Fig. 31B).

Bearing in mind that CAR NK cells secrete IFN-γ [284], and this cytokine augments HLA-E expression on MM cells [378], we quantified the amount of IFN-γ produced by CAR NKAE cells for 24 hours. Flow cytometry analysis revealed that CAR NKAE cells, in the absence of tumor cells (590.87 ± 136.75 pg/ml in NKG2D-CAR NKAE cells and 97.41 ± 9.31 pg/ml in BCMA-CAR NKAE cells) or in co-culture with XG-1 cells (693.14 ± 200.69 pg/ml in NKG2D-CAR NKAE cells and 236.05 ± 53.24 pg/ml in BCMA-CAR NKAE cells), release a high concentration of IFN-γ, compared to XG-1 cultures (4.24 ± 0.14 pg/ml) (Fig. 31C).

Taken together, these findings suggest that HLA-E expression may further enhance on MM cells after CAR NK cell treatment, increasing the resistance to CAR NK cell therapy mediated by HLA-E/NKG2A immune checkpoint.

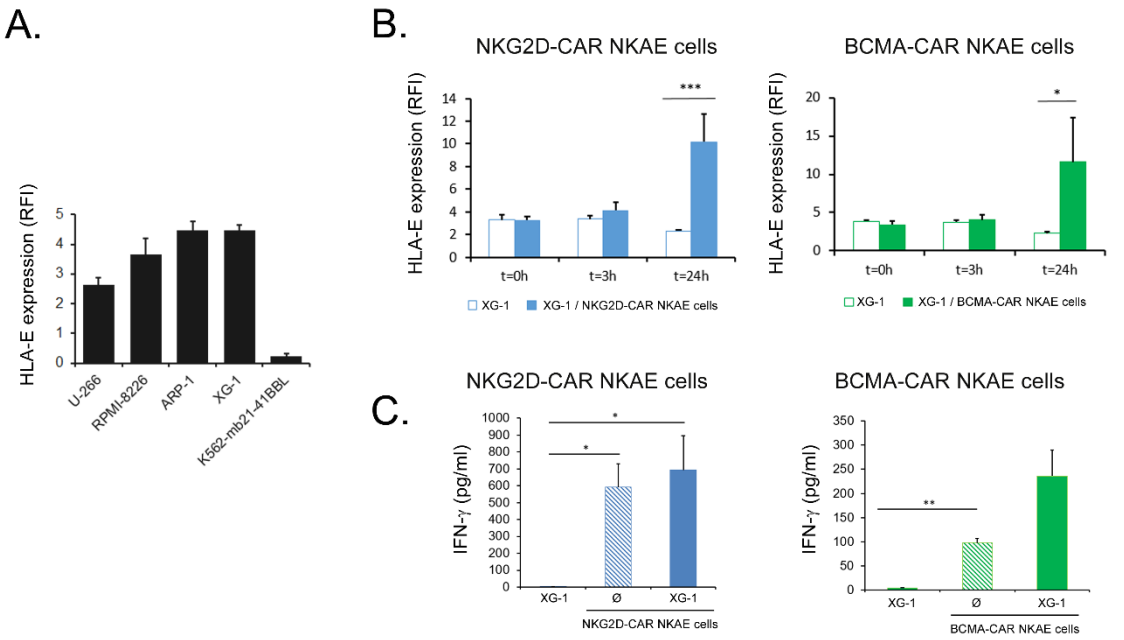

Figure 31. HLA-E expression increases on MM cells after co-culture with CAR NKAE cells that release high concentrations of IFN-γ. A) Flow cytometry analysis of HLA-E expression on U-266, RPMI-8226, ARP-1 and XG-1 MM cells and the feeder cell K562-mb21-41BBL (n=5). Means ± SEM are shown. B) Flow cytometry analysis of HLA-E expression on XG-1 cells alone or in co-culture with NKG2D- (n=4) or BCMA-CAR NKAE cells (n=3) at 0, 3 and 24 hours. The mean ± SEM is shown. C) IFN-γ quantification in NKG2D- or BCMA-CAR NKAE cell supernatants alone or after 24 hours co-culture with XG-1 MM cells, at 1:2 T:E ratio, by LEGENDplex bead-based immunoassay (n=3). *p<0.05; **p<0.01; ***p<0.001.

4.2.4. NKG2A blockade enhances CAR NKAE cell cytotoxicity against MM cell lines

Given that a high percentage of NKG2D- and BCMA-CAR NKAE cells are NKG2A^{+}, and that HLA-E is overexpressed on MM cell lines and primary MM cells, whose expression is even higher after CAR therapies co-cultures, we used the two α-NKG2A Abs (mouse Z199 and human BMS-986315) to disrupt this inhibitory immune checkpoint.

First, we evaluated the expression of CAR targets, NKG2D-L and BCMA, on different MM cell lines. U-266 (17.77 ± 0.61 RFI) and ARP-1 (6.29 ± 0.48 RFI) cells have a high NKG2D-L expression, whereas XG-1 (2.52 ± 0.15 RFI) and RPMI-8226 (4.09 ± 0.53 RFI) cell NKG2D-L expression is low. U-266 (15.14 ± 1.1 RFI) and RPMI-8226 (14.49 ± 3.93 RFI) cells have high expression of BCMA, while XG-1 (7.17 ± 0.84 RFI) and ARP-1 (7.17 ± 0.84 RFI) cells present lower levels (Fig. 32A).

To test the efficacy of NKG2A blockade to improve CAR NKAE cell killing capacity against MM cell lines, XG-1, ARP-1, U-266, and RPMI-8226 cells were co-cultured with CAR effectors pretreated with the mouse (Z199) or human (BMS-986315) α-NKG2A Abs, or their corresponding isotypes. Calcein-release assays demonstrated that blocking with either the mouse or the human α-NKG2A Abs significantly increases NKG2D- (Fig. 32B) and BCMA-CAR NKAE cell cytotoxicity (Fig. 32C) against all MM cell lines at different T:E ratios.

In subsequent studies, we tested the efficacy of both α-NKG2A Abs after increasing HLA-E expression on RPMI-8226 cells with a 24-hour IFN-γ treatment. Calcein-release assay results indicate a lower CAR NKAE cytotoxicity against RPMI-8226 cells when pretreated with IFN-γ. However, even in this increased resistance setting, both α-NKG2A blocking Abs were also able to potentiate NKG2D- and BCMA-CAR NKAE anti-MM activity (Fig. 32D).

Altogether, these *in vitro* experiments demonstrate that the blockade of the inhibitory receptor NKG2A fosters CAR NKAE cytotoxic activity against HLA-E^{+} MM cell lines.

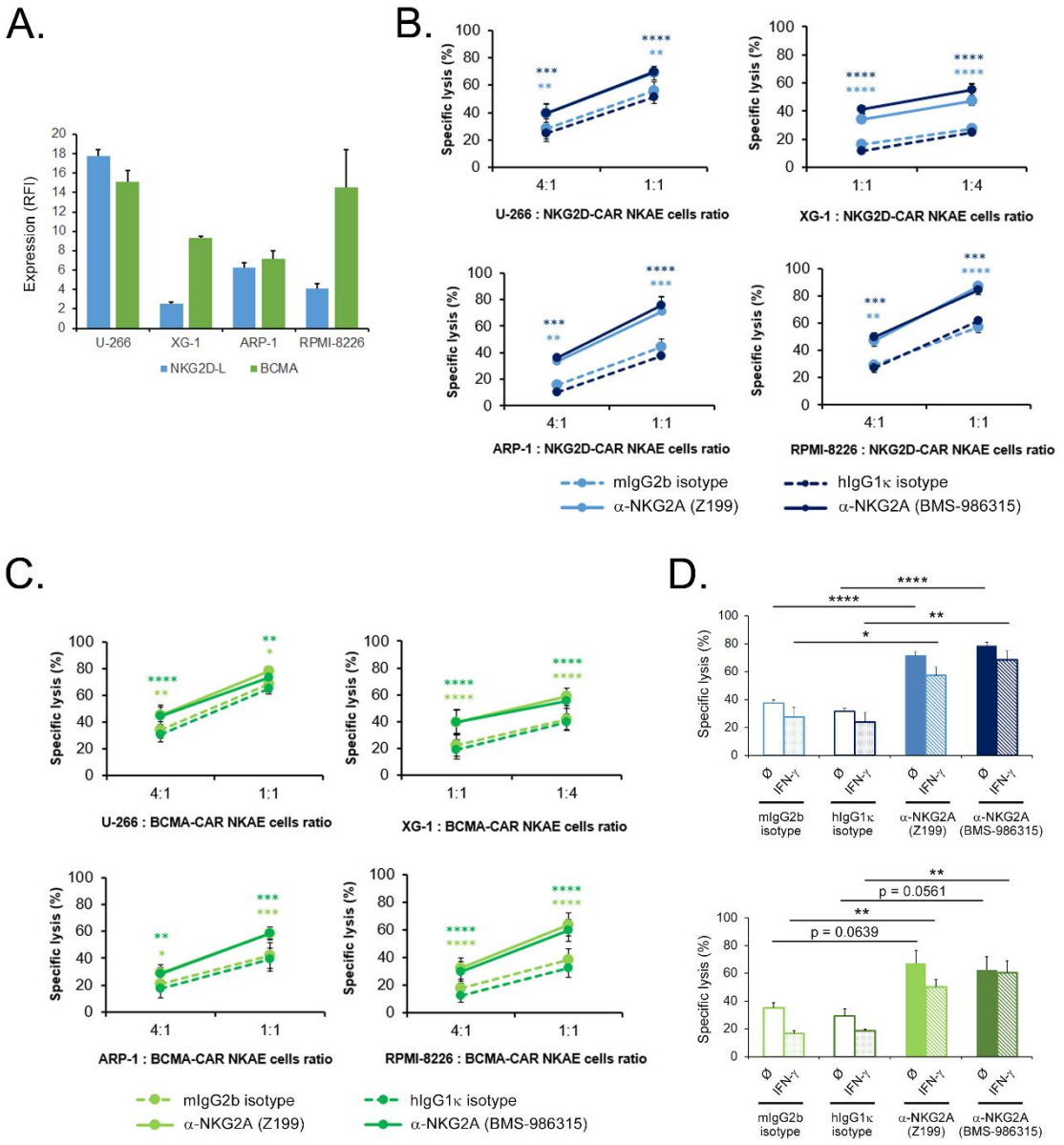

Figure 32. NKG2D- and BCMA-CAR NKAE cells in combination with α-NKG2A blocking Abs exhibit higher cytotoxicity against MM cell lines, even after 24h-treatment of tumor cells with IFN-γ. A) Flow cytometry analysis of NKG2D-L (ULBP1, ULBP 2/5/6, ULBP 3 and MICA/B) and BCMA expression on U-266, RPMI-8226, XG-1, and ARP-1 MM cells (n=6). Means ± SEM are shown. B-C) Specific lysis of NKG2D- (B) and BCMA-CAR NKAE cells (C) treated with either the mouse (Z199) or the human (BMS-986315) α-NKG2A Abs or their corresponding isotypes (mouse IgG2b and human IgG1κ, respectively) against the MM cells U-266, XG-1, ARP-1, and RPMI-8226, at different T:E ratios, analyzed by 3h-Calcein release assay (n=3-6). The mean ± SEM is shown. D) Specific lysis of NKG2D- and BCMA-CAR NKAE cells treated with either the mouse (Z199) or the human (BMS-986315) α-NKG2A Abs or their corresponding isotypes (mouse IgG2b and human IgG1κ, respectively) against the MM cells RPMI-8226, at 1:1 ratio, analyzed by 3h-Calcein release assay (n=3). Where indicated, RPMI-8226 cells are pretreated with IFN-γ for 24 hours. The mean ± SEM is shown. *p<0.05; **p<0.01; ***p<0.001; ****p<0.0001.

4.2.5. NKG2A blockade increases CAR NKAE degranulation levels and IFN-γ release during co-culture with MM cell lines

Another hallmark of NK cell activation by tumor cells is the degranulation capacity. NK cells hold cytotoxic granules containing perforins and granzymes, among other cytolytic proteins, which are directly released when these cells interact with target cells. Since the protein CD107a, also known as LAMP-1, is expressed on the membrane of these cytotoxic granules, the detection of this molecule has been described as a marker of NK and $CD8^+$ T cells degranulation, an indirect method to measure effector cytotoxicity [470] (Fig. 33A).

Both NKG2D- and BCMA-CAR NKAE cells pretreated with the α-NKG2A Abs heighten their degranulation levels against all the MM cell lines tested, but not against the HLA-E^- feeder cell K562-mb21-41BBL. Against ARP-1 cell line, 20.4 ± 4.47% or 27.04 ± 4.38% of NKG2D-CAR NKAE cells pretreated with mIgG2b or hIgG1κ, respectively, are $CD107a^+$, but increase to 35.98 ± 3.98% or 44.27 ± 5.21% in cells pretreated with Z199 or BMS-986315 α-NKG2A Abs, respectively. The pretreatment of BCMA-CAR NKAE cells with α-NKG2A Abs also potentiates degranulation levels (22.91 ± 1.17 % or 24.73 ± 4.03 % NKAE cells pretreated with mIgG2b or hIgG1κ vs 39.26 ± 2.95 % or 42.5 ± 3.77 % NKAE cells pretreated with Z199 or BMS-986315 α-NKG2A Abs) (Fig. 33B).

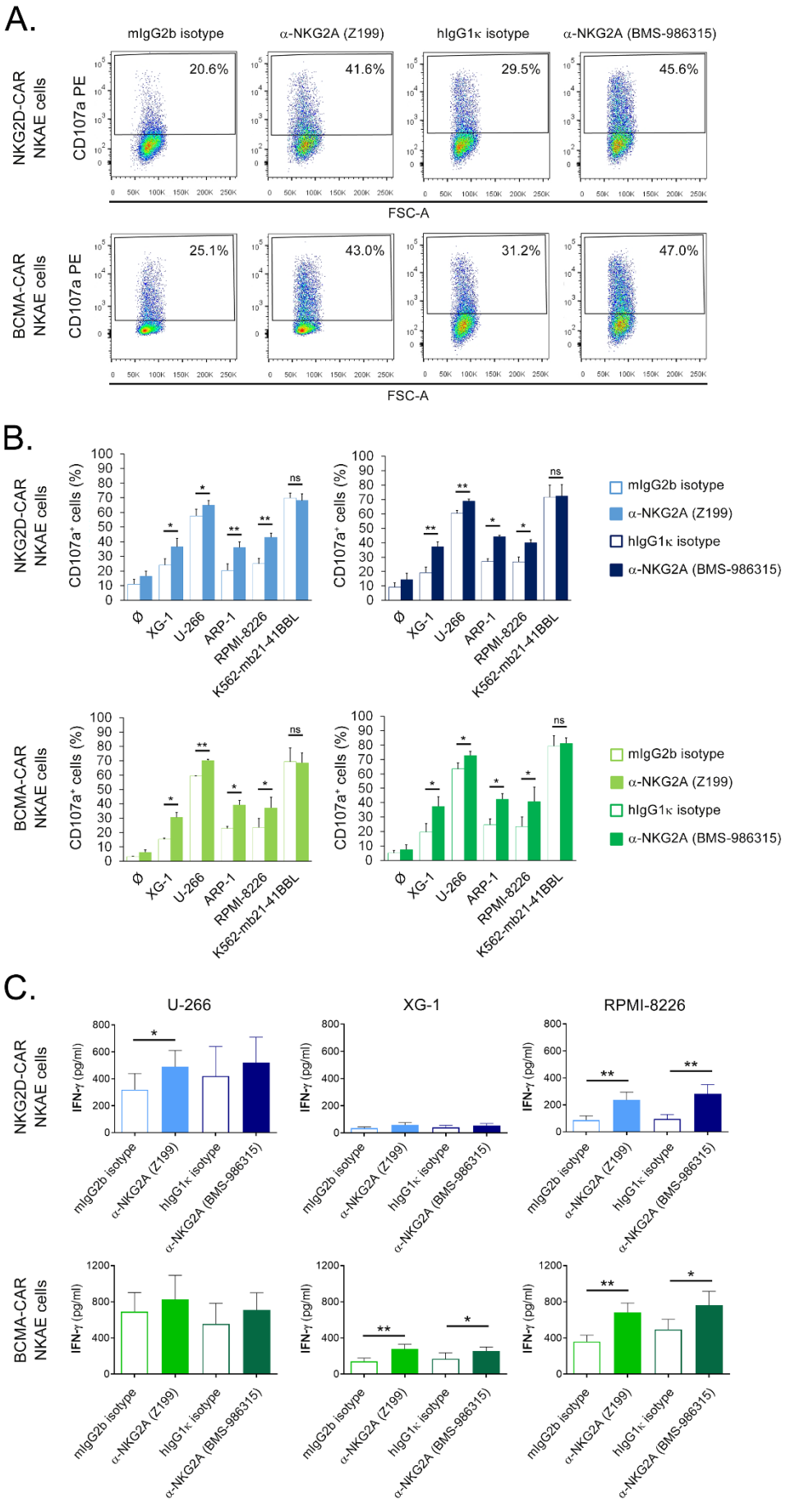
A.
mIgG2b isotype
α-NKG2A (Z199)
hIgG1κ isotype
α-NKG2A (BMS-986315)
NKG2D-CAR NKAE cells
BCMA-CAR NKAE cells
CD107a PE
20.6%
41.6%
29.5%
45.6%
25.1%
43.0%
31.2%
47.0%
FSC-A
B.
CD107a+ cells (%)
Ø
XG-1
U-266
ARP-1
RPMI-8226
K562-mb21-41BBL
ns
C.
U-266
XG-1
RPMI-8226
IFN-γ (pg/ml)

Figure 33. Higher degranulation capacity and IFN-γ release are exhibited by α-NKG2A-pretreated NKG2D- and BCMA-CAR NKAE cells. A) Representative flow cytometry dot plot of CD107a staining in NKG2D- and BCMA-CAR NKAE cells pretreated with α-NKG2A blocking Abs (Z199 or BMS-986315) or their corresponding isotypes (mIgG2b or hIgG1κ, respectively) and co-cultured with the ARP-1 MM cells for 4h. B) Flow cytometry analysis of CD107a expression on NKG2D- (n=5) and BCMA-CAR NKAE cells (n=3) pretreated with α-NKG2A blocking Abs (Z199 or BMS-986315) or their corresponding isotypes (mIgG2b or hIgG1κ, respectively), alone or after 4-hour co-culture with the XG-1, U-266, ARP-1, and RPMI-8226 MM cell lines, and the feeder cell HLA-E^{-}, K562-mb21-41BBL, at 1:1 ratio. The mean ± SEM is shown. C) Quantification of IFN-γ release after NKG2D- or BCMA-CAR NKAE cells pretreated with either the mouse (Z199) or human (BMS-986315) α-NKG2A Abs or their corresponding isotypes (mouse IgG2b or human IgG1κ, respectively) upon 24-hour co-culture with the MM cells U-266, XG-1, and RPMI-8226, at 1:2 T:E ratio, by LEGENDplex bead-based immunoassay (n=8). The mean ± SEM is shown. ns: not significant; *p<0.05; **p<0.01.

As the NKG2A blockade enhances CAR NKAE cell degranulation, we studied which cytokines or cytolytic proteins are increased. NKG2A-blocked NKG2D- and BCMA-CAR NKAE cells were cultured alone or with the MM cells U-266, XG-1 or RPMI-8226, or the feeder cell line K562-mb21-41BBL for 24 hours. Then, supernatants were collected and IL-2, IL-4, IL-6, IL-10, IL-17A, IFN-γ, TNF-α, soluble Fas, soluble FasL, granzyme A, granzyme B, perforin and granulysin release were analyzed by flow cytometry. Of note, the concentration of IFN-γ measured into NKG2D-CAR NKAE cell co-cultures against RPMI-8226 increases up to 236.23 ± 58.89 pg/ml and 282.8 ± 67.22 pg/ml in cultures of CAR NK cells pretreated with mouse or human α-NKG2A Abs, compared to 88.52 ± 30.57 pg/ml and 95.78 ± 32.78 pg/ml in cells pretreated with the mIgG2b or hIgG1κ, respectively. In addition, the pretreatment of BCMA-CAR NKAE cells with mouse or human α-NKG2A Abs raises IFN-γ concentration to 682.01 ± 103.99 pg/ml and 760.87 ± 154.15 pg/ml, respectively, whereas the concentration with their corresponding isotypes is 359.43 ± 70.85 pg/ml and 493 ± 112.39 pg/ml (Fig. 33C).

Collectively, these results demonstrate that breaking off the HLA-E/NKG2A interaction by means of NKG2A blocking Abs potentiates NKG2D-CAR and BCMA-CAR NKAE cell cytolytic capacity against MM cell lines.

4.2.6. α-NKG2A treatment does not significantly affect CAR NKAE cell activation or inhibition marker expression, but increases ZAP70/Syk phosphorylation

To investigate whether NKG2A blockade has an impact on NK cell phenotype, the expression of different activation and inhibition surface markers was analyzed by mass (Fig. 34A) and flow cytometry (Fig. 34B) on NKG2D- and BCMA-CAR NKAE cells pretreated with the human α-NKG2A Ab or its corresponding isotype after co-culture with RPMI-8226 cells for 24 hours.

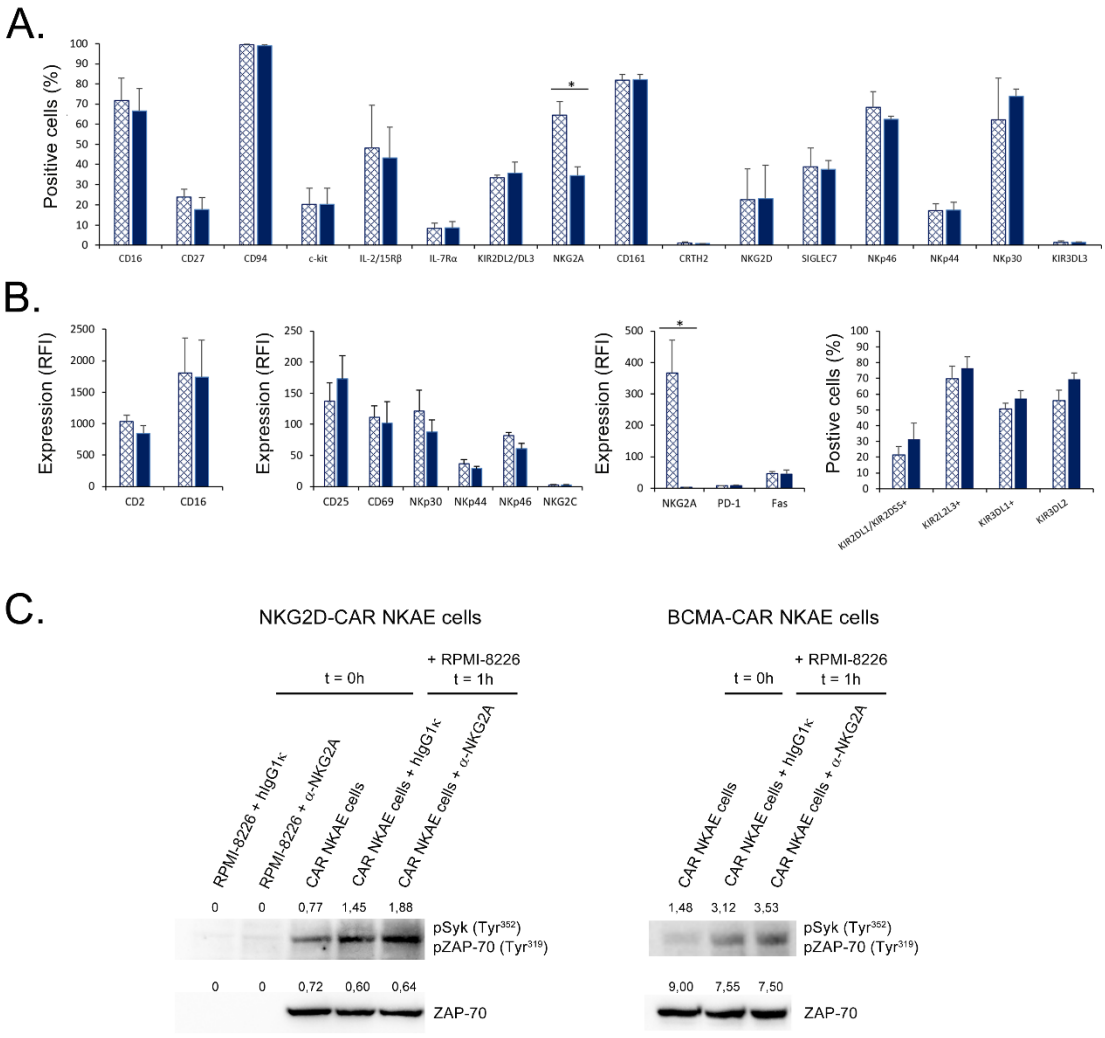

Figure 34. NKG2D-CAR NKAE cell immunophenotype is not markedly altered by NKG2A blockade but ZAP70/Syk phosphorylation is potentiated after tumor stimulation. A) Mass cytometry analysis of several markers in NKG2D-CAR NKAE cells ($CD56^{+}$) pretreated with the BMS-986315 α-NKG2A Ab or the human IgG1κ isotype, after 24-hour co-culture with the MM cells RPMI-8226 (n=3). B) Flow cytometry

analysis of different markers expressed on the surface of NKG2D-CAR NKAE cells ($CD56^+CD3^-$) after pretreatment with the BMS-986315 α-NKG2A Ab or the human IgG1κ isotype, and 24-hour co-culture with the MM cells RPMI-8226 (n=3). C) Western blot analysis of ZAP-70 (Tyr^{319}) / Syk (Tyr^{352}) phosphorylation in NKG2D- and BCMA-CAR NKAE cells, pretreated with BMS-986315 α-NKG2A Ab or the human IgG1κ isotype after 1-hour co-culture with the RPMI-8226 MM cells. Where indicated, RPMI-8226 cells, pretreated with BMS-986315 Ab or IgG1κ isotype, as well as NKG2D- and BCMA-CAR NKAE cells, are collected at time 0. Cell lysates were separated by SDS-PAGE. A rabbit anti-human phospho-ZAP-70 (Tyr^{319}) / Syk (Tyr^{352}) Ab was used to detect the phosphorylation of ZAP-70/Syk. ZAP70 was used as loading control. *$p<0.05$.

The detection of NKG2A by both cytometry techniques is diminished, indicating that α-NKG2A blocking Ab binds to NK cells and compete with α-NKG2A staining and/or foster the reduction of the receptor in the cell surface by internalization. Apart from that, NKG2A blockade did not significantly affect the expression of other NK cell surface receptors studied, including CD69, CD25, NKp30, NKp44, NKp46, NKG2C, and PD-1. Consequently, intracellular signaling was examined by assessing the phosphorylation of Syk and zeta-chain-associated protein kinase 70 (ZAP-70) by western blot. The co-culture with RPMI-8226 cells increments the phosphorylation of Syk (Tyr^{352}) and ZAP-70 (Tyr^{319}) in human isotype-pretreated NKG2D- and BCMA-CAR NKAE cell co-cultures but increases even more with the blockade of NKG2A (Fig. 34C).

Overall, these results suggest that blocking NKG2A does not modify the expression of the main activating and inhibiting receptors of CAR NK cells, but intracellular signaling pathways seem to be differentially activated.

4.2.7. Pretreatment with α-NKG2A Abs enhances the cytotoxicity of NKG2D- and BCMA-CAR NKAE therapies over MM primary cells without compromising $CD34^+$ population

After studying the ability of the blockade of NKG2A to strengthen the antitumor potency of both CAR NKAE treatments against MM cell lines, we sought to investigate the killing activity over primary PC and $CD34^+$ progenitors from MM patients. BM samples of 7 newly diagnosed patients and 2 differently treated patients at progression were used for these assays (for detailed patient characteristics see Table 13).

	Age	Status	ISS	Treatment	Isotype	PC (%)	NKG2D-L (RFI)	BCMA (RFI)	HLA-E (RFI)	$CD34^+$ (%)
#1	73	ND	-	-	IgG kappa	6.11	21.45	32.12	4.72	3.41
#2	62	ND	R-ISS II	-	IgG kappa	36.7	21.68	41.83	4.63	0.25
#3	89	ND	ISS-III	-	IgG kappa	36.03	5.65	27.76	6.39	1.9
#4	79	ND	ISS-III	-	IgG kappa	13.55	4.03	13.58	11.97	1.46
#5	53	ND	R-ISS II	-	IgG kappa	8.38	3.32	13.62	11.37	1.95
#6	71	ND	ISS-II	-	Light chain kappa	8.55	16.54	20.1	4.21	0.69
#7	58	ND	R-ISS III	-	IgG lambda	46.56	7.04	16.15	5.67	2.62
#8	59	RR	ISS-II	DRd (1^{st} line)	IgG lambda	18.6	15.94	27.6	8.99	0.67
#9	57	RR	R-ISS II	DKd (3^{rd} line)	IgG kappa	39.3	12.12	30.33	5.25	0.13

Table 13. Characteristics of MM patients used in ex vivo experiments. ISS: International Staging System; PC: plasma cell; RFI: relative fluorescence intensity; NKG2D-L: NKG2D ligands; ND: newly diagnosed; RR: relapsed or refractory; DRd: daratumumab, lenalidomide and dexamethasone; DKd: daratumumab, carfilzomib and dexamethasone; Ig: immunoglobulin.

To mimic the TME surrounding PC in MM, BMMCs from patients were obtained through density gradient and cultures were performed in the presence of the own patient BM plasma. The percentage of $CD34^+$ cells and PC, as well as the expression of NKG2D-L, BCMA, and HLA-E within this population, were studied by flow cytometry (Table 13).

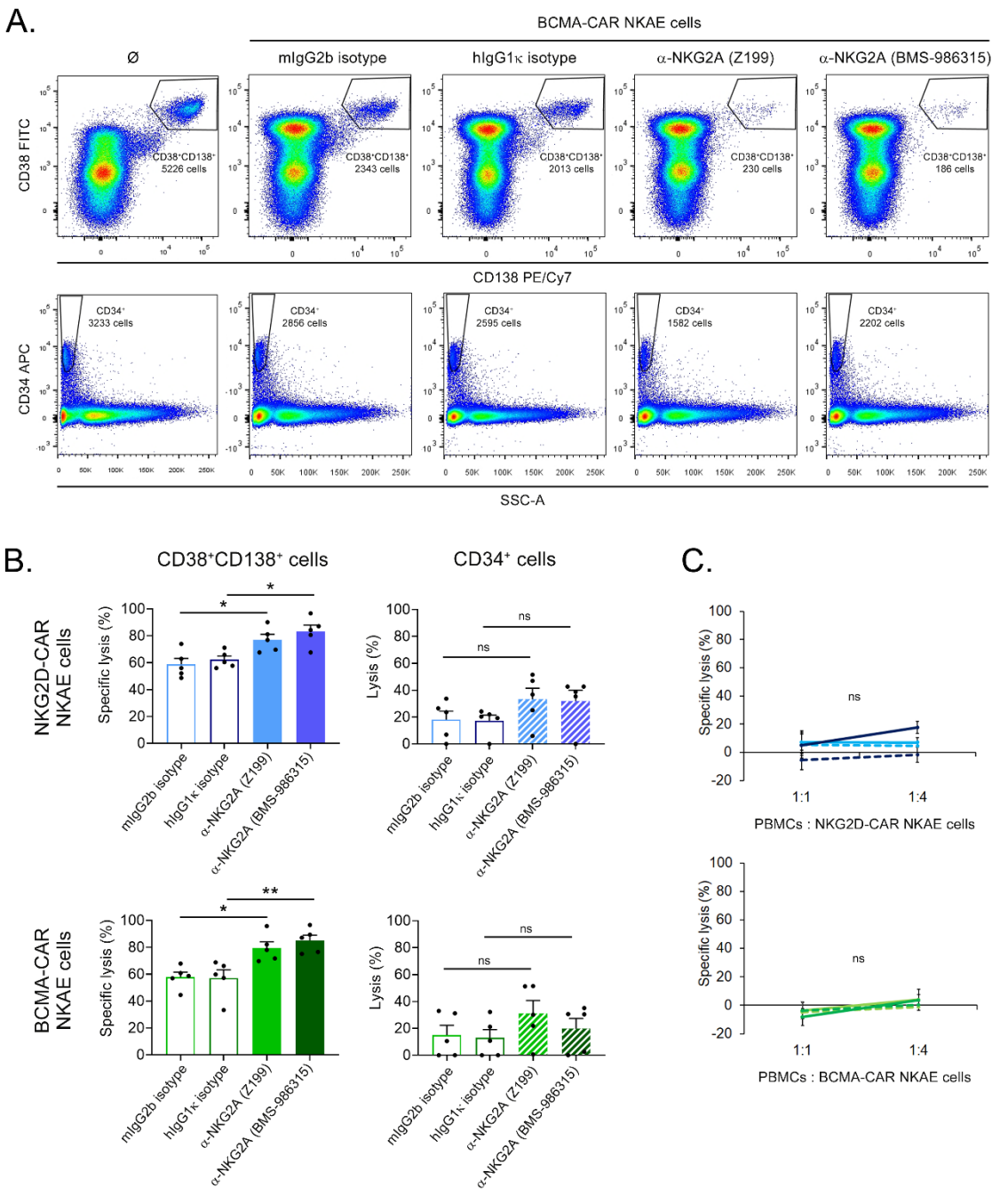

Figure 35. NKG2D- and BCMA-CAR NKAE cells pretreated with α-NKG2A Abs exhibit a higher antitumor activity against PC from MM patients, with low toxicity over CD34$^+$ cells from the same patient and PBMCs from HD. A) Representative flow cytometry dot plots of PC (CD38$^+$CD138$^+$) and CD34$^+$ cells gating in BCMA-CAR NKAE cell and BMMC 24h-co-cultures. B) Specific lysis of NKG2D- and BCMA-CAR NKAE cells treated with either the mouse (Z199) or the human (BMS-986315) α-NKG2A Ab, or their corresponding isotypes (mIgG2b or hIgG1κ), against PC (CD38$^+$CD138$^+$) or CD34$^+$ cells from MM patient BMMCs for 24 hours, analyzed by flow cytometry (Attune CytPix Flow Cytometer). PC : CAR NKAE cell ratio (1:10 for NKG2D-CAR NKAE cell experiments and 1:5 for BCMA-CAR NKAE cell experiments) was determined taking into account the percentage of PC within BMMCs. The mean ± SEM is shown (n=5). C) Specific lysis of NKG2D- and BCMA-CAR NKAE cells treated with either the mouse (Z199) or the human (BMS-986315) α-NKG2A Ab, or their corresponding isotypes (mIgG2b and hIgG1κ), against HD PBMCs analyzed by 3h-Calcein release assay. The mean ± SEM is shown (n=6). ns: not significant; *p<0.05; **p<0.01.

An increased cytotoxic activity against PC was achieved at 1:10 T:E ratio with NKG2D-CAR NKAE cells pretreated with α-NKG2A Abs (77.15 ± 4.07% with Z199 and 83.37 ± 4.74% with BMS-986315) compared to NKG2D-CAR NKAE cells pretreated with their corresponding isotypes (58.79 ± 4.49% with mIgG2b and 62.27 ± 2.78% with hIgG1κ) (Fig. 35A, B). Similarly, α-NKG2A Ab pretreated BCMA-CAR NKAE cells increment the tumor cell lysis at 1:5 T:E ratio (79.55 ± 4.64% with Z199 and 85.03 ± 4.04% with BMS-986315) with respect to isotype pretreated cells (57.87 ± 3.79% with mIgG2b and 57.11 ± 6.28% with hIgG1κ). No significant killing activity was observed over $CD34^+$ progenitors with NKG2A blocked NKG2D- (33.26 ± 8.2% with Z199 and 31.92 ± 8.1% with BMS-986315) and BCMA-CAR NKAE therapies (31.1 ± 9.58% with Z199 and 19.76 ± 7.59% with BMS-986315) compared to isotype pretreated NKG2D- (18.16 ± 6.31% with mIgG2b and 17.19 ± 4.38% with hIgG1κ) and BCMA-CAR NKAE cells (14.94 ± 7.26% with mIgG2b and 12.85 ± 6.25% with hIgG1κ).

Considering the improved efficacy of CAR populations pretreated with the α-NKG2A Abs, we performed additional toxicity assays against mature blood cells from HD. None of the combinations proposed cause toxicity against these PBMCs from HD. The maximum percentage of cell lysis was 17.8 ± 4.32% obtained with α-NKG2A blocked NKG2D-CAR NKAE cells at a ratio of 1:4 (T:E) (Fig. 35C).

Taken together, these data demonstrate that NKG2A blockade enhances the cytolytic capacity of NKG2D- and BCMA-CAR NKAE cells against primary MM cells whereas exhibits low hematotoxicity.

4.2.8. Pretreatment of NKG2D-CAR NKAE cells with the BMS-986315 α-NKG2A blocking Ab increases survival in disseminated MM xenograft mouse model

Once we had demonstrated the *in vitro* antitumor efficacy and reduced hematotoxicity of the combination of α-NKG2A blocking Abs with NKG2D- or BCMA-CAR NKAE cells, we tested its anti-MM activity *in vivo*. As only the human α-NKG2A Ab provided by BMS, BMS-986315, could be used in clinical practice, mouse experiments were carried out comparing this human Ab and its corresponding IgG1κ isotype treatment.

For this purpose, we selected the mouse strain NOD.Cg-Prkdc^{scid} Il2rg^{tm1Wjl} Tg(IL15)1Sz/SzJ, NSG-Tg(Hu-IL15) with physiological serum levels of human IL-15 that facilitates the maintenance of functional human NK cells. Additionally, as we have demonstrated that IL-15 promotes NKG2A expression, the use of NSG-Tg(Hu-IL15) strain enables the examination of these therapies efficacy in a more challenging/resistant scenario.

In a first experiment, 5 x 10^5 RPMI-8226 ffLucGFP cells (Fig. 36A) were intravenously injected in sublethally irradiated mice. After 72 hours, 8 x 10^6 NKG2D- or BCMA-CAR NKAE cells pretreated with either the human α-NKG2A Ab or the corresponding hIgG1κ isotype were intravenously infused. To guarantee the blockade of NKG2A on CAR NKAE cells for a longer time, we intraperitoneally administered 250 µg of the hIgG1κ isotype or the α-NKG2A Ab at day 0 and day 11. Scheme treatments are shown in figure 36B. The CAR-NK transduction efficiency on the day of infusion was 41.6% for NKG2D-CAR and 49.5% for BCMA-CAR (Fig. 36C). In addition, NKG2A blockade on CAR NKAE cells was corroborated by flow cytometry. The expression of NKG2A cells in NKG2D-CAR NKAE population diminished from 83.61 RFI in cells pretreated with hIgG1κ to 11 RFI in cells incubated with α-NKG2A. Similarly, BCMA-CAR NKAE cells reduced the expression of NKG2A cells from 133.6 RFI in cells pretreated with hIgG1κ to 13.46 RFI in α-NKG2A-treated cells.

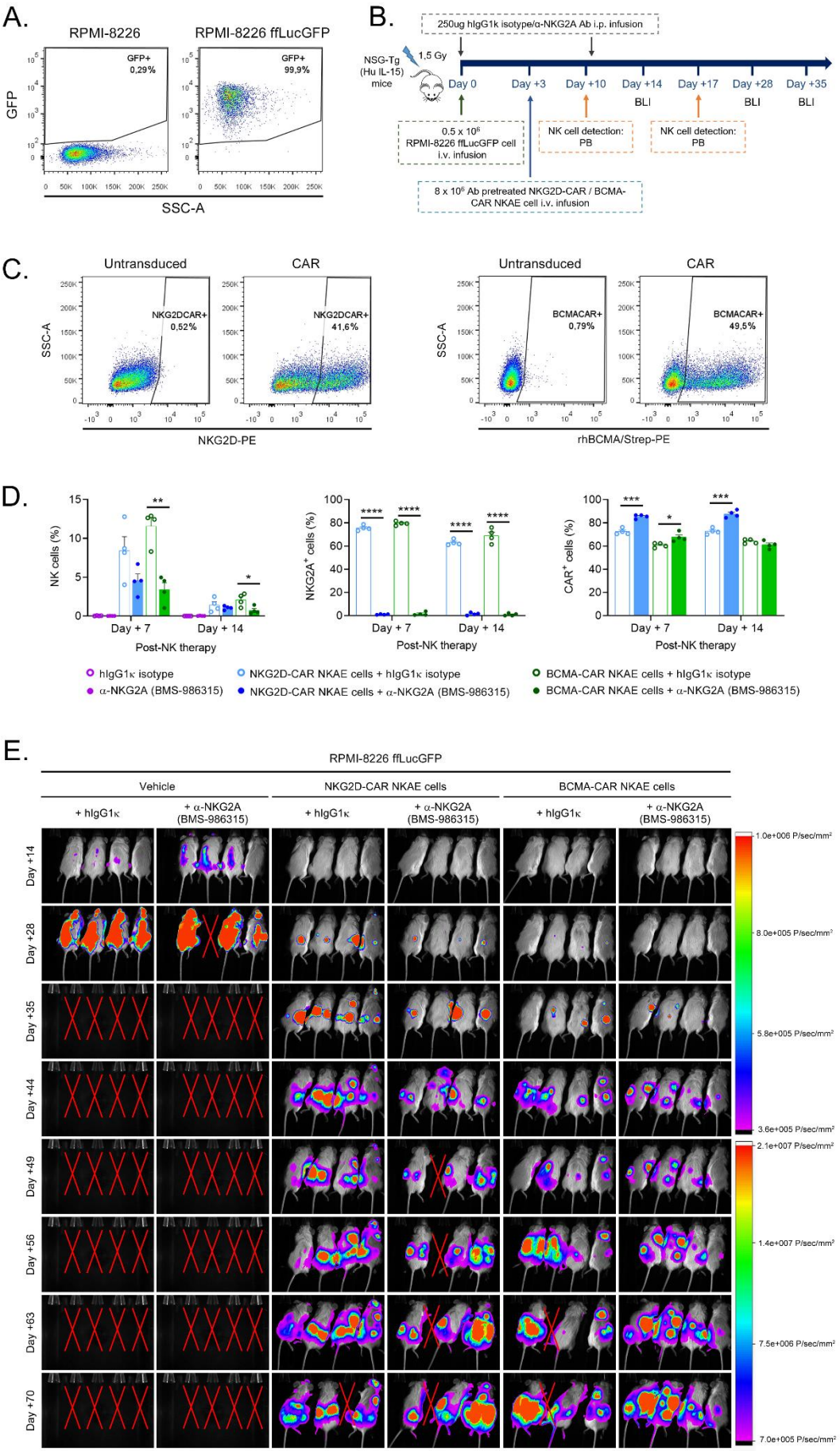
A.
RPMI-8226
RPMI-8226 ffLucGFP
GFP+ 0,29%
GFP+ 99,9%
GFP
SSC-A
B.
250ug hIgG1k isotype/α-NKG2A Ab i.p. infusion
NSG-Tg (Hu IL-15) mice
1,5 Gy
Day 0
Day +3
Day +10
Day +14
Day +17
Day +28
Day +35
BLI
BLI
BLI
0.5 x 10^6 RPMI-8226 ffLucGFP cell i.v. infusion
NK cell detection: PB
NK cell detection: PB
8 x 10^6 Ab pretreated NKG2D-CAR / BCMA-CAR NKAE cell i.v. infusion
C.
Untransduced
CAR
NKG2DCAR+ 0,52%
NKG2DCAR+ 41,6%
SSC-A
NKG2D-PE
Untransduced
CAR
BCMACAR+ 0,79%
BCMACAR+ 49,5%
SSC-A
rhBCMA/Strep-PE
D.
NK cells (%)
Day + 7
Day + 14
Post-NK therapy
NKG2A+ cells (%)
Day + 7
Day + 14
Post-NK therapy
CAR+ cells (%)
Day + 7
Day + 14
Post-NK therapy
hIgG1κ isotype
α-NKG2A (BMS-986315)
NKG2D-CAR NKAE cells + hIgG1κ isotype
NKG2D-CAR NKAE cells + α-NKG2A (BMS-986315)
BCMA-CAR NKAE cells + hIgG1κ isotype
BCMA-CAR NKAE cells + α-NKG2A (BMS-986315)
E.
RPMI-8226 ffLucGFP
Vehicle
NKG2D-CAR NKAE cells
BCMA-CAR NKAE cells
+ hIgG1κ
+ α-NKG2A (BMS-986315)
+ hIgG1κ
+ α-NKG2A (BMS-986315)
+ hIgG1κ
+ α-NKG2A (BMS-986315)
Day +14
Day +28
Day +35
Day +44
Day +49
Day +56
Day +63
Day +70
1.0e+006 P/sec/mm²
8.0e+005 P/sec/mm²
5.8e+005 P/sec/mm²
3.6e+005 P/sec/mm²
2.1e+007 P/sec/mm²
1.4e+007 P/sec/mm²
7.5e+006 P/sec/mm²
7.0e+005 P/sec/mm²

Figure 36. Intraperitoneally infusion of BMS-986315 α-NKG2A Ab in mice decreases NKG2D- and BCMA-CAR NKAE cell percentages *in vivo*. A) Representative flow cytometry dot plot of GFP expression on RPMI-8226 and RPMI-8266 ffLucGFP cells purified by cell sorting. B) Experimental design of the MM disseminated orthotopic NSG-Tg(Hu-IL15) mouse model generated through the intravenous (i.v.) infusion of 5 x 10^5 RPMI-8226 ffLucGFP cells followed by an i.v. infusion of 8 x 10^6 NKG2D- or BCMA-CAR NKAE cells pretreated with either the human α-NKG2A (BMS-986315) or its corresponding isotype (hIgG1κ) at day 3. Additionally, 250 µg of the α-NKG2A or the hIgG1κ isotype Abs were intraperitoneally (i.p.) infused at day 0 and day 11. PB was extracted for NK cell detection analysis by flow cytometry at day 7 and 14 after CAR NKAE cell infusion. Tumor burden was monitored weekly by BLI. C) Flow cytometry dot plot of NKG2D-CAR$^+$ and BCMA-CAR$^+$ cell percentages at infusion. D) Flow cytometry analysis of the percentage of NK cells and NKG2A$^+$ and CAR$^+$ within NK cells from mouse PB samples at day 7 and 14 after NK cell infusion (n=4). The mean ± SEM is shown. E) Imaging of tumor burden, monitored by bioluminescence, at the indicated time points from NSG-Tg(Hu-IL15) mice bearing RPMI-8226 ffLucGFP without treatment or treated with intraperitoneal Ab infusion and NKG2D- or BCMA-CAR NKAE cells, preincubated with either BMS-986315 or the hIgG1κ isotype. *p<0.05; **p<0.01; ***p<0.001; ****p<0.0001.

Strikingly, few percentages of NK cells were detected in mice treated with the α-NKG2A Ab at day 7 (4.55 ± 0.87% in α-NKG2A NKG2D-CAR NKAE cell vs 8.43 ± 1.79% IgG1κ NKG2D-CAR NKAE cell treated mice and 3.41 ± 0.89% in α-NKG2A BCMA-CAR NKAE cell vs 11.58 ± 1.09% IgG1κ BCMA-CAR NKAE cell treated mice) and day 14 (1.06 ± 0.13% in α-NKG2A NKG2D-CAR NKAE cell vs 1.41 ± 0.43% IgG1κ NKG2D-CAR NKAE cell treated mice and 0.73 ± 0.24% in α-NKG2A BCMA-CAR NKAE cell vs 2.08 ± 0.41% IgG1κ BCMA-CAR NKAE cell treated mice) (Fig. 36D). All NK cells from α-NKG2A treated mice were NKG2A$^-$, while high NKG2A expression was maintained in NK cells from isotype-treated mouse groups. Remarkably, CAR expression was superior in α-NKG2A pretreated populations compared to the isotype at day 7: 85.48 ± 0.87% in α-NKG2A NKG2D-CAR NKAE cells vs 72.43 ± 1.33% IgG1κ NKG2D-CAR NKAE cells and 67.58 ± 2.01% in α-NKG2A BCMA-CAR NKAE cells vs 60.73 ± 0.97% IgG1κ BCMA-CAR NKAE cells.

First results from BLI studies shown that α-NKG2A treatment in combination with both CAR therapies delayed disease progression but, after 44 days, tumor burden was quite similar among all treated groups. Moreover, most mice did not have tumor cells in BM at necropsy, but they developed extramedullary tumors (Fig. 36E).

Due to the decreased NK cell percentage in the α-NKG2A-treated groups, probably caused by a fratricide effect among NKG2A$^-$ cells, and the inability to properly measure MM cells within their niche when using the RPMI-8226 ffLucGFP model, we tested the efficacy of these combination therapies against another MM cell line, the U-266

ffLucGFP (Fig. 37A), maintaining the pretreatment CAR NK cell approach, but eliminating the intraperitoneal Ab administrations.

A pilot experiment was undertaken to find the optimal CAR NK cell dose range. 5 x 10^5 U-266 ffLucGFP cells were intravenously injected in sublethally irradiated NSG-Tg(Hu-IL15) mice. After 3 days, 8 x 10^6 NKG2D- or BCMA-CAR NKAE cells pretreated with either the human α-NKG2A Ab or the hIgG1κ isotype were intravenously administered (Fig. 37B). As in the previous experiment, CAR expression (Fig. 37C) (6.9% NKG2D-CAR$^+$ and 17.8% BCMA-CAR$^+$) and the blockade of NKG2A on NK cells in α-NKG2A pretreated mice (5 NKG2A RFI in α-NKG2A NKG2D-CAR NKAE cells vs 112.78 RFI in hIgG1κ NKG2D-CAR NKAE cells and 6.29 NKG2A RFI in α-NKG2A BCMA-CAR NKAE cells vs 106.42 RFI in IgG1κ BCMA-CAR NKAE cells) were corroborated on the day of NK cell infusion.

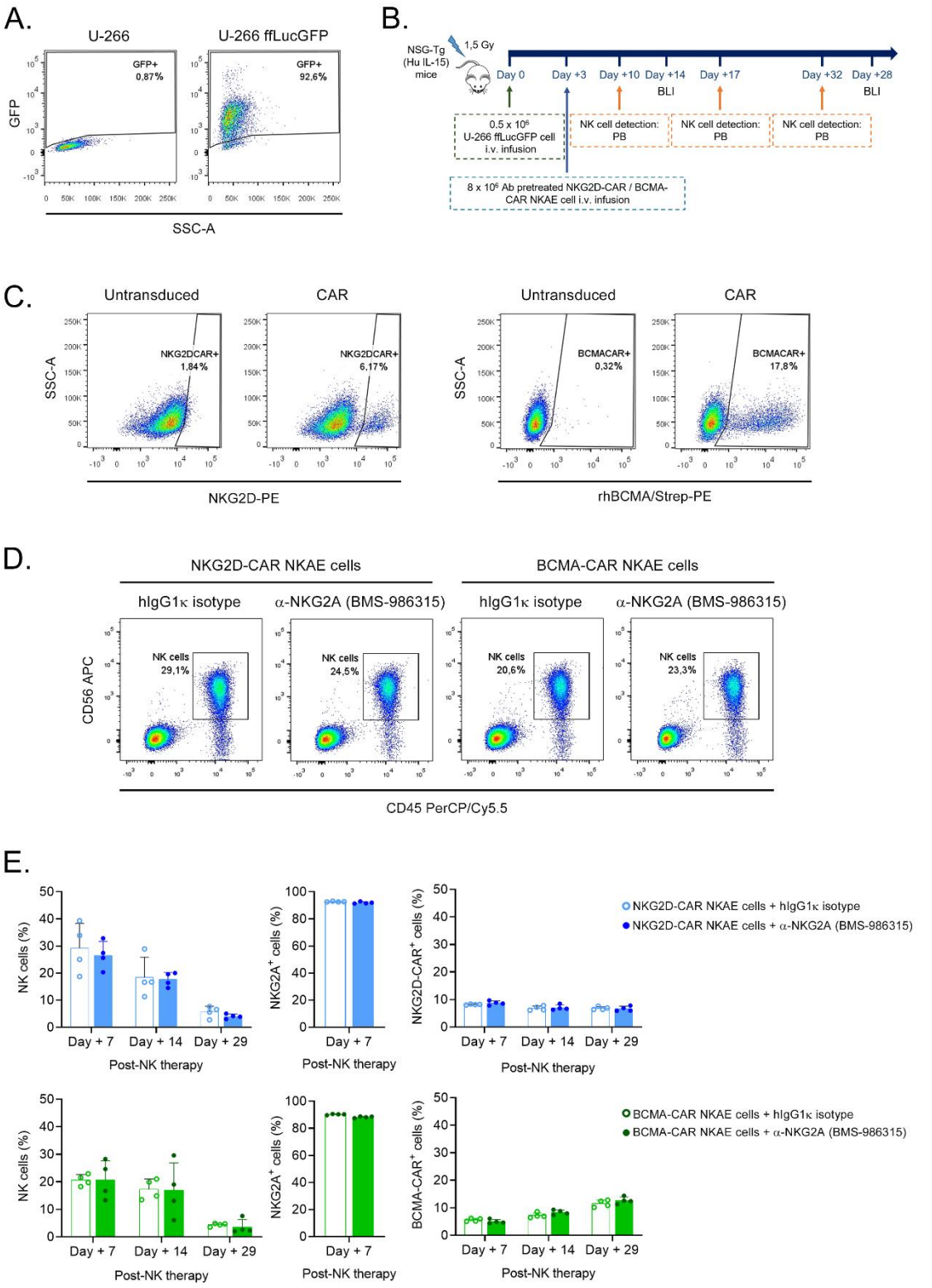

Figure 37. NKG2D- and BCMA-CAR NKAE cells persist for at least 29 days in NSG-Tg(Hu-IL15) mice bearing U-266 ffLucGFP MM cells. A) Representative flow cytometry dot plot of GFP expression on U-266 ffLucGFP cells purified by cell sorting. B) Experimental design of the disseminated MM NSG-Tg(Hu-IL15) mouse model generated through the intravenous (i.v.) infusion of 5 x 10^5 U-266 ffLucGFP cells followed by an i.v. infusion of 8 x 10^6 NKG2D- or BCMA-CAR NKAE cells pretreated with either the human α-NKG2A (BMS-986315) or its corresponding isotype (hIgG1κ) at day 3. PB was extracted for NK cell detection analysis by flow cytometry at day 7, 14, and 29 after CAR NKAE cell infusion. Tumor

burden was monitored fortnightly by BLI. C) Flow cytometry dot plot of the NKG2D-CAR$^+$ and BCMA-CAR$^+$ cell percentages at infusion. D) Representative flow cytometry dot plot of NK cells gating in NKG2D- or BCMA-CAR NKAE cells pretreated with BMS-986315 α-NKG2A Ab or its isotype (hIgG1κ) at day 7 post-NK cell infusion. E) Flow cytometry analysis of the percentage of NK cells and NKG2A$^+$ and CAR$^+$ within NK cells from PB mouse samples at day 7, 14, or 29 after NK cell infusion (n=4). The mean ± SEM is shown.

PB samples collected at day 7, 14, and 29 post-NK administration revealed the CAR expression stability and NK cell persistence for at least 29 days post-therapy infusion. At day 14, the percentage of human NK cells was 18.38 ± 3.73% in hIgG1κ and 17.63 ± 1.32% in BMS-986315 pretreated NKG2D-CAR NKAE cell mouse group and 17.33 ± 1.84% in hIgG1κ and 16.95 ± 4.98% in BMS-986315 pretreated BCMA-CAR NKAE cell mouse group. No significant differences in NK cell frequencies or CAR expression were observed between mice infused with hIgG1κ or α-NKG2A-pretreated CAR NK cells. Moreover, since intraperitoneally infusions of BMS-986315 were replaced by pretreatment, at day 7, all CAR NKAE expressed a high percentage of NKG2A (Fig. 37 D, E).

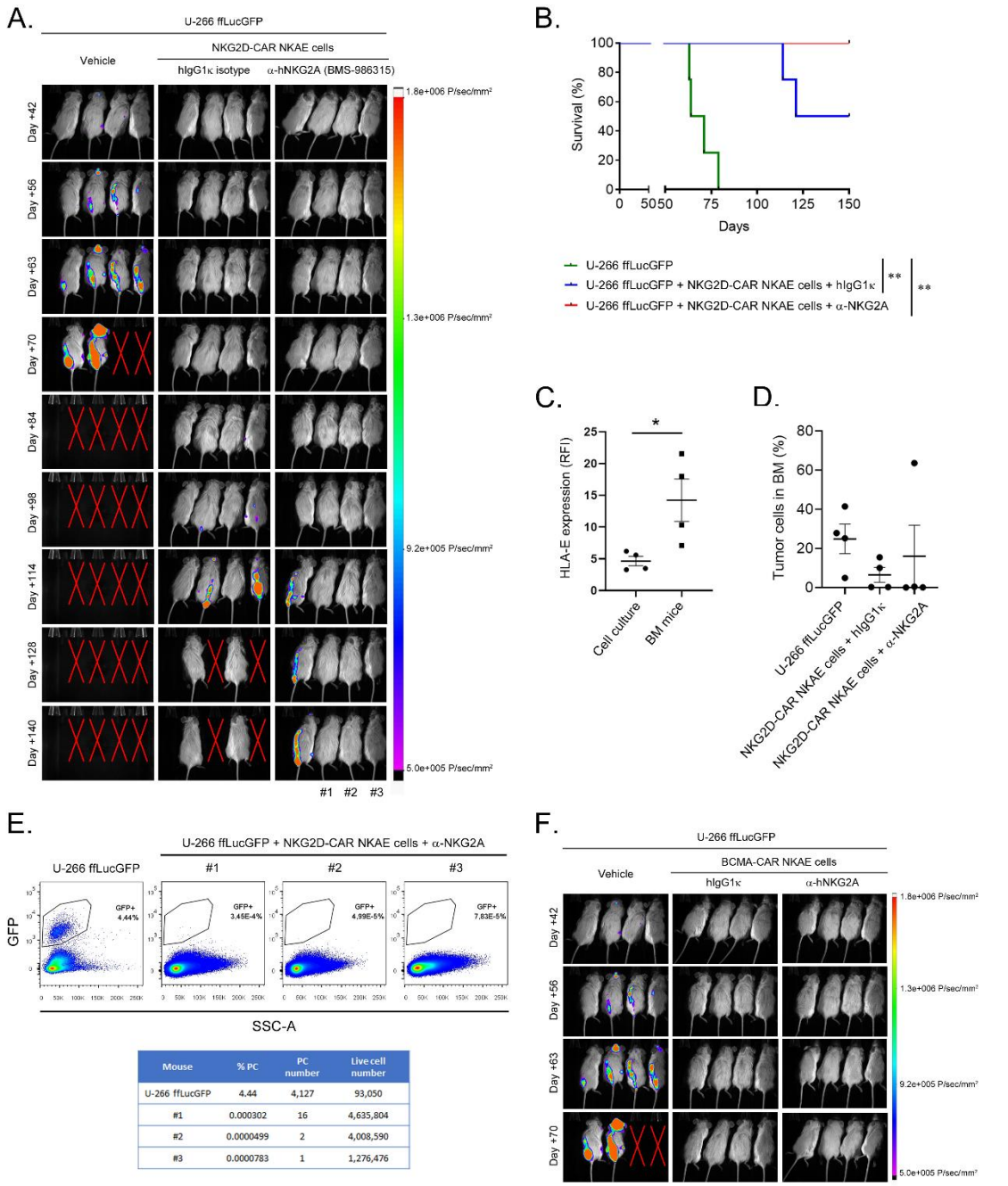

Mouse	% PC	PC number	Live cell number
U-266 ffLucGFP	4.44	4,127	93,050
#1	0.000302	16	4,635,804
#2	0.0000499	2	4,008,590
#3	0.0000783	1	1,276,476

Figure 38. NKG2D-CAR NKAE cells pretreated with either the BMS-986315 Ab or its isotype significantly reduce tumor burden in NSG-Tg(Hu-IL15) mice bearing U-266 ffLucGFP MM cells. A) Imaging of tumor burden monitored by bioluminescence at the indicated time points from NSG-Tg(Hu-IL15) mice bearing U-266 ffLucGFP cells without treatment or treated with NKG2D-CAR NKAE cells, preincubated with either BMS-986315 or the hIgG1κ isotype. B) Kaplan-Meier survival curve of mice described in (A) (n=4). C) Flow cytometry analysis of HLA-E expression on U-266 ffLucGFP cells in culture or collected from BM mice at necropsy (n=4). The mean ± SEM is shown. D) Flow cytometry analysis of GFP^+ tumor cells in BM mice at necropsy from the indicated experimental groups (n=4). The mean ± SEM is shown. E) Flow cytometry dot plot of residual tumor cells in the BM of indicated mice in (A). Flow cytometry analysis of the number of U-266 ffLucGFP cells detected in the BM of mice #1, #2, and #3 from α-NKG2A-pretreated NKG2D-CAR NKAE cell group, sacrificed at day 150. One U-266 ffLucGFP untreated mouse analysis is shown. F) Imaging of tumor burden monitored by bioluminescence, at the indicated time points from NSG-Tg(Hu-IL15) mice bearing U-266 ffLucGFP cells without treatment

or treated with BCMA-CAR NKAE cells, preincubated with either BMS-986315 or the hIgG1κ isotype. *p<0.05; **p<0.01.

Regarding NKG2D-CAR NKAE cells, both pretreated, α-NKG2A (undefined) and isotype (>135.5 days), CAR NKAE cells significantly prolong mice survival compared to the vehicle group (67.5 days) (Fig. 38A, B). Of note, HLA-E expression was significantly superior on U-266 ffLucGFP from mice analyzed at necropsy (14.24 ± 3.34 RFI) compared to U-266 ffLucGFP in cell culture (4.64 ± 0.74 RFI) (Fig. 38C).

Tumor cells were detected at necropsy in BM mice by flow cytometry (Fig. 38D). Remarkably, after 150 days, 2 mice from the isotype and 3 from the NKG2A blockade group did not have clinical signs of the disease or BLI signal and, consequently, the experiment was discontinued. Flow cytometry analysis was conducted to assess residual MM cells in the BM of these mice: #1 (16 PC on 4.64 x 10^6 viable events), #2 (2 PC on 4.01 x 10^6 viable events), and #3 (2 PC on 1.28 x 10^6 viable events) (Fig. 38E). Concerning BCMA-CAR NKAE cells, all mice were rescued from death (Fig. 38F). These results indicated that both NKG2D- and BCMA-CAR NKAE therapies were able to eliminate tumor burden in 62.5% and 100% of mice, respectively. For that reason, we reduced the number of infused CAR NK cells to test the efficacy of NKG2A-blocked CAR NK cells under suboptimal conditions, mimicking low therapy:tumor cell proportions in RRMM patients.

For this purpose, 4 x 10^6 NKG2D- or BCMA-CAR NKAE cells pretreated with either the human α-NKG2A Ab or the hIgG1κ isotype, were infused in mice sublethally irradiated 72h after U-266 ffLucGFP infusion (5 x 10^5 cells), as indicated in Figure 39A. Once again, we confirmed CAR expression (37.2% NKG2D-CAR$^+$ and 30.1% BCMA-CAR$^+$) (Fig. 39B) and NKG2A blockade in all infused populations (18.2 NKG2A RFI in α-NKG2A NKG2D-CAR NKAE cells vs 126.39 RFI in hIgG1κ NKG2D-CAR NKAE cells, and 12.78 NKG2A RFI in α-NKG2A BCMA-CAR NKAE cells vs 71.51 RFI in hIgG1κ BCMA-CAR NKAE cells).

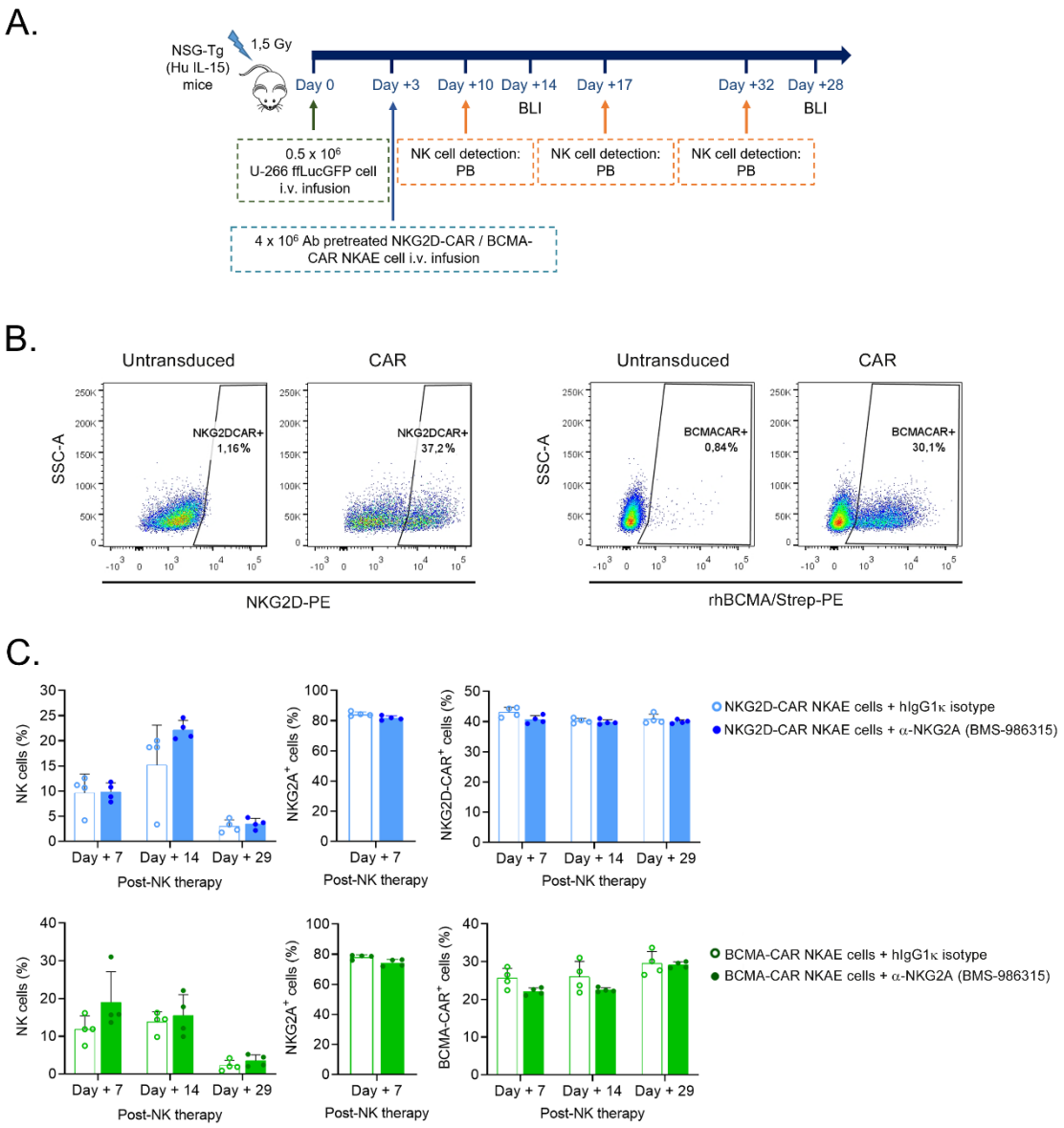

Figure 39. Lower doses of NKG2D- and BCMA-CAR NKAE cells can be also detected at least 29 days from infusion in NSG-Tg(Hu-IL15) mice bearing U-266 ffLucGFP MM. A) Experimental design of the disseminated MM NSG-Tg(Hu-IL15) mouse model generated through the intravenous (i.v.) infusion of 5 x 10^5 U-266 ffLucGFP cells followed by an i.v. infusion of 4 x 10^6 NKG2D- or BCMA-CAR NKAE cells pretreated with either the human α-NKG2A (BMS-986315) or its corresponding isotype (IgG1κ) at day 3. PB was extracted for NK cell detection analysis by flow cytometry at day 7, 14, and 29 after CAR NKAE cell infusion. Tumor burden was monitored fortnightly by BLI. B) Flow cytometry dot plot of NKG2D-CAR$^+$ and BCMA-CAR$^+$ cell percentages at infusion. C) Flow cytometry analysis of the percentage of NK cells and NKG2A$^+$ and CAR$^+$ within NK cells from mouse PB samples at day 7, day 14, or day 29 after NK cell infusion (n=4). The mean ± SEM is shown.

Despite having halved the cell therapy dose compared to the previous *in vivo* study, NK cells remain detected at least 29 days post infusion in all experimental mice, showing also a stable CAR expression (Fig. 39C). Regarding NKG2D-CAR therapy, both CAR NK

cell conditions increased mice survival over untreated (71 days), but the blockade of the NKG2A significantly delayed tumor development (>143 days) compared to the isotype group (93.5 days) (Fig. 40A, B). Quantification of the luminescence photon flux signal was measured along the experiment (Fig. 40C) and tumor cells in the BM of all mice were analyzed at necropsy by flow cytometry (Fig. 40D). At day 154, the experiment was discontinued and tumor cell infiltration in the BM of the remaining live mice (#1 and #2) was studied (Fig. 40E).

Surprisingly, hIgG1κ and α-NKG2A-pretreated BCMA-CAR NKAE cells rescued all mice from death (Fig. 40F). Therefore, we could not evaluate the differences in antitumor activity between the BCMA-CAR NKAE cell treatments.

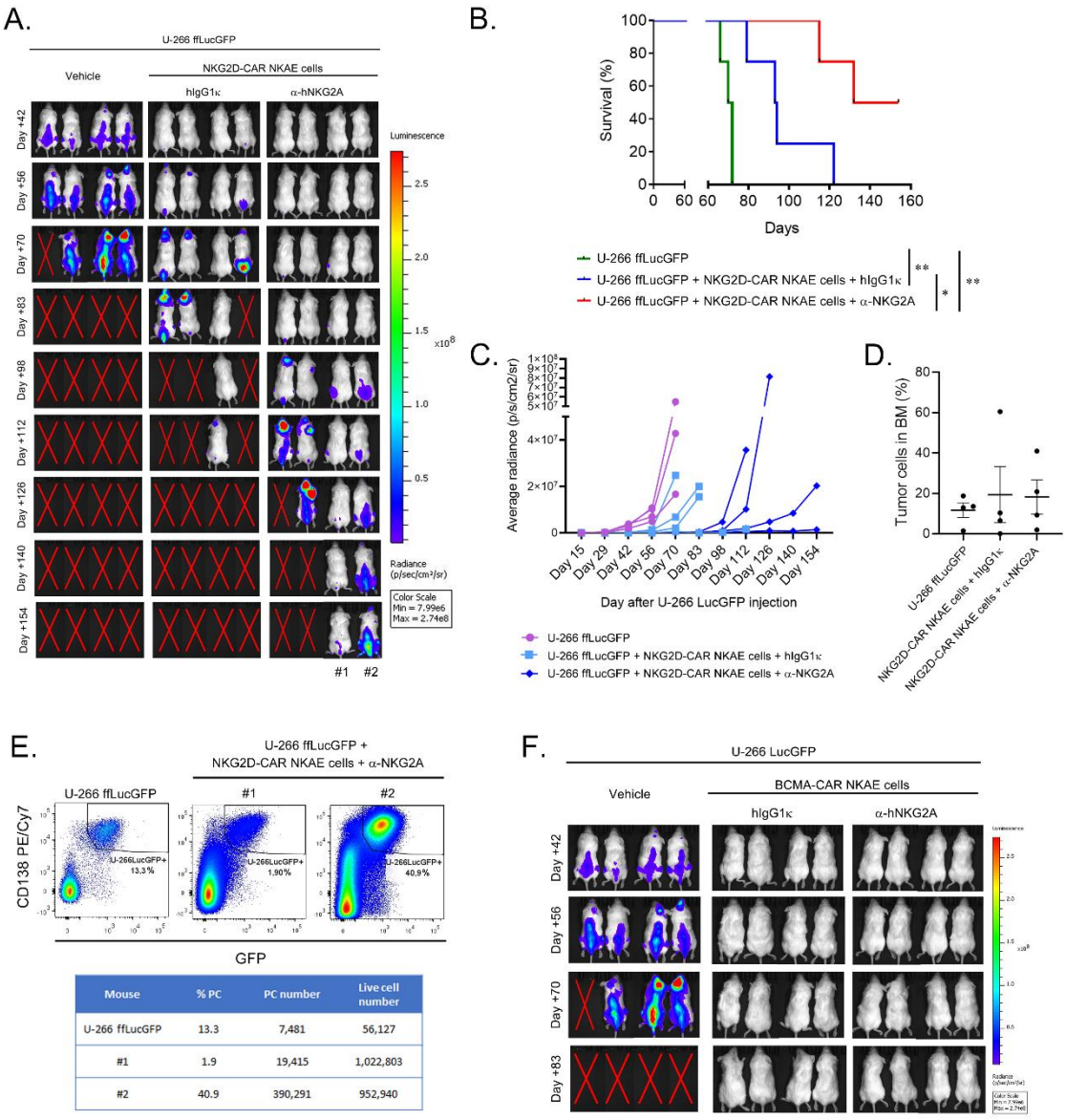

Mouse	% PC	PC number	Live cell number
U-266 ffLucGFP	13.3	7,481	56,127
#1	1.9	19,415	1,022,803
#2	40.9	390,291	952,940

Figure 40. BMS-986315 pretreatment on NKG2D-CAR NKAE cells significantly prolongs mouse survival in NSG-Tg(Hu-IL15) mice bearing U-266 ffLucGFP MM cells. A) Imaging of tumor burden monitored by bioluminescence, at the indicated time points from NSG-Tg(Hu-IL15) mice bearing U-266 ffLucGFP cells without treatment or treated with NKG2D-CAR NKAE cells, preincubated with either BMS-986315 or the hIgG1κ isotype. B) Kaplan-Meier survival curve of mice described in (A) (n=4). C) Quantification of luminescence per mouse at different time points. D) Flow cytometry analysis of $CD138^{+}GFP^{+}$ tumor cells in BM mice at necropsy from the indicated experimental groups (n=4). The mean ± SEM is shown. E) Flow cytometry dot plot of tumor cells in the BM of mice indicated in (A). Flow cytometry analysis of the number of U-266 ffLucGFP cells detected in the BM of mice #1 and #2 from α-NKG2A-pretreated NKG2D-CAR NKAE cell groups, sacrificed at day 154. One U-266 ffLucGFP untreated mouse is shown. F) Imaging of tumor burden monitored by bioluminescence at the indicated time points from NSG-Tg(Hu-IL15) mice bearing U-266 ffLucGFP cells without treatment or treated with BCMA-CAR NKAE cells, preincubated with either BMS-986315 or the hIgG1κ isotype. *p<0.05; **p<0.01.

Taken together, these results demonstrate that NKG2A blockade improves the *in vivo* killing efficacy of NKG2D-CAR NK cells, but further experiments with lower CAR NK cell doses would be required to evaluate the effect of blocking NKG2A in BCMA-CAR NKAE cells.

4.3. NKG2D-CAR CIML-NKAE cells have superior efficacy against MM cells *in vitro* and *in vivo*

4.3.1. Generation of NKG2D-CAR NKAE and CIML-NKAE cells from HD PB samples is feasible

CIML-NK cells are a unique approach to heighten *in vivo* expansion, persistence, and antitumor responses of NK cells [437, 457]. As the memory phenotype is induced through a short exposure to IL-12, IL-15, and IL-18 on fresh purified NK cells [432], we asked whether we could potentiate our NKG2D-CAR NKAE therapy with additional characteristics described for CIML cells by the incubation with this cytokine cocktail. NKG2D-CAR NKAE cells were generated as previously detailed and, right after lentivector removal, were exposed to IL-12, IL-15, and IL-18 for 16 hours. After 5-7 days, experiments to characterize this population were carried out.

Characterization of NKG2D-CAR CIML-NKAE and NKAE cells was performed by flow cytometry (Fig. 41A). These CAR NKAE cells were generated from PB samples with a low percentage of NK cells (5.78 ± 0.74% of $CD56^{+}$ cells), mostly $CD16^{+}$ (75.33 ±

5.93%), and a high percentage of T cells (55.48 ± 5.97% of $CD3^+$ cells). At day 14, both NKG2D-CAR NKAE cell cultures achieved a purity of more than 96% $CD56^+$ cells (97.85 ± 0.39% in the CIML-NKAE and 96.24 ± 0.79% in NKAE cultures), most of them $CD16^+$ (83.97 ± 2.68% in the CIML population and 88.08 ± 2.72% in the NKAE subset), with extremely low contamination of $CD3^+$ cells (0.02 ± 0.01% in CIML-NKAE cells and 0.04 ± 0.02% in NKAE cells) (Fig. 41B).

Flow cytometry data showed no significant differences in NKG2D-CAR transduction levels between both populations, with a mean value of 15.65 ± 2.85% in NKAE cells and 19.89 ± 3.49% in the CIML-NKAE cells (Fig. 41C, D). VCN results were similar between therapies, 0.25 ± 0.08 copies per cell in NKG2D-CAR NKAE cells and 0.31 ± 0.07 copies per cell in NKG2D-CAR CIML-NKAE cells (Fig. 41D). Remarkably, transduction percentages, analyzed by flow cytometry, and VCN values, obtained by q-PCR, have a high correlation (R^2=0.971 in NKG2D-CAR NKAE cells and R^2=0.9372 in NKG2D-CAR CIML-NKAE cells) (Fig. 41E). Additionally, we used Quantibrite™ beads to specifically compare the amount of NKG2D molecules on the surface of these populations. It is important to take into account that the number of molecules includes not only the CAR constructs but also the endogenous NKG2D receptor. Results show that transduction with the NKG2D-CAR enhances the presence of this receptor on both NKG2D-CAR CIML-NKAE cells (2,087.13 ± 278.46 molecules on the CAR subset vs 832.58 ± 170.57 on untransduced CIML-NKAE cells) and NKG2D-CAR NKAE cells (1,667.35 ± 366.92 molecules on the CAR population vs 631.47 ± 234.63 on untransduced NKAE cells) (Fig. 41F).

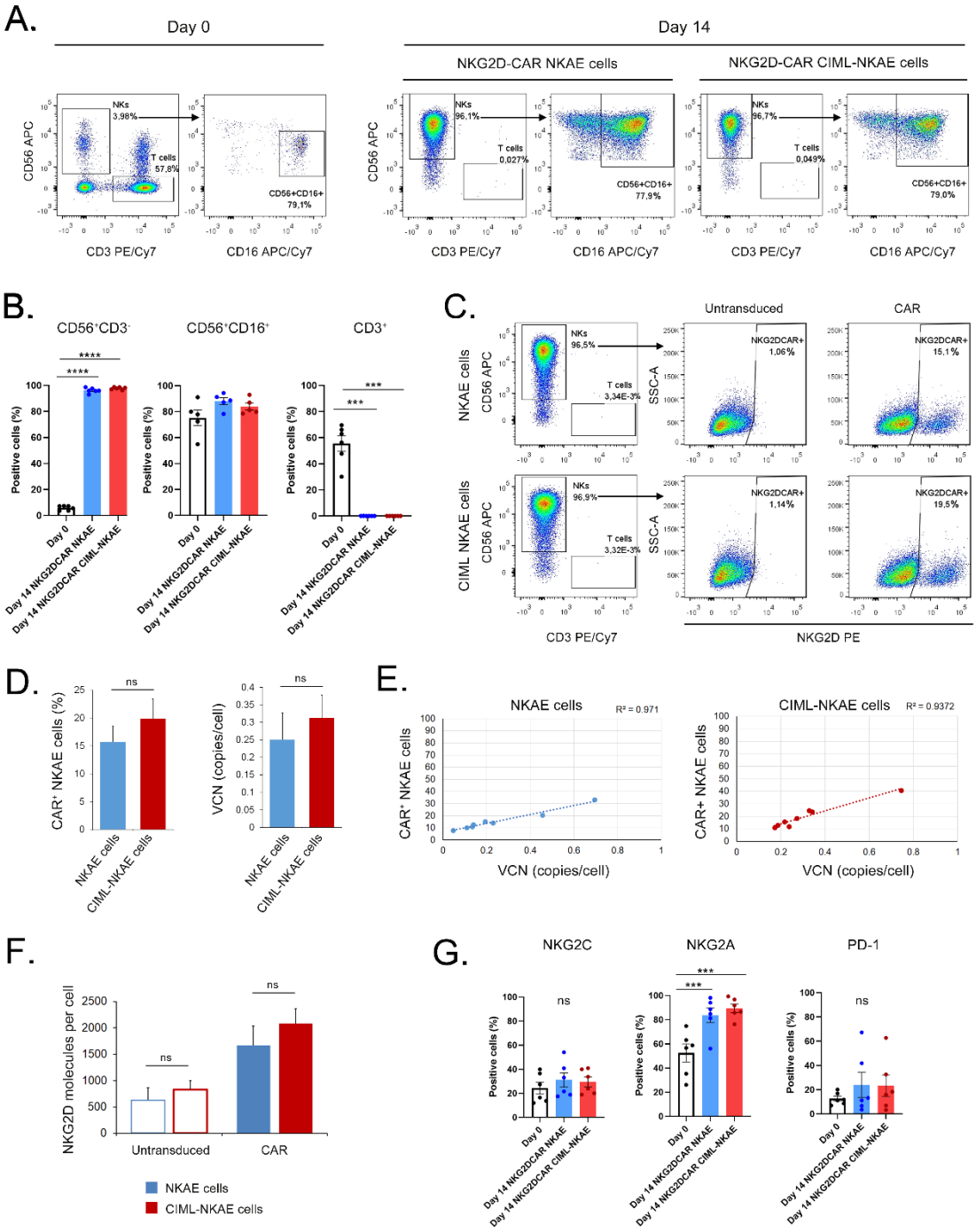

Figure 41. CIML-NKAE and NKAE cells are efficiently generated and stably transduced with lentivectors containing NKG2D-CAR. A) Representative flow cytometry dot plot of NK cells ($CD56^+CD3^-$), cytotoxic NK cells ($CD56^+CD16^+$), and T cells ($CD3^+$) from NKG2D-CAR CIML-NKAE and NKAE cell cultures at day 0 and day 14. B) Flow cytometry analysis of the percentage of NK cells ($CD56^+CD3^-$), cytotoxic NK cells ($CD56^+CD16^+$), and T cells ($CD3^+$) cells in NKG2D-CAR CIML-NKAE and NKAE cell cultures at day 0 and day 14 (n=6). Means ± SEM are shown. C) Representative flow cytometry dot plot of NKG2D-CAR expression on the surface of CIML-NKAE and NKAE cells at 6 days post-transduction. D) Flow cytometry analysis and vector copy number (VCN) quantification by q-PCR of NKG2D-CAR in CIML-NKAE and NKAE cells at day 6 post-transduction (n=8). The mean ± SEM is shown. E) Correlation between the percentage of NKG2D-CAR^+ cells and the VCN per cell on CIML-NKAE and NKAE cells after 6 days from transduction (n=8). F) Quantification of the NKG2D molecules

on the cell surface of the CIML-NKAE and NKAE cells, untransduced or transduced with the NKG2D-CAR lentivector (n=5) by Quantibrite™ beads for flow cytometry analysis at 6 days post-transduction. Means ± SEM are shown. G) Flow cytometry analysis of the percentage of $NKG2C^+$, $NKG2A^+$ and $PD\text{-}1^+$ cells within $CD56^+CD3^-$ populations on NKG2D-CAR CIML-NKAE and NKAE cell cultures at day 0 and day 14 (n=6). Means ± SEM are shown. ns: not significant; ***p<0.001; ****p<0.0001.

Moreover, we studied the expression changes regarding other NKG2 receptors, NKG2C and NKG2A, and PD-1. NKG2C (29.59 ± 4.05% $NKG2C^+$ cells within NKG2D-CAR CIML-NKAE cells and 31.02 ± 5.93% in NKG2D-CAR NKAE cells at day 14 vs 24.39 ± 4.93 at day 0) and PD-1 expression (23.29 ± 8.94% $PD\text{-}1^+$ cells within NKG2D-CAR CIML-NKAE cells and 23.97 ± 10.32% in NKG2D-CAR NKAE cells at day 14 vs 12.59 ± 2.04 at day 0) did not experiment any change during CAR NKAE cell generation, while NKG2A expression (89.46 ± 3.42% $NKG2A^+$ cells within NKG2D-CAR CIML-NKAE cells and 83.88 ± 6.08% in NKG2D-CAR NKAE cells at day 14 vs 52.49 ± 7.44 at day 0) augmented after activation and expansion of NK cells (Fig. 41G).

These results indicate the feasibility of generating NKG2D-CAR CIML-NKAE cells from NKG2D-CAR NKAE cells, with similar CAR transduction efficiency and expression of NKG2 and PD-1 receptors.

4.3.2. NKG2D-CAR CIML-NKAE cells exhibit higher cytotoxicity and degranulation capacity against MM cell lines

To test their anti-MM activity, both NKG2D-CAR populations were co-cultured with the MM cell lines XG-1 and RPMI-8226 at different T:E ratios. NKG2D-CAR CIML-NKAE cells are significantly more efficient in killing these two MM cell lines, XG-1 (58.03 ± 2.88% specific lysis vs 41.23 ± 5.18%, at 1:8 T:E ratio) and RPMI-8226 (80.02 ± 4.45% specific lysis vs 62.81 ± 7.11%, at 1:8 T:E ratio), than NKG2D-CAR NKAE cells (Fig. 42A).

Furthermore, we studied the antitumor ability of NKG2D-CAR CIML-NKAE or NKAE cells against the MM cell line, L-363, which has the capacity to grow forming colonies in methylcellulose semi-solid medium. At 4:1 T:E co-culture, NKG2D-CAR CIML-NKAE cells significantly reduce L-363 colony percentage (53.93 ± 11.29%), compared to NKG2D-CAR NKAE cells (85.59 ± 4.34%) (Fig. 42B).

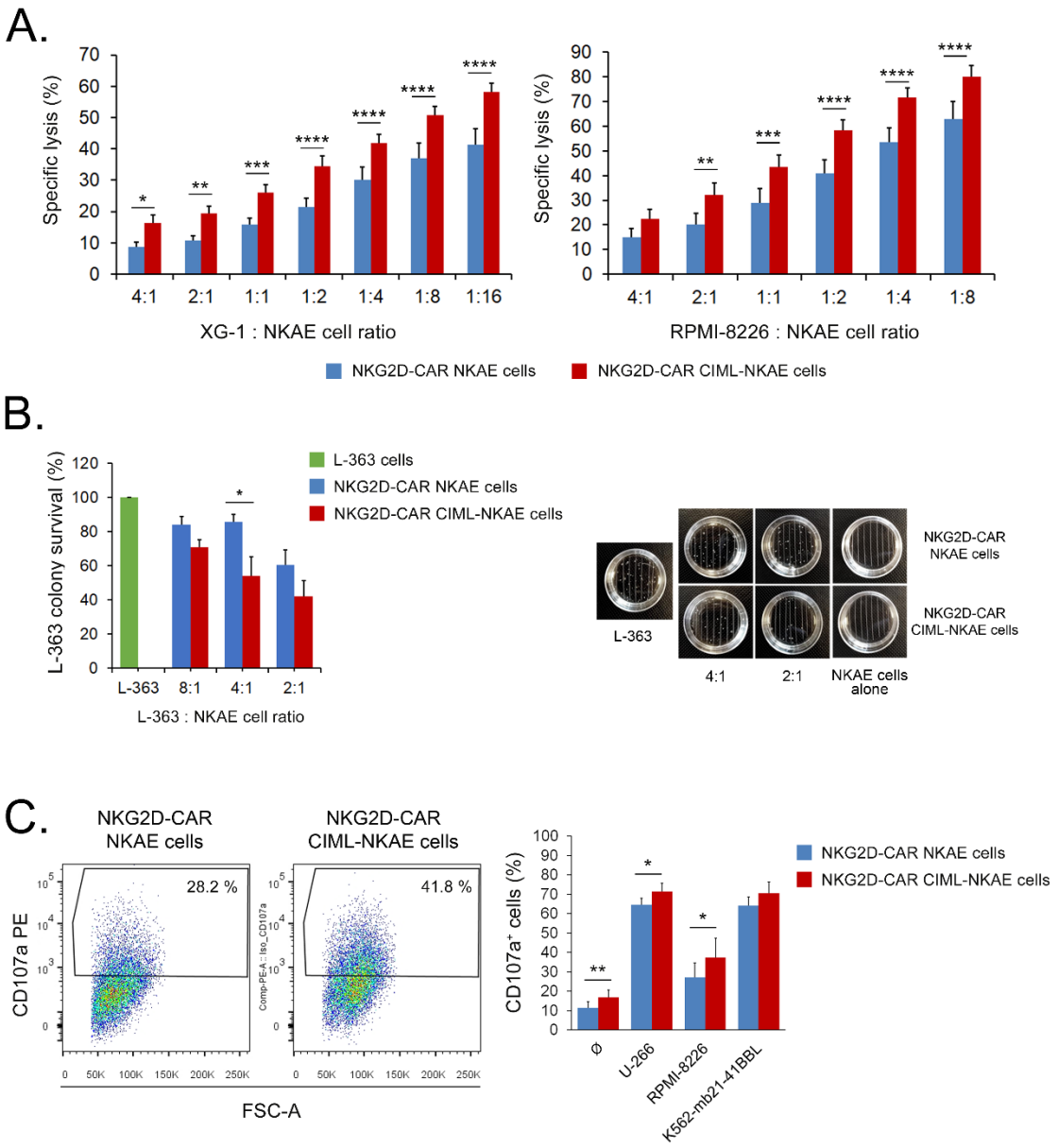

Figure 42. Anti-MM and degranulation activity is augmented in NKG2D-CAR CIML-NKAE cells. A) Specific lysis of NKG2D-CAR CIML-NKAE and NKAE cells against the MM cells RPMI-8226 (n=6) and XG-1 (n=7) analyzed by 3h-Calcein release assay. The mean ± SEM is shown. B) At the left, quantification of the percentage of L-363 colonies after 14 days of co-culture with NKG2D-CAR CIML-NKAE or NKAE cells in methylcellulose semi-solid medium (n=3). At the right, representative images of plates containing L-363 cells alone or after co-culture with CAR NKAE cells at different T:E ratios. CAR NKAE cell control plates are also shown. C) At the left, representative flow cytometry dot plot of $CD107a^+$ staining in NKG2D-CAR CIML-NKAE and NKAE cells after 4h co-culture with RPMI-8226 cells. At the right, flow cytometry analysis of CD107a expression on NKG2D-CAR CIML-NKAE and NKAE cells (n=4) alone or after 4-hour co-culture with the MM cells U-266 and RPMI-8226, or the feeder cell K562-mb21-41BBL at 1:1 ratio. The mean ± SEM is shown. *p<0.05; **p<0.01; ***p<0.001; ****p<0.0001.

To corroborate the higher cytolytic potential of NKG2D-CAR CIML-NKAE cells, degranulation assays were performed. A compilation of 4 experiments shows that

NKG2D-CAR CIML-NKAE cells have increased degranulation levels, compared to NKG2D-CAR NKAE cells, against the MM cell lines U-266 (71.39 ± 4.21% vs 64.48 ± 3.41%) and RPMI-8226 cells (37.34 ± 9.97% vs 27.12 ± 7.57%) (Fig. 42C).

Altogether, although NKG2D-CAR NKAE cells display high cytotoxicity and degranulation levels against MM target cells, the induction of the memory phenotype in these cells significantly improves their killing activity.

4.3.3. Cytotoxic cytokine production is increased in NKG2D-CAR CIML-NKAE cells

Because of cytokine release profile is key for NK cell killing activity, we studied whether NKG2D-CAR CIML-NKAE cells secrete more cytotoxic cytokines or cytolytic proteins after interaction with tumor cells. First, intracellular IFN-γ was measured by flow cytometry in both therapies after their co-culture with two MM cell lines, U-266 and RPMI-8226. In addition, we included in the assay the modified feeder cell K562-mb21-41BBL, used to generate these populations, as CIML-NK cells have been described to quickly react to previous stimuli [431].

Results show that NKG2D-CAR CIML-NKAE cells present high intracellular IFN-γ levels against U-266 (44.87 ± 7.2% vs 28.21 ± 5.84%), RPMI-8226 (41.68 ± 11.01% vs 25.99 ± 7.06%) and K562-mb21-41BBL (65.32 ± 8.21 vs 47.64 ± 8.75%), compared to NKG2D-CAR NKAE cells (Fig. 43A).

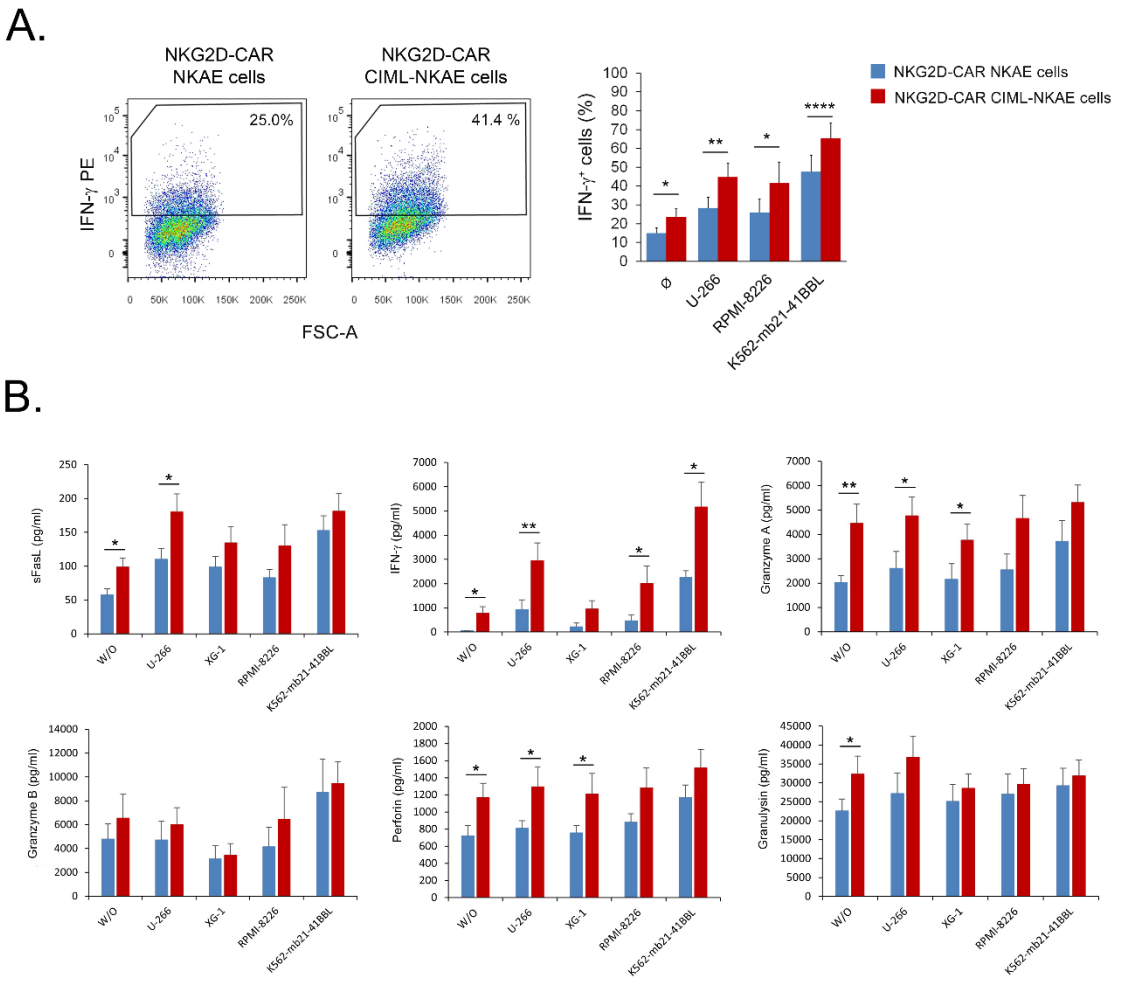

Figure 43. NKG2D-CAR CIML-NKAE cells have higher IFN-γ intracellular production and IFN-γ, perforin, sFasL and granzyme A release, compared to NKG2D-CAR NKAE cells. A) At the left, representative flow cytometry dot plot of IFN-γ staining in NKG2D-CAR CIML-NKAE and NKAE cells after 4h co-culture with RPMI-8226 cells. At the left, flow cytometry analysis of IFN-γ intracellular expression on NKG2D-CAR CIML-NKAE and NKAE cells alone or after 4-hour co-culture with the MM cells U-266 and RPMI-8226, and the feeder cell K562-mb21-41BBL, at ratio 1:1 (n=4). The mean ± SEM is shown. B) Quantification of cytokine/cytolytic proteins (IFN-γ, soluble FasL, granzyme A, granzyme B, perforin and granulysin) in supernatants of NKG2D-CAR CIML-NKAE or NKAE cells 24-hour alone or co-cultured with the MM cells U-266, XG-1, and RPMI-8226, or the feeder cell line K562-mb21-41BBL, at 1:2 T:E ratio, by LEGENDplex bead-based immunoassay (n=9). The mean ± SEM is shown. ns: not significant; *p<0.05; **p<0.01; ****p<0.0001.

To characterize the secretion profile of NK cells, a panel of 13 cytotoxic and cytolytic proteins, including IL-2, IL-4, IL-6, IL-10, IL-17A, IFN-γ, TNF-α, soluble Fas, soluble FasL, granzyme A, granzyme B, perforin, and granulysin, was analyzed by flow cytometry. NKG2D-CAR NKAE and CIML-NKAE cells were cultured alone or with the U-266, XG-1, RPMI-8226 and K562-mb21-41BBL cells for 24h and the collected supernatant was used for cytokine/cytolytic protein release determination. As shown in

Figure 43B, NKG2D-CAR CIML-NKAE cells secrete higher concentrations of IFN-γ, perforin, granzyme A and soluble FasL, alone or after co-culture with tumor cell lines, compared to NKG2D-CAR NKAE cells. After 24h co-culture of NKG2D-CAR CIML-NKAE cells with U-266 cells, the concentration of IFN-γ was 2,939.18 ± 734.2 pg/ml, of perforin 1,294.6 ± 232.39 pg/ml, of granzyme A 4764.72 ± 772.3 pg/ml, and of soluble FasL 179.73 ± 26.98 pg/ml compared to 922.48 ± 411.23 pg/ml IFN-γ, 810.73 ± 86.68 pg/ml perforin, 2,608.64 ± 690.49 pg/ml granzyme A, and 109.98 ± 15.85 pg/ml soluble FasL in NKG2D-CAR NKAE cell co-cultures.

Overall, these results show that memory induction on NKG2D-CAR NKAE cells is able to modify the cytokine and cytolytic protein production, enhancing NK cell antitumor efficacy.

4.3.4. NKG2D-CAR CIML-NKAE cells have enhanced proliferation activity *in vitro*

One of the main characteristics of the CIML population is its high proliferation and persistence potential [436, 439]. For this reason, we studied NKG2D-CAR CIML-NKAE proliferative capacity through two assays: by measuring the percentage of $Ki67^+$ cells within the total population and the percentage of cells that are duplicating their DNA and entering mitosis (phases S, G2, and M). An average of 77.94 ± 2.62% of NKG2D-CAR CIML-NKAE cells are $Ki67^+$, compared to 71.73 ± 2.66% of NKG2D-CAR NKAE cells (Fig. 44A). Consistently, the percentage of NKG2D-CAR CIML-NKAE cells entering mitosis is higher in NKG2D-CAR CIML-NKAE cells (32.33 ± 2.2%) than in NKG2D-CAR NKAE population (24.19 ± 2.47%) (Fig. 44B).

Both assays demonstrate that the exposure of NKG2D-CAR NKAE cells to IL-12, IL-15, and IL-18 enhances cell proliferation capacity.

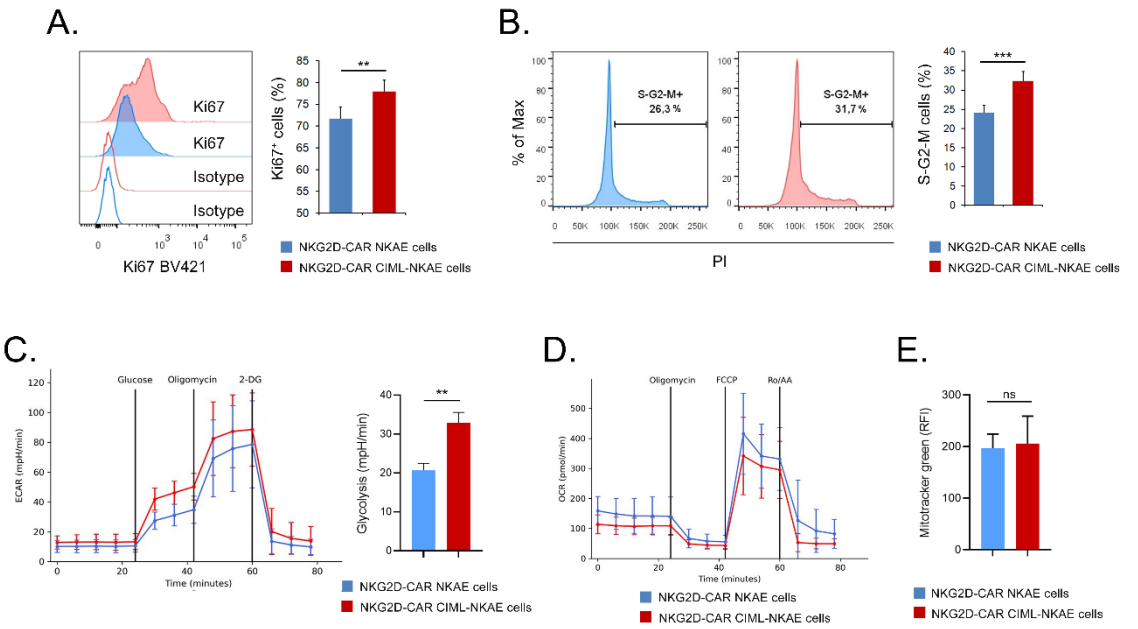

Figure 44. Cytokine-induction of memory promotes proliferation activity and glycolytic state in CAR NKAE cells. A) Representative flow cytometry histogram of Ki67 staining of NKG2D-CAR CIML-NKAE and NKAE cells (left). Flow cytometry analysis of the percentage of $Ki67^+$ cells on NKG2D-CAR CIML-NKAE and NKAE cell populations (right). B) Representative flow cytometry histogram of cell cycle propidium iodide-stained NKG2D-CAR CIML-NKAE and NKAE cells (left). Flow cytometry cell cycle analysis of the percentage of S-G2-M cells on NKG2D-CAR CIML-NKAE and NKAE cells (right). The mean ± SEM is shown (n=14). C) At the left, ECAR measured by Seahorse assay comparing NKG2D-CAR CIML-NKAE and NKAE cells. At the right, bar graphs summarize the glycolytic activity (n=5). The mean ± SEM is shown. D) OCR measured by Seahorse assay comparing NKG2D-CAR CIML-NKAE and NKAE cells (n=5). E) MitoTracker Green flow cytometry staining in NKG2D-CAR CIML-NKAE and NKAE cells (n=4). The mean ± SEM is shown. ns: not significant; **p<0.01; ***p<0.001

4.3.5. NKG2D-CAR CIML-NKAE cells have increased glycolysis

As the short exposure to IL-12/IL-15/IL-18 prompts a sustained metabolic switch of NK cells towards glycolysis [453], we compared the ECAR and OCR between both populations. Our results suggest that NKG2D-CAR CIML-NKAE cells have increased glycolysis (32.94 ± 2.63 mpH/min) compared to NKG2D-CAR NKAE cells (20.72 ± 1.77 mpH/min) (Fig. 44C). However, NKG2D-CAR CIML-NKAE cells do not have superior mitochondrial oxidative phosphorylation compared to NKG2D-CAR NKAE cells (Fig. 44D).

To assess whether the differences in glycolysis were caused by cellular mitochondrial content, we evaluated mitochondrial mass using MitoTracker Green staining. Results show that there is no differential mitochondrial mass between NKG2D-CAR CIML-NKAE and NKAE cells.

These results suggest that NKG2D-CAR CIML-NKAE has an increase glucose metabolism.

4.3.6. NKG2D-CAR NKAE and CIML-NKAE cells have a differential transcriptome and epigenome profile

To better characterize the NKG2D-CAR CIML-NKAE cells, RNA-seq transcriptome analysis was performed in both populations. First, samples were analyzed based on the PC variations. Considering the 3,000 genes with the higher variability between NKG2D-CAR NKAE and CIML-NKAE cells, the most variation (PC1) and the second most variation (PC2) were determined. PC1 had a 52% of variance while PC2 had 26%. As expected, most differences are between individuals and not by cell type (Fig. 45A).

However, 162 differentially expressed genes (DEG) were found between CAR NKAE populations. It is noteworthy the upregulated expression of genes involved in cell proliferation, including CCND2 (cyclin D2) [471], TNRF11A (RANK) [472], MANF [473], and CD71 [453] in NKG2D-CAR CIML-NKAE cells, as well as the chemokine receptors CCR4 and CCR7. Additionally, CABLES1 [474] and KLRG1 [475] expression is downregulated in this population, proteins that negatively regulate NK cell growth and function. By contrast, higher expression levels of the immune checkpoint TIGIT were showed in NKG2D-CAR NKAE cells.

To understand the biological significance of these 162 DEG in NK cells, gene ontology (GO) analysis was conducted. NKG2D-CAR CIML-NKAE cells are enriched for pathways related to migration, regulation of IL-12 production and chemotaxis. The ratio (quantity of genes that belong to a specific group) and the odd ratio (probability of a DEG to belong to a specific group), including its $-\log_{10}$(APVAL), are represented in figure 45A.

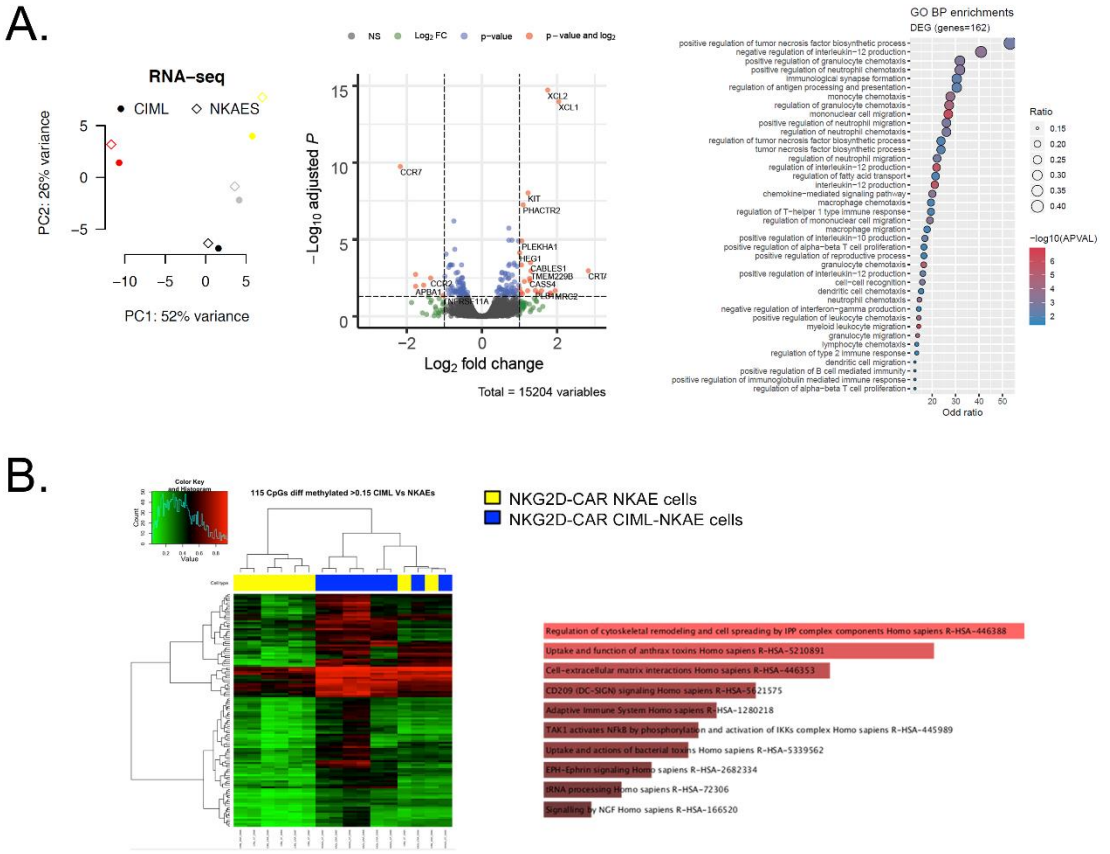

Figure 45. NKG2D-CAR CIML-NKAE cells have a differential epigenetic and transcriptomic profile, compared to NKG2D-CAR NKAE cells. A) At the left, principal component analysis among 4 paired NKG2D-CAR CIML-NKAE and NKAE cells. In the middle, volcano plot of RNA-seq transcriptomic analysis. At the right, gene ontology biological process enrichments from 162 DEG. B) At the left, supervised hierarchical clustering of differentially methylated CpG sites between NKG2D-CAR CIML-NKAE and NKAE cells (n=4). At the right, gene ontology analysis of genes containing CpG sites differentially expressed in the NKG2D-CAR CIML-NKAE cells, obtained from Reactome pathway.

To further investigate the differences associated with cytokine memory induction, the epigenetic profile of NKG2D-CAR CIML-NKAE and paired NKG2D-CAR NKAE cells from 4 HD was analyzed. DNA methylation levels differed between both populations at 115 CpG sites, located in regions that potentially impact on the expression of 86 genes. GO analysis revealed that the most overrepresented pathways are involved in cytokine signaling, cytoskeletal remodeling, and cell-extracellular matrix interactions (Fig. 45B).

Taken together, the transcriptomic and epigenomic analyses reveal different expression profiles between CAR effectors due to the exposure to IL-12, IL-15, and IL-18.

4.3.7. NKG2D-CAR NKAE and CIML-NKAE cells exhibit differential expression of extracellular markers

To validate the results obtained by RNA-seq and to identify additional NK cell extracellular markers with different expression levels between both CAR populations, a detailed flow cytometry phenotyping was conducted.

Results reveal that NKG2D-CAR CIML-NKAE cells have higher expression of the costimulatory protein CD2 (1,747 ± 222.6 vs 1,409 ± 192.1 RFI), the activation receptor CD25 (164.6 ± 31.59 vs 80.12 ± 21.92 RFI) and the transferrin receptor CD71 (495.2 ± 134.3 vs 325.4 ± 84.1 RFI), compared to NKG2D-CAR NKAE cells. By contrast, the expression of the activating receptors NKp30 (113.1 ± 14.04 vs 131.4 ± 17.36 RFI), NKp44 (28.18 ± 4.681 vs 53.26 ± 8.505 RFI), NKp46 (79.45 ± 11.77 vs 91.93 ± 12.81 RFI) is downregulated on NKG2D-CAR CIML-NKAE cells. Similarly, NKG2D-CAR CIML-NKAE cells have lower levels of CD57 (6.78 ± 2.12 vs 11.71 ± 3.38 RFI) and the glucose transporter GLUT1 (37.64 ± 13.39 vs 57.99 ± 19.65 RFI). Moreover, CD62L expression (49.26 ± 16.39 vs 15.11 ± 2.2 RFI) is slightly higher in NKG2D-CAR CIML-NKAE cells, while NKG2A expression diminishes (415.6 ± 100.5 vs 807.4 ± 218.5 RFI), although these last results are not statistically significant (Fig. 46).

These results suggest that NKG2D-CAR CIML-NKAE cells have increased activation (CD25) as well as a high costimulation, through CD2. Besides, CD71 is highly expressed, corroborating RNA-seq results. However, NCRs expression is lower compared to NKG2D-CAR NKAE cells, although functional assays have demonstrated a higher cytotoxicity. Remarkably, decreased CD57 expression means NKG2D-CAR CIML-NKAE population is less mature.

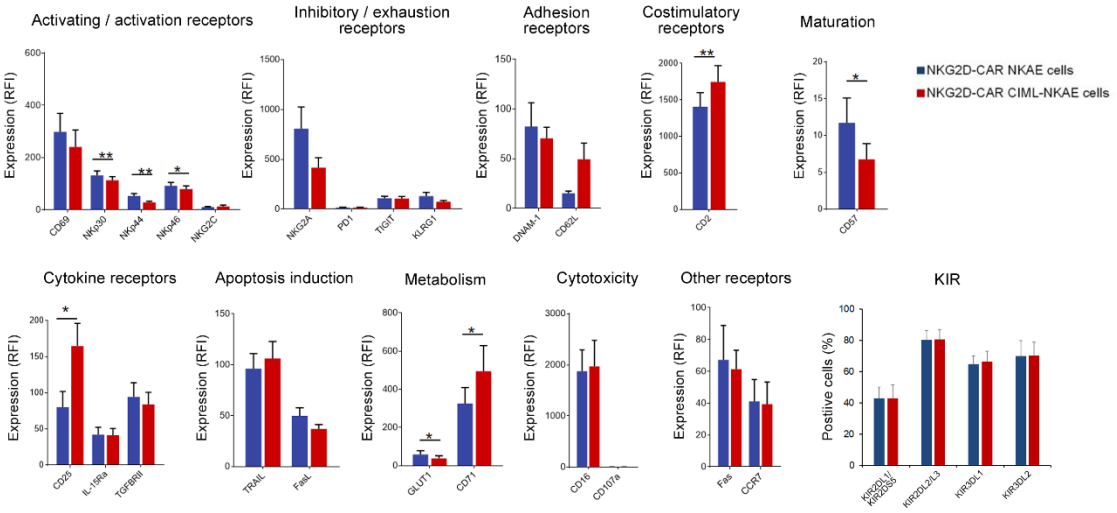

Figure 46. NKG2D-CAR CIML-NKAE cells have a higher expression of CD25, CD2 and CD71, while display a reduced expression of NCRs, GLUT1, and CD57. Flow cytometry analysis of different markers expressed on the surface of NKG2D-CAR CIML-NKAE or NKAE cells (n=7). *p<0.05; **p<0.01.

4.3.8. NKG2D-CAR CIML-NKAE cells display higher cytotoxicity against primary MM cells with low toxicity over CD34$^+$ hematopoietic stem cells

After demonstrating NKG2D-CAR CIML-NKAE cell superior antitumor activity against MM cell lines, we tested their efficacy against primary MM cells. For this purpose, NKG2D-CAR NKAE and CIML-NKAE cells were co-cultured with BMMCs from 3 MM patients (Table 13) for 24 hours, as previously described.

The cytotoxic capacity of NKG2D-CAR NKAE cells was 29.72 ± 2.43% at ratio 1:10 (T:E), whereas the NKG2D-CAR CIML-NKAE population achieved a mean value of 53.65 ± 7.23% . Remarkably, the killing activity against CD34$^+$ progenitors did not show significant differences between both populations (8 ± 4.35% in NKG2D-CAR NKAE cells and 10.61 ± 5.55% in NKG2D-CAR CIML-NKAE cells) (Fig. 47A).

To corroborate the absence of toxicity of NKG2D-CAR CIML-NKAE cells against healthy tissues, clonogenic assays were performed in methylcellulose semi-solid medium by co-culturing both CAR NK therapies with CD34$^+$ cells, obtained from CB. At the highest T:E ratio 1:16, CFU-GM colony percentage is similar to the condition without effector cells and BFU-E colony percentage only decreases by a mean of 23% (Fig. 47B). In both cases, colony average percentages did not significantly differ with respect to the culture with CD34$^+$ cells alone.

Taken together, these results reveal that NKG2D-CAR CIML-NKAE cells exert a higher antitumor activity against primary MM cells without provoking hematotoxicity.

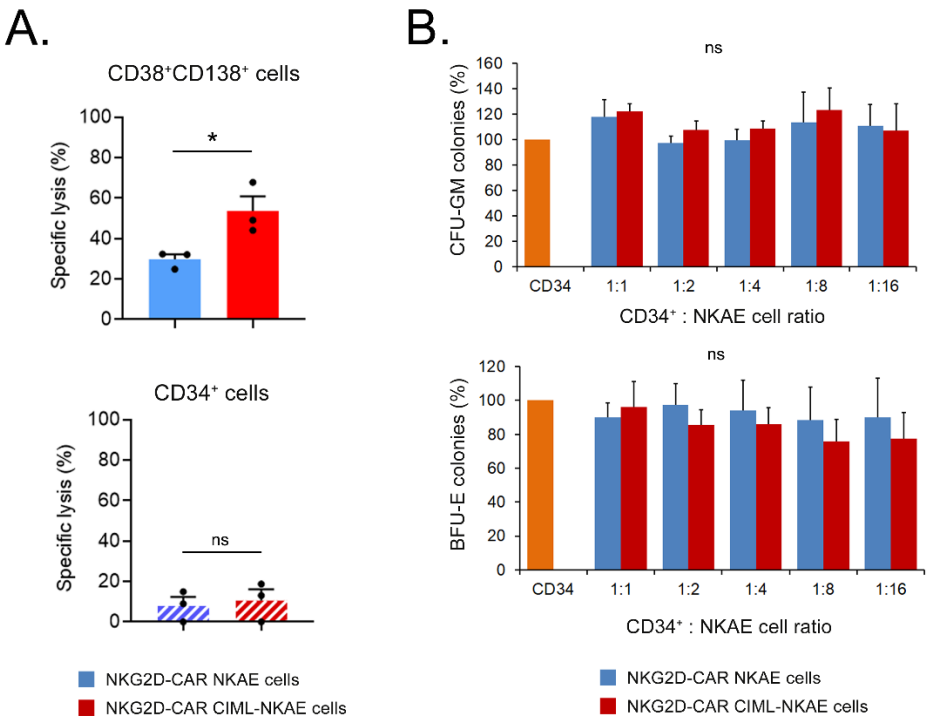

Figure 47. Cytokine-induction of memory in NKG2D-CAR NKAE cells significantly improves the lysis of PC from MM patients, without compromising CD34⁺ population from the same patients or isolated from CB samples. A) Specific lysis of NKG2D-CAR CIML-NKAE or NKAE cells against PC ($CD38^+CD138^+$) or $CD34^+$ progenitors from MM patient BMMCs after 24h-co-culture analyzed by flow cytometry (Attune CytPix Flow Cytometer). PC : CAR NKAE cell ratio (1:10) was determined taking into account the percentage of PC within BMMCs. The mean ± SEM is shown (n=3). B) Quantification of the percentage of CFU-GM (at the top) and BFU-E colonies (at the bottom) after 14 days co-cultured of $CD34^+$ cells with NKG2D-CAR CIML-NKAE or NKAE cells at different T:E ratios in methylcellulose semi-solid medium (n=4). Means ± SEM are shown. ns: not significant; *$p<0.05$.

4.3.9. NKG2D-CAR CIML-NKAE cells display heightened antitumor efficacy in a disseminated MM xenograft mouse model

NKG2D-CAR CIML-NKAE cell *in vivo* efficacy and persistence were evaluated in a disseminated MM xenograft NSG-Tg(Hu-IL15) mouse model. At day 0, sublethally irradiated mice were intravenously injected with 5 x 10^5 U-266 ffLucGFP cells. After 3 days, 4 x 10^6 NKG2D-CAR NKAE or CIML-NKAE cells were intravenously administered (Fig. 48A). The percentage of NKG2D-CAR$^+$ cells was 37.2% in NKG2D-CAR NKAE cells and 48.1% in NKG2D-CAR CIML-NKAE cells (Fig. 48B).

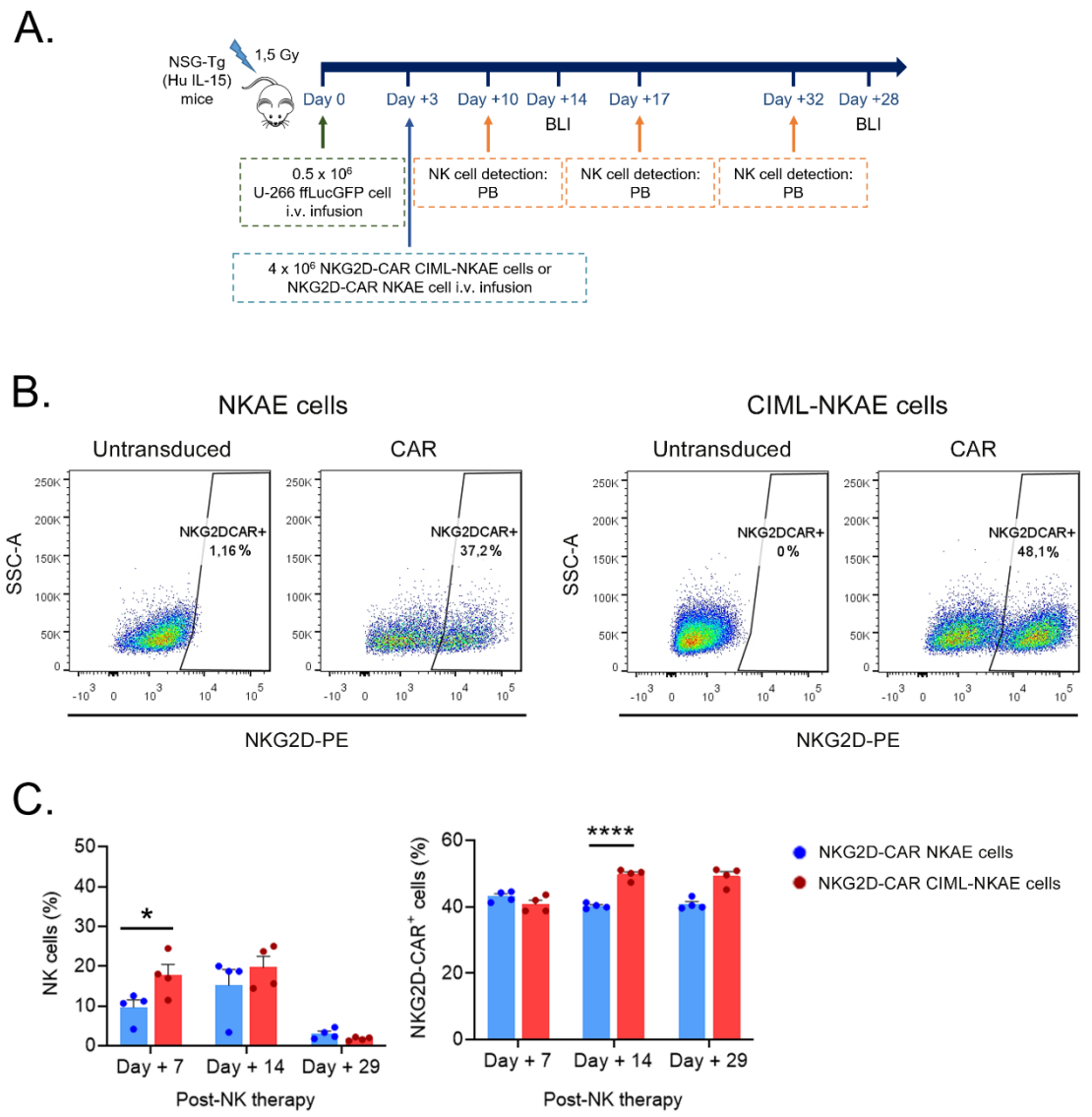

Figure 48. The percentage of NKG2D-CAR CIML-NKAE cells in mouse PB is superior, compared to NKG2D-CAR NKAE cells at day 7 post-NK cell infusion. A) Experimental design of the MM disseminated orthotopic NSG-Tg(Hu-IL15) mouse model generated through the intravenous (i.v.) infusion of 5 x 10^5 U-266 ffLucGFP cells followed by an i.v. infusion of 4 x 10^6 NKG2D-CAR CIML-NKAE and NKAE cells at day 3. PB was extracted for NK cell detection analysis by flow cytometry at day 7, 14, and 29 after CAR NKAE cell infusion. Tumor burden was monitored fortnightly by BLI. B) Flow cytometry dot plot of the percentage of NKG2D-CAR^+ cells at infusion. C) Flow cytometry analysis of the percentage of NK cells and CAR^+ NK cells from mouse PB samples at day 7, day 14, or day 29 after NK cell infusion (n=4). The mean ± SEM is shown. *p<0.05; ****p<0.0001.

PB analysis was carried out at 7-, 14-, and 29-days post-therapy infusion to evaluate NK cell persistence in mice. At day 7, the average infiltration of human NK cells was significantly higher in the NKG2D-CAR CIML-NKAE cells (17.73 ± 2.67%), compared to the NKG2D-CAR NKAE cells (9.64 ± 1.87%) (Fig. 48C). In addition, at day 14, NK

cell percentage was still superior in the memory group and, remarkably, at this point, the percentage of NKG2D-CAR$^+$ CIML-NKAE cells was significantly higher (49.75 ± 0.81%), which could signify that CAR$^+$ cells were proliferating more in the memory group, compared to NKG2D-CAR NKAE cells (40.25 ± 0.41%). However, at day 29, the percentage of NK cells was similar in both groups, suggesting that NKG2D-CAR CIML-NKAE cells do not exhibit a higher persistence, compared to NKG2D-CAR NKAE cells.

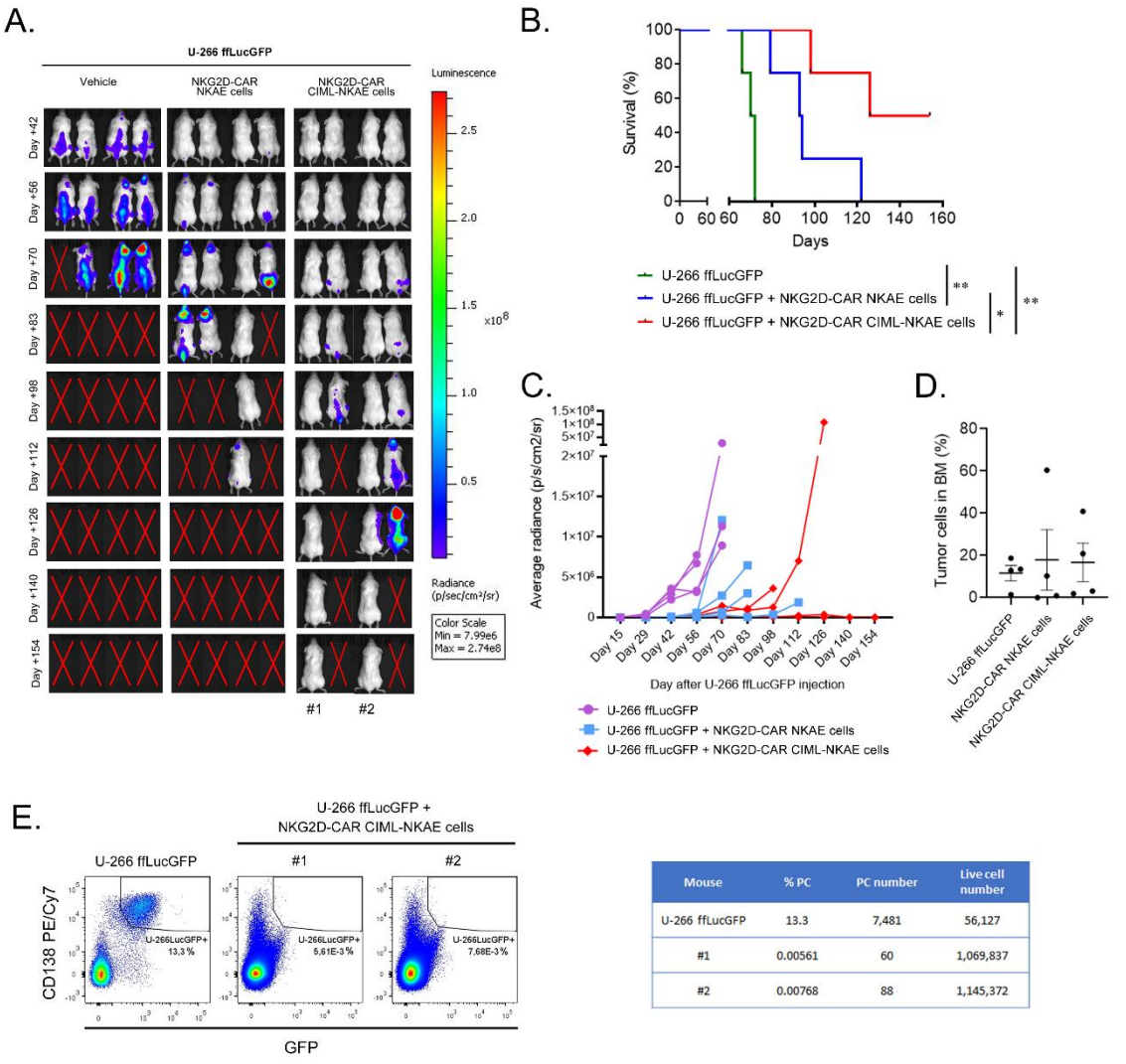

Mouse	% PC	PC number	Live cell number
U-266 ffLucGFP	13.3	7,481	56,127
#1	0.00561	60	1,069,837
#2	0.00768	88	1,145,372

Figure 49. NKG2D-CAR CIML-NKAE cells significantly prolong mice survival in NSG-Tg(Hu-IL15) mice bearing U-266 ffLucGFP MM cells. A) Imaging of tumor burden monitored by bioluminescence, at the indicated time points from NSG-Tg(Hu-IL15) mice bearing U-266 ffLucGFP cells without treatment or treated with NKG2D-CAR CIML-NKAE or NKAE cells. B) Kaplan-Meier survival curve of mice described in (A) (n=4). C) Quantification of luminescence per mouse at different time points. D) Flow cytometry of CD138$^+$GFP$^+$ tumor cells in BM mice at necropsy from the indicated experimental groups (n=4). The mean ± SEM is shown. E) Flow cytometry dot plots of residual tumor cells in the BM of the indicated mice in (A). Flow cytometry analysis of the number of U-266 ffLucGFP detected in the BM of

mice #1 and #2 from NKG2D-CAR CIML-NKAE cell groups, sacrificed at day 154. One U-266 ffLucGFP untreated mouse is shown. *p<0.05; **p<0.01.

In this experiment, both CAR NK cell therapy delayed tumor progression, but NKG2D-CAR CIML-NKAE cells significantly increased mice survival (>140 days) compared to the NKG2D-CAR NKAE cell treatment (93.5 days), and the vehicle group (71 days) (Fig. 49A, B). Quantification of the luminescence photon flux signal was measured along the experiment (Fig. 49C) and tumor cells in the BM of all mice were analyzed by flow cytometry (Fig. 49D). Notably, 2 mice did not have clinical signs of disease neither BLI signal in NKG2D-CAR CIML-NKAE cells at day 150 and the experiment was discontinued. Residual MM cells in the BM of these mice by flow cytometry were detected: 60 PC on 1.07 x 10^6 viable events in mouse #1 and 88 PC on 1.15 x 10^6 viable events in mouse #2 (Fig. 49E).

Altogether, these results support that cytokine memory induction of NKG2D-CAR NKAE cells potentiates anti-MM activity *in vivo*.

4.3.10. NKG2A blockade enhances NKG2D-CAR CIML-NKAE cells cytotoxicity against MM cells *in vitro*

Due to all the results above-described and, taking into account that NKG2D-CAR CIML-NKAE cells also express high levels of NKG2A, we combined both approaches: memory induction through IL-12, IL-15, and IL-18 exposure with Z199 NKG2A blockade.

In vitro cytotoxicity assays performed against XG-1, ARP-1, and RPMI-8226 MM cell lines demonstrated that the blockade of NKG2A is able to increase even more NKG2D-CAR CIML-NKAE cell antitumor efficacy. At a ratio 4:1 (T:E) against RPMI-8226 cells, the specific lysis of NKG2D-CAR NKAE cells pretreated with isotype is 23.55 ± 4.16% and with NKG2A Ab rises to 49.91 ± 4.52%. Interestingly, isotype pretreated NKG2D-CAR CIML-NKAE cells achieve 37.66 ± 4.28% of specific lysis, which increases up to 62.43 ± 3.23% in when pretreated with α-NKG2A Ab (Fig. 50).

Overall, although NKG2D-CAR CIML-NKAE cells produce a high antitumor response with respect to CAR NKAE cells, NKG2A blockade can potentiate their cytolytic activity.

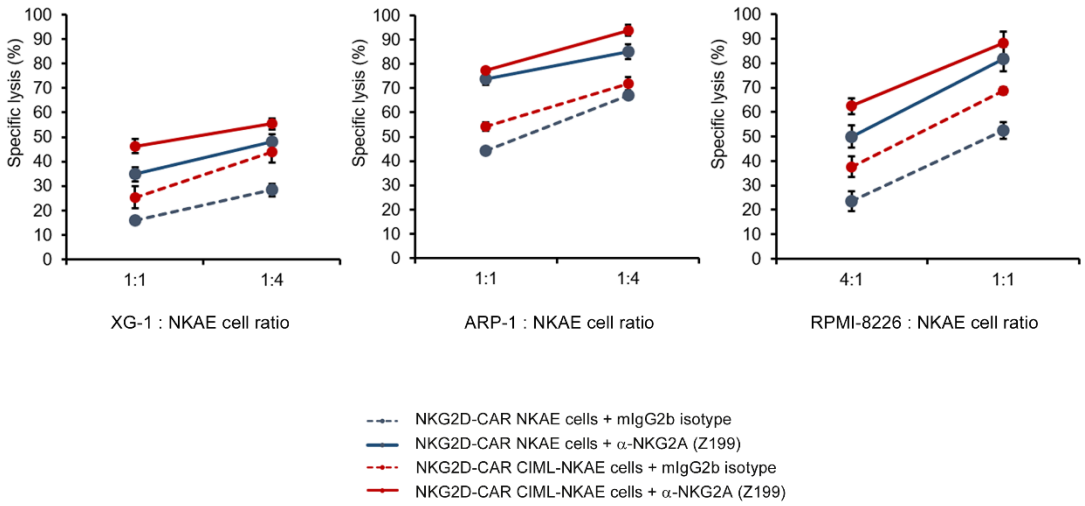

NG2D-CAR NKAE cells	XG-1	ARP-1	RPMI -8226	NKG2D-CAR CIML-NKAE cells
IgG2b isotype 4:1			****	IgG2b isotype 4:1
α-NKG2A (Z199) 4:1			****	α-NKG2A (Z199) 4:1
IgG2b isotype 1:1	****	****	****	IgG2b isotype 1:1
α-NKG2A (Z199) 1:1	****	ns	*	α-NKG2A (Z199) 1:1
IgG2b isotype 1:4	****	*		IgG2b isotype 1:4
α-NKG2A (Z199) 1:4	***	ns		α-NKG2A (Z199) 1:4

IgG2b isotype	XG-1	ARP-1	RPMI-8226	α-NKG2A (Z199)
NKG2D-CAR NKAE cells 4:1			****	NKG2D-CAR NKAE cells 4:1
NKG2D-CAR CIML-NKAE cells 4:1			****	NKG2D-CAR CIML-NKAE cells 4:1
NKG2D-CAR NKAE cells 1:1	****	****	****	NKG2D-CAR NKAE cells 1:1
NKG2D-CAR CIML-NKAE cells 1:1	****	****	****	NKG2D-CAR CIML-NKAE cells 1:1
NKG2D-CAR NKAE cells 1:4	****	****		NKG2D-CAR NKAE cells 1:4
NKG2D-CAR CIML-NKAE cells 1:4	****	***		NKG2D-CAR CIML-NKAE cells 1:4

Figure 50. The blockade of NKG2A significantly augments NKG2D-CAR CIML-NKAE efficacy against MM cell lines. Specific lysis of NKG2D-CAR CIML-NKAE and NKAE cells treated with either the mouse α-NKG2A Ab (Z199) or its corresponding isotype (mIgG2b) against the MM cells ARP-1 (n=3), RPMI-8226 (n=4), and XG-1 (n=5) analyzed by 3h-Calcein release assay. The mean ± SEM is shown. Statistical analysis is included in the table. ns: not significant; *p<0.05; **p<0.01; ***p<0.001; ****p<0.0001.

5. DISCUSSION

Although MM overall survival has increased over the last decades due to the therapeutic armamentarium available, MM is still an incurable disease. Within the TME, MM cells are sustained by soluble factors and direct cell-cell interactions that promote their proliferation, while exhausting NK and T cells, especially in the RRMM scenario. This immunosuppressive context arises the need to find new strategies to eradicate this tumor. In this setting, the main objective of this thesis is the generation of enhanced allogeneic CAR NK cell therapies for RRMM patients, in combination with immune checkpoint inhibitors to improve CAR NK cell efficacy, as well as with the induction of memory properties to increase CAR NK cell persistence.

On the one hand, based on previous preclinical and clinical studies not only in other hematological malignancies, but also in solid tumors, immune checkpoints seem to play a key role in NK and T cell dysfunction, promoting tumor escape. In concrete, HLA-E, a non-classical class I molecule, has been found overexpressed in many tumors [348, 377, 379-383, 399], correlating with lower overall survival [379, 384-386, 388, 389]. As the treatment with α-KIR and α-PD-1 or α-PD-L1 Abs to disrupt immune checkpoint inhibitory signals has reported severe toxicities in MM patients [356, 476], the interaction of HLA-E and NKG2A has become an interesting alternative to potentiate NK cell activity in this tumor. In this thesis, we have tested the combination of CAR NK cells redirected to two main targets in MM, NKG2D ligands and BCMA, with a novel human clinical-candidate α-NKG2A Ab, to overcome this shortcoming.

On the other hand, *in vivo* persistence after adoptive transfer has been previously reported to correlate with clinical responses. NK cell short lifespan and limited proliferative capacity caused by the host immunosuppressive TME may be responsible for the low sustenance of CAR NK therapies. In this study, we have analyzed the *in vivo* efficacy and persistence of a new cytokine-induced memory-like NKG2D-CAR NKAE cell therapy for RRMM patients.

5.1. HLA-E is overexpressed in pathologic plasma cells from RRMM patients compared to healthy populations

In this first set of experiments, our results show that HLA-E expression is increased on PC from a large cohort of MM patients (n=54) compared to HD (Fig. 25A). Similar results were described by other groups that also studied HLA-E expression by flow cytometry on PC from 30 NDMM patients and 7 HD [125] and 8 MM patients and 1 PCL patient [378].

To our knowledge, this is the first time that HLA-E expression on pPC has been compared to normal populations (nPC and $CD34^+$ cells) from the same patients on MGUS, MM at diagnosis and MM at progression BM samples, resulting in an increased HLA-E expression in patients at progression, compared to the other stages. This fact suggests that HLA-E expression augments along MM progression and that its presence on the cell membrane is significantly high compared to healthy cells (Fig. 25B). Comparison with $CD34^+$ cells is intuitive because a high HLA-E expression would predict a possible multi-lineage cytopenia after HLA-E/NKG2A targeted therapies. Due to the improved clinical management of CRS, pancytopenia is currently the main severe adverse after CAR T cell treatments [477].

Since HLA-E expression is increased in patients at progression, we then compared PFS between MM patients at diagnosis with high (pPC/$CD34^+$ ratio > 1.1) and low (pPC/$CD34^+$ ratio ≤ 1.1) HLA-E expression. Our results show a shorter PFS tendency in the high HLA-E expression ratio, but a larger cohort of patients would be needed to propose HLA-E expression ratio as a prognostic factor. Unfortunately, a higher HLA-E expression ratio between pPC and $CD34^+$ cells does not impact on patient overall survival (Fig. 25C). Since mediated responses by immune effectors in the BM may be fine-tuned via different signals beyond HLA-E/NKG2A axis, these results may suggest that other factors could be dominantly affecting MM survival. Although HLA-E may not result in a biomarker of the progression of MM, it could be conditioning adoptive therapy responses.

Nevertheless, Lagana's study reported a shorter PFS within the high HLA-E expression group after studying 436 NDMM patients, but this measurement was inferred from HLA-A data from CoMMpass study, as HLA-E expression is not available in this dataset [387]. In line with the impact of HLA-E over prognostic markers, Yang's group stratified the

previously-mentioned 30 NDMM patients and obtained a significant correlation between HLA-E expression and an advanced ISS stage and a high cytogenetic risk [125].

Additionally, we have studied the relevance of several cytokines present in TME, not only to unveil possible cytokines involved in HLA-E modulation, but also their possible impact on CAR adoptive therapy efficacy. Previously, some groups have already reported different cytokine expression levels in this tumor compared to healthy samples. IL-10, MCP-1, IL-6, CXCL2, IL-2 and TNF-α, among others, have been found increased in samples from MM patients, while lower levels of IL-3, IL-13 and GM-CSF have been observed [478, 479]. However, IFN-γ levels in MM patients are controversial. Pérez-Andrés et al. described a higher IFN-γ concentration (around 20 pg/ml) in BM samples from MM patients compared to HD [130], while Sharma's and Zheng's studies found lower levels of this cytokine in PB samples [478, 480]. In our project, we have analyzed the concentration of diverse cytokines in BM samples from 32 patients at different stages, obtaining higher levels of MCP-1, IL-6, in line with previous published results [478, 479], TGF-β, and IFN-γ (around 15 pg/ml), compared to HD (Fig. 26A). This result suggests, according to Pérez-Andrés et al., that IFN-γ levels are increased in the MM microenvironment, in the BM but not in the PB of these patients, where it may play a key role in the immune escape of this tumor. In this sense, although IFN-γ is essential in NK and T cell immunomodulation, this cytokine can also upregulate molecules, which mediates immune effector exhaustion (eg. PD-L1), in tumor cells [137].

In this context, we tested the influence of this proinflammatory cytokine on HLA-E expression. Previous studies had already reported that IFN-γ increased HLA-E expression on tumor cells [348, 377, 394, 395], including MM cells [349, 393]. IFN-γ transcriptionally augments HLA-E mRNA [481]. Moreover, HLA-E is stabilized on the cell surface when loading signal peptides derived from HLA molecules [88]. In the presence of IFN-γ or TNF-α, a dynamic equilibrium between the formation of the proteasome and the immunoproteasome occurs. Furthermore, BTZ is able to inhibit the β5 subunit of the proteasome along with the β5 induced subunit in the immunoproteasome, causing ER stress and a lack of loading peptides on HLA-E, reducing its presence on the cell membrane [482].

Our results also corroborated this effect over primary MM cells, from diagnosis and progression samples (Fig. 26B), and the MM cell lines RPMI-8226 and NCI-H929 (Fig. 26C). Moreover, we included, in this set of experiments, two MM cell lines resistant to

20 nM BTZ, to study the effect of this cytokine over BTZ-resistant MM cells. As we expected, IFN-γ also augments HLA-E presence on these cells, suggesting that BTZ-resistant patients would also have increased HLA-E expression on PC after IFN-γ exposure. Additionally, BTZ treatment diminishes HLA-E expression on sensitive MM cells, even if its expression had been previously induced by IFN-γ. Remarkably, since HLA-E expression was not reduced after IFN-γ exposure on BTZ-resistant cells, HLA-E levels may remain high in MM BTZ-resistant patients with increased IFN-γ levels within the BM.

5.1.1. α-NKG2A Ab monotherapy does not restore immune effector activity in BM MM patient samples

Given the high expression of HLA-E detected in MM cells, we studied the expression of its activating receptor NKG2C and its inhibiting receptor NKG2A on cytotoxic NK and T cells. In our results, there is a higher percentage of NK cells expressing the inhibiting receptor NKG2A than the activating NKG2C in BM samples from MM patients, reaching 50% of $NKG2A^+$ NK cells in samples from patients at progression (Fig. 27A). On the contrary, cytotoxic tumor-infiltrating T cells expressed a very low percentage of $NKG2A^+$ or $NKG2C^+$ cells, while around 60% of these T cells were $PD\text{-}1^+$(Fig. 27B). These studies suggest that NK cell activity against tumors, but not T cells, may be impaired by the inhibitory signaling fostered by the binding of NKG2A to HLA-E in the tumor cells. Thus, the disruption of this axis could reactivate NK cell antitumor efficacy.

Related to these results, around 60% of tumor-infiltrating NK cells have been found $NKG2A^+$ in B-cell lymphoma bearing mice [399], although no significant differences were detected regarding this receptor between the NK cells from CLL patients and HD [348]. Moreover, low expression of NKG2A has been reported on tumor-infiltrating T cells from mice bearing B-cell lymphoma [399] and gynecological cancer samples at diagnosis [379], but these studies did not analyze the expression of NKG2A on NK cells. The importance of this inhibitory receptor in patient survival is unclear. High expression of NKG2A has been found to correlate with a poor prognosis in liver cancer [483] and HNSCC, while it has been associated with a failure to achieve remission in AML patients [103]. By contrast, a higher expression of NKG2A has been reported to correlate with a better survival in breast cancer and no associations were found in other solid tumors [484].

Regarding α-NKG2A treatments in monotherapy, Monalizumab, a humanized α-NKG2A blocking Ab, has reported activity restoring immune effector activity in CLL and EBV^+ lymphomas *in vitro* [348], but it has not shown efficacy *in vivo* in immunocompetent mice against B-cell lymphomas [399] and PDAC [383]. Due to commercial market issues and availability, our study has been focused on the use of another α-NKG2A Ab, the BMS-986315, which specifically neutralizes the NKG2A receptor, compared to a standard mouse α-NKG2A Ab, the Z199, widely used on diverse studies. Battin et al. reported a strong binding of Z199 to NKG2A, as well as a high efficacy targeting HLA-E^+ tumor cells that were loading different leader peptides [402]. Moreover, Z199 activity was compared to the use of PEBL, designed with the same scFv, where both showed a significant increase in NK cell cytotoxicity [394]. In keeping with this, the efficacy of the human α-NKG2A included in this study, provided by BMS (BMS-986315), is being tested in two clinical trials against NSCLC (NCT06094296) and solid tumors (NCT04349267), in combination with other drugs, but neither preclinical nor clinical efficacy data have been published yet.

In this thesis we have compared, for the first time, to our knowledge, the efficacy of two α-NKG2A Abs (Z199 and BMS-986315) over BMMCs from MM patients. These cultures imply a native context, including PC as well as NK, T, DCs, among others, supplemented with own sample plasma, to test the effect of these Abs in the most similar conditions to the TME. Neither the use of the human nor the mouse α-NKG2A Ab were able to reactivate NK cell activity against MM cells (Fig. 27C). Probably, the challenging culture context would explain our results in this experiment. However, our findings are consistent with the negative outcomes reported in clinical trials, where Monalizumab only achieved modest responses in HNSCC [408] and gynecologic malignancies [407]. For this reason, most clinical trials are now combining Monalizumab with other blocking Abs and have reported better results [410, 411]. Having demonstrated that α-NKG2A Abs in monotherapy have not shown efficacy and, considering the reported toxicities with common mAbs (α-PD-1 and α-KIR) in MM patients, we hypothesized that by combining CAR NK adoptive therapy and α-NKG2A Abs, it might be possible to foster NK antitumor responses still further.

5.2. NKG2D- and BCMA-CAR NKAE cells are efficiently generated

CAR NK cells have emerged as a safer but equally [293], or even more effective therapy [155, 485], compared to CAR T cells *in vitro*. In the clinical setting, unlike CD19 CAR NK cells showed equal outcomes with regard to CAR T cells, BCMA-CAR NK therapies have reported modest and low durable responses (Table 4). This fact has promoted the development of new strategies to enhance CAR NK cell antitumor efficacy.

CAR NK cell preclinical studies have used different specificities to target MM, as CS1, CD138, BCMA and CD19 [206, 330-333]. Our lab has been focused on two targets, BCMA and NKG2D-L, utilizing a BCMA-CAR based on a scFv that specifically binds BCMA and a NKG2D-CAR designed from the natural ectodomain of NKG2D receptor. BCMA has been described as the first MM target with limited expression on healthy cells. In fact, extraordinary outcomes of the two FDA-approved BCMA-CAR T therapies (ide-cel and cilta-cel) have been reported. This target is virtually expressed on all PC, as we have demonstrated in different MM cell lines (Fig. 32A) as well as in primary MM cells (Table 13). Moreover, NKG2D-L have been also found overexpressed on MM cells, especially on the side population [155], which suggests the importance of targeting these ligands in this tumor. However, few clinical trials using NKG2D-CAR T cells have not met the expected results in MM patients [160, 266]. Probably, the poor efficacy may be caused by the absence of lymphodepletion prior to CAR T infusion, the use of first-generation NKG2D-CAR or the low levels of NKG2D-L in those patients. However, we have detected a high expression of the NKG2D-L, not only on MM cell lines (Fig. 32A), but also on all the primary MM cells we have analyzed (Table 13).

One of the main benefits of CAR NK therapy, regarding target-cell interaction, is that CAR NK cells are not restricted to HLA-TCR recognition. CAR NK cells can be used in an allogeneic context, without the need of engineering the TCR, as allogeneic CAR T cells, being a universal and off-the-self treatment option for cancer patients. Allogeneic CAR T cells have inferior clinical outcomes, probably due to genotoxicity, caused by gene-editing, and immunogenicity [486].

Expansion and transduction of CAR NK cells are quite challenging. CAR NK cells can be generated from different sources, although most preclinical studies use PB

leukapheresis [286], PB buffy coats [335, 487] or umbilical CB [419]. Our study is based on obtaining a great amount of CAR NK cells from 18 ml of PB from HD, a less invasive and expensive method. However, most sources, including ours, need feeder cells (e.g K562-mb21-41BBL) to expand and activate NK cells [155, 488], resulting in a diverse NK cell clonal repertoire [489]. The use of K562-mb21-41BBL in co-culture with PBMCs generated a large amount of NKAE cells (up to 4 x 10^8 cells, 100-fold, data not shown), almost 100% $CD56^+$, around 70% of them were cytotoxic ($CD56^+CD16^+$) and a very low contamination of $CD3^+$ cells was observed (lower than 0.5%) (Fig. 28B). Interestingly, this feeder cell or the K562-mb15-41BBL have been used in numerous clinical trials, demonstrating a large NK cell expansion ratio. Besides, no toxicity or oncogenic risk were reported due to their manufacturing use, as these cells have to be previously irradiated [255, 490, 491].

Another key point is NK cell transduction. Lentiviral vectors are the most selected method for CAR delivery. These particles can infect dividing and non-dividing cells, while γ-retrovirus only infect dividing cells and can produce a higher insertional oncogenesis risk compared to lentivirus, as they are normally inserted near transcriptional start sites, reasons why they have been discarded from many studies. Moreover, lentiviral transduction implies CAR integration in the DNA, between exons and introns, preferentially far from transcriptional start sites, and a long-lasting CAR expression on the cell membrane, compared to the transient expression obtained by mRNA or DNA transfection methods (3 or 15 days, respectively). Commonly, lentiviral vectors are pseudotyped with the VSV-G envelope. However, its receptor, the LDL-R, is poorly expressed on activated NK cells. For this reason, to favor the interaction between lentivectors and NK cells, several strategies as the use of cationic polymers (polybrene or protamine sulfate) to avoid virion-cell repulsion, crosslinking agents as Retronectin or Vectofusin-1, spinoculation or multiple rounds of transduction have been utilized to enhance CAR integration efficiency [492]. We have optimized NKG2D- and BCMA-CAR transduction on our NKAE cells using retronectin-coated plates and spinoculation to enhance CAR integration. Moreover, due to differences in CAR expression between NKG2D- and BCMA-CAR NKAE cells, we have used a higher MOI (MOI 8) and 2 rounds of transduction for BCMA-CAR. Our results showed an average of 34% and 22% of CAR efficiency expression in NKG2D- and BCMA-CAR NKAE cells, respectively, quite similar between populations, as it was also demonstrated after VCN measurement

(0.82 vs 0.55 copies/cell) (Fig. 29B). Other groups have reported similar data in NK cells derived from PB. Published results from our group described a median of 20% NKG2D-CAR$^+$ NKAE cells, derived from PB from MM patients [155], while Herrera et al. achieved around 45% of CAR$^+$ NK cells, after 7 days from transduction [325]. However, Muller et al. only reached a median of 10% CAR$^+$ cells with lentiviral vectors [487], according to several studies that have reported the superior refractoriness of PB NK cells to engineering. Moreover, a higher sensitivity to apoptosis after lentiviral infection has been reported [493]. Nevertheless, NK cells derived from CB are more permissive [492], as described in clinical trials, achieving a median of 50% CAR$^+$ NK cells [326]. Besides, unpublished results from our lab have showed a 67% and 53% of NKG2D- and BCMA-CAR$^+$ NKAE cells when generating these therapies from CB.

To improve the transduction of NK cells derived from PB, some groups have proposed the use of another envelope, the Baboon envelope (BaEV), which receptors, ASCT-1 and ASCT-2 are highly expressed on activated NK cells [492, 494]. Dong et al. reported a median of 65% transduction efficiency when using BaEv lentiviral vectors [458], although our experience with the production of lentivectors containing the BaEv envelope resulted in 100-fold low titers, compared to VSV-G lentivectors. Due to the high lability of BaEv and that our transduction efficiency in NK cells was similar to VSV-G (around 30%), we have not used this envelope in this thesis. Moreover, other intrinsic antiviral mechanisms may be hampering NK cell transduction, which can be inhibited by other molecules (eg. BX-795) [324].

Several publications reported an increased NKG2A and NKG2D expression on NK cells after ex vivo activation [155, 405, 495]. Tognarelli et al. demonstrated that, compared to resting NK cells, cytokine stimulation increases the percentage of NKG2A$^+$ and NKG2D$^+$ NK cells up to 80 and 100%, respectively [393]. According to these reports, we have observed a higher percentage of NKG2A$^+$ and NKG2D$^+$ CAR NKAE cells, 90 and 60%, respectively (Fig. 30A), suggesting that the activation of NK cells not only augments activating receptors such as NKG2D but also inhibiting receptors, as NKG2A, to counterbalance this excessive activation, which could produce an autoimmune effect. Moreover, we have studied the impact of different cytokines, used to generate NKAE cells or that are present in the MM microenvironment, on NKG2A expression. In 48-hour NK cell cultures, we showed a mainly IL-15-dependent NKG2A induction on cytotoxic NK cells (RFI of 100 with IL-15 compared to RFI of 55 on unstimulated NK cells). The

same fold was obtained after IL-2 and IL-21 addition, cytokines commonly used to expand NK cells. However, TGF-β did not increase NKG2A expression (Fig. 30B). IL-21, IL-15, IL-12, IL-10 and TGF-β have been described to induce NKG2A expression on NK cells [396]. Although we cannot properly compare NKG2A induction measure to other studies, Hromadnikova et al. reported an increase in the percentage of $NKG2A^+$ cells up to 55 and 52% after IL-2 or IL-15 addition, respectively, compared to 30 and 45% without cytokines, after 4 days of culture [496]. Moreover, Skak et al. also described a synergistic effect of IL-2 and IL-21, raising NKG2A percentage from 41% without stimulation, to 59% with IL-2 and IL-21. These results indicate that all distinct cytokines that could be used to activate and expand NK cells would increase NKG2A expression, being an important inhibitory signal for NKAE cells when binding HLA-E on tumor cells.

According to what we observed in primary MM cell analysis, the MM cell lines used in this project (U-266, RPMI-8226, XG-1, and ARP-1) also express different levels of HLA-E, results that were previously reported by Sarkar et al. [378] (Fig. 31A). Although HLA-E expression may seem low (RFI of 2.5-4.5), MM cells co-culture with NKG2D- or BCMA-CAR NKAE cells significantly increases the expression of HLA-E on MM cell lines (RFI of 10 and 12, respectively) (Fig. 31B). The high IFN-γ release by NKG2D- and BCMA-CAR NKAE cells (around 600 pg/ml) suggests the potential role of this cytokine in MM resistance to CAR NK therapy (Fig. 31C), which implies a positive feedback, as CAR NKAE cells produce more IFN-γ, when they are co-cultured with cell lines, increasing even more HLA-E expression on target cells. A similar study was performed on AML cells, where they observed an increase in HLA-E expression, induced by the IFN-γ secreted by immature NK cells [497]. In this way, tumor cells are protected from NK cell lysis via HLA-E/NKG2A signaling.

5.3. The blockade of NKG2A enhances NKG2D- and BCMA-CAR NKAE efficacy against MM cells

NKG2A, as well as KIRs, are involved in NK cell licensing. Therefore, a total elimination of NKG2A could induce hyporesponsiveness in NK cells. Zhang et al. suggested that partial deletion of NKG2A is more favorable than the complete blockade of this axis [498]. In this setting, different approaches have been carried out to disrupt NKG2A/HLA-

E binding. Kamiya et al. described the use of PEBL, molecules that concomitantly bind NKG2A and the ER to retain NKG2A receptors, impeding its presence on the cell membrane and therefore its binding to HLA-E [394]. However, two recent publications have knocked out by CRISPR-Cas9 the gene that codifies NKG2A, *KLRC1*, on NK cells, showing enhanced cytotoxicity against MM (80 vs 60% at 1:1 ratio against MM1.S cells and 40 vs 18% against U-266 pretreated with IFN-γ) [349] and solid tumors [495]. Nevertheless, most studies have been carried out using an α-NKG2A blocking Ab. Combination of ex vivo NK cells with α-NKG2A Abs enhances their antitumor activity against leukemia [404], CLL [348], PDAC [383], HNSCC [395] and MM [393]. This last study observed a significant increase in activated NK cell cytotoxicity in combination with the Z199 against different MM cell lines (75 vs 65% at 1:2 T:E ratio against U-266), even if they were previously incubated with IFN-γ to augment HLA-E expression (75 vs 50% at 1:2 T:E ratio against U-266 pretreated with IFN-γ). Since CAR NK cells have not been studied in combination with complete or partial elimination of NKG2A against tumors, we cannot properly compare our results. We found that both mouse (Z199) and human (BMS-986315) α-NKG2A Abs significantly enhance NKG2D- and BCMA-CAR NKAE cells cytolytic activity against the MM cell lines U-266 (70 vs 50% at 1:1 ratio with NKG2D-CAR NKAE cells), RPMI-8226, XG-1 and ARP-1 (Fig. 32B) and primary cells from MM patients (Fig. 35B). Besides, we also corroborated the efficacy of these combinations against the RPMI-8226 cell line, after 24-hour exposure to IFN-γ (57 vs 27% at 1:1 ratio with Z199 pretreated NKG2D-CAR NKAE cells) (Fig. 32D). Remarkably, experiments against primary cells were performed co-culturing both pretreated CAR NKAE cells with BMMCs. These BMMCs contained not only PC, but also immune cells, including immunosuppressive cells and $CD34^+$ cells. Moreover, soluble factors (ADO, IDO, TGF-β) and platelets contained in the plasma of BM samples were added to sustain PC and test the efficacy of CAR NKAE cells in a challenging scenario. In this context, we have tested the efficacy of the α-NKG2A pretreatment on CAR NKAE cells mimicking TME, where both therapies have demonstrated great antitumor activity. Of note, although we did not observe differences in terms of efficacy between both CARs against MM cell lines, we used a lower T:E ratio for BCMA-CAR comparisons suggesting that BCMA-CAR has a higher efficacy eliminating PC (80 vs 50% 1:5 T:E), than NKG2D-CAR (80 vs 60% at 1:10 T:E) (Fig. 35B). Blockade of NKG2A on activated NK cells also enhanced cytotoxicity against AML primary cells, previously treated with IFN-γ (around 50 vs 30% at 1:1 or 1:2 T:E) [394] and knock out

of NKG2A on activated NK cells resulted in an enhanced lysis of IFN-γ against primary MM cells (40 vs 20% at 1:1 T:E) [349].

Furthermore, we have measured the degranulation capacity of both CAR therapies against the MM cell lines previously mentioned and against the feeder cell K562-mb21-41BBL that lacks HLA-I and HLA-E expression. Again, both combinations demonstrated an increased degranulation capacity compared to isotypes except against the feeder cell, where, as expected, no differences were found due to the absence of HLA-E on the target cells (Fig. 33B). By contrast, Mahaweni et al. did not observe differences on degranulation levels after NKG2A blockade on NK cells against primary MM cells, only some efficacy was described when KIR mismatched samples were selected [406]. In addition, Oei et al. suggested that the presence of CAR molecules on NK cells overcomes the inhibition caused by the interaction between NKG2A and HLA-E, although they do not combine CAR NK cells with NKG2A blockade [499]. Our results demonstrate that even CAR NKAE cells have enhanced antitumor efficacy, the blockade of the inhibitory receptor NKG2A is able to increase even more this effect.

Additionally, NKG2D- and BCMA-CAR NKAE cells secreted high concentrations of cytolytic cytokines. However, only IFN-γ concentration was significantly higher after CAR NKAE cells blockade with the α-NKG2A Abs, when co-cocultured with MM cell lines (Fig. 33C). Published results from our group regarding NKG2D-CAR NKAE cells, generated from MM patient PB samples, reported low levels of these cytokines alone (a median of 50 pg/ml of IFN-γ) [155] compared to the average of 600 pg/ml that we obtained. Notably, since cytokine concentration is augmented when exposed to MM cells, we cannot compare the release of other soluble molecules with the ones obtained in the cited publication [155]. Besides, Bexte et al. did not find significant differences in IFN-γ production between *KLRC1* KO NK cells and non-treated NK cells after co-culture with tumor cells, but a higher tendency in the KO group was noticed [349]. Remarkably, our blocked cells neither expressed IL-6 nor IL-10 (data not shown), cytokines directly related to CRS. Although there is no direct correlation between cytokines produced *in vitro* and in patients, the absence of IL-6 and IL-10 production *in vitro* may suggest the low risk of this side effect when using CAR NK therapies *in vivo* [326].

This improved anti-MM activity could be expected to produce toxicities. On the one hand, most preclinical studies in MM have not studied CAR NK cell toxicity against healthy cells. Leivas et al. demonstrated low toxicity of NKG2D-CAR NKAE cells against a lung

cell line (25%) and HD PBMCs (20%), but a considered lysis against a colon cell line (40%), at 1:4 T:E ratio [155]. However, these healthy cell lines may not have the same marker profile as healthy tissues, where NKG2D-L expression might be lower. Moreover, CD19 CAR NK cells used in clinical trials have shown transitory grade 4 hematologic toxic events (neutropenia and lymphopenia), but both trials have associated them with the lymphodepleting chemotherapy prior to CAR NK cell infusion (NCT03056339 [326] and NCT05020678). NKG2D-CAR NK therapy (NKX101) caused grade 3 or higher anemia and neutropenia in 50% of AML and MDS patients (3/6; NCT04623944), probably related to the lymphodepletion treatment. On the other hand, monalizumab, as a single agent, has not shown severe hematologic side effects in clinical trials. A phase II study treating HNSCC tumors detected grade 1 or 2 anemia in 7% of patients [408], while a gynecologic tumor clinical trial reported grade 3 or higher anemia in 2 out of 40 patients [407]. In this thesis, we have tested NKG2D- and BCMA-CAR NKAE cells toxicity when pretreated with the α-NKG2A Abs against HD PBMCs (Fig. 35C) and $CD34^+$ from MM patients in a native-context culture (Fig. 35B). Toxicity against PBMCs was quite low, less than 20%, using the α-NKG2A NKG2D-CAR treatment, as Leivas et al. reported [155], and less than 5% of killing with the BCMA-CAR combined therapy, at the highest ratio (1:4 T:E). Moreover, we chose to test toxicity against hematopoietic progenitors because one of the most severe CAR T cell side effects is prolonged cytopenias, associated with a higher risk of infections [500]. Notably, the combination of α-NKG2A Abs with NKG2D- or BCMA-CAR NKAE cells displayed low cytolytic activity against MM patient $CD34^+$ cells, suggesting that they concomitantly lyse primary PC without affecting these hematopoietic stem cells, in line with most CAR NK cells and monalizumab clinical trial results, separately. Remarkably, the use of the BMS-986315 Ab did not increase the toxicity caused by CAR NKAE cells incubated with the isotype (Fig. 35B).

Unfortunately, we have not found differential expression on diverse expression markers studied by flow cytometry and CyTOF (Fig. 34A, B), as other groups have already reported when disrupting HLA-E/NKG2A axis [349, 394], except from a downregulation on NKG2A expression. By contrast, as a paradigmatic example, Mac Donald et al. reported a higher expression of NKG2C on $KLRC1^{KO}$ NK cells, which partially participates in the augmented cytotoxicity of the KO NK cells, and suggested that NKG2C increase is caused by the NK cell expansion using IL-21. However, we activated

and expanded NK cells with the feeder cell K562-mb21-41BBL that contains IL-21 and did not observe an increased expression of NKG2C during NK cell expansion or when treated with the α-NKG2A Ab.

Although differences in cytotoxicity are appreciated between CAR NKAE cells pretreated with the α-NKG2A Ab or the isotype and other markers may be affecting the activating/inhibiting NK balance, we have found an increased phosphorylation of downstream ZAP70/Syk kinases after blocking with BMS Ab (Fig. 34C), which could explain the higher efficacy of this combination *per se*. Further phosphoproteomic studies of other kinases are needed to unveil the complete signaling pattern.

5.3.1. Pretreatment of NKG2D-CAR NKAE cells with BMS-986315 α-NKG2A Ab significantly reduces tumor burden *in vivo*

First *in vivo* attempt in immunodeficient NSG-Tg(Hu-IL15) mice bearing RPMI-8226 ffLucGFP cells comprised NKG2D- or BCMA-CAR NKAE cells pretreated with either the human BMS-986315 or the hIgG1κ and additional infusions of the corresponding Abs to maintain the blockade of NKG2A over time. PB analysis at day 7 and day 14 revealed a significant NK cell percentage decrease within α-NKG2A pretreated CAR NK cells, which may be caused by the prolonged NKG2A absence, fostering CAR NKAE cell recognition of their siblings and inducing fratricide (Fig. 36). Of note, this effect is not caused by an enhanced ADCC, as Fc region from BMS-986315 Ab is mutated [414]. Ruggeri et al. also described this effect after repeated doses of α-NKG2A Ab in mice, suggesting NK cell auto-killing [404]. However, this fratricide effect has not been reported *in vitro*. For example, Bexte et al. knocked-out the NKG2A encoded gene, *KLRC1,* and demonstrated that the lack of NKG2A did not impact on NK cell viability. These cells even had a 10-fold expansion after 18 days from CRIPSR-Cas9 edition [349].

Since NKG2A blocked CAR NKAE cell persistence was reduced, we tested the efficacy of the blockade of NKG2A on both therapies, NKG2D- and BCMA-CAR NKAE cells, only as a pretreatment, against the modified U-266 ffLucGFP cell line in the disseminated orthotopic NSG-Tg(Hu-IL15) mouse model. As we and others have reported [378], although HLA-E expression is quite low in this cell line, it increases *in vivo* (5 vs 15 RFI) (Fig. 38C), becoming an appropriate model to assess our treatments.

CAR NK cells have shown efficacy *in vivo* against MM cells. Regarding NKG2D-CAR, our group has already published that NKG2D-CAR NKAE cells efficiently eliminate tumor burden in 25% of mice against the same cell line, U-266 ffLucGFP, although there are some differences between that study and ours. Leivas et al. generated NKG2D-CAR NKAE cells from MM patients PB, not HD samples, and for the *in vivo* experiment they infused this therapy at a 1:3 T:E ratio in NSG mice [155]. Our first *in vivo* experiment against U-266 ffLucGFP cells was designed at a 1:16 T:E ratio. Under these circumstances, even mice from the isotype control treatment were rescued from dead (50%), and in the α-NKG2A blocking therapy, 75% were MRD^- (Fig. 38). Using a low T:E ratio, 1:8, we significantly delayed tumor development in the α-NKG2A NKG2D-CAR NKAE cells treatment (>143 days) compared to the isotype (93.5 days) (Fig. 40), suggesting that the disruption of the HLA-E/NKG2A axis enhances the antitumor efficacy of CAR NK cells.

Other studies have also reported the benefit of hampering the binding of NKG2A to HLA-E in NK cells, out of CAR context. Ruggeri et al. rescued from death 100% of immunodeficient mice bearing AML, pretreating activated NK cells with monalizumab α-NKG2A Ab [404]. Similarly, α-NKG2A PEBL-transduced NK cells were able to eliminate Ewing sarcoma cells in 5 out of 7 immunodeficient mice, after 269 days of follow-up [394]. In addition, the CRISPR-Cas9 KO of the *KLRC1* gene on NK cells delayed breast cancer proliferation (59 vs 48 days) in NSG-Tg(Hu-IL15) mice [495].

Unfortunately, in our two U-266 ffLucGFP *in vivo* experiments (1:16 and 1:8 T:E), we could not evaluate differences between α-NKG2A blocked BCMA-CAR NKAE cells and the isotype (Fig. 38 and 40). These results indicate that BCMA-CAR has more efficacy than NKG2D-CAR in eradicating MM cells, as we also detected against primary cells. New experiments with low BCMA-CAR NKAE cell doses are ongoing. Previous studies have also reported high efficacy of this BCMA-CAR on NK cells in MM mouse models. Ng et al. engineered PB NK cells to co-express BCMA-CAR and CXCR4 to improve CAR NK cells homing to the BM, obtaining a higher mice survival over the BCMA-CAR NK cells group (1:6 T:E ratio) [335]. In line with BCMA-CAR NK cell modifications, Cichocki et al. modified iPSC-derived NK cells to express a BCMA-CAR, mbIL-15 and IL-15R, CD38 KO as well as a non-cleavable CD16, to augment ADCC in combination with daratumumab, and showed their efficacy at an extremely high ratio (1:150 T:E ratio) against the MM cell MM1.S [340]. Our experience suggests that redirecting BCMA-CAR

NKAE cells with chemokines receptors or daratumumab to increase their potential are not needed to fully eradicate tumor burden in our MM bearing mouse models.

The enhanced NKG2D- and BCMA-CAR NKAE cell antitumor efficacy is probably caused by the long persistence of CAR NKAE cells in mice. We were able to detect NK cells in all mice treated with CAR NKAE therapies up to 29 days and, in both U-266 ffLucGFP experiments, CAR expression remained stable (Fig. 37 and 39). Of note, no significant differences were obtained regarding NK cell percentage in mice between CAR-NKAE cells pretreated with the α-NKG2A Ab and the isotype. These results suggest that the release of human IL-15 in these mice plays a key role in NK cell persistence. Moreover, the expression levels of transgenic human IL-15 expressed by NSG-Tg(Hu-IL15) mice are similar to the levels that can be found in humans (around 7.1 pg/ml) [469], suggesting that our model resembles the IL-15-*milieu* that these therapies would find in patients. Several studies have recommended the addition of interleukins, such as IL-2 or IL-15, to promote NK cell sustenance in mice [501]. Another strategy is the incorporation of the human IL-15 and the CAR sequence in a bicistronic construct, as a soluble factor or as a membrane ligand [336, 340, 419]. In particular, Liu et al. obtained a longer mice survival when CB CAR NK cells auto-produced IL-15, with a bicistronic construct, up to 68 days, compared to CAR NK cells lacking IL-15, and demonstrated that exogenous IL-15 results more toxic than the production of this cytokine by engineering CAR NK cells. By contrast, Thangaraj et al. detected NK cells at necropsy (63-91 days) in all NK treatments in the mouse BM from NSG-bearing MM, suggesting that no exogenous or IL-15 self-production on NK cells is needed to maintain these cells for extended periods [390]. Seemly in contrast, none of our mice had NK cells at necropsy (later than 90 days).

Altogether, the combination of the human α-NKG2A with NKG2D-CAR NKAE cells displays high efficacy *in vivo* and could be a novel therapy for RRMM treatment.

5.4. NKG2D-CAR CIML-NKAE cells exhibit a higher efficacy than NKG2D-CAR NKAE cells *in vitro* and *in vivo*

Previous exposures to haptens, virus or even tumor cells have been reported to induce a higher proliferation in NK cells, especially after a second exposure to the stimulus [423, 424]. Interestingly, Fehniger et al. tested the effect of different interleukins (IL-12, IL-15 and IL-18) on NK cell functions [430] and, in 2009, Cooper et al. combined these three molecules and first described the induction of memory-like properties on NK cells through cytokine exposure, the CIML-NK cells [431]. Thus, the discovery of memory properties in NK cells has resulted in a multitude of studies trying to unveil the mechanisms underlying this phenomenon.

Most studies obtained NK cells from PB leukapheresis or buffy coats and cultured them overnight with IL-12, IL-15, and IL-18. Conventional NK cells were maintained with IL-15 only as a control [437, 442], although this population is obsolete, and is no longer use in modern clinical trials. Moreover, CAR transduction was normally performed the day after cytokine exposure [454, 456, 458]. Our study wanted to combine the benefits of generating CAR NKAE cells from a small amount of PB and the co-culture with the feeder cell K562-mb21-41BBL with the induction of memory properties. Moreover, we have compared the CAR CIML population with our best-developed therapy, the CAR NKAE cell, not the conventional IL-15-activated NK cells. Only a recent study has generated CAR CIML-NK cells using a similar strategy. He et al. first purified NK cells and exposed them to IL-12, IL-15, and IL-18 for 16 hours. Then, memory-like NK cells were co-cultured with the feeder cell to expand and activate these NK cells and after 4 days, they were retrovirally transduced with a CD19-CAR [457]. In this thesis, CAR NKAE cells were generated as previously described. First, PBMCs were co-cultured with the feeder cell to increase NK cell number and activation and after NK cell purification, NKAE cells were lentivirally transduced with a NKG2D-CAR. The following day, CAR NKAE cells were exposed to IL-12, IL-15, and IL-18. This way, since memory is induced after CAR NKAE cells are generated, NK cell reprogramming takes place after. However, He et al. interfere CIML reprogramming with feeder cell expansion, which could modify memory-like proper characteristics.

NKG2D-CAR CIML-NKAE or NKAE cells were efficiently generated from HD PB. At day 14, after activation, purification, and transduction, both populations were almost 100% $CD56^+$, most of them $CD56^+CD16^+$, with less than 1% of $CD3^+$ cells (Fig. 41B). Although a lower expression of $CD16^+$ has been reported after IL-12 and IL-18 addition [502], we did not observe significant differences between groups. Moreover, NKG2D-CAR CIML-NKAE cells significantly augmented NKG2A expression compared to day 0, while NKG2C and PD-1 expression remained unchanged (Fig. 41G), suggesting that NKG2A is still a critical checkpoint after memory induction, as Berrien-Elliott et al. also described in conventional CIML-NK cells [445].

NKG2D-CAR transduction, using lentivectors with VSV-G envelope, was efficient and stable after 6 days, as we demonstrated by flow cytometry (around 20% of NKG2D-CAR CIML-NKAE cells were CAR^+) and q-PCR (Fig. 41D). Remarkably, there was a high correlation (R^2=0.93) between the percentage of NKG2D-CAR^+ NK cells and the VCN, indicating that the integration of the CAR construct correlates with its expression on the cell membrane. Besides, we could quantify the number of NKG2D-CAR molecules per cell (around 1,000 molecules) (Fig. 41F). Although there were no significant differences in NK cell transduction between the two populations, a higher tendency was observed in the NKG2D-CAR CIML-NKAE cells. Our results are in line with other studies that used lentivectors and the VSV-G envelope. They detected around 15-20% of CAR^+ NK cells and also suggested a higher transduction efficacy in the CIML population [454, 456]. However, it has been reported that the use of BaEv-lentiviral vectors [458] or RD114 feline envelope-gammaretroviral vectors [457] could achieve a higher percentage of CAR^+ CIML-NK cells, 65% and 70%, respectively. Although transduction efficacy using the VSV-G envelope is lower, our NKG2D-CAR CIML-NKAE cells have demonstrated a relevant anti-MM activity.

NKG2D-CAR CIML-NKAE cells exhibited a significantly higher cytotoxicity against MM cell lines (Fig. 42A) and notably, against primary MM cells (Fig. 47A). This last experiment was performed maintaining TME conditions, where we also demonstrated the superiority of the CIML population. Besides, we detected an increased efficacy against the clonogenic MM cell line L-363 (40% survival at 2:1 T:E ratio) (Fig. 42B), indicating that NKG2D-CAR CIML-NKAE cells are able to efficiently kill clonogenic tumor cells, also described by Leivas et al., using NKG2D-CAR NKAE cells (70% of colony survival at 1:1 ratio) [155]. Moreover, we observed that NKG2D-CAR CIML-NKAE cells

degranulate more (Fig. 42C) and have a higher percentage of IFN-γ$^+$ NK cells compared to the control population (Fig. 43A), NKG2D-CAR NKAE cells, alone or during co-culture with MM cell lines. These results are in line with several studies where CIML-NK cells have demonstrated a higher cytolytic capacity against other hematological malignancies as ALL [437, 447] and AML [437, 442, 445], compared to conventional NK cells. Regarding CAR CIML-NK cells, these cells also displayed a higher cytotoxicity, degranulation and IFN-γ production against B-cell malignancies [457], lymphomas [456] and HNSCC [454], with regard to conventional CAR NK cells. These studies also compared CAR CIML-NK cell efficacy with untransduced CIML-NK cells, as their aim was demonstrating CAR superiority too. In this thesis, since we aimed to improve the functionality of our best effector, the NKG2D-CAR NKAE cells, the differences that we studied are due to the induction of the memory properties, not CAR transduction.

Moreover, we have also studied the release of cytolytic proteins. NKG2D-CAR CIML-NKAE cells secreted more soluble FasL, IFN-γ, granzyme A and perforin compared to control NKG2D-CAR NKAE cells (200, 3,000, 5,000 and 1,200 pg/ml secreted by NKG2D-CAR CIML-NKAE cells against U-266, respectively) (Fig. 43B). Most CIML-NK cells studies measured the percentage of IFN-γ$^+$ cells within NK cells instead of analyzing the levels of cytolytic proteins that they release. However, two publications reported a higher concentration of IFN-γ regarding CIML-NK cells, compared to conventional IL-15-activated NK cells. Zhuang et al. showed a median concentration of 1,000 pg/ml of IFN-γ in supernatants from CIML-NK cells in co-culture with liver cancer cell lines [448]. In line with this, Lusty et al. studied the release of IFN-γ at different time points and interleukin combinations to reprogram NK cells. They detected the maximum IFN-γ concentration 24 hours after interleukins exposure, obtaining similar and the highest levels in IL-12 plus IL-18 condition (around 80,000 pg/ml) and the CIML combination, IL-12, IL-15 and IL-18 (around 60,000 pg/ml). Then, IFN-γ concentration decreased with time (60 pg/ml after 72 hours) [435]. Nevertheless, we found high levels of this cytokine 6 days after memory induction (800 pg/ml without target and up to 5,000 after co-culture with K562-mb21-41BBL). Huber et al. detected a higher percentage of perforin$^+$ NK cells [438], as well as Romee et al, who also described an increased production of granzyme B on CIML-NK cells [442]. These results correlate with our findings regarding perforin, but we did not observe significant differences in granzyme B release. Moreover, NKG2D-CAR CIML-NKAE cells did not release CRS-associated

cytokines as IL-6 and IL-10 (data not shown). Of note, a phase I trial with ML NK cells did not report CRS in AML patients [418].

Not only NKG2D-CAR CIML-NKAE cells displayed a great efficacy against MM cells but also, they did not affect $CD34^+$ cells derived from CB (Fig. 47B) or from MM patients (Fig. 47A). We demonstrated that the CAR CIML population increases its cytotoxic capacity against PC from MM patients without compromising the $CD34^+$ cells present in those samples, suggesting the absence of hematotoxicity of this therapy regarding hematopoietic progenitors. In this sense, no hematological adverse effects were described in the CIML-NK cell NCT02782546 clinical trial, where most patients achieved neutrophil and platelet engraftment within the first month of treatment [417]. In line with this, NCT03068819 study reported hematological grade 3-4 side effects in only 1 out of 9 patients treated [418]. However, Saphiro et al. observed pancytopenia in 4 out of 6 patients with myeloid malignancies, 2 of them had prolonged pancytopenias and $CD34^+$ cells from the same patients were infused, recovering neutrophils within the first 14 days [459]. Point-of-care all these trials infused CIML-NK cells after hematopoietic cell transplant, suggesting the hematological toxicities reported may be a consequence of the allogeneic transplant and not of the CIML therapy.

CIML-NK cells have been also reported to have an increased metabolic activity. Our results showed that NKG2D-CAR CIML-NKAE cells have higher glycolysis compared to NKG2D-CAR NKAE cells, although no differences were observed in OXPHOS analysis (Fig. 44C, D). These results correlate with Terren et al., where CIML-NK cells had a higher ECAR tendency without significant differences in the OCR test [453]. However, other studies suggested that CIML-NK cells not only have a higher glycolytic capacity but also an augmented OXPHOS [451, 452]. Regarding metabolic receptors, Terren et al. reported a higher expression of nutrient transporters such as the glucose transporters GLUT1 and GLUT3, the transferrin receptor CD71 and the amino acid transporter CD98 [453]. Although we corroborated the higher CD71 expression on our NKG2D-CAR CIML-NKAE population, we observed a significantly lower GLUT1 expression, compared to NKG2D-CAR NKAE cells (Fig. 46).

Different results were also obtained compared to other studies regarding diverse surface markers, except from CD25 (Fig. 46). CD25, the γ-chain of the IL-2 receptor, was significantly increased on NKG2D-CAR CIML-NKAE cells as well as in most CIML studies [434, 436, 438, 439, 441, 451, 453, 503], suggesting that the high expression of

the γ-chain IL-2 receptor may be involved in the higher proliferation of CIML-NK cells in response to low doses of IL-2. In addition, our results indicated a lower expression of NCRs, NKp30, NKp44 and NKp46, as well as of the maturation antigen CD57, while a significantly higher expression of CD2 was observed (Fig. 46). However, previously published studies reported other differences in markers expression, in comparison to conventional NK cells. CD69, NKG2A, CD56 [437], Sca-1 [438] and SEMA7A [440] are upregulated in CIML-NK cells, while a decreased expression of CD62L, CD16 [438], CXCR4 [439], TGFβR and KIRs [443] has been reported.

Regarding RNA-seq analysis, we detected 162 DEG between NKG2D-CAR CIML-NKAE and NKAE cells (Fig. 45A), indicating that the induction of memory through the exposure of IL-12, IL-15, and IL-18 is able to modify gene expression program. It is worth noting that the transferrin receptor, CD71, not only was overexpressed on NKG2D-CAR CIML-NKAE in the RNA-seq study, but also we could corroborate it by flow cytometry. Since CD71 is also a target of cMyc, this receptor is involved in NK cell proliferation [504] and could be related to the higher Ki67 expression and the augmented percentage of S-G2-M^+ NK cells we found within the NKG2D-CAR CIML-NKAE population. By the same token, the increased transcription of the CCND2, RANK and MANF genes, mainly related to cell growth [471-473], may be involved in this incremented proliferation. However, some studies have discovered that the expression of RANK on NK cells diminishes their antitumor efficacy when binding to RANKL but, remarkably, the treatment with denosumab, an antibody that targets RANKL, counteract this effect [505, 506]. Therefore, in MM, a concomitant use of denosumab with CAR CIML-NKAE cells not only would decrease osteoclast activity, but also may augment this NK therapy efficacy. Another transcription factor involved in cell growth is CABLES1. Our RNA-seq data indicate a lower transcription of this gene in the NKG2D-CAR CIML-NKAE cells, which decreases CDK2 kinase activity and negatively impact on cell proliferation and/or differentiation, also in line with our Ki67 and cell cycle analysis [474, 507]. Moreover, relevant inhibitory receptors such as TIGIT [303] and KLRG1 were found underexpressed on the memory population, suggesting a lower sensitivity to be inhibited. Since KLRG1 has been also described as a marker of differentiation or senescence [308], our NKG2D-CAR CIML-NKAE cells seem to display a less mature and senescent phenotype. In addition, NKG2D-CAR CIML-NKAE cells have an increased expression of chemokines receptors (CCR4 and CCR7), which

may enhance their ability to respond to chemokines and increase their homing to tumor sites [508, 509]. Of note, NKG2D-CAR CIML-NKAE cells were enriched for pathways involved in migration, regulation of IL-12 production and chemotaxis. Furthermore, a high expression of CCR7 has been also associated with a less mature NK cell subset ($CD56^{bright}CD16^{-}$) [510], matching with the lower KLRG1 transcription. Altogether, these modifications might be also responsible for the higher anti-MM activity of the NKG2D-CAR CIML-NKAE cells. Although this is the first study comparing RNA expression in CAR CIML-NKAE cells and CAR NKAE cells, other groups have also reported differences regarding CIML-NK cell populations versus conventional NK cells. Kerbauy et al. found an enrichment of genes involved in IFN-γ, TNF, IL-2/STAT5 and IL-6/JAK/STAT3 signaling and mTOR signaling [455], while Berrien-Elliott et al. found a higher enrichment in GATA3 target genes [445]. Of note, Becker-Hapak identified an increased induction of the *IFNG* gene [451]. Despite we have not identified this gene overexpressed in our NKG2D-CAR CIML-NKAE cells, their intracellular IFN-γ concentration (Fig. 42C), as well as their IFN-γ release (Fig. 43B), are significantly high compared to NKG2D-CAR NKAE cells.

Furthermore, we have observed 115 CpG sites differentially methylated between NKG2D-CAR CIML-NKAE cells and NKG2D-CAR NKAE cells, related to cytokine signaling, cytoskeletal remodeling and cell-extracellular matrix interactions (Fig. 45B). Most common demethylated gene observed between CIML-NK cells and conventional NK cells is the CNS-1 region of the IFN-γ locus [451]. Differences in RNA-seq and epigenomic studies compared to other published reports in CIML-NK cells may probably lie in the different control populations.

The most relevant induced memory property in CIML-NK cells is persistence *in vivo*. Several studies have reported that CIML-NK cells have a higher proliferation compared to control NK cells [432, 439, 441]. Our results correlate with these published outcomes *in vitro*. NKG2D-CAR CIML-NKAE cells had a higher percentage of $Ki67^{+}$ cells as well as a higher percentage of cells entering mitosis ($S\text{-}G2\text{-}M^{+}$), 6 days after memory reprogramming (Fig. 44A, B). Remarkably, NKG2D-CAR CIML-NKAE cells had a significantly higher percentage of NK cells at day 7 in mice, and CAR expression was superior at day 14 and 29 (Fig. 48C). Thus, *in vivo* results corroborate our *in vitro* results, showing that the exposure of NKG2D-CAR NKAE cells to the interleukins IL-12, IL-15 and IL-18 enhances the percentage of NKG2D-CAR CIML-NKAE cells in mouse PB,

probably due to a higher proliferation *in vivo*. Moreover, other studies have reported the longer persistence or proliferation of CIML-NK cells in mice models, compared to conventional NK cells [434, 436, 437, 441]. Notably, He et al. also demonstrated a higher relative percentage of CAR CIML-NK cells (0.5% of NK cells) in mouse PB, compared to CAR NK cells (nearly 0%) at day 7 [457]. Of note, our NKG2D-CAR CIML-NKAE cells represented a median of 18% at day 7, much superior to what this study obtained. Nevertheless, we have not observed, at any kinetic time point, the presence of NKG2D-CAR CIML-NKAE cells, once NKG2D-CAR NKAE cells cannot be detected. Thus, we cannot assure a higher persistence of the CIML population.

The superior percentage of NKG2D-CAR CIML-NKAE cells at day 7 and 14 may be one of the main responsible for the higher antitumor responses *in vivo*. NKG2D-CAR CIML-NKAE cells rescued 50% of mice from death, using a 1:8 T:E ratio (Fig. 49). Notably, these mice were MRD^- at necropsy after 154 days from U-266 ffLucGFP infusion. This result correlates with another CAR CIML-NK cell publication. He et al. also observed a higher *in vivo* efficacy in the CAR CIML-NK cell group against a lymphoma cell line, compared to conventional CAR NK cells [457]. Other studies support the superior *in vivo* activity of CIML-NK cells compared to conventional NK cells, without CAR [441, 442, 448-451, 511].

CIML-NK cell efficacy could be increased by different strategies [512]. Although our NKG2D-CAR CIML-NKAE cells have demonstrated great anti-MM activity *in vivo*, after enhancing their potential including genetic modifications (CAR transduction) and improving their expansion (co-culture with K562-mb21-41BBL), we tested the effect of inhibiting the NKG2A receptor with a neutralizing α-NKG2A Ab. Berrien-Elliott et al. reported that NKG2A was transcriptionally induced in CIML-NK cells and demonstrated that the KO of the NKG2A-encoding gene *KLRC1* increases their anti-AML responses [445]. Taking into account our results blocking the HLA-E/NKG2A axis in NKG2D- and BCMA-CAR NKAE cells and the high expression of the NKG2A inhibitory receptor on NKG2D-CAR CIML-NKAE cells, we also pretreated these cells with an α-NKG2A Ab. Analysis against three different MM cell lines confirmed the synergistic effect of the induction of the memory phenotype and the blockade of NKG2A eradicating MM cells *in vitro* (Fig. 50). Subsequent *in vivo* studies are ongoing to fully corroborate this enhanced anti-MM efficacy.

This study has certain limitations. Although the blockade of NKG2A on our CAR NKAE populations has exhibited an enhanced efficacy against MM cells, we have not studied the HLA-E peptidome. Depending on the nature or the sequence of the peptide, the stability of HLA-E on the cell membrane and its binding to NKG2A can be modified, modulating NK cell response (eg. Hsp60 or CMV peptides) [513, 514]. Battin et al. recently reported that the blockade of this inhibitory receptor also depends on the peptides presented by HLA-E. In the mentioned study, they demonstrated that monalizumab was more effective when HLA-E loaded HLA-A, HLA-B and HLA-C peptides compared to HLA-G peptides presentation [402]. Further analysis would be needed to specifically confirm the absence of efficacy of BMS-986315 Ab in monotherapy against BMMCs from MM patients cultured in a native context. In line with this, we have studied the *in vivo* activity of NKG2D- and BCMA-CAR NKAE cells in combination with BMS-986315 Ab in NSG mice that constitutively express human IL-15. However, a humanized mouse model engrafting not only primary MM cells, but also a complete immune system from the same patient, to study the efficacy of these combinations in the human context would have reported more accurate results. The difficulty engrafting primary MM cells as well as a complete TME [515] reflect the lack of PDX-His MM mouse models to properly evaluate treatment efficacy and safety. Regarding our *in vivo* studies, we have also found other limitations. The first study was conducted by combining NKG2D- and BCMA-CAR NKAE cells and BMS-986315 Ab, in pretreatment and intraperitoneally infused in NSG-Tg(Hu-IL15) mice bearing RPMI-8226 ffLucGFP MM cells. The lower percentage of CAR NKAE cells in BMS-986315 groups compared to the isotypes suggested a fratricide effect that we did not detect in the subsequent studies, after eliminating the intraperitoneally Ab administration. However, the pretreatment with the human α-NKG2A only blocked NKG2A expression on CAR NKAE cells for 48 hours. In this regard, other strategies to permanently abolish or reduce NKG2A expression on CAR NKAE cells, such as siRNA or PEBL, will be further tested. In our lab, the knock out of the *KLRC1* gene, which encodes NKG2A, is being studied in BCMA-CAR NKAE cells and preliminary results have not reported a fratricide effect after eliminating NKG2A expression *in vitro*. CRISPR-Cas9 technology can completely and permanently eliminate NKG2A expression compared to Ab blockade, but this technique has a higher cost in GMP-setting because nucleofection procedures are needed. Furthermore, the total elimination of this receptor could affect NK cell licensing, suggesting that a partial deletion could have better results [103]. In addition to this, although the objectives of this

thesis are focused on the clinical translation of enhanced CAR NKAE effectors, we have slightly investigated the molecular mechanisms underlying NKG2A signaling after BMS-986315 pretreatment. In this context, the study of the phosphoproteome of other proteins involved in this balance signaling, such as VAV-1, SHP-2 and FYN, or proteins that participate in CAR NKAE cell synapsis, would arise a better knowledge about the effect of NKG2A blockade on CAR NKAE cells.

Regarding NKG2D-CAR CIML-NKAE cells, massive analysis and flow cytometry studies revealed a multitude of DEG, methylations and differentially expressed markers on the cell surface, but unfortunately, we have not identified a set of candidate genes, overlapping between our NKG2D-CAR CIML-NKAE cells and conventional CIML-NK cells compared to NKG2D-CAR NKAE cells or conventional NK cells, respectively. Thus, common candidates associated with universal memory-induced properties, which could be targeted to redirect CAR NK cells towards a memory-like phenotype, remain unveiled.

In continuation with this line of work, the efficacy of NKG2D- or BCMA-CAR NKAE cells as well as NKG2D-CAR CIML-NKAE cells can be improved by redirecting these effector cells to other tumor antigens using BiKEs. As our NKG2D-CAR CIML-NKAE have a high expression of CD16, in contrast to conventional CIML-NK cells, we are currently designing a BiKE molecule that specifically targets CD16 on the CAR NKAE cell and CD44v6 on the MM cell. This strategy would not only enhance tumor cell recognition through CAR binding but also trigger CAR NK cell activity through other endogenous signaling molecules (CD16).

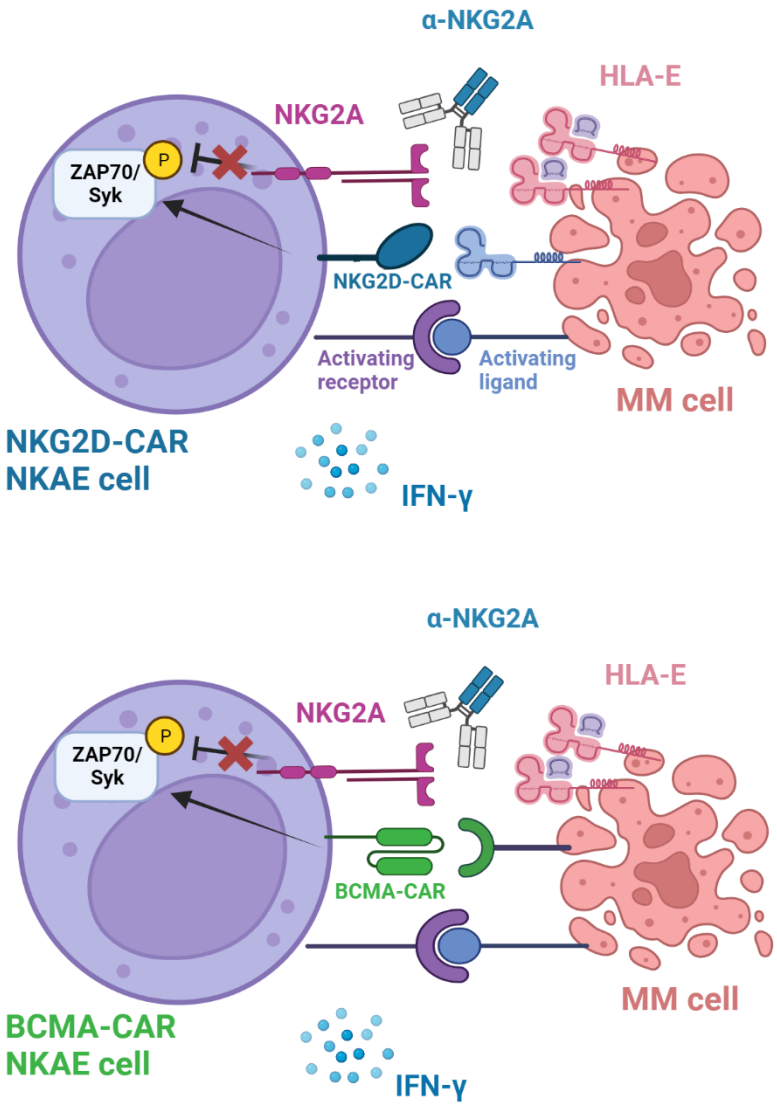

Figure 51. The blockade of NKG2A enhances NKG2D- and BCMA-CAR NKAE cells against MM cells. The use of neutralizing α-NKG2A Abs impairs NKG2A binding to HLA-E in MM cells. CAR signaling, together with native activating receptors, augment NK cell cytotoxicity against tumor cells and IFN-γ production, probably mediated by a higher phosphorylation of intracellular kinases as ZAP70 and Syk. NKG2A: natural killer group 2 member A; HLA: human leukocyte antigen; NKG2D: natural killer group 2 member D; CAR: chimeric antigen receptor; ZAP-70: zeta-chain-associated protein kinase 70; SYK: spleen tyrosine kinase; MM: multiple myeloma; IFN-γ: interferon-γ; BCMA: B-cell maturation antigen. Created with BioRender.com.

In summary, we propose two models to enhance CAR NKAE therapies for the treatment of RRMM. We have studied the antitumoral activity of NKG2A blockade in combination with NKG2D- and BCMA-CAR NKAE cells (Fig. 51). First preclinical data combining the BMS-986315 α-NKG2A Ab and two novel CAR NK cell adoptive therapies, targeting NKG2D-L and BCMA on MM cells demonstrate an enhanced efficacy against MM cells

in vitro and *in vivo*. Furthermore, we have cytokine-induced a memory phenotype in NKG2D-CAR NKAE cells to target, for the first time, MM, demonstrating an improved antitumor ability *in vitro* and *in vivo*. The brief exposure to IL-12, IL-15, and IL-18 is able to reprogram NKG2D-CAR CIML-NKAE cells towards a more proliferative and glycolytic cell through transcriptomic and epigenetic changes (Fig. 52). Thus, the blockade of NKG2A or the induction of memory properties on CAR NKAE cells entail two new strategies to treat not only MM patients, but also other patients with HLA-E^{+} tumors.

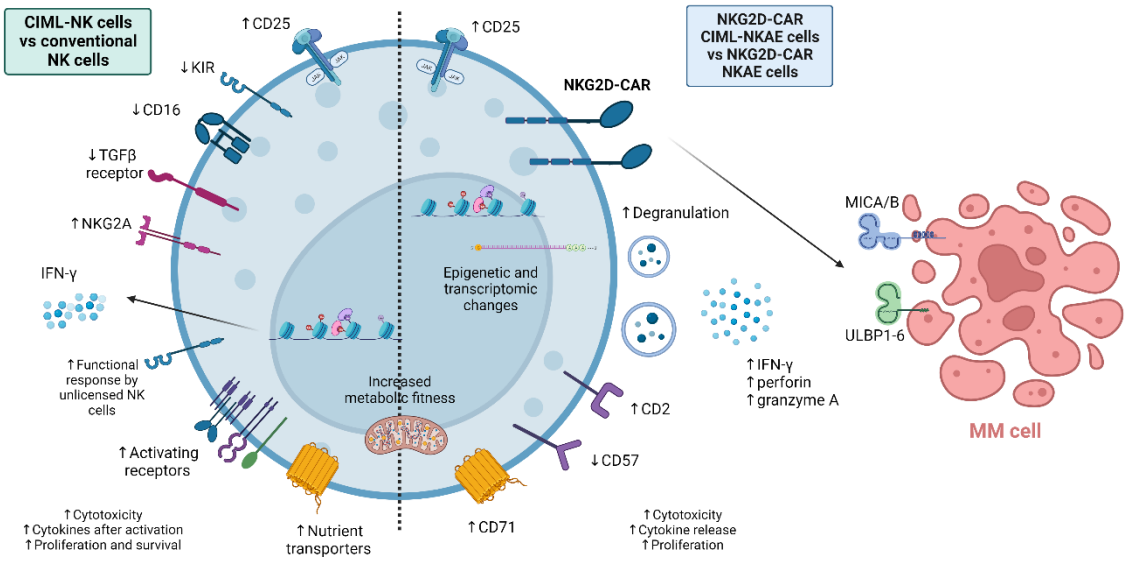

Figure 52. The induction of memory properties improves NKG2D-CAR NKAE cells cytotoxicity against MM cells. The exposure to IL-12, IL-15, and IL-18 is able to induce epigenetic and transcriptomic changes on NKG2D-CAR NKAE cells. The new NKG2D-CAR CIML-NKAE population exerts a higher cytotoxicity against MM cells through an augmented degranulation and IFN-γ, perforin and granzyme A production, as well as a higher proliferation. Furthermore, these enhance cells have a high expression of CD25, CD2 and CD71, together with a superior glycolysis, and reduced CD57. CIML: cytokine-induced memory-like; TGF-β: transforming growth factor-β; NKG2D: natural killer group 2 member D; CAR: chimeric antigen receptor; IFN-γ: interferon-γ; MM: multiple myeloma; MICA/B: major histocompatibility complex class I chain-related protein A/B; ULBP1-6: unique long 16 binding protein 1-6. Created with BioRender.com.

6. CONCLUSIONES

Las principales conclusiones extraídas de este trabajo se enumeran a continuación:

1. La expresión de HLA-E es mayor en las células plasmáticas de pacientes de MM comparada con la de las células plasmáticas de donantes sanos. HLA-E está sobre-expresado en las células plasmáticas patológicas de pacientes de MM con respecto a las células plasmáticas normales y las células $CD34^+$ del mismo paciente, especialmente en progresión.

2. Tanto el IFN-γ como el BTZ modulan la expresión de HLA-E en líneas celulares y células primarias de MM.

3. Aunque las células NK citotóxicas presentes en la médula ósea de pacientes de MM muestran una alta expresión de NKG2A y las células plasmáticas sobre-expresan HLA-E, el tratamiento en monoterapia con dos anticuerpos de bloqueo α-NKG2A (Z199 o BMS-986315) no restaura la capacidad anti-MM de las células NK *in vitro*.

4. La generación de células alogénicas NKG2D- o BCMA-CAR NKAE a partir de sangre periférica de donantes sanos es factible. Las señales que participan en el proceso de expansión y activación de estas células inducen un aumento de la expresión de NKG2A en ambas poblaciones.

5. El pretratamiento de las células NKG2D- o BCMA-CAR NKAE con el anticuerpo de bloqueo α-NKG2A BMS-986315 aumenta la eficacia de las CAR NKAE frente a células de MM *in vitro* e *in vivo*.

6. El aumento de eficacia *in vitro* de las células NKG2D- o BCMA-CAR NKAE en combinación con los anticuerpos de bloqueo de NKG2A se asocia con una mayor función de la célula NK mediada por un incremento de la degranulación y de la secreción de IFN-γ, sin alteraciones importantes en el inmunofenotipo.

7. El tratamiento con células NKG2D- o BCMA-CAR NKAE en combinación con anticuerpos α-NKG2A no produce toxicidad relevante sobre células $CD34^+$ de pacientes de MM ni sobre células maduras de sangre periférica de donantes sanos.

8. Es factible la generación de células NKG2D-CAR CIML-NKAE a partir de volúmenes reducidos de sangre periférica de donantes sanos.

9. La exposición de las células NKG2D-CAR NKAE a las interleuquinas IL-12, IL-15 e IL-18 induce cambios a nivel epigenético, transcriptómico e inmunofenotípico, que solapan parcialmente con los descritos en las células CIML-NK convencionales.

10. Las células NKG2D-CAR CIML-NKAE se caracterizan por un aumento de la degranulación, producción de proteínas citolíticas, metabolismo glucolítico y proliferación *in vitro*, así como una mayor actividad anti-MM *in vitro* e *in vivo*, comparadas con las células NKG2D-CAR NKAE.

11. El aumento de la eficacia anti-MM *in vivo* de las células NKG2D-CAR CIML-NKAE no está relacionado con una mayor persistencia respecto a las células NKG2D-CAR NKAE, si no que se asocia con un aumento en la proporción de las células NKG2D-CAR CIML-NKAE en los ratones.

7. CONCLUSIONS

Main conclusions drawn from this work are listed below:

1. HLA-E expression is higher on PC from MM patients compared to PC from HD. HLA-E is overexpressed on pPC with respect to nPC and $CD34^+$ cells from the same MM patients, especially at progression.

2. Both IFN-γ and BTZ modulate HLA-E expression on cell lines and primary MM cells.

3. Although cytotoxic NK cells from MM patient BM show a high expression of NKG2A and PC overexpress HLA-E, monotherapy treatment with two blocking Abs (Z199 or BMS-986315) does not restore the anti-MM NK cell capacity *in vitro.*

4. Allogeneic NKG2D- or BCMA-CAR NKAE cell generation from HD PB is feasible. The signals that participate in NK cell expansion and activation process induce an increase of NKG2A expression in both populations.

5. NKG2D- or BCMA-CAR NKAE cell pretreatment with BMS-986315 α-NKG2A Ab augments CAR NKAE cell efficacy against MM cells *in vitro* and *in vivo.*

6. The increase of *in vitro* efficacy of NKG2D- or BCMA-CAR NKAE cells in combination with NKG2A blocking Abs is associated with a higher NK function mediated by an augmented degranulation and IFN-γ secretion, without major immunophenotype alterations.

7. NKG2D- or BCMA-CAR NKAE treatment in combination with α-NKG2A Abs do not produce a relevant toxicity against either $CD34^+$ cells from MM patients or mature PB cells from HD.

8. NKG2D-CAR CIML-NKAE cell generation is feasible starting from reduced HD PB volumes.

9. The exposure of NKG2D-CAR NKAE cells to IL-12, IL-15, and IL-18 interleukins induces epigenetic, transcriptomic, and immunophenotypic changes that partially overlaps with the ones described in conventional CIML-NK cells.

10. NKG2D-CAR CIML-NKAE cells are characterized by an increased degranulation, cytolytic protein production, glycolytic metabolism, and proliferation *in vitro*, as well as by an augmented anti-MM activity *in vitro* and *in vivo*, compared to NKG2D-CAR NKAE cells.

11. The increase of the NKG2D-CAR CIML-NKAE cell *in vivo* anti-MM efficacy is not related to a higher persistence with respect to NKG2D-CAR NKAE cells, but it is associated with an augmented NKG2D-CAR CIML-NKAE frequency in mice.

8. ABBREVIATIONS

2-DG: 2-desoxy-D-glucose

21spe-MLL5: splice variant mixed-lineage leukemia-5

4-1BBL: 4-1BB ligand

A

A2AR: adenosine A2a receptor

Ab: antibody

ADAM10/17: a disintegrin and metallopeptidase 10/17

ADC: antibody-drug conjugate

ADCC: antibody-dependent cellular cytotoxicity

ADCP: antibody-dependent cellular phagocytosis

ADO: adenosine

ADP: adenosine diphosphate

AKT: Ak strain transforming

ALL: acute lymphocytic leukemia

AML: acute myeloid leukemia

ANLL: acute nonlymphocytic leukemia

ANOVA: analysis of variance

APC: allophycocyanin

APC/Cy7: allophycocyanin-cyanine7

APRIL: a proliferation-inducing ligand

APVAL: adjusted p-value

ARM: antibody recruiting molecule

ASCT: autologous stem cell transplant

ASCT-1/2: alanine/serine/cysteine transporter 1/2

ATP: adenosine triphosphate

B

B2-m: β-2 microglobulin

B7-H6: B7 homolog 6

BaEv: Baboon envelope

BAFF: B-cell activating factor

BAG6: B-cell lymphoma 2 associated athanogene 6

BCL-2: B-cell lymphoma 2

BCMA: B-cell maturation antigen

BCR: B-cell receptor

BFU-E: burst forming unit erythroid

BiAbs: bispecific antibodies

BiKE: bispecific killer cell engager

BIRC2/3: baculoviral IAP repeat containing 2/3

BiTE: bispecific T-cell engager

BLI: bioluminescent imaging

BM: bone marrow

BMMCs: bone marrow mononuclear cells

BMS: Bristol Myers Squibb

BMSCs: bone marrow mesenchymal stromal cells

BPDCN: blastic plasmacytoid dendritic cell neoplasm

BRCA2: breast cancer gene 2

Bregs: regulatory B cells

BSA: bovine serum albumin

BTZ: bortezomib

C

CABLES1: cyclin-dependent kinase-5 and Abelson murine leukemia 1 enzyme substrate 1

Calcein-AM: calcein-acetoxymethylester

CAR: chimeric antigen receptor

Cas9: clustered regularly interspaced short palindromic repeats associated protein 9

CB: cord blood

CB-NK: cord blood natural killer cells

CCL: CC chemokine ligand

CCR: CC chemokine receptor

CCND2: cyclin D2

CD44v6: CD44 variant domain 6

CDC: complement-dependent cytotoxicity

CDKN1B: cyclin dependent kinase inhibitor 1B

CDKN2C: cyclin-dependent kinase 4 inhibitor C

CFU-GM: colony-forming unit granulocyte-macrophage

Cilta-cel: ciltacabtagene autoleucel

CIML: cytokine-induced memory-like

CLEC2D: C-type lectin domain family 2 member D

CLL: chronic lymphocytic leukemia

CMV: cytomegalovirus

CR: complete response

CRAB: hypercalcemia, renal failure, anemia and bone lesions

CRISPR: clustered regularly interspaced short palindromic repeats

CRS: cytokine release syndrome

CRTAM: MHC class I–restricted T cell–associated molecule

CT: computed tomography

CTLA-4: cytotoxic T-lymphocyte antigen 4

CXCL: CXC chemokine ligand

CXCR: CXC chemokine receptor

CyTOF: cytometry by time of flight

D

DAP10/12: DNAX-activating protein 10/12

DAPI: 4',6-diamidino-2-phenylindole

DC: dendritic cell

DEG: differentially expressed genes

DLBCL: diffuse large B cell lymphoma

DKK1: Dickkopf 1

DMSO: dimethyl sulfoxide

DNA: deoxyribonucleic acid

DNAM-1: DNAX accessory molecule-1

E

EBV: Epstein-Barr virus

ECAR: extracellular acidification rate

ECL: enhanced chemiluminescence

EDTA: ethylenediaminetetraacetic acid

EMA: European Medicines Agency

EPO: erythropoietin

ER: endoplasmic reticulum

ERK: extracellular signal-regulated kinase

F

FAM46C: family with sequence similarity 46 member C

FasL: Fas ligand

FBS: fetal bovine serum

FCCP: fluoro-carbonyl cyanide phenylhydrazone

FcεRIγ: γ-chain high-affinity IgE receptor

FcRγ: Fc receptor γ-chain

FcRH5: Fc receptor-homolog 5

FDA: Food and Drug Administration

FGFBP2: fibroblast growth factor binding protein 2

FGFR3: fibroblast growth factor receptor 3

FISH: fluorescence in situ hybridization

FITC: fluorescein isothiocyanate

FLC: free light chain

FMO: fluorescence minus one

FSC: forward side channel

G

GFP: green fluorescent protein

GFR: glomerular filtration rate

GLUT1/3: glucose transporter 1/3

GM-CSF: granulocyte macrophage colony-stimulating factor

GO BP: gene ontology biological processes

GPRC5D: G protein-coupled receptor class C group 5 member D

Grb2: growth factor receptor-bound protein 2

GvHD: graft versus host disease

H

h-MM: hyperdiploid multiple myeloma

H12O: *Hospital 12 de Octubre*

HAMA: human anti-mouse antibody

HCV: hepatitis C virus

HD: healthy donor

HDAC: histone deacetylase

HER2: human epidermal growth factor receptor 2

hESC: human embryonic stem cells

HLA: human leukocyte antigen

HNSCC: head and neck squamous cell carcinoma

HR: hazard ratio

HSPCs: hematopoietic stem/progenitor cells

HRP: horseradish peroxidase

I

i.p: intraperitoneal

i.v: intravenous

ICANS: immune effector cell-associated neurotoxicity syndrome

ICI: immune checkpoint inhibitors

ICOS: inducible costimulatory

Ide-cel: idecabtagene vicleucel

IDH3A: isocitrate dehydrogenase subunit alpha

IDO: indoleamine-pyrrole 2,3-dioxygenase

IFN-γ: interferon-γ

Ig: immunoglobulin

IgH: immunoglobulin heavy chain

IgL: immunoglobulin light chain

IKZF1/3: Ikaros family zinc finger 1/3

IL: interleukin

IMDM: Iscove´s Modified Dulbecco´s Medium

IMiD: immunomodulatory agents

iPSCs: induced pluripotent stem cells

IRAK3: interleukin 1 receptor associated kinase 3

IRS2: insulin receptor substrate 2

ISS: international staging system

ITAM: immunoreceptor tyrosine-based activation motif

ITIM: immunoreceptor tyrosine-based inhibitory motif

ITT: Ig tyrosine tail

J

JAK/STAT: Janus kinase/signal transducers and activators of transcription

K

KI: knock in

KIR: killer-cell immunoglobulin-like receptors

KLRC1: killer cell lectin-like receptor C1

KLRG1: killer cell lectin-like receptor G1

KO: knock out

L

LAG3: lymphocyte activation gene 3

LCK: lymphocyte-specific protein tyrosine kinase

LDH: lactate dehydrogenase

LDL-R: low density lipoprotein receptor

M

mAb: monoclonal antibody

MAC: membrane attack complex

MANF3: mesencephalic astrocyte-derived neurotrophic factor 3

MAPK: mitogen-activated protein kinase

MCP-1: monocyte chemoattractant protein-1

MDS: myelodysplastic syndrome

MDSCs: myeloid-derived suppressor cells

MFI: median fluorescence intensity

MGUS: monoclonal gammopathy of undetermined significance

MHC: major histocompatibility complex

MICA/B: major histocompatibility complex class I chain-related protein A/B

MIL: marrow-infiltrating lymphocyte

MIP-1α: macrophage inflammatory protein-1α

MM: multiple myeloma

MMP: matrix metalloproteinase

MOI: multiplicity of infection

MR: minimal response

MRD: minimal residual disease

MRI: magnetic resonance imaging

mRNA: messenger RNA

MUC1: mucin 1

N

NAADP: nicotinic acid adenine dinucleotide phosphate

NAD: nicotinamide adenine dinucleotide

NADP: nicotinamide adenine dinucleotide phosphate

NCR: natural cytotoxicity receptors

NCT: national clinical trial

NDMM: newly diagnosed multiple myeloma

NF-κB: nuclear factor κ B

nh-MM: non-hyperdiploid multiple myeloma

NHL: non-Hodgkin lymphoma

NK: natural killer

NKG2A/B/C/D/E: natural killer group 2 member A/B/C/D/E

NKG2D-L: natural killer group 2 member D ligands

nPC: normal plasma cell

NPM1: nucleophosmin 1

NRROS: negative regulator of reactive oxygen species

NSCLC: non-small cell lung cancer

O

OCR: oxygen consumption rate

OPG: osteoprotegerin

ORR: overall response rate

OS: overall survival

OXPHOS: oxidative phosphorylation

P

P/S: penicillin streptomycin

PB: peripheral blood

PBMCs: peripheral blood mononuclear cells

PBS: phosphate-buffered saline

PC: plasma cell

PCNA: proliferating cell nuclear antigen

PD-1: programmed cell death 1

PD-L1/2: programmed cell death ligand 1/2

PDAC: pancreatic ductal adenocarcinoma

PE: phycoerythrin

PE/Cy7: phycoerythrin-cyanine7

PEBL: protein expression blocker

PerCP/Cy5.5: peridinin chlorophyll protein-Cyanine5.5

PET-CT: positron emission tomography and computed tomography

PFS: progression-free survival

PGE2: prostaglandin E2

PI: proteosome inhibitor

PI3K: phosphoinositide 3-kinase

pPC: pathologic plasma cell

PR: partial response

PVR: poliovirus receptor

PYHIN1: pyrin and hematopoietic expression, interferon-inducible nature, and nuclear localization domain family member 1

Q

q-PCR: quantitative polymerase chain reaction

R

R-ISS: revised international staging system

RANK: receptor activator for nuclear factor κ B

RANKL: receptor activator for nuclear factor κ B ligand

RAS: rat sarcoma

RB1: retinoblastoma protein

RHAMM: receptor for hyaluronan-mediated motility

RNA: ribonucleic acid

RPMI: Roswell Park Memorial Institute

RRMM: relapsed/refractory multiple myeloma

RT: room temperature

S

SEM: standard error of the mean

SCF: stem cell factor

scFv: single-chain variable fragment

SCLC: small-cell lung cancer

SDS-PAGE: sodium dodecyl sulfate polyacrylamide gel electrophoresis

SEMA: semaphoring

SHP-1: Src homology region 2 domain-containing phosphatase-1

SIRPα: signal regulatory protein α

SLAMF7: signaling lymphocyte activation molecule family member 7

SMM: smoldering multiple myeloma

SNAP: self-labeling protein tag

SSC: side scatter channel

STAT1/3: signal transducer and activator of transcription 1/3

SYK: spleen tyrosine kinase

SYNE1: synaptic nuclear envelope protein 1

synNotch: synthetic Notch

T

T:E: target: effector

TACI: transmembrane activator and calcium modulator and cyclophilin ligand interactor

TBS: tris-buffered saline

TBS-T: tris-buffered saline with 0.1% Tween 20

TCF7: transcription factor 7

TCR: T cell receptor

TGF-β: transforming growth factor-β

TGFBRII: transforming growth factor-β receptor 2

TFRC: transferrin receptor

TIGIT: T cell immunoreceptor with Ig and ITIM domains

TIM-3: T cell immunoglobulin domain and mucin domain-3

TIML-NK: tumor-induced memory-like NK cell

TLR1: toll-like receptor 1

TME: tumor microenvironment

TNF-α: tumor necrosis factor α

TNFR11A: tumor necrosis factor receptor superfamily member 11a

TP53: tumor protein p53

TRAIL: tumor necrosis factor related apoptosis-inducing ligand

TRAIL-R: tumor necrosis factor related apoptosis-inducing ligand receptor

Tregs: regulatory T cells

U

ULBP: unique long 16 binding protein

V

VCAM-1: vascular cell adhesion protein 1

VCN: vector copy number

VEGF: vascular endothelial growth factor

VGPR: very good partial response

VRd: Bortezomib, lenalidomide, and dexamethasone

VSV-G: vesicular stomatitis virus G

W

WB: western blot

WHSC1: Wolf-Hirschhorn syndrome candidate 1

WNT: wingless-related integration site

WWOX: WW domain containing oxidoreductase

X

XCL: chemokine (C motif) ligand

XPO1: exportin 1

Z

ZAP-70: zeta-chain-associated protein kinase 70

9. BIBLIOGRAPHY

1. Rajkumar, S.V., *Multiple myeloma: 2022 update on diagnosis, risk stratification, and management.* Am J Hematol, 2022. **97**(8): p. 1086-1107.
2. Kyle, R.A., *Multiple myeloma: an odyssey of discovery.* Br J Haematol, 2000. **111**(4): p. 1035-44.
3. Kyle, R.A., et al., *Clinical course of light-chain smouldering multiple myeloma (idiopathic Bence Jones proteinuria): a retrospective cohort study.* Lancet Haematol, 2014. **1**(1): p. e28-e36.
4. Fernandez de Larrea, C., et al., *Primary plasma cell leukemia: consensus definition by the International Myeloma Working Group according to peripheral blood plasma cell percentage.* Blood Cancer J, 2021. **11**(12): p. 192.
5. Kumar, S.K., et al., *Multiple myeloma.* Nat Rev Dis Primers, 2017. **3**: p. 17046.
6. Siegel, R.L., et al., *Cancer statistics, 2023.* CA Cancer J Clin, 2023. **73**(1): p. 17-48.
7. (ACS), A.C.S. *Cancer Stat Facts: Myeloma*. 2023; Available from: https://seer.cancer.gov/statfacts/html/mulmy.html.
8. (AECC), A.E.C.e.C. *Mieloma Múltiple*. 2021; Available from: https://www.contraelcancer.es/es/todo-sobre-cancer/tipos-cancer/mieloma-multiple/epidemiolog%C3%ADa#:~:text=De%20acuerdo%20con%20los%20datos,1.354%20casos%20nuevos%20respectivamente%20en.
9. Kyle, R.A. and S.V. Rajkumar, *Multiple myeloma.* Blood, 2008. **111**(6): p. 2962-72.
10. Landgren, O., et al., *Risk of monoclonal gammopathy of undetermined significance (MGUS) and subsequent multiple myeloma among African American and white veterans in the United States.* Blood, 2006. **107**(3): p. 904-6.
11. Korde, N., S.Y. Kristinsson, and O. Landgren, *Monoclonal gammopathy of undetermined significance (MGUS) and smoldering multiple myeloma (SMM): novel biological insights and development of early treatment strategies.* Blood, 2011. **117**(21): p. 5573-81.
12. Boffetta, P., et al., *Exposure to ultraviolet radiation and risk of malignant lymphoma and multiple myeloma--a multicentre European case-control study.* Int J Epidemiol, 2008. **37**(5): p. 1080-94.
13. Friedman, G.D., *Multiple myeloma: relation to propoxyphene and other drugs, radiation and occupation.* Int J Epidemiol, 1986. **15**(3): p. 424-6.
14. Ichimaru, M., et al., *Multiple myeloma among atomic bomb survivors in Hiroshima and Nagasaki, 1950-76: relationship to radiation dose absorbed by marrow.* J Natl Cancer Inst, 1982. **69**(2): p. 323-8.
15. Landgren, O., et al., *Pesticide exposure and risk of monoclonal gammopathy of undetermined significance in the Agricultural Health Study.* Blood, 2009. **113**(25): p. 6386-91.
16. Khuder, S.A. and A.B. Mutgi, *Meta-analyses of multiple myeloma and farming.* Am J Ind Med, 1997. **32**(5): p. 510-6.
17. Altekruse, S.F., S.J. Henley, and M.J. Thun, *Deaths from hematopoietic and other cancers in relation to permanent hair dye use in a large prospective study (United States).* Cancer Causes Control, 1999. **10**(6): p. 617-25.
18. Preston, D.L., et al., *Cancer incidence in atomic bomb survivors. Part III. Leukemia, lymphoma and multiple myeloma, 1950-1987.* Radiat Res, 1994. **137**(2 Suppl): p. S68-97.
19. Marques-Mourlet, C., et al., *Obesity and myeloma: Clinical and mechanistic contributions to disease progression.* Front Endocrinol (Lausanne), 2023. **14**: p. 1118691.
20. Rodriguez-Garcia, A., et al., *Efficacy of Antiviral Treatment in Hepatitis C Virus (HCV)-Driven Monoclonal Gammopathies Including Myeloma.* Front Immunol, 2021. **12**: p. 797209.
21. Nair, S., et al., *Antigen-mediated regulation in monoclonal gammopathies and myeloma.* JCI Insight, 2018. **3**(8).

22. Nair, S., et al., *Clonal Immunoglobulin against Lysolipids in the Origin of Myeloma.* N Engl J Med, 2016. **374**(6): p. 555-61.
23. Maldonado, J.E. and R.A. Kyle, *Familial myeloma. Report of eight families and a study of serum proteins in their relatives.* Am J Med, 1974. **57**(6): p. 875-84.
24. Altieri, A., et al., *Familial risks and temporal incidence trends of multiple myeloma.* Eur J Cancer, 2006. **42**(11): p. 1661-70.
25. Vachon, C.M., et al., *Increased risk of monoclonal gammopathy in first-degree relatives of patients with multiple myeloma or monoclonal gammopathy of undetermined significance.* Blood, 2009. **114**(4): p. 785-90.
26. Morgan, G.J., B.A. Walker, and F.E. Davies, *The genetic architecture of multiple myeloma.* Nat Rev Cancer, 2012. **12**(5): p. 335-48.
27. Pinto, V., et al., *Multiple Myeloma: Available Therapies and Causes of Drug Resistance.* Cancers (Basel), 2020. **12**(2).
28. Amodio, N., et al., *Epigenetic modifications in multiple myeloma: recent advances on the role of DNA and histone methylation.* Expert Opin Ther Targets, 2017. **21**(1): p. 91-101.
29. Hideshima, T., et al., *Understanding multiple myeloma pathogenesis in the bone marrow to identify new therapeutic targets.* Nat Rev Cancer, 2007. **7**(8): p. 585-98.
30. Barwick, B.G., et al., *Cell of Origin and Genetic Alterations in the Pathogenesis of Multiple Myeloma.* Front Immunol, 2019. **10**: p. 1121.
31. Papadhimitriou, S.I., et al., *The Cytogenetic Profile of Primary and Secondary Plasma Cell Leukemia: Etiopathogenetic Perspectives, Prognostic Impact and Clinical Relevance to Newly Diagnosed Multiple Myeloma with Differential Circulating Clonal Plasma Cells.* Biomedicines, 2022. **10**(2).
32. Dimopoulos, K., P. Gimsing, and K. Gronbaek, *The role of epigenetics in the biology of multiple myeloma.* Blood Cancer J, 2014. **4**(5): p. e207.
33. Garcia-Ortiz, A., et al., *The Role of Tumor Microenvironment in Multiple Myeloma Development and Progression.* Cancers (Basel), 2021. **13**(2).
34. Manier, S., et al., *Bone marrow microenvironment in multiple myeloma progression.* J Biomed Biotechnol, 2012. **2012**: p. 157496.
35. Palumbo, A. and K. Anderson, *Multiple myeloma.* N Engl J Med, 2011. **364**(11): p. 1046-60.
36. Maiso, P., et al., *Bone Marrow Mesenchymal Stromal Cells in Multiple Myeloma: Their Role as Active Contributors to Myeloma Progression.* Cancers (Basel), 2021. **13**(11).
37. Oyajobi, B.O., *Multiple myeloma/hypercalcemia.* Arthritis Res Ther, 2007. **9 Suppl 1**(Suppl 1): p. S4.
38. Chatziravdeli, V., et al., *A systematic review and meta-analysis of interventional studies of bisphosphonates and denosumab in multiple myeloma and future perspectives.* J Musculoskelet Neuronal Interact, 2022. **22**(4): p. 596-621.
39. Borrello, I., *Can we change the disease biology of multiple myeloma?* Leuk Res, 2012. **36 Suppl 1**(0 1): p. S3-12.
40. Panaroni, C., A.J. Yee, and N.S. Raje, *Myeloma and Bone Disease.* Curr Osteoporos Rep, 2017. **15**(5): p. 483-498.
41. Dimopoulos, M.A., et al., *Pathogenesis and treatment of renal failure in multiple myeloma.* Leukemia, 2008. **22**(8): p. 1485-93.
42. Garcia-Sanz, R., M.V. Mateos, and J.F. San Miguel, *[Multiple myeloma].* Med Clin (Barc), 2007. **129**(3): p. 104-15.
43. Cowan, A.J., et al., *Diagnosis and Management of Multiple Myeloma: A Review.* JAMA, 2022. **327**(5): p. 464-477.
44. Liu, L., et al., *Multiple myeloma hinders erythropoiesis and causes anaemia owing to high levels of CCL3 in the bone marrow microenvironment.* Sci Rep, 2020. **10**(1): p. 20508.

45. Ludwig, H., G. Pohl, and A. Osterborg, *Anemia in multiple myeloma.* Clin Adv Hematol Oncol, 2004. **2**(4): p. 233-41.
46. Sorrig, R., et al., *Immunoparesis in newly diagnosed Multiple Myeloma patients: Effects on overall survival and progression free survival in the Danish population.* PLoS One, 2017. **12**(12): p. e0188988.
47. Nucci, M. and E. Anaissie, *Infections in patients with multiple myeloma in the era of high-dose therapy and novel agents.* Clin Infect Dis, 2009. **49**(8): p. 1211-25.
48. Schutt, P., et al., *Immune parameters in multiple myeloma patients: influence of treatment and correlation with opportunistic infections.* Leuk Lymphoma, 2006. **47**(8): p. 1570-82.
49. Rajkumar, S.V., et al., *International Myeloma Working Group updated criteria for the diagnosis of multiple myeloma.* Lancet Oncol, 2014. **15**(12): p. e538-48.
50. Rajkumar, S.V. and S. Kumar, *Multiple Myeloma: Diagnosis and Treatment.* Mayo Clin Proc, 2016. **91**(1): p. 101-19.
51. Hillengass, J., et al., *International myeloma working group consensus recommendations on imaging in monoclonal plasma cell disorders.* Lancet Oncol, 2019. **20**(6): p. e302-e312.
52. Johnsen, H.E., et al., *Multiparametric flow cytometry profiling of neoplastic plasma cells in multiple myeloma.* Cytometry B Clin Cytom, 2010. **78**(5): p. 338-47.
53. Radzevicius, M., et al., *Multiple Myeloma Immunophenotype Related to Chromosomal Abnormalities Used in Risk Assessment.* Diagnostics (Basel), 2022. **12**(9).
54. Bataille, R., et al., *CD117 (c-kit) is aberrantly expressed in a subset of MGUS and multiple myeloma with unexpectedly good prognosis.* Leuk Res, 2008. **32**(3): p. 379-82.
55. Paiva, B., et al., *Clinical significance of CD81 expression by clonal plasma cells in high-risk smoldering and symptomatic multiple myeloma patients.* Leukemia, 2012. **26**(8): p. 1862-9.
56. Palumbo, A., et al., *Revised International Staging System for Multiple Myeloma: A Report From International Myeloma Working Group.* J Clin Oncol, 2015. **33**(26): p. 2863-9.
57. D'Agostino, M., et al., *Second Revision of the International Staging System (R2-ISS) for Overall Survival in Multiple Myeloma: A European Myeloma Network (EMN) Report Within the HARMONY Project.* J Clin Oncol, 2022. **40**(29): p. 3406-3418.
58. Tan, J.L.C., et al., *The second revision of the International Staging System (R2-ISS) stratifies progression-free and overall survival in multiple myeloma: Real world data results in an Australian and New Zealand Population.* Br J Haematol, 2023. **200**(2): p. e17-e21.
59. Blade, J., et al., *Treatment of alkylating resistant multiple myeloma with vincristine, BCNU, doxorubicin and prednisone (VBAP).* Eur J Cancer Clin Oncol, 1986. **22**(10): p. 1193-7.
60. Durie, B.G.M., et al., *Bortezomib with lenalidomide and dexamethasone versus lenalidomide and dexamethasone alone in patients with newly diagnosed myeloma without intent for immediate autologous stem-cell transplant (SWOG S0777): a randomised, open-label, phase 3 trial.* Lancet, 2017. **389**(10068): p. 519-527.
61. Aguilar Franco, C., et al., *Hematoguía Mieloma*. 2023.
62. Moreau, P., et al., *Maintenance with daratumumab or observation following treatment with bortezomib, thalidomide, and dexamethasone with or without daratumumab and autologous stem-cell transplant in patients with newly diagnosed multiple myeloma (CASSIOPEIA): an open-label, randomised, phase 3 trial.* Lancet Oncol, 2021. **22**(10): p. 1378-1390.
63. Mateos, M.V., et al., *Daratumumab Plus Bortezomib, Melphalan, and Prednisone Versus Bortezomib, Melphalan, and Prednisone in Transplant-Ineligible Newly Diagnosed*

Multiple Myeloma: Frailty Subgroup Analysis of ALCYONE. Clin Lymphoma Myeloma Leuk, 2021. **21**(11): p. 785-798.
64. Parrondo, R.D., et al., *Autologous Stem-Cell Transplantation for Multiple Myeloma in the Era of Novel Therapies.* JCO Oncol Pract, 2020. **16**(2): p. 56-66.
65. Michel Attal, V.L.-C., Cyrille Hulin, Thierry Facon, Denis Caillot, Martine Escoffre, Bertrand Arnulf, Margaret MACRO, Karim Belhadj, Laurent Garderet, Murielle Roussel, Claire Mathiot, Herve Avet-Loiseau, Nikhil C. Munshi, Paul G. Richardson, Kenneth C. Anderson, jean Luc Harousseau, Philippe Moreau, *Autologous Transplantation for Multiple Myeloma in the Era of New Drugs: A Phase III Study of the Intergroupe Francophone Du Myelome (IFM/DFCI 2009 Trial).* ASH, 2015.
66. Ntanasis-Stathopoulos, I., et al., *Multiple myeloma: Role of autologous transplantation.* Cancer Treat Rev, 2020. **82**: p. 101929.
67. Bazarbachi, A.H., et al., *Induction therapy prior to autologous stem cell transplantation (ASCT) in newly diagnosed multiple myeloma: an update.* Blood Cancer J, 2022. **12**(3): p. 47.
68. More, S., et al., *Autologous Stem Cell Transplantation in Multiple Myeloma: Where Are We and Where Do We Want to Go?* Cells, 2022. **11**(4).
69. Gagelmann, N., et al., *Tandem Autologous Stem Cell Transplantation Improves Outcomes in Newly Diagnosed Multiple Myeloma with Extramedullary Disease and High-Risk Cytogenetics: A Study from the Chronic Malignancies Working Party of the European Society for Blood and Marrow Transplantation.* Biol Blood Marrow Transplant, 2019. **25**(11): p. 2134-2142.
70. Minnie, S.A. and G.R. Hill, *Autologous Stem Cell Transplantation for Myeloma: Cytoreduction or an Immunotherapy?* Front Immunol, 2021. **12**: p. 651288.
71. Orrantia, A., et al., *NK Cell Reconstitution After Autologous Hematopoietic Stem Cell Transplantation: Association Between NK Cell Maturation Stage and Outcome in Multiple Myeloma.* Front Immunol, 2021. **12**: p. 748207.
72. Ito, T., et al., *Identification of a primary target of thalidomide teratogenicity.* Science, 2010. **327**(5971): p. 1345-50.
73. Quach, H., et al., *Mechanism of action of immunomodulatory drugs (IMiDS) in multiple myeloma.* Leukemia, 2010. **24**(1): p. 22-32.
74. Heim, C. and M.D. Hartmann, *High-resolution structures of the bound effectors avadomide (CC-122) and iberdomide (CC-220) highlight advantages and limitations of the MsCI4 soaking system.* Acta Crystallogr D Struct Biol, 2022. **78**(Pt 3): p. 290-298.
75. Fionda, C., et al., *The IMiDs targets IKZF-1/3 and IRF4 as novel negative regulators of NK cell-activating ligands expression in multiple myeloma.* Oncotarget, 2015. **6**(27): p. 23609-30.
76. Richardson, P.G., et al., *Mezigdomide plus Dexamethasone in Relapsed and Refractory Multiple Myeloma.* N Engl J Med, 2023.
77. Kotla, V., et al., *Mechanism of action of lenalidomide in hematological malignancies.* J Hematol Oncol, 2009. **2**: p. 36.
78. Jungkunz-Stier, I., et al., *Modulation of natural killer cell effector functions through lenalidomide/dasatinib and their combined effects against multiple myeloma cells.* Leuk Lymphoma, 2014. **55**(1): p. 168-76.
79. Lagrue, K., et al., *Lenalidomide augments actin remodeling and lowers NK-cell activation thresholds.* Blood, 2015. **126**(1): p. 50-60.
80. Davies, F.E., et al., *Thalidomide and immunomodulatory derivatives augment natural killer cell cytotoxicity in multiple myeloma.* Blood, 2001. **98**(1): p. 210-6.
81. Corral, L.G., et al., *Differential cytokine modulation and T cell activation by two distinct classes of thalidomide analogues that are potent inhibitors of TNF-alpha.* J Immunol, 1999. **163**(1): p. 380-6.

82. Delforge, M. and H. Ludwig, *How I manage the toxicities of myeloma drugs.* Blood, 2017. **129**(17): p. 2359-2367.
83. Manasanch, E.E. and R.Z. Orlowski, *Proteasome inhibitors in cancer therapy.* Nat Rev Clin Oncol, 2017. **14**(7): p. 417-433.
84. Besse, A., et al., *Proteasome Inhibition in Multiple Myeloma: Head-to-Head Comparison of Currently Available Proteasome Inhibitors.* Cell Chem Biol, 2019. **26**(3): p. 340-351 e3.
85. Carlsten, M., et al., *Bortezomib sensitizes multiple myeloma to NK cells via ER-stress-induced suppression of HLA-E and upregulation of DR5.* Oncoimmunology, 2019. **8**(2): p. e1534664.
86. Nencioni, A., et al., *Proteasome inhibitors: antitumor effects and beyond.* Leukemia, 2007. **21**(1): p. 30-6.
87. Mattingly, L.H., R.A. Gault, and W.J. Murphy, *Use of systemic proteasome inhibition as an immune-modulating agent in disease.* Endocr Metab Immune Disord Drug Targets, 2007. **7**(1): p. 29-34.
88. Wieten, L., et al., *Clinical and immunological significance of HLA-E in stem cell transplantation and cancer.* Tissue Antigens, 2014. **84**(6): p. 523-35.
89. Shi, J., et al., *Bortezomib down-regulates the cell-surface expression of HLA class I and enhances natural killer cell-mediated lysis of myeloma.* Blood, 2008. **111**(3): p. 1309-17.
90. Niu, C., et al., *Low-dose bortezomib increases the expression of NKG2D and DNAM-1 ligands and enhances induced NK and gammadelta T cell-mediated lysis in multiple myeloma.* Oncotarget, 2017. **8**(4): p. 5954-5964.
91. Hallett, W.H., et al., *Sensitization of tumor cells to NK cell-mediated killing by proteasome inhibition.* J Immunol, 2008. **180**(1): p. 163-70.
92. Zheng, Y., et al., *Cardiovascular Toxicity of Proteasome Inhibitors in Multiple Myeloma Therapy.* Curr Probl Cardiol, 2023. **48**(3): p. 101536.
93. Poczta, A., A. Rogalska, and A. Marczak, *Treatment of Multiple Myeloma and the Role of Melphalan in the Era of Modern Therapies-Current Research and Clinical Approaches.* J Clin Med, 2021. **10**(9).
94. Samur, M.K., et al., *High-dose melphalan treatment significantly increases mutational burden at relapse in multiple myeloma.* Blood, 2023. **141**(14): p. 1724-1736.
95. Palumbo, A., et al., *Daratumumab, Bortezomib, and Dexamethasone for Multiple Myeloma.* N Engl J Med, 2016. **375**(8): p. 754-66.
96. Dimopoulos, M.A., et al., *Daratumumab plus lenalidomide and dexamethasone versus lenalidomide and dexamethasone in relapsed or refractory multiple myeloma: updated analysis of POLLUX.* Haematologica, 2018. **103**(12): p. 2088-2096.
97. Rajkumar, S.V., et al., *Consensus recommendations for the uniform reporting of clinical trials: report of the International Myeloma Workshop Consensus Panel 1.* Blood, 2011. **117**(18): p. 4691-5.
98. Gandhi, U.H., et al., *Outcomes of patients with multiple myeloma refractory to CD38-targeted monoclonal antibody therapy.* Leukemia, 2019. **33**(9): p. 2266-2275.
99. Podar, K., et al., *Selinexor for the treatment of multiple myeloma.* Expert Opin Pharmacother, 2020. **21**(4): p. 399-408.
100. Moreau, P., et al., *Treatment of relapsed and refractory multiple myeloma: recommendations from the International Myeloma Working Group.* Lancet Oncol, 2021. **22**(3): p. e105-e118.
101. Fisher, J.G., et al., *Selinexor Enhances NK Cell Activation Against Malignant B Cells via Downregulation of HLA-E.* Front Oncol, 2021. **11**: p. 785635.
102. Hu, F., et al., *Drug resistance biomarker ABCC4 of selinexor and immune feature in multiple myeloma.* Int Immunopharmacol, 2022. **108**: p. 108722.

103. Fisher, J.G., et al., *Disruption of the NKG2A:HLA-E Immune Checkpoint Axis to Enhance NK Cell Activation against Cancer.* Vaccines (Basel), 2022. **10**(12).
104. Ray, A., et al., *A novel alkylating agent Melflufen induces irreversible DNA damage and cytotoxicity in multiple myeloma cells.* Br J Haematol, 2016. **174**(3): p. 397-409.
105. Pour, L., et al., *Efficacy and safety of melflufen plus daratumumab and dexamethasone in relapsed/refractory multiple myeloma: results from the randomized, open-label, phase III LIGHTHOUSE study.* Haematologica, 2023.
106. (EMA), E.M.A., 2023.
107. Foundation, I.M., *Current FDA-Approved Medications: Multiple Myeloma Drugs.* 2023.
108. Rodriguez-Otero, P., et al., *Ide-cel or Standard Regimens in Relapsed and Refractory Multiple Myeloma.* N Engl J Med, 2023. **388**(11): p. 1002-1014.
109. San-Miguel, J., et al., *Cilta-cel or Standard Care in Lenalidomide-Refractory Multiple Myeloma.* N Engl J Med, 2023.
110. Moreau, P., et al., *Teclistamab in Relapsed or Refractory Multiple Myeloma.* N Engl J Med, 2022. **387**(6): p. 495-505.
111. Lesokhin, A.M., et al., *Elranatamab in relapsed or refractory multiple myeloma: phase 2 MagnetisMM-3 trial results.* Nat Med, 2023. **29**(9): p. 2259-2267.
112. Chari, A., et al., *Talquetamab, a T-Cell-Redirecting GPRC5D Bispecific Antibody for Multiple Myeloma.* N Engl J Med, 2022. **387**(24): p. 2232-2244.
113. Jimenez-Zepeda, V.H., et al., *Second autologous stem cell transplantation as salvage therapy for multiple myeloma: impact on progression-free and overall survival.* Biol Blood Marrow Transplant, 2012. **18**(5): p. 773-9.
114. Dhakal, B., et al., *Salvage second transplantation in relapsed multiple myeloma.* Leukemia, 2021. **35**(4): p. 1214-1217.
115. Kumar, S., et al., *Efficacy of venetoclax as targeted therapy for relapsed/refractory t(11;14) multiple myeloma.* Blood, 2017. **130**(22): p. 2401-2409.
116. Sidiqi, M.H., et al., *Venetoclax for the treatment of multiple myeloma: Outcomes outside of clinical trials.* Am J Hematol, 2021. **96**(9): p. 1131-1136.
117. Kumar, S.K., et al., *Venetoclax or placebo in combination with bortezomib and dexamethasone in patients with relapsed or refractory multiple myeloma (BELLINI): a randomised, double-blind, multicentre, phase 3 trial.* Lancet Oncol, 2020. **21**(12): p. 1630-1642.
118. Pan, D., et al., *Outcomes with panobinostat in heavily pretreated multiple myeloma patients.* Semin Oncol, 2023. **50**(1-2): p. 40-48.
119. Maouche, N., et al., *Panobinostat in combination with bortezomib and dexamethasone in multiply relapsed and refractory myeloma; UK routine care cohort.* PLoS One, 2022. **17**(7): p. e0270854.
120. Minnie, S.A. and G.R. Hill, *Immunotherapy of multiple myeloma.* J Clin Invest, 2020. **130**(4): p. 1565-1575.
121. Visram, A., et al., *Relapsed multiple myeloma demonstrates distinct patterns of immune microenvironment and malignant cell-mediated immunosuppression.* Blood Cancer J, 2021. **11**(3): p. 45.
122. Pessoa de Magalhaes, R.J., et al., *Analysis of the immune system of multiple myeloma patients achieving long-term disease control by multidimensional flow cytometry.* Haematologica, 2013. **98**(1): p. 79-86.
123. El-Sherbiny, Y.M., et al., *The requirement for DNAM-1, NKG2D, and NKp46 in the natural killer cell-mediated killing of myeloma cells.* Cancer Res, 2007. **67**(18): p. 8444-9.
124. Carbone, E., et al., *HLA class I, NKG2D, and natural cytotoxicity receptors regulate multiple myeloma cell recognition by natural killer cells.* Blood, 2005. **105**(1): p. 251-8.
125. Yang, Y., et al., *HLA-E Binding Peptide as a Potential Therapeutic Candidate for High-Risk Multiple Myeloma.* Front Oncol, 2021. **11**: p. 670673.

126. Racanelli, V., et al., *Alterations in the antigen processing-presenting machinery of transformed plasma cells are associated with reduced recognition by CD8+ T cells and characterize the progression of MGUS to multiple myeloma.* Blood, 2010. **115**(6): p. 1185-93.
127. Konjevic, G., et al., *Decreased CD161 activating and increased CD158a inhibitory receptor expression on NK cells underlies impaired NK cell cytotoxicity in patients with multiple myeloma.* J Clin Pathol, 2016.
128. Rosenblatt, J., et al., *PD-1 blockade by CT-011, anti-PD-1 antibody, enhances ex vivo T-cell responses to autologous dendritic cell/myeloma fusion vaccine.* J Immunother, 2011. **34**(5): p. 409-18.
129. Liu, J., et al., *Plasma cells from multiple myeloma patients express B7-H1 (PD-L1) and increase expression after stimulation with IFN-gamma and TLR ligands via a MyD88-, TRAF6-, and MEK-dependent pathway.* Blood, 2007. **110**(1): p. 296-304.
130. Perez-Andres, M., et al., *Characterization of bone marrow T cells in monoclonal gammopathy of undetermined significance, multiple myeloma, and plasma cell leukemia demonstrates increased infiltration by cytotoxic/Th1 T cells demonstrating a squed TCR-Vbeta repertoire.* Cancer, 2006. **106**(6): p. 1296-305.
131. Jinushi, M., et al., *MHC class I chain-related protein A antibodies and shedding are associated with the progression of multiple myeloma.* Proc Natl Acad Sci U S A, 2008. **105**(4): p. 1285-90.
132. Uhl, C., et al., *Natural killer cells activity against multiple myeloma cells is modulated by osteoblast-induced IL-6 and IL-10 production.* Heliyon, 2022. **8**(3): p. e09167.
133. Ratta, M., et al., *Dendritic cells are functionally defective in multiple myeloma: the role of interleukin-6.* Blood, 2002. **100**(1): p. 230-7.
134. D'Andrea, A., et al., *Interleukin 10 (IL-10) inhibits human lymphocyte interferon gamma-production by suppressing natural killer cell stimulatory factor/IL-12 synthesis in accessory cells.* J Exp Med, 1993. **178**(3): p. 1041-8.
135. Rana, P.S., et al., *Targeting TGF-beta signaling in the multiple myeloma microenvironment: Steering CARs and T cells in the right direction.* Front Cell Dev Biol, 2022. **10**: p. 1059715.
136. Strobl, H. and W. Knapp, *TGF-beta1 regulation of dendritic cells.* Microbes Infect, 1999. **1**(15): p. 1283-90.
137. Iwasa, M., et al., *PD-L1 upregulation in myeloma cells by panobinostat in combination with interferon-gamma.* Oncotarget, 2019. **10**(20): p. 1903-1917.
138. Ray, A., et al., *Targeting tryptophan catabolic kynurenine pathway enhances antitumor immunity and cytotoxicity in multiple myeloma.* Leukemia, 2020. **34**(2): p. 567-577.
139. Katz, J.B., A.J. Muller, and G.C. Prendergast, *Indoleamine 2,3-dioxygenase in T-cell tolerance and tumoral immune escape.* Immunol Rev, 2008. **222**: p. 206-21.
140. Li, W., et al., *CD38: An important regulator of T cell function.* Biomed Pharmacother, 2022. **153**: p. 113395.
141. Rebmann, V., et al., *Soluble MICA as an independent prognostic factor for the overall survival and progression-free survival of multiple myeloma patients.* Clin Immunol, 2007. **123**(1): p. 114-20.
142. Diaz-Tejedor, A., et al., *Immune System Alterations in Multiple Myeloma: Molecular Mechanisms and Therapeutic Strategies to Reverse Immunosuppression.* Cancers (Basel), 2021. **13**(6).
143. Dosani, T., et al., *The cellular immune system in myelomagenesis: NK cells and T cells in the development of MM and their uses in immunotherapies.* Blood Cancer J, 2015. **5**(7): p. e321.
144. Richardson, P.G., et al., *Isatuximab plus pomalidomide and low-dose dexamethasone versus pomalidomide and low-dose dexamethasone in patients with relapsed and*

refractory multiple myeloma (ICARIA-MM): follow-up analysis of a randomised, phase 3 study. Lancet Oncol, 2022. **23**(3): p. 416-427.
145. Shah, N., et al., *B-cell maturation antigen (BCMA) in multiple myeloma: rationale for targeting and current therapeutic approaches.* Leukemia, 2020. **34**(4): p. 985-1005.
146. Van Oekelen, O., et al., *Neurocognitive and hypokinetic movement disorder with features of parkinsonism after BCMA-targeting CAR-T cell therapy.* Nat Med, 2021. **27**(12): p. 2099-2103.
147. Cho, S.F., et al., *Promising Antigens for the New Frontier of Targeted Immunotherapy in Multiple Myeloma.* Cancers (Basel), 2021. **13**(23).
148. Giordano, D., et al., *B cell-activating factor (BAFF) from dendritic cells, monocytes and neutrophils is required for B cell maturation and autoantibody production in SLE-like autoimmune disease.* Front Immunol, 2023. **14**: p. 1050528.
149. Hahne, M., et al., *APRIL, a new ligand of the tumor necrosis factor family, stimulates tumor cell growth.* J Exp Med, 1998. **188**(6): p. 1185-90.
150. Moreaux, J., et al., *BAFF and APRIL protect myeloma cells from apoptosis induced by interleukin 6 deprivation and dexamethasone.* Blood, 2004. **103**(8): p. 3148-57.
151. Ndacayisaba, L.J., et al., *Characterization of BCMA Expression in Circulating Rare Single Cells of Patients with Plasma Cell Neoplasms.* Int J Mol Sci, 2022. **23**(21).
152. Tai, Y.T., et al., *APRIL and BCMA promote human multiple myeloma growth and immunosuppression in the bone marrow microenvironment.* Blood, 2016. **127**(25): p. 3225-36.
153. Wiedemann, A., et al., *Soluble B-cell maturation antigen as a monitoring marker for multiple myeloma.* Pathol Oncol Res, 2023. **29**: p. 1611171.
154. Pont, M.J., et al., *gamma-Secretase inhibition increases efficacy of BCMA-specific chimeric antigen receptor T cells in multiple myeloma.* Blood, 2019. **134**(19): p. 1585-1597.
155. Leivas, A., et al., *NKG2D-CAR-transduced natural killer cells efficiently target multiple myeloma.* Blood Cancer J, 2021. **11**(8): p. 146.
156. Allez, M., et al., *CD4+NKG2D+ T cells in Crohn's disease mediate inflammatory and cytotoxic responses through MICA interactions.* Gastroenterology, 2007. **132**(7): p. 2346-58.
157. Saez-Borderias, A., et al., *Expression and function of NKG2D in CD4+ T cells specific for human cytomegalovirus.* Eur J Immunol, 2006. **36**(12): p. 3198-206.
158. Upshaw, J.L., et al., *NKG2D-mediated signaling requires a DAP10-bound Grb2-Vav1 intermediate and phosphatidylinositol-3-kinase in human natural killer cells.* Nat Immunol, 2006. **7**(5): p. 524-32.
159. Roda-Navarro, P. and H.T. Reyburn, *The traffic of the NKG2D/Dap10 receptor complex during natural killer (NK) cell activation.* J Biol Chem, 2009. **284**(24): p. 16463-16472.
160. Sallman, D.A., et al., *CYAD-01, an autologous NKG2D-based CAR T-cell therapy, in relapsed or refractory acute myeloid leukaemia and myelodysplastic syndromes or multiple myeloma (THINK): haematological cohorts of the dose escalation segment of a phase 1 trial.* Lancet Haematol, 2023. **10**(3): p. e191-e202.
161. Gasser, S., et al., *The DNA damage pathway regulates innate immune system ligands of the NKG2D receptor.* Nature, 2005. **436**(7054): p. 1186-90.
162. Ward, J., et al., *HIV modulates the expression of ligands important in triggering natural killer cell cytotoxic responses on infected primary T-cell blasts.* Blood, 2007. **110**(4): p. 1207-14.
163. Pende, D., et al., *Major histocompatibility complex class I-related chain A and UL16-binding protein expression on tumor cell lines of different histotypes: analysis of tumor susceptibility to NKG2D-dependent natural killer cell cytotoxicity.* Cancer Res, 2002. **62**(21): p. 6178-86.

164. Groh, V., et al., *Cell stress-regulated human major histocompatibility complex class I gene expressed in gastrointestinal epithelium.* Proc Natl Acad Sci U S A, 1996. **93**(22): p. 12445-50.
165. Raulet, D.H., et al., *Regulation of ligands for the NKG2D activating receptor.* Annu Rev Immunol, 2013. **31**: p. 413-41.
166. Fionda, C., et al., *NKG2D and DNAM-1 Ligands: Molecular Targets for NK Cell-Mediated Immunotherapeutic Intervention in Multiple Myeloma.* Biomed Res Int, 2015. **2015**: p. 178698.
167. Zhang, T., A. Barber, and C.L. Sentman, *Generation of antitumor responses by genetic modification of primary human T cells with a chimeric NKG2D receptor.* Cancer Res, 2006. **66**(11): p. 5927-33.
168. Atamaniuk, J., et al., *Overexpression of G protein-coupled receptor 5D in the bone marrow is associated with poor prognosis in patients with multiple myeloma.* Eur J Clin Invest, 2012. **42**(9): p. 953-60.
169. Pillarisetti, K., et al., *A T-cell-redirecting bispecific G-protein-coupled receptor class 5 member D x CD3 antibody to treat multiple myeloma.* Blood, 2020. **135**(15): p. 1232-1243.
170. Hasselbalch Riley, C., et al., *RG6234, a novel GPRC5D T-cell engaging bispecific antibody, induces rapid responses in patients with relapsed/refractory multiple myeloma: preliminary results from a first-in-human trial.* EHA, 2022.
171. Smith, E.L., et al., *GPRC5D is a target for the immunotherapy of multiple myeloma with rationally designed CAR T cells.* Sci Transl Med, 2019. **11**(485).
172. Elkins, K., et al., *FcRL5 as a target of antibody-drug conjugates for the treatment of multiple myeloma.* Mol Cancer Ther, 2012. **11**(10): p. 2222-32.
173. Jiang, D., et al., *Chimeric antigen receptor T cells targeting FcRH5 provide robust tumour-specific responses in murine xenograft models of multiple myeloma.* Nat Commun, 2023. **14**(1): p. 3642.
174. Stewart, A.K., et al., *Phase I study of the anti-FcRH5 antibody-drug conjugate DFRF4539A in relapsed or refractory multiple myeloma.* Blood Cancer J, 2019. **9**(2): p. 17.
175. Piedra-Quintero, Z.L., et al., *CD38: An Immunomodulatory Molecule in Inflammation and Autoimmunity.* Front Immunol, 2020. **11**: p. 597959.
176. Ogiya, D., et al., *The JAK-STAT pathway regulates CD38 on myeloma cells in the bone marrow microenvironment: therapeutic implications.* Blood, 2020. **136**(20): p. 2334-2345.
177. Saltarella, I., et al., *Mechanisms of Resistance to Anti-CD38 Daratumumab in Multiple Myeloma.* Cells, 2020. **9**(1).
178. van de Donk, N. and S.Z. Usmani, *CD38 Antibodies in Multiple Myeloma: Mechanisms of Action and Modes of Resistance.* Front Immunol, 2018. **9**: p. 2134.
179. Zambello, R., et al., *NK cells and CD38: Implication for (Immuno)Therapy in Plasma Cell Dyscrasias.* Cells, 2020. **9**(3).
180. Wang, Y., et al., *Fratricide of NK Cells in Daratumumab Therapy for Multiple Myeloma Overcome by Ex Vivo-Expanded Autologous NK Cells.* Clin Cancer Res, 2018. **24**(16): p. 4006-4017.
181. Kind, S., et al., *Prevalence of Syndecan-1 (CD138) Expression in Different Kinds of Human Tumors and Normal Tissues.* Dis Markers, 2019. **2019**: p. 4928315.
182. Akhmetzyanova, I., et al., *Dynamic CD138 surface expression regulates switch between myeloma growth and dissemination.* Leukemia, 2020. **34**(1): p. 245-256.
183. Kawano, Y., et al., *Multiple myeloma cells expressing low levels of CD138 have an immature phenotype and reduced sensitivity to lenalidomide.* Int J Oncol, 2012. **41**(3): p. 876-84.

184. Beauvais, D.M., et al., *Syndecan-1 (CD138) Suppresses Apoptosis in Multiple Myeloma by Activating IGF1 Receptor: Prevention by SynstatinIGF1R Inhibits Tumor Growth.* Cancer Res, 2016. **76**(17): p. 4981-93.
185. Lovell, R., et al., *Soluble syndecan-1 level at diagnosis is an independent prognostic factor in multiple myeloma and the extent of fall from diagnosis to plateau predicts for overall survival.* Br J Haematol, 2005. **130**(4): p. 542-8.
186. Rapraeger, A.C., *Syndecan-regulated receptor signaling.* J Cell Biol, 2000. **149**(5): p. 995-8.
187. Coombe, D.R., *Biological implications of glycosaminoglycan interactions with haemopoietic cytokines.* Immunol Cell Biol, 2008. **86**(7): p. 598-607.
188. Casu, B., A. Naggi, and G. Torri, *Heparin-derived heparan sulfate mimics to modulate heparan sulfate-protein interaction in inflammation and cancer.* Matrix Biol, 2010. **29**(6): p. 442-52.
189. Moreaux, J., et al., *APRIL and TACI interact with syndecan-1 on the surface of multiple myeloma cells to form an essential survival loop.* Eur J Haematol, 2009. **83**(2): p. 119-29.
190. Heider, K.H., et al., *CD44v6: a target for antibody-based cancer therapy.* Cancer Immunol Immunother, 2004. **53**(7): p. 567-79.
191. Casucci, M., et al., *CD44v6-targeted T cells mediate potent antitumor effects against acute myeloid leukemia and multiple myeloma.* Blood, 2013. **122**(20): p. 3461-72.
192. Todaro, M., et al., *CD44v6 is a marker of constitutive and reprogrammed cancer stem cells driving colon cancer metastasis.* Cell Stem Cell, 2014. **14**(3): p. 342-56.
193. Jung, T., W. Gross, and M. Zoller, *CD44v6 coordinates tumor matrix-triggered motility and apoptosis resistance.* J Biol Chem, 2011. **286**(18): p. 15862-74.
194. Ponta, H., L. Sherman, and P.A. Herrlich, *CD44: from adhesion molecules to signalling regulators.* Nat Rev Mol Cell Biol, 2003. **4**(1): p. 33-45.
195. Shirure, V.S., et al., *CD44 variant isoforms expressed by breast cancer cells are functional E-selectin ligands under flow conditions.* Am J Physiol Cell Physiol, 2015. **308**(1): p. C68-78.
196. Jijiwa, M., et al., *CD44v6 regulates growth of brain tumor stem cells partially through the AKT-mediated pathway.* PLoS One, 2011. **6**(9): p. e24217.
197. Khan, F., et al., *Identification of novel CD44v6-binding peptides that block CD44v6 and deliver a pro-apoptotic peptide to tumors to inhibit tumor growth and metastasis in mice.* Theranostics, 2021. **11**(3): p. 1326-1344.
198. Wang, Z., et al., *CD44/CD44v6 a Reliable Companion in Cancer-Initiating Cell Maintenance and Tumor Progression.* Front Cell Dev Biol, 2018. **6**: p. 97.
199. Riechelmann, H., et al., *Phase I trial with the CD44v6-targeting immunoconjugate bivatuzumab mertansine in head and neck squamous cell carcinoma.* Oral Oncol, 2008. **44**(9): p. 823-9.
200. Awuah, D., et al., *Developing a Safer Anti-CD44v6 Chimeric Antigen Receptor T Cell Against Hematological Cancers By Mitigating on-Target Off-Tumor Toxicity.* Blood, 2021. **138**: p. 2796.
201. Braumuller, H., et al., *CD44v6 cell surface expression is a common feature of macrophages and macrophage-like cells - implication for a natural macrophage extravasation mechanism mimicked by tumor cells.* FEBS Lett, 2000. **476**(3): p. 240-7.
202. Bruno, B., et al., *European Myeloma Network perspective on CAR T-Cell therapies for multiple myeloma.* Haematologica, 2021. **106**(8): p. 2054-2065.
203. Kumaresan, P.R., et al., *CS1, a novel member of the CD2 family, is homophilic and regulates NK cell function.* Mol Immunol, 2002. **39**(1-2): p. 1-8.
204. Chan, W.K., et al., *A CS1-NKG2D Bispecific Antibody Collectively Activates Cytolytic Immune Cells against Multiple Myeloma.* Cancer Immunol Res, 2018. **6**(7): p. 776-787.

205. Malaer, J.D. and P.A. Mathew, *CS1 (SLAMF7, CD319) is an effective immunotherapeutic target for multiple myeloma.* Am J Cancer Res, 2017. **7**(8): p. 1637-1641.
206. Chu, J., et al., *CS1-specific chimeric antigen receptor (CAR)-engineered natural killer cells enhance in vitro and in vivo antitumor activity against human multiple myeloma.* Leukemia, 2014. **28**(4): p. 917-27.
207. O'Neal, J., et al., *CS1 CAR-T targeting the distal domain of CS1 (SLAMF7) shows efficacy in high tumor burden myeloma model despite fratricide of CD8+CS1 expressing CAR-T cells.* Leukemia, 2022. **36**(6): p. 1625-1634.
208. Li, X., et al., *CD19, from bench to bedside.* Immunol Lett, 2017. **183**: p. 86-95.
209. Barsan, V., et al., *Tisagenlecleucel utilisation and outcomes across refractory, first relapse and multiply relapsed B-cell acute lymphoblastic leukemia: a retrospective analysis of real-world patterns.* EClinicalMedicine, 2023. **65**: p. 102268.
210. Schuster, S.J., et al., *Tisagenlecleucel in Adult Relapsed or Refractory Diffuse Large B-Cell Lymphoma.* N Engl J Med, 2019. **380**(1): p. 45-56.
211. Wang, Y., et al., *Long-Term Follow-Up of Combination of B-Cell Maturation Antigen and CD19 Chimeric Antigen Receptor T Cells in Multiple Myeloma.* J Clin Oncol, 2022. **40**(20): p. 2246-2256.
212. Garfall, A.L., et al., *Anti-CD19 CAR T cells with high-dose melphalan and autologous stem cell transplantation for refractory multiple myeloma.* JCI Insight, 2018. **3**(8).
213. Wang, Y., et al., *BCMA-targeting Bispecific Antibody That Simultaneously Stimulates NKG2D-enhanced Efficacy Against Multiple Myeloma.* J Immunother, 2020. **43**(6): p. 175-188.
214. Shi, X., et al., *Anti-CD19 and anti-BCMA CAR T cell therapy followed by lenalidomide maintenance after autologous stem-cell transplantation for high-risk newly diagnosed multiple myeloma.* Am J Hematol, 2022. **97**(5): p. 537-547.
215. Radhakrishnan, S.V., et al., *CD229 CAR T cells eliminate multiple myeloma and tumor propagating cells without fratricide.* Nat Commun, 2020. **11**(1): p. 798.
216. Hosen, N., et al., *The activated conformation of integrin beta(7) is a novel multiple myeloma-specific target for CAR T cell therapy.* Nat Med, 2017. **23**(12): p. 1436-1443.
217. Larson, R.C., et al., *Anti-TACI single and dual-targeting CAR T cells overcome BCMA antigen loss in multiple myeloma.* Nat Commun, 2023. **14**(1): p. 7509.
218. Anderson, G.S.F., et al., *Unbiased cell surface proteomics identifies SEMA4A as an effective immunotherapy target for myeloma.* Blood, 2022. **139**(16): p. 2471-2482.
219. Soekojo, C.Y., et al., *Immunotherapy in Multiple Myeloma.* Cells, 2020. **9**(3).
220. Krejcik, J., et al., *Daratumumab depletes CD38+ immune regulatory cells, promotes T-cell expansion, and skews T-cell repertoire in multiple myeloma.* Blood, 2016. **128**(3): p. 384-94.
221. Dimopoulos, M.A., et al., *Overall Survival With Daratumumab, Lenalidomide, and Dexamethasone in Previously Treated Multiple Myeloma (POLLUX): A Randomized, Open-Label, Phase III Trial.* J Clin Oncol, 2023. **41**(8): p. 1590-1599.
222. Sonneveld, P., et al., *Overall Survival With Daratumumab, Bortezomib, and Dexamethasone in Previously Treated Multiple Myeloma (CASTOR): A Randomized, Open-Label, Phase III Trial.* J Clin Oncol, 2023. **41**(8): p. 1600-1609.
223. Nijhof, I.S., et al., *CD38 expression and complement inhibitors affect response and resistance to daratumumab therapy in myeloma.* Blood, 2016. **128**(7): p. 959-70.
224. Naeimi Kararoudi, M., et al., *CD38 deletion of human primary NK cells eliminates daratumumab-induced fratricide and boosts their effector activity.* Blood, 2020. **136**(21): p. 2416-2427.
225. Verkleij, C.P.M., et al., *NK Cell Phenotype Is Associated With Response and Resistance to Daratumumab in Relapsed/Refractory Multiple Myeloma.* Hemasphere, 2023. **7**(5): p. e881.

226. De Luca, F., et al., *Monoclonal Antibodies: The Greatest Resource to Treat Multiple Myeloma.* Int J Mol Sci, 2023. **24**(4).
227. Dhillon, S., *Isatuximab: First Approval.* Drugs, 2020. **80**(9): p. 905-912.
228. Martin, T., et al., *Isatuximab, carfilzomib, and dexamethasone in patients with relapsed multiple myeloma: updated results from IKEMA, a randomized Phase 3 study.* Blood Cancer J, 2023. **13**(1): p. 72.
229. Moreau, P., et al., *Isatuximab, carfilzomib, and dexamethasone in relapsed multiple myeloma (IKEMA): a multicentre, open-label, randomised phase 3 trial.* Lancet, 2021. **397**(10292): p. 2361-2371.
230. Moore, D.C., et al., *Hepatitis B reactivation in patients with multiple myeloma treated with anti-CD38 monoclonal antibody-based therapies: a pharmacovigilance analysis.* Int J Clin Pharm, 2023.
231. Gozzetti, A., et al., *Anti CD38 monoclonal antibodies for multiple myeloma treatment.* Hum Vaccin Immunother, 2022. **18**(5): p. 2052658.
232. Hiemstra, I.H., et al., *Preclinical anti-tumour activity of HexaBody-CD38, a next-generation CD38 antibody with superior complement-dependent cytotoxic activity.* EBioMedicine, 2023. **93**: p. 104663.
233. Magen, H. and E. Muchtar, *Elotuzumab: the first approved monoclonal antibody for multiple myeloma treatment.* Ther Adv Hematol, 2016. **7**(4): p. 187-95.
234. Tai, Y.T., et al., *Anti-CS1 humanized monoclonal antibody HuLuc63 inhibits myeloma cell adhesion and induces antibody-dependent cellular cytotoxicity in the bone marrow milieu.* Blood, 2008. **112**(4): p. 1329-37.
235. Ritchie, D. and M. Colonna, *Mechanisms of Action and Clinical Development of Elotuzumab.* Clin Transl Sci, 2018. **11**(3): p. 261-266.
236. Liu, Y.C., S. Szmania, and F. van Rhee, *Profile of elotuzumab and its potential in the treatment of multiple myeloma.* Blood Lymphat Cancer, 2014. **2014**(4): p. 15-27.
237. Dimopoulos, M.A., et al., *Elotuzumab Plus Pomalidomide and Dexamethasone for Relapsed/Refractory Multiple Myeloma: Final Overall Survival Analysis From the Randomized Phase II ELOQUENT-3 Trial.* J Clin Oncol, 2023. **41**(3): p. 568-578.
238. Ray, U. and R.Z. Orlowski, *Antibody-Drug Conjugates for Multiple Myeloma: Just the Beginning, or the Beginning of the End?* Pharmaceuticals (Basel), 2023. **16**(4).
239. Markham, A., *Belantamab Mafodotin: First Approval.* Drugs, 2020. **80**(15): p. 1607-1613.
240. Lonial, S., et al., *Belantamab mafodotin for relapsed or refractory multiple myeloma (DREAMM-2): a two-arm, randomised, open-label, phase 2 study.* Lancet Oncol, 2020. **21**(2): p. 207-221.
241. Katja Weisel, V.T.H., Atanas Radinoff, Sosana Delimpasi, Gabor Mikala, Tamas Masszi,, M.C. Jian Li, Morio Matsumoto, Neal Sule, Mary Li, Astrid McKeown, Wei He, Shelley Bright,, and J.B. Brooke Currie, Joanna Opalinska, Meletios A. Dimopoulos, *A phase 3, open-label, randomized study to evaluate the efficacy and safety of singleagent belantamab mafodotin (belamaf) compared to pomalidomide plus low-dose dexamethasone (Pd) in patients (pts) with relapsed/refractory multiple myeloma (RRMM): DREAMM-3.* Journal of Clinical Oncology, 2023.
242. Martin, T.G., et al., *Cilta-cel, a BCMA-targeting CAR-T therapy for heavily pretreated patients with relapsed/refractory multiple myeloma.* Future Oncol, 2023.
243. de la Rubia, J., et al., *Belantamab Mafodotin in Patients with Relapsed/Refractory Multiple Myeloma: Results of the Compassionate Use or the Expanded Access Program in Spain.* Cancers (Basel), 2023. **15**(11).
244. Abramson, H.N., *Immunotherapy of Multiple Myeloma: Current Status as Prologue to the Future.* Int J Mol Sci, 2023. **24**(21).
245. Cho, S.F., et al., *Bispecific antibodies in multiple myeloma treatment: A journey in progress.* Front Oncol, 2022. **12**: p. 1032775.

246. Pillarisetti, K., et al., *Teclistamab is an active T cell-redirecting bispecific antibody against B-cell maturation antigen for multiple myeloma.* Blood Adv, 2020. **4**(18): p. 4538-4549.
247. Verkleij, C.P.M., et al., *Preclinical activity and determinants of response of the GPRC5DxCD3 bispecific antibody talquetamab in multiple myeloma.* Blood Adv, 2021. **5**(8): p. 2196-2215.
248. Zhao, J., et al., *Bispecific antibodies targeting BCMA, GPRC5D, and FcRH5 for multiple myeloma therapy: latest updates from ASCO 2023 Annual Meeting.* J Hematol Oncol, 2023. **16**(1): p. 92.
249. Li, J., et al., *Membrane-Proximal Epitope Facilitates Efficient T Cell Synapse Formation by Anti-FcRH5/CD3 and Is a Requirement for Myeloma Cell Killing.* Cancer Cell, 2017. **31**(3): p. 383-395.
250. Suzanne Trudel, A.D.C., Amrita Y. Krishnan, Rafael Fonseca, Andrew Spencer, Jesús G. Berdeja, Alexander Lesokhin, Peter A Forsberg, Jacob P. Laubach, Luciano J. Costa, Paula Rodriguez-Otero, Rayan Kaedbey, Joshua Richter, Maria-Victoria Mateos, Sheeba K Thomas, Chihunt Wong, Mengsong Li, Voleak Choeurng, Anjali Vaze, Divya Samineni, Teiko Sumiyoshi, James Cooper, Simon J Harrison, *Cevostamab Monotherapy Continues to Show Clinically Meaningful Activity and Manageable Safety in Patients with Heavily Pre-Treated Relapsed/Refractory Multiple Myeloma (RRMM): Updated Results from an Ongoing Phase I Study.* ASH 2021, 2021.
251. Rahman, M.M. and G. McFadden, *Oncolytic Viruses: Newest Frontier for Cancer Immunotherapy.* Cancers (Basel), 2021. **13**(21).
252. Cook, J., et al., *Oncolytic virotherapy - Forging its place in the immunomodulatory paradigm for Multiple Myeloma.* Cancer Treat Res Commun, 2021. **29**: p. 100473.
253. Stewart, G., A. Chantry, and M. Lawson, *The Use of Oncolytic Viruses in the Treatment of Multiple Myeloma.* Cancers (Basel), 2021. **13**(22).
254. Boussi, L.S., Z.M. Avigan, and J. Rosenblatt, *Immunotherapy for the treatment of multiple myeloma.* Front Immunol, 2022. **13**: p. 1027385.
255. Leivas, A., et al., *Novel treatment strategy with autologous activated and expanded natural killer cells plus anti-myeloma drugs for multiple myeloma.* Oncoimmunology, 2016. **5**(12): p. e1250051.
256. Verheye, E., et al., *Dendritic Cell-Based Immunotherapy in Multiple Myeloma: Challenges, Opportunities, and Future Directions.* Int J Mol Sci, 2022. **23**(2).
257. Daher, M. and K. Rezvani, *Outlook for New CAR-Based Therapies with a Focus on CAR NK Cells: What Lies Beyond CAR-Engineered T Cells in the Race against Cancer.* Cancer Discov, 2021. **11**(1): p. 45-58.
258. Tokarew, N., et al., *Teaching an old dog new tricks: next-generation CAR T cells.* Br J Cancer, 2019. **120**(1): p. 26-37.
259. Mullard, A., *FDA approves first CAR T therapy.* Nat Rev Drug Discov, 2017. **16**(10): p. 669.
260. Maude, S.L., et al., *Tisagenlecleucel in Children and Young Adults with B-Cell Lymphoblastic Leukemia.* N Engl J Med, 2018. **378**(5): p. 439-448.
261. Chen, Y.J., B. Abila, and Y. Mostafa Kamel, *CAR-T: What Is Next?* Cancers (Basel), 2023. **15**(3).
262. Berdeja, J.G., et al., *Ciltacabtagene autoleucel, a B-cell maturation antigen-directed chimeric antigen receptor T-cell therapy in patients with relapsed or refractory multiple myeloma (CARTITUDE-1): a phase 1b/2 open-label study.* Lancet, 2021. **398**(10297): p. 314-324.
263. Mailankody, S. and O. Landgren, *T-Cell Engagers - Modern Immune-Based Therapies for Multiple Myeloma.* N Engl J Med, 2022. **387**(6): p. 558-561.
264. Barber, A., et al., *Chimeric NKG2D receptor-expressing T cells as an immunotherapy for multiple myeloma.* Exp Hematol, 2008. **36**(10): p. 1318-28.

265. Lonez, C., et al., *Study protocol for THINK: a multinational open-label phase I study to assess the safety and clinical activity of multiple administrations of NKR-2 in patients with different metastatic tumour types.* BMJ Open, 2017. **7**(11): p. e017075.
266. Baumeister, S.H., et al., *Phase I Trial of Autologous CAR T Cells Targeting NKG2D Ligands in Patients with AML/MDS and Multiple Myeloma.* Cancer Immunol Res, 2019. **7**(1): p. 100-112.
267. Rodriguez-Otero, P. and J.F. San-Miguel, *Cellular therapy for multiple myeloma: what's now and what's next.* Hematology Am Soc Hematol Educ Program, 2022. **2022**(1): p. 180-189.
268. Khan, A.N., et al., *Immunogenicity of CAR-T Cell Therapeutics: Evidence, Mechanism and Mitigation.* Front Immunol, 2022. **13**: p. 886546.
269. Zhu, X., Q. Li, and X. Zhu, *Mechanisms of CAR T cell exhaustion and current counteraction strategies.* Front Cell Dev Biol, 2022. **10**: p. 1034257.
270. Gumber, D. and L.D. Wang, *Improving CAR-T immunotherapy: Overcoming the challenges of T cell exhaustion.* EBioMedicine, 2022. **77**: p. 103941.
271. Roeven, M.W., et al., *Immunotherapeutic approaches to treat multiple myeloma.* Hum Vaccin Immunother, 2014. **10**(4): p. 896-910.
272. Fernandez de Larrea, C., et al., *Defining an Optimal Dual-Targeted CAR T-cell Therapy Approach Simultaneously Targeting BCMA and GPRC5D to Prevent BCMA Escape-Driven Relapse in Multiple Myeloma.* Blood Cancer Discov, 2020. **1**(2): p. 146-154.
273. Ruffo, E., et al., *Post-translational covalent assembly of CAR and synNotch receptors for programmable antigen targeting.* Nat Commun, 2023. **14**(1): p. 2463.
274. Martin, T., et al., *Ciltacabtagene Autoleucel, an Anti-B-cell Maturation Antigen Chimeric Antigen Receptor T-Cell Therapy, for Relapsed/Refractory Multiple Myeloma: CARTITUDE-1 2-Year Follow-Up.* J Clin Oncol, 2023. **41**(6): p. 1265-1274.
275. Zhang, X., et al., *CAR-T cell therapy in multiple myeloma: Current limitations and potential strategies.* Front Immunol, 2023. **14**: p. 1101495.
276. Chen, D., et al., *Subsequent anti-myeloma therapy after maturation antigen (BCMA) chimeric antigen receptor (CAR)-T cell (HDS269B) treatment in patients with relapsed/refractory multiple myeloma.* Am J Hematol, 2022. **97**(12): p. E478-E481.
277. Morris, E.C., et al., *Cytokine release syndrome and associated neurotoxicity in cancer immunotherapy.* Nat Rev Immunol, 2022. **22**(2): p. 85-96.
278. Hines, M.R., et al., *Hemophagocytic lymphohistiocytosis-like toxicity (carHLH) after CD19-specific CAR T-cell therapy.* Br J Haematol, 2021. **194**(4): p. 701-707.
279. Jain, T., T.S. Olson, and F.L. Locke, *How I treat cytopenias after CAR T-cell therapy.* Blood, 2023. **141**(20): p. 2460-2469.
280. Valeri, A., et al., *Overcoming tumor resistance mechanisms in CAR-NK cell therapy.* Front Immunol, 2022. **13**: p. 953849.
281. Sanber, K., B. Savani, and T. Jain, *Graft-versus-host disease risk after chimeric antigen receptor T-cell therapy: the diametric opposition of T cells.* Br J Haematol, 2021. **195**(5): p. 660-668.
282. Sivori, S., et al., *NK Cell-Based Immunotherapy for Hematological Malignancies.* J Clin Med, 2019. **8**(10).
283. Shah, N.N. and T.J. Fry, *Mechanisms of resistance to CAR T cell therapy.* Nat Rev Clin Oncol, 2019. **16**(6): p. 372-385.
284. Marofi, F., et al., *Renaissance of armored immune effector cells, CAR-NK cells, brings the higher hope for successful cancer therapy.* Stem Cell Res Ther, 2021. **12**(1): p. 200.
285. Cozar, B., et al., *Tumor-Infiltrating Natural Killer Cells.* Cancer Discov, 2021. **11**(1): p. 34-44.
286. Caruso, S., et al., *Safe and effective off-the-shelf immunotherapy based on CAR.CD123-NK cells for the treatment of acute myeloid leukaemia.* J Hematol Oncol, 2022. **15**(1): p. 163.

287. Biederstadt, A. and K. Rezvani, *Engineering the next generation of CAR-NK immunotherapies.* Int J Hematol, 2021. **114**(5): p. 554-571.
288. Zhang, Y., et al., *In vivo kinetics of human natural killer cells: the effects of ageing and acute and chronic viral infection.* Immunology, 2007. **121**(2): p. 258-65.
289. Glienke, W., et al., *Advantages and applications of CAR-expressing natural killer cells.* Front Pharmacol, 2015. **6**: p. 21.
290. Burga, R.A., et al., *Improving efficacy of cancer immunotherapy by genetic modification of natural killer cells.* Cytotherapy, 2016. **18**(11): p. 1410-1421.
291. Wlodarczyk, M. and B. Pyrzynska, *CAR-NK as a Rapidly Developed and Efficient Immunotherapeutic Strategy against Cancer.* Cancers (Basel), 2022. **15**(1).
292. Berrien-Elliott, M.M., R. Romee, and T.A. Fehniger, *Improving natural killer cell cancer immunotherapy.* Curr Opin Organ Transplant, 2015. **20**(6): p. 671-80.
293. Gong, Y., et al., *Chimeric antigen receptor natural killer (CAR-NK) cell design and engineering for cancer therapy.* J Hematol Oncol, 2021. **14**(1): p. 73.
294. Rafei, H., M. Daher, and K. Rezvani, *Chimeric antigen receptor (CAR) natural killer (NK)-cell therapy: leveraging the power of innate immunity.* Br J Haematol, 2021. **193**(2): p. 216-230.
295. Cichocki, F., et al., *Epigenetic regulation of NK cell differentiation and effector functions.* Front Immunol, 2013. **4**: p. 55.
296. Berrien-Elliott, M.M., M.T. Jacobs, and T.A. Fehniger, *Allogeneic natural killer cell therapy.* Blood, 2023. **141**(8): p. 856-868.
297. Jonsson, A.H. and W.M. Yokoyama, *Natural killer cell tolerance licensing and other mechanisms.* Adv Immunol, 2009. **101**: p. 27-79.
298. Debska-Zielkowska, J., et al., *KIR Receptors as Key Regulators of NK Cells Activity in Health and Disease.* Cells, 2021. **10**(7).
299. Zhang, Y., et al., *KIR-HLA interactions extend human CD8+ T cell lifespan in vivo.* J Clin Invest, 2023. **133**(12).
300. Zhong, X., et al., *PD-L2 expression extends beyond dendritic cells/macrophages to B1 cells enriched for V(H)11/V(H)12 and phosphatidylcholine binding.* Eur J Immunol, 2007. **37**(9): p. 2405-10.
301. Yearley, J.H., et al., *PD-L2 Expression in Human Tumors: Relevance to Anti-PD-1 Therapy in Cancer.* Clin Cancer Res, 2017. **23**(12): p. 3158-3167.
302. Ghosh, C., G. Luong, and Y. Sun, *A snapshot of the PD-1/PD-L1 pathway.* J Cancer, 2021. **12**(9): p. 2735-2746.
303. Harjunpaa, H. and C. Guillerey, *TIGIT as an emerging immune checkpoint.* Clin Exp Immunol, 2020. **200**(2): p. 108-119.
304. Cifaldi, L., et al., *DNAM-1 chimeric receptor-engineered NK cells: a new frontier for CAR-NK cell-based immunotherapy.* Front Immunol, 2023. **14**: p. 1197053.
305. Wolf, Y., A.C. Anderson, and V.K. Kuchroo, *TIM3 comes of age as an inhibitory receptor.* Nat Rev Immunol, 2020. **20**(3): p. 173-185.
306. Lamb, M.G., et al., *Natural killer cell therapy for hematologic malignancies: successes, challenges, and the future.* Stem Cell Res Ther, 2021. **12**(1): p. 211.
307. Borys, S.M., et al., *The Yin and Yang of Targeting KLRG1(+) Tregs and Effector Cells.* Front Immunol, 2022. **13**: p. 894508.
308. Henson, S.M. and A.N. Akbar, *KLRG1--more than a marker for T cell senescence.* Age (Dordr), 2009. **31**(4): p. 285-91.
309. Borrego, F., et al., *The CD94/NKG2 family of receptors: from molecules and cells to clinical relevance.* Immunol Res, 2006. **35**(3): p. 263-78.
310. Kaiser, B.K., et al., *Interactions between NKG2x immunoreceptors and HLA-E ligands display overlapping affinities and thermodynamics.* J Immunol, 2005. **174**(5): p. 2878-84.

311. Medjouel Khlifi, H., et al., *Role of the ITAM-Bearing Receptors Expressed by Natural Killer Cells in Cancer.* Front Immunol, 2022. **13**: p. 898745.
312. de Andrade, L.F., M.J. Smyth, and L. Martinet, *DNAM-1 control of natural killer cells functions through nectin and nectin-like proteins.* Immunol Cell Biol, 2014. **92**(3): p. 237-44.
313. Sanchez-Correa, B., et al., *DNAM-1 and the TIGIT/PVRIG/TACTILE Axis: Novel Immune Checkpoints for Natural Killer Cell-Based Cancer Immunotherapy.* Cancers (Basel), 2019. **11**(6).
314. Rezvani, K., et al., *Engineering Natural Killer Cells for Cancer Immunotherapy.* Mol Ther, 2017. **25**(8): p. 1769-1781.
315. Guillerey, C., N.D. Huntington, and M.J. Smyth, *Targeting natural killer cells in cancer immunotherapy.* Nat Immunol, 2016. **17**(9): p. 1025-36.
316. Chiossone, L. and E. Vivier, *Bringing natural killer cells to the clinic.* J Exp Med, 2022. **219**(10).
317. Klingemann, H., *Are natural killer cells superior CAR drivers?* Oncoimmunology, 2014. **3**: p. e28147.
318. Kang, L., et al., *Characterization and ex vivo Expansion of Human Placenta-Derived Natural Killer Cells for Cancer Immunotherapy.* Front Immunol, 2013. **4**: p. 101.
319. Wen, W., et al., *Enhancing cord blood stem cell-derived NK cell growth and differentiation through hyperosmosis.* Stem Cell Res Ther, 2023. **14**(1): p. 295.
320. Guo, X., et al., *CBLB ablation with CRISPR/Cas9 enhances cytotoxicity of human placental stem cell-derived NK cells for cancer immunotherapy.* J Immunother Cancer, 2021. **9**(3).
321. Schmidt, D., et al., *Engineering CAR-NK cells: how to tune innate killer cells for cancer immunotherapy.* Immunother Adv, 2022. **2**(1): p. ltac003.
322. Zhang, L., et al., *Natural killer cells: of-the-shelf cytotherapy for cancer immunosurveillance.* Am J Cancer Res, 2021. **11**(4): p. 1770-1791.
323. Hermanson, D.L. and D.S. Kaufman, *Utilizing chimeric antigen receptors to direct natural killer cell activity.* Front Immunol, 2015. **6**: p. 195.
324. Sutlu, T., et al., *Inhibition of intracellular antiviral defense mechanisms augments lentiviral transduction of human natural killer cells: implications for gene therapy.* Hum Gene Ther, 2012. **23**(10): p. 1090-100.
325. Herrera, L., et al., *Adult peripheral blood and umbilical cord blood NK cells are good sources for effective CAR therapy against CD19 positive leukemic cells.* Sci Rep, 2019. **9**(1): p. 18729.
326. Liu, E., et al., *Use of CAR-Transduced Natural Killer Cells in CD19-Positive Lymphoid Tumors.* N Engl J Med, 2020. **382**(6): p. 545-553.
327. Shin, M.H., et al., *NK Cell-Based Immunotherapies in Cancer.* Immune Netw, 2020. **20**(2): p. e14.
328. Zhang, L., et al., *CAR-NK cells for cancer immunotherapy: from bench to bedside.* Biomark Res, 2022. **10**(1): p. 12.
329. Wu, X. and S. Matosevic, *Gene-edited and CAR-NK cells: Opportunities and challenges with engineering of NK cells for immunotherapy.* Mol Ther Oncolytics, 2022. **27**: p. 224-238.
330. Jiang, H., et al., *Transfection of chimeric anti-CD138 gene enhances natural killer cell activation and killing of multiple myeloma cells.* Mol Oncol, 2014. **8**(2): p. 297-310.
331. Roex, G., et al., *Two for one: targeting BCMA and CD19 in B-cell malignancies with off-the-shelf dual-CAR NK-92 cells.* J Transl Med, 2022. **20**(1): p. 124.
332. Luanpitpong, S., et al., *Selective Cytotoxicity of Single and Dual Anti-CD19 and Anti-CD138 Chimeric Antigen Receptor-Natural Killer Cells against Hematologic Malignancies.* J Immunol Res, 2021. **2021**: p. 5562630.

333. Motais, B., et al., *Anti-BCMA-CAR NK Cells Expressing Soluble TRAIL: Promising Therapeutic Approach for Multiple Myeloma in Combination with Bortezomib and γ-Secretase Inhibitors.* ASH, 2022.
334. Golubovskaya, V., et al., *CAR-NK Cells Generated with mRNA-LNPs Kill Tumor Target Cells In Vitro and In Vivo.* Int J Mol Sci, 2023. **24**(17).
335. Ng, Y.Y., et al., *CXCR4 and anti-BCMA CAR co-modified natural killer cells suppress multiple myeloma progression in a xenograft mouse model.* Cancer Gene Ther, 2022. **29**(5): p. 475-483.
336. Wang, X., et al., *Inducible MyD88/CD40 synergizes with IL-15 to enhance antitumor efficacy of CAR-NK cells.* Blood Adv, 2020. **4**(9): p. 1950-1964.
337. Karvouni, M., et al., *Challenges in alphaCD38-chimeric antigen receptor (CAR)-expressing natural killer (NK) cell-based immunotherapy in multiple myeloma: Harnessing the CD38dim phenotype of cytokine-stimulated NK cells as a strategy to prevent fratricide.* Cytotherapy, 2023. **25**(7): p. 763-772.
338. Brophy, S., et al., *CB derived, optimized affinity CD38 CAR-NK cells with CD38 KO show promising in-vivo activity in a Multiple Myeloma model.* IMS 2022, 2022.
339. Reiser, J., et al., *FT555: Off-the-Shelf CAR-NK Cell Therapy Co-Targeting GPRC5D and CD38 for the Treatment of Multiple Myeloma.* ASH, 2022.
340. Cichocki, F., et al., *Quadruple gene-engineered natural killer cells enable multi-antigen targeting for durable antitumor activity against multiple myeloma.* Nat Commun, 2022. **13**(1): p. 7341.
341. Dhakal, B., et al., *Interim phase I clinical data of FT576 as monotherapy and in combination with daratumumab in subjects with relapsed/refractory multiple myeloma.* ASH, 2022.
342. Li, Y., et al., *KIR-based inhibitory CARs overcome CAR-NK cell trogocytosis-mediated fratricide and tumor escape.* Nat Med, 2022. **28**(10): p. 2133-2144.
343. Cichocki, F., et al., *GSK3 Inhibition Drives Maturation of NK Cells and Enhances Their Antitumor Activity.* Cancer Res, 2017. **77**(20): p. 5664-5675.
344. Afolabi, L.O., et al., *Synergistic Tumor Cytolysis by NK Cells in Combination With a Pan-HDAC Inhibitor, Panobinostat.* Front Immunol, 2021. **12**: p. 701671.
345. Chen, X., et al., *A combinational therapy of EGFR-CAR NK cells and oncolytic herpes simplex virus 1 for breast cancer brain metastases.* Oncotarget, 2016. **7**(19): p. 27764-77.
346. Xiao, X., et al., *Bispecific NK-cell engager targeting BCMA elicits stronger antitumor effects and produces less proinflammatory cytokines than T-cell engager.* Front Immunol, 2023. **14**: p. 1113303.
347. Zhang, C., et al., *Bispecific antibody-mediated redirection of NKG2D-CAR natural killer cells facilitates dual targeting and enhances antitumor activity.* J Immunother Cancer, 2021. **9**(10).
348. McWilliams, E.M., et al., *Therapeutic CD94/NKG2A blockade improves natural killer cell dysfunction in chronic lymphocytic leukemia.* Oncoimmunology, 2016. **5**(10): p. e1226720.
349. Bexte, T., et al., *CRISPR-Cas9 based gene editing of the immune checkpoint NKG2A enhances NK cell mediated cytotoxicity against multiple myeloma.* Oncoimmunology, 2022. **11**(1): p. 2081415.
350. Daher, M., et al., *Targeting a cytokine checkpoint enhances the fitness of armored cord blood CAR-NK cells.* Blood, 2021. **137**(5): p. 624-636.
351. Benson, D.M., Jr., et al., *IPH2101, a novel anti-inhibitory KIR antibody, and lenalidomide combine to enhance the natural killer cell versus multiple myeloma effect.* Blood, 2011. **118**(24): p. 6387-91.

352. Nijhof, I.S., et al., *Daratumumab-mediated lysis of primary multiple myeloma cells is enhanced in combination with the human anti-KIR antibody IPH2102 and lenalidomide.* Haematologica, 2015. **100**(2): p. 263-8.
353. Benson, D.M., Jr., et al., *A phase 1 trial of the anti-KIR antibody IPH2101 in patients with relapsed/refractory multiple myeloma.* Blood, 2012. **120**(22): p. 4324-33.
354. Carlsten, M., et al., *Checkpoint Inhibition of KIR2D with the Monoclonal Antibody IPH2101 Induces Contraction and Hyporesponsiveness of NK Cells in Patients with Myeloma.* Clin Cancer Res, 2016. **22**(21): p. 5211-5222.
355. Laskowski, T.J., A. Biederstadt, and K. Rezvani, *Natural killer cells in antitumour adoptive cell immunotherapy.* Nat Rev Cancer, 2022. **22**(10): p. 557-575.
356. Benson, D.M., Jr., et al., *A Phase I Trial of the Anti-KIR Antibody IPH2101 and Lenalidomide in Patients with Relapsed/Refractory Multiple Myeloma.* Clin Cancer Res, 2015. **21**(18): p. 4055-61.
357. Judge, S.J., et al., *Minimal PD-1 expression in mouse and human NK cells under diverse conditions.* J Clin Invest, 2020. **130**(6): p. 3051-3068.
358. Yang, C., et al., *Dual-targeted CAR-NK cell therapy: optimized CAR design to prevent antigen escape and elicit a deep and durable response in multiple myeloma.* Cancer Research, 2023.
359. Benson, D.M., Jr., et al., *The PD-1/PD-L1 axis modulates the natural killer cell versus multiple myeloma effect: a therapeutic target for CT-011, a novel monoclonal anti-PD-1 antibody.* Blood, 2010. **116**(13): p. 2286-94.
360. Badros, A.Z., et al., *Long-term remissions after stopping pembrolizumab for relapsed or refractory multiple myeloma.* Blood Adv, 2019. **3**(11): p. 1658-1660.
361. D'Souza, A., et al., *A Phase 2 Study of Pembrolizumab during Lymphodepletion after Autologous Hematopoietic Cell Transplantation for Multiple Myeloma.* Biol Blood Marrow Transplant, 2019. **25**(8): p. 1492-1497.
362. Mateos, M.V., et al., *Pembrolizumab plus pomalidomide and dexamethasone for patients with relapsed or refractory multiple myeloma (KEYNOTE-183): a randomised, open-label, phase 3 trial.* Lancet Haematol, 2019. **6**(9): p. e459-e469.
363. Liu, Z.Y., et al., *CD155/TIGIT signalling plays a vital role in the regulation of bone marrow mesenchymal stem cell-induced natural killer-cell exhaustion in multiple myeloma.* Clin Transl Med, 2022. **12**(7): p. e861.
364. Jo, D.H., et al., *Simultaneous engineering of natural killer cells for CAR transgenesis and CRISPR-Cas9 knockout using retroviral particles.* Mol Ther Methods Clin Dev, 2023. **29**: p. 173-184.
365. Brauneck, F., et al., *Combined Blockade of TIGIT and CD39 or A2AR Enhances NK-92 Cell-Mediated Cytotoxicity in AML.* Int J Mol Sci, 2021. **22**(23).
366. Maas, R.J., et al., *TIGIT blockade enhances functionality of peritoneal NK cells with altered expression of DNAM-1/TIGIT/CD96 checkpoint molecules in ovarian cancer.* Oncoimmunology, 2020. **9**(1): p. 1843247.
367. Zhang, Q., et al., *Blockade of the checkpoint receptor TIGIT prevents NK cell exhaustion and elicits potent anti-tumor immunity.* Nat Immunol, 2018. **19**(7): p. 723-732.
368. Jiang, W., et al., *Tim-3 Blockade Elicits Potent Anti-Multiple Myeloma Immunity of Natural Killer Cells.* Front Oncol, 2022. **12**: p. 739976.
369. Rakova, J., et al., *TIM-3 levels correlate with enhanced NK cell cytotoxicity and improved clinical outcome in AML patients.* Oncoimmunology, 2021. **10**(1): p. 1889822.
370. Gleason, M.K., et al., *Tim-3 is an inducible human natural killer cell receptor that enhances interferon gamma production in response to galectin-9.* Blood, 2012. **119**(13): p. 3064-72.
371. Ulbrecht, M., et al., *Cell surface expression of HLA-E: interaction with human beta2-microglobulin and allelic differences.* Eur J Immunol, 1999. **29**(2): p. 537-47.

372. Paech, C., et al., *HLA-E diversity unfolded: Identification and characterization of 170 novel HLA-E alleles.* HLA, 2021. **97**(5): p. 389-398.
373. Braud, V.M., et al., *HLA-E binds to natural killer cell receptors CD94/NKG2A, B and C.* Nature, 1998. **391**(6669): p. 795-9.
374. Ulbrecht, M., et al., *Interaction of HLA-E with peptides and the peptide transporter in vitro: implications for its function in antigen presentation.* J Immunol, 1998. **160**(9): p. 4375-85.
375. Borst, L., S.H. van der Burg, and T. van Hall, *The NKG2A-HLA-E Axis as a Novel Checkpoint in the Tumor Microenvironment.* Clin Cancer Res, 2020. **26**(21): p. 5549-5556.
376. van Hall, T., et al., *Monalizumab: inhibiting the novel immune checkpoint NKG2A.* J Immunother Cancer, 2019. **7**(1): p. 263.
377. Altvater, B., et al., *HLA-G and HLA-E Immune Checkpoints Are Widely Expressed in Ewing Sarcoma but Have Limited Functional Impact on the Effector Functions of Antigen-Specific CAR T Cells.* Cancers (Basel), 2021. **13**(12).
378. Sarkar, S., et al., *Optimal selection of natural killer cells to kill myeloma: the role of HLA-E and NKG2A.* Cancer Immunol Immunother, 2015. **64**(8): p. 951-63.
379. Gooden, M., et al., *HLA-E expression by gynecological cancers restrains tumor-infiltrating CD8(+) T lymphocytes.* Proc Natl Acad Sci U S A, 2011. **108**(26): p. 10656-61.
380. Nguyen, S., et al., *NK-cell reconstitution after haploidentical hematopoietic stem-cell transplantations: immaturity of NK cells and inhibitory effect of NKG2A override GvL effect.* Blood, 2005. **105**(10): p. 4135-42.
381. Gross, C., et al., *An Hsp70 peptide initiates NK cell killing of leukemic blasts after stem cell transplantation.* Leuk Res, 2008. **32**(4): p. 527-34.
382. Derre, L., et al., *Expression and release of HLA-E by melanoma cells and melanocytes: potential impact on the response of cytotoxic effector cells.* J Immunol, 2006. **177**(5): p. 3100-7.
383. Liu, X., et al., *Immune checkpoint HLA-E:CD94-NKG2A mediates evasion of circulating tumor cells from NK cell surveillance.* Cancer Cell, 2023. **41**(2): p. 272-287 e9.
384. Talebian Yazdi, M., et al., *The positive prognostic effect of stromal CD8+ tumor-infiltrating T cells is restrained by the expression of HLA-E in non-small cell lung carcinoma.* Oncotarget, 2016. **7**(3): p. 3477-88.
385. de Kruijf, E.M., et al., *HLA-E and HLA-G expression in classical HLA class I-negative tumors is of prognostic value for clinical outcome of early breast cancer patients.* J Immunol, 2010. **185**(12): p. 7452-9.
386. Andersson, E., et al., *Non-classical HLA-class I expression in serous ovarian carcinoma: Correlation with the HLA-genotype, tumor infiltrating immune cells and prognosis.* Oncoimmunology, 2016. **5**(1): p. e1052213.
387. Lagana, A., et al., *Increased HLA-E Expression Correlates with Early Relapse in Multiple Myeloma.* ASH, 2018.
388. Kren, L., et al., *Expression of immune-modulatory molecules HLA-G and HLA-E by tumor cells in glioblastomas: an unexpected prognostic significance?* Neuropathology, 2011. **31**(2): p. 129-34.
389. Bossard, C., et al., *HLA-E/beta2 microglobulin overexpression in colorectal cancer is associated with recruitment of inhibitory immune cells and tumor progression.* Int J Cancer, 2012. **131**(4): p. 855-63.
390. Thangaraj, J.L., et al., *Expanded natural killer cells augment the antimyeloma effect of daratumumab, bortezomib, and dexamethasone in a mouse model.* Cell Mol Immunol, 2021. **18**(7): p. 1652-1661.
391. Yun, H.D., et al., *Dinaciclib enhances natural killer cell cytotoxicity against acute myelogenous leukemia.* Blood Adv, 2019. **3**(16): p. 2448-2452.

392. Enqvist, M., et al., *Selenite induces posttranscriptional blockade of HLA-E expression and sensitizes tumor cells to CD94/NKG2A-positive NK cells.* J Immunol, 2011. **187**(7): p. 3546-54.
393. Tognarelli, S., et al., *Enhancing the Activation and Releasing the Brakes: A Double Hit Strategy to Improve NK Cell Cytotoxicity Against Multiple Myeloma.* Front Immunol, 2018. **9**: p. 2743.
394. Kamiya, T., et al., *Blocking expression of inhibitory receptor NKG2A overcomes tumor resistance to NK cells.* J Clin Invest, 2019. **129**(5): p. 2094-2106.
395. Lee, J., et al., *Monalizumab efficacy correlates with HLA-E surface expression and NK cell activity in head and neck squamous carcinoma cell lines.* J Cancer Res Clin Oncol, 2023. **149**(9): p. 5705-5715.
396. Wang, X., H. Xiong, and Z. Ning, *Implications of NKG2A in immunity and immune-mediated diseases.* Front Immunol, 2022. **13**: p. 960852.
397. Plougastel, B., T. Jones, and J. Trowsdale, *Genomic structure, chromosome location, and alternative splicing of the human NKG2A gene.* Immunogenetics, 1996. **44**(4): p. 286-91.
398. Wagner, J.A., et al., *Cytokine-Induced Memory-Like Differentiation Enhances Unlicensed Natural Killer Cell Antileukemia and FcgammaRIIIa-Triggered Responses.* Biol Blood Marrow Transplant, 2017. **23**(3): p. 398-404.
399. Andre, P., et al., *Anti-NKG2A mAb Is a Checkpoint Inhibitor that Promotes Anti-tumor Immunity by Unleashing Both T and NK Cells.* Cell, 2018. **175**(7): p. 1731-1743 e13.
400. Masilamani, M., et al., *CD94/NKG2A inhibits NK cell activation by disrupting the actin network at the immunological synapse.* J Immunol, 2006. **177**(6): p. 3590-6.
401. Das, J. and S.I. Khakoo, *NK cells: tuned by peptide?* Immunol Rev, 2015. **267**(1): p. 214-27.
402. Battin, C., et al., *NKG2A-checkpoint inhibition and its blockade critically depends on peptides presented by its ligand HLA-E.* Immunology, 2022. **166**(4): p. 507-521.
403. Figueiredo, C., A. Seltsam, and R. Blasczyk, *Permanent silencing of NKG2A expression for cell-based therapeutics.* J Mol Med (Berl), 2009. **87**(2): p. 199-210.
404. Ruggeri, L., et al., *Effects of anti-NKG2A antibody administration on leukemia and normal hematopoietic cells.* Haematologica, 2016. **101**(5): p. 626-33.
405. Melero, I., et al., *Intratumoral co-injection of NK cells and NKG2A-neutralizing monoclonal antibodies.* EMBO Mol Med, 2023: p. e17804.
406. Mahaweni, N.M., et al., *NKG2A Expression Is Not per se Detrimental for the Anti-Multiple Myeloma Activity of Activated Natural Killer Cells in an In Vitro System Mimicking the Tumor Microenvironment.* Front Immunol, 2018. **9**: p. 1415.
407. Tinker, A.V., et al., *Dose-Ranging and Cohort-Expansion Study of Monalizumab (IPH2201) in Patients with Advanced Gynecologic Malignancies: A Trial of the Canadian Cancer Trials Group (CCTG): IND221.* Clin Cancer Res, 2019. **25**(20): p. 6052-6060.
408. Galot, R., et al., *A phase II study of monalizumab in patients with recurrent/metastatic squamous cell carcinoma of the head and neck: The I1 cohort of the EORTC-HNCG-1559 UPSTREAM trial.* Eur J Cancer, 2021. **158**: p. 17-26.
409. Cohen, R.B., et al., *Combination of monalizumab and cetuximab in patients with recurrent or metastatic head and neck squamous cell cancer previously treated with platinum-based chemotherapy and PD-(L)1 inhibitors: a phase II expansion study.* ASCO, 2020.
410. Colevas, D.A., et al., *Monalizumab, cetuximab and durvalumab in first-line treatment of recurrent or metastatic squamous cell carcinoma of the head and neck (R/M SCCHN): A phase II trial.* Annals of Oncology, 2023.
411. Herbst, R.S., et al., *COAST: An Open-Label, Phase II, Multidrug Platform Study of Durvalumab Alone or in Combination With Oleclumab or Monalizumab in Patients With*

Unresectable, Stage III Non-Small-Cell Lung Cancer. J Clin Oncol, 2022. **40**(29): p. 3383-3393.
412. Geurts, V.C.M., et al., *Unleashing NK- and CD8 T cells by combining monalizumab and trastuzumab for metastatic HER2-positive breast cancer: Results of the MIMOSA trial.* Breast, 2023. **70**: p. 76-81.
413. Devillier, R., et al., *Safety of Anti-NKG2A Blocking Antibody Monalizumab As Maintenance Therapy after Allogeneic Hematopoietic*

Stem Cell Transplantation: A Phase I Study. ASH, 2021.
414. Bezman, N., et al., *ANTI-NKG2A ANTIBODIES AND USES THEREOF*. 2020: USA.
415. Grzywacz, B., et al., *Natural Killer Cell Homing and Persistence in the Bone Marrow After Adoptive Immunotherapy Correlates With Better Leukemia Control.* J Immunother, 2019. **42**(2): p. 65-72.
416. Curti, A., et al., *Successful transfer of alloreactive haploidentical KIR ligand-mismatched natural killer cells after infusion in elderly high risk acute myeloid leukemia patients.* Blood, 2011. **118**(12): p. 3273-9.
417. Berrien-Elliott, M.M., et al., *Hematopoietic cell transplantation donor-derived memory-like NK cells functionally persist after transfer into patients with leukemia.* Sci Transl Med, 2022. **14**(633): p. eabm1375.
418. Bednarski, J.J., et al., *Donor memory-like NK cells persist and induce remissions in pediatric patients with relapsed AML after transplant.* Blood, 2022. **139**(11): p. 1670-1683.
419. Liu, E., et al., *Cord blood NK cells engineered to express IL-15 and a CD19-targeted CAR show long-term persistence and potent antitumor activity.* Leukemia, 2018. **32**(2): p. 520-531.
420. Li, L., et al., *Loss of metabolic fitness drives tumor resistance after CAR-NK cell therapy and can be overcome by cytokine engineering.* Sci Adv, 2023. **9**(30): p. eadd6997.
421. Fernandez, R.A., et al., *Improving NK cell function in multiple myeloma with NKTR-255, a novel polymer-conjugated human IL-15.* Blood Adv, 2023. **7**(1): p. 9-19.
422. Rosario, M., et al., *The IL-15-Based ALT-803 Complex Enhances FcgammaRIIIa-Triggered NK Cell Responses and In Vivo Clearance of B Cell Lymphomas.* Clin Cancer Res, 2016. **22**(3): p. 596-608.
423. Berrien-Elliott, M.M., J.A. Wagner, and T.A. Fehniger, *Human Cytokine-Induced Memory-Like Natural Killer Cells.* J Innate Immun, 2015. **7**(6): p. 563-71.
424. Pal, M., et al., *Tumor-priming converts NK cells to memory-like NK cells.* Oncoimmunology, 2017. **6**(6): p. e1317411.
425. Kujur, W., et al., *Memory like NK cells display stem cell like properties after Zika virus infection.* PLoS Pathog, 2020. **16**(12): p. e1009132.
426. Foley, B., et al., *Cytomegalovirus reactivation after allogeneic transplantation promotes a lasting increase in educated NKG2C+ natural killer cells with potent function.* Blood, 2012. **119**(11): p. 2665-74.
427. Schlums, H., et al., *Cytomegalovirus infection drives adaptive epigenetic diversification of NK cells with altered signaling and effector function.* Immunity, 2015. **42**(3): p. 443-56.
428. Merino, A., et al., *Chronic stimulation drives human NK cell dysfunction and epigenetic reprograming.* J Clin Invest, 2019. **129**(9): p. 3770-3785.
429. Orchard, K., et al., *In Vivo Generation of Memory-like NK Cells for the Treatment of AML and Myelodysplastic Syndrome; Early Clinical Applications of INKmuneTM.* ASH, 2022.
430. Fehniger, T.A., et al., *Differential cytokine and chemokine gene expression by human NK cells following activation with IL-18 or IL-15 in combination with IL-12: implications for the innate immune response.* J Immunol, 1999. **162**(8): p. 4511-20.

431. Cooper, M.A., et al., *Cytokine-induced memory-like natural killer cells.* Proc Natl Acad Sci U S A, 2009. **106**(6): p. 1915-9.
432. Romee, R., et al., *Cytokine activation induces human memory-like NK cells.* Blood, 2012. **120**(24): p. 4751-60.
433. Tarannum, M. and R. Romee, *Cytokine-induced memory-like natural killer cells for cancer immunotherapy.* Stem Cell Res Ther, 2021. **12**(1): p. 592.
434. Leong, J.W., et al., *Preactivation with IL-12, IL-15, and IL-18 induces CD25 and a functional high-affinity IL-2 receptor on human cytokine-induced memory-like natural killer cells.* Biol Blood Marrow Transplant, 2014. **20**(4): p. 463-73.
435. Lusty, E., et al., *IL-18/IL-15/IL-12 synergy induces elevated and prolonged IFN-gamma production by ex vivo expanded NK cells which is not due to enhanced STAT4 activation.* Mol Immunol, 2017. **88**: p. 138-147.
436. Ni, J., et al., *Sustained effector function of IL-12/15/18-preactivated NK cells against established tumors.* J Exp Med, 2012. **209**(13): p. 2351-65.
437. Tanzi, M., et al., *Cytokine-Induced Memory-Like NK Cells with High Reactivity against Acute Leukemia Blasts and Solid Tumor Cells Suitable for Adoptive Immunotherapy Approaches.* Cancers (Basel), 2021. **13**(7).
438. Huber, C.M., J.M. Doisne, and F. Colucci, *IL-12/15/18-preactivated NK cells suppress GvHD in a mouse model of mismatched hematopoietic cell transplantation.* Eur J Immunol, 2015. **45**(6): p. 1727-35.
439. Terren, I., et al., *Implication of Interleukin-12/15/18 and Ruxolitinib in the Phenotype, Proliferation, and Polyfunctionality of Human Cytokine-Preactivated Natural Killer Cells.* Front Immunol, 2018. **9**: p. 737.
440. Ghofrani, J., et al., *Semaphorin 7A modulates cytokine-induced memory-like responses by human natural killer cells.* Eur J Immunol, 2019. **49**(8): p. 1153-1166.
441. Uppendahl, L.D., et al., *Cytokine-induced memory-like natural killer cells have enhanced function, proliferation, and in vivo expansion against ovarian cancer cells.* Gynecol Oncol, 2019. **153**(1): p. 149-157.
442. Romee, R., et al., *Cytokine-induced memory-like natural killer cells exhibit enhanced responses against myeloid leukemia.* Sci Transl Med, 2016. **8**(357): p. 357ra123.
443. Pahl, J.H.W., A. Cerwenka, and J. Ni, *Memory-Like NK Cells: Remembering a Previous Activation by Cytokines and NK Cell Receptors.* Front Immunol, 2018. **9**: p. 2796.
444. Orr, M.T. and L.L. Lanier, *Natural killer cell education and tolerance.* Cell, 2010. **142**(6): p. 847-56.
445. Berrien-Elliott, M.M., et al., *Multidimensional Analyses of Donor Memory-Like NK Cells Reveal New Associations with Response after Adoptive Immunotherapy for Leukemia.* Cancer Discov, 2020. **10**(12): p. 1854-1871.
446. Vendrame, E., et al., *Mass Cytometry Analytical Approaches Reveal Cytokine-Induced Changes in Natural Killer Cells.* Cytometry B Clin Cytom, 2017. **92**(1): p. 57-67.
447. Boieri, M., et al., *IL-12, IL-15, and IL-18 pre-activated NK cells target resistant T cell acute lymphoblastic leukemia and delay leukemia development in vivo.* Oncoimmunology, 2017. **6**(3): p. e1274478.
448. Zhuang, L., et al., *Activity of IL-12/15/18 primed natural killer cells against hepatocellular carcinoma.* Hepatol Int, 2019. **13**(1): p. 75-83.
449. Marin, N.D., et al., *Memory-like Differentiation Enhances NK Cell Responses to Melanoma.* Clin Cancer Res, 2021. **27**(17): p. 4859-4869.
450. Ni, J., et al., *Adoptively transferred natural killer cells maintain long-term antitumor activity by epigenetic imprinting and CD4(+) T cell help.* Oncoimmunology, 2016. **5**(9): p. e1219009.
451. Becker-Hapak, M.K., et al., *A Fusion Protein Complex that Combines IL-12, IL-15, and IL-18 Signaling to Induce Memory-Like NK Cells for Cancer Immunotherapy.* Cancer Immunol Res, 2021. **9**(9): p. 1071-1087.

452. Kedia-Mehta, N., et al., *Cytokine-induced natural killer cell training is dependent on cellular metabolism and is defective in obesity.* Blood Adv, 2021. **5**(21): p. 4447-4455.
453. Terren, I., et al., *Metabolic changes of Interleukin-12/15/18-stimulated human NK cells.* Sci Rep, 2021. **11**(1): p. 6472.
454. Jacobs, M.T., et al., *Memory-like differentiation, tumor targeting monoclonal antibodies, and chimeric antigen receptors enhance natural killer cell responses to head and neck cancer.* Clin Cancer Res, 2023.
455. Kerbauy, L.N., et al., *Combining AFM13, a Bispecific CD30/CD16 Antibody, with Cytokine-Activated Blood and Cord Blood-Derived NK Cells Facilitates CAR-like Responses Against CD30(+) Malignancies.* Clin Cancer Res, 2021. **27**(13): p. 3744-3756.
456. Gang, M., et al., *CAR-modified memory-like NK cells exhibit potent responses to NK-resistant lymphomas.* Blood, 2020. **136**(20): p. 2308-2318.
457. He, B., et al., *Cytokines induced memory-like NK cells engineered to express CD19 CAR exhibit enhanced responses against B cell malignancies.* Front Immunol, 2023. **14**: p. 1130442.
458. Dong, H., et al., *Memory-like NK cells armed with a neoepitope-specific CAR exhibit potent activity against NPM1 mutated acute myeloid leukemia.* Proc Natl Acad Sci U S A, 2022. **119**(25): p. e2122379119.
459. Shapiro, R.M., et al., *Expansion, persistence, and efficacy of donor memory-like NK cells infused for posttransplant relapse.* J Clin Invest, 2022. **132**(11).
460. Rutella, S., et al., *WU-NK-101: an Enhanced NK Cell Therapy Optimized for Function in the Tumor Microenvironment (TME).* ESMO, 2022.
461. Rastelli, L., et al., *A first-in-class ex vivo combination between cytokine-induced memory like (CIML) NK cells and a CD38 targeting antibody recruiting molecule (ARM) as a novel approach to target NK cells without cellular engineering for the treatment of multiple myeloma.* ASCO, 2020.
462. Sevilla-Movilla, S., et al., *Upregulated expression and function of the alpha4beta1 integrin in multiple myeloma cells resistant to bortezomib.* J Pathol, 2020. **252**(1): p. 29-40.
463. Denman, C.J., et al., *Membrane-bound IL-21 promotes sustained ex vivo proliferation of human natural killer cells.* PLoS One, 2012. **7**(1): p. e30264.
464. Wang, R.N., et al., *Optimized protocols for gammadelta T cell expansion and lentiviral transduction.* Mol Med Rep, 2019. **19**(3): p. 1471-1480.
465. Song, D.G., et al., *Chimeric NKG2D CAR-expressing T cell-mediated attack of human ovarian cancer is enhanced by histone deacetylase inhibition.* Hum Gene Ther, 2013. **24**(3): p. 295-305.
466. Amiot, M., et al., *Identification and Hierarchy of Clonogenic Factors for Human Myeloma Cells: IL-6 for CD45+ Versus IL-6 and Growth Factors for CD45-.* ASH, 2005.
467. Scholzen, T. and J. Gerdes, *The Ki-67 protein: from the known and the unknown.* J Cell Physiol, 2000. **182**(3): p. 311-22.
468. Love, M.I., W. Huber, and S. Anders, *Moderated estimation of fold change and dispersion for RNA-seq data with DESeq2.* Genome Biol, 2014. **15**(12): p. 550.
469. Aryee, K.E., et al., *Enhanced development of functional human NK cells in NOD-scid-IL2rg(null) mice expressing human IL15.* FASEB J, 2022. **36**(9): p. e22476.
470. Alter, G., J.M. Malenfant, and M. Altfeld, *CD107a as a functional marker for the identification of natural killer cell activity.* J Immunol Methods, 2004. **294**(1-2): p. 15-22.
471. Tiedemann, R.E., et al., *Identification of kinetin riboside as a repressor of CCND1 and CCND2 with preclinical antimyeloma activity.* J Clin Invest, 2008. **118**(5): p. 1750-64.
472. Kukita, A. and T. Kukita, *Multifunctional properties of RANKL/RANK in cell differentiation, proliferation and metastasis.* Future Oncol, 2013. **9**(11): p. 1609-22.

473. Lindahl, M., et al., *MANF is indispensable for the proliferation and survival of pancreatic beta cells.* Cell Rep, 2014. **7**(2): p. 366-375.
474. Shi, Z., et al., *Cables1 complex couples survival signaling to the cell death machinery.* Cancer Res, 2015. **75**(1): p. 147-158.
475. Ito, M., et al., *Killer cell lectin-like receptor G1 binds three members of the classical cadherin family to inhibit NK cell cytotoxicity.* J Exp Med, 2006. **203**(2): p. 289-95.
476. Jelinek, T., B. Paiva, and R. Hajek, *Update on PD-1/PD-L1 Inhibitors in Multiple Myeloma.* Front Immunol, 2018. **9**: p. 2431.
477. Sharma, N., P.M. Reagan, and J.L. Liesveld, *Cytopenia after CAR-T Cell Therapy-A Brief Review of a Complex Problem.* Cancers (Basel), 2022. **14**(6).
478. Zheng, M.M., et al., *The systemic cytokine environment is permanently altered in multiple myeloma.* PLoS One, 2013. **8**(3): p. e58504.
479. Zingone, A., et al., *Altered cytokine and chemokine profiles in multiple myeloma and its precursor disease.* Cytokine, 2014. **69**(2): p. 294-7.
480. Sharma, A., et al., *Dysregulation in T helper 1/T helper 2 cytokine ratios in patients with multiple myeloma.* Leuk Lymphoma, 2010. **51**(5): p. 920-7.
481. Gustafson, K.S. and G.D. Ginder, *Interferon-gamma induction of the human leukocyte antigen-E gene is mediated through binding of a complex containing STAT1alpha to a distinct interferon-gamma-responsive element.* J Biol Chem, 1996. **271**(33): p. 20035-46.
482. Ettari, R., et al., *Immunoproteasome-selective and non-selective inhibitors: A promising approach for the treatment of multiple myeloma.* Pharmacol Ther, 2018. **182**: p. 176-192.
483. Sun, C., et al., *High NKG2A expression contributes to NK cell exhaustion and predicts a poor prognosis of patients with liver cancer.* Oncoimmunology, 2017. **6**(1): p. e1264562.
484. Salome, B., et al., *NKG2A and HLA-E define an alternative immune checkpoint axis in bladder cancer.* Cancer Cell, 2022. **40**(9): p. 1027-1043 e9.
485. Quintarelli, C., et al., *Efficacy of third-party chimeric antigen receptor modified peripheral blood natural killer cells for adoptive cell therapy of B-cell precursor acute lymphoblastic leukemia.* Leukemia, 2020. **34**(4): p. 1102-1115.
486. Rasche, L., M. Hudecek, and H. Einsele, *CAR T-Cell Therapy in Multiple Myeloma: Mission Accomplished?* Blood, 2023.
487. Muller, S., et al., *High Cytotoxic Efficiency of Lentivirally and Alpharetrovirally Engineered CD19-Specific Chimeric Antigen Receptor Natural Killer Cells Against Acute Lymphoblastic Leukemia.* Front Immunol, 2019. **10**: p. 3123.
488. Yang, Y., et al., *Superior Expansion and Cytotoxicity of Human Primary NK and CAR-NK Cells from Various Sources via Enriched Metabolic Pathways.* Mol Ther Methods Clin Dev, 2020. **18**: p. 428-445.
489. Allan, D.S.J., et al., *Expanded NK cells used for adoptive cell therapy maintain diverse clonality and contain long-lived memory-like NK cell populations.* Mol Ther Oncolytics, 2023. **28**: p. 74-87.
490. Ciurea, S.O., et al., *Phase 1 clinical trial using mbIL21 ex vivo-expanded donor-derived NK cells after haploidentical transplantation.* Blood, 2017. **130**(16): p. 1857-1868.
491. Vela, M., et al., *Haploidentical IL-15/41BBL activated and expanded natural killer cell infusion therapy after salvage chemotherapy in children with relapsed and refractory leukemia.* Cancer Lett, 2018. **422**: p. 107-117.
492. Schmidt, P., M.J. Raftery, and G. Pecher, *Engineering NK Cells for CAR Therapy-Recent Advances in Gene Transfer Methodology.* Front Immunol, 2020. **11**: p. 611163.
493. Dagher, O.K. and A.D. Posey, Jr., *Forks in the road for CAR T and CAR NK cell cancer therapies.* Nat Immunol, 2023. **24**(12): p. 1994-2007.

494. Colamartino, A.B.L., et al., *Efficient and Robust NK-Cell Transduction With Baboon Envelope Pseudotyped Lentivector.* Front Immunol, 2019. **10**: p. 2873.
495. Mac Donald, A., et al., *KLRC1 knockout overcomes HLA-E-mediated inhibition and improves NK cell antitumor activity against solid tumors.* Front Immunol, 2023. **14**: p. 1231916.
496. Hromadnikova, I., P. Pirkova, and L. Sedlackova, *Influence of in vitro IL-2 or IL-15 alone or in combination with Hsp-70-derived 14-mer peptide (TKD) on the expression of NK cell activatory and inhibitory receptors.* Mediators Inflamm, 2013. **2013**: p. 405295.
497. Nguyen, S., et al., *HLA-E upregulation on IFN-gamma-activated AML blasts impairs CD94/NKG2A-dependent NK cytolysis after haplo-mismatched hematopoietic SCT.* Bone Marrow Transplant, 2009. **43**(9): p. 693-9.
498. Zhang, X., et al., *Synergized regulation of NK cell education by NKG2A and specific Ly49 family members.* Nat Commun, 2019. **10**(1): p. 5010.
499. Oei, V.Y.S., et al., *Intrinsic Functional Potential of NK-Cell Subsets Constrains Retargeting Driven by Chimeric Antigen Receptors.* Cancer Immunol Res, 2018. **6**(4): p. 467-480.
500. Logue, J.M., et al., *Early cytopenias and infections after standard of care idecabtagene vicleucel in relapsed or refractory multiple myeloma.* Blood Adv, 2022. **6**(24): p. 6109-6119.
501. Carlsten, M. and R.W. Childs, *Genetic Manipulation of NK Cells for Cancer Immunotherapy: Techniques and Clinical Implications.* Front Immunol, 2015. **6**: p. 266.
502. Romee, R., et al., *NK cell CD16 surface expression and function is regulated by a disintegrin and metalloprotease-17 (ADAM17).* Blood, 2013. **121**(18): p. 3599-608.
503. Carreira-Santos, S., et al., *Enhanced expression of natural cytotoxicity receptors on cytokine-induced memory-like natural killer cells correlates with effector function.* Front Immunol, 2023. **14**: p. 1256404.
504. Littwitz-Salomon, E., et al., *Metabolic requirements of NK cells during the acute response against retroviral infection.* Nat Commun, 2021. **12**(1): p. 5376.
505. Schmiedel, B.J., et al., *Receptor activator for NF-kappaB ligand in acute myeloid leukemia: expression, function, and modulation of NK cell immunosurveillance.* J Immunol, 2013. **190**(2): p. 821-31.
506. Gomez-Aleza, C., et al., *Inhibition of RANK signaling in breast cancer induces an anti-tumor immune response orchestrated by CD8+ T cells.* Nat Commun, 2020. **11**(1): p. 6335.
507. Zhang, H., et al., *Aberrant splicing of cables gene, a CDK regulator, in human cancers.* Cancer Biol Ther, 2005. **4**(11): p. 1211-5.
508. Schomer, N.T., et al., *CCR7 expression in CD19 chimeric antigen receptor-engineered natural killer cells improves migration toward CCL19-expressing lymphoma cells and increases tumor control in mice with human lymphoma.* Cytotherapy, 2022. **24**(8): p. 827-834.
509. Lachota, M., et al., *Mapping the chemotactic landscape in NK cells reveals subset-specific synergistic migratory responses to dual chemokine receptor ligation.* EBioMedicine, 2023. **96**: p. 104811.
510. Hong, H.S., et al., *Loss of CCR7 expression on CD56(bright) NK cells is associated with a CD56(dim)CD16(+) NK cell-like phenotype and correlates with HIV viral load.* PLoS One, 2012. **7**(9): p. e44820.
511. Song, Y., et al., *IL-12/IL-18-preactivated donor NK cells enhance GVL effects and mitigate GvHD after allogeneic hematopoietic stem cell transplantation.* Eur J Immunol, 2018. **48**(4): p. 670-682.
512. Bakhtiyaridovvombaygi, M., et al., *Cytokine-Induced Memory-Like NK Cells: Emerging strategy for AML immunotherapy.* Biomed Pharmacother, 2023. **168**: p. 115718.
513. Michaelsson, J., et al., *A signal peptide derived from hsp60 binds HLA-E and interferes with CD94/NKG2A recognition.* J Exp Med, 2002. **196**(11): p. 1403-14.

514. Huisman, B.D., et al., *High-throughput characterization of HLA-E-presented CD94/NKG2x ligands reveals peptides which modulate NK cell activation.* Nat Commun, 2023. **14**(1): p. 4809.
515. Mehdi, S.H., et al., *Animal Models of Multiple Myeloma Bone Disease.* Front Genet, 2021. **12**: p. 640954.